Biogeochemistry of Sulfur in Small Forested Catchments of the Great Smoky Mountains National Park

A Dissertation Presented for the
Doctor of Philosophy
Degree
The University of Tennessee, Knoxville

Adrian Miguel Gonzalez
May 2018

Copyright © 2018 by Adrian Miguel Gonzalez
All rights reserved.

DEDICATION

To the three women in my life who encourage, challenge and cheer me on to conquer on their behalf: Catherine, Elizabeth, and Nicole

ACKNOWLEDGEMENTS

This research was funded by the U.S. Department of Interior, Southern Appalachian Cooperative Ecosystems Studies Unit, CA No. P14AC00882, Task Agreement No. P14AC00867. Field activities were permitted by the U.S. Department of Interior National Park Service under permit No. GRSM-2016-SCI-1248, and soil sampling areas were checked for cultural or archeological artifacts by NPS archeologist.

Special thanks go to Dr. John Schwartz for guiding my journey through this doctorate experience. I often told family and friends during my time in the program that there could not have been a better student-advisor fit for me. John too worked through his doctoral program in the middle-ages of life, so he more than most was well-equipped for understanding my perspective as a "late-bloomer" student. Not only did he provide excellent technical guidance, but his relaxed perspective on academia in the larger context of living life was very helpful and welcome. I hope that I can be the same to those with whom I collaborate in the future.

I would also like to thank the other members of my committee for contributing to my experience and knowledge, both in and out of the classroom. Three of my favorite courses were taught by Dr. Anna Szynkiewicz and Dr. Michael Essington (Dr. "E"), which I tried to put to good use in this research, and my most challenging course was taught by Dr. Qiang He. Thanks also go to the National Park Service and the Great Smoky Mountains National Park, and specifically to Matt Kulp for his role in funding, contracts, and for the general research ideas regarding sulfur biogeochemistry in the Park.

I had the honor of working beside numerous fellow students, some who provided much appreciated assistance in lab and field work, some who I gladly assisted and collaborated with in their

programs, and some who just befriended the old guy in the lab for whom they had pity. It would be an effort to list everyone I worked with over the years; I'd forget some and leave them out.

My support network on campus was only half of the community of people helped me get through this doctoral program in my late 40s/early 50s. They vicariously lived through the program with me, but I'm sure they were quite contented that it was me doing the work and not they! Special support came from my two daughters, Nicole and Elizabeth. Not only did they help with water sampling on occasion, but I shared the unique experience of being fellow college students together. Even more rare was the joy I got in being in the same UTK Civil Engineering department with Nicole during her junior and senior years. I am so grateful for the experiences of seeing her in class down the hall from the graduate student offices, having her gently knock on the window next to my cubicle to be let in for a quick visit, and walking to the Student Union together for a Chick-Fil-A lunch. It's been such a blessing for me to share daily academic life with my grown daughter. I also have such gratitude and pride in being an inspiration to my other daughter Elizabeth in pursuing graduate education for herself. Perhaps she reasoned: "if my old man can do, this should be a piece of cake for me!" I especially enjoyed our conversations on academia or graduate studies or sharing advice on writing or navigating relationships with fellow students or professors.

Lastly, special acknowledgement goes to my dearest wife and friend, Catherine. Such sacrifice from her to allow me to achieve this goal and bucket-list item! Amazing! Taking on roles of primary income earner and family-budget manager to keep expenses below our combined incomes of a non-profit employee and a student stipend! Showing grace and patience in being left alone for hours on end while I shuttled back to the lab to finish running samples or to the student offices to write! Thank you doesn't come close to breaking even, but I'll start there. I have the rest of our life together to work on paying it back.

ABSTRACT

This dissertation presents three studies designed to investigate sources and biogeochemical processing of sulfur in the Great Smoky Mountains National Park (GRSM). First, a geochemical study of first- and second-order streams throughout the GRSM was conducted to determine variability in water quality and the influence of natural land disturbances on the water quality. The study identified three categories of sites, each with distinct water chemistry: lower elevation sites, high-elevation sites, and sites influence by sulfidic bedrock. Stream water chemistry was statistically significantly different in catchments with and without known areas of land disturbances that exposed sulfidic bedrock to the atmosphere. A second study focused on soil/stream water geochemistry and the influence of bedrock composition on it. Three sites overlying sulfidic bedrock were statistically compared to two overlying sandstone and two overlying a bedrock transition zone. Stream water from the two sites adjacent to exposed sulfidic bedrock had the lowest pH and acid-neutralizing capacity, the highest sulfate concentrations, as well as the highest metals and cations concentrations. Results also showed that the soil organic phase was the primary locus of sulfur retention in high-elevation forest catchments. The third study focused on stable isotope geochemistry in the same seven catchments. It showed that stream water chemistry, and the sulfur ($\delta^{34}S$) and oxygen ($\delta^{18}O$) isotope composition of stream water sulfate and soil sulfur, reflects atmospheric sulfate in the absence of significant sulfur/sulfate inputs from sulfidic bedrock. All three studies were consistent in providing evidence that influence of sulfidic bedrock on stream water geochemistry in high-elevation catchments is dependent on the bedrock's exposure to the atmosphere. The soil mantel has a stronger direct influence on GRSM stream water chemistry than bedrock composition, as indicated by the sulfur and oxygen isotope composition of soil sulfur and soil organic sulfur and by the similarity in sulfur isotope composition of sulfate

in stream water and subsurface soil. Geochemical indicators of acidification of GRSM stream water and soil at the selected study sites appear to be caused by the characteristically low-neutralizing potential of high-elevation soil than to the composition of underlying bedrock.

PREFACE

“Modern man has no real ‘value’ for the ocean [or the environment generally]. All he has is the most crass form of egoist, pragmatic value for it. He treats it as a ‘thing’ in the worst possible sense, to exploit it for the ‘good’ of man. The man who believes things are there only by chance cannot give things a real value. But for the Christian, the value of a thing is not in itself autonomously, but because God made it. It deserves this respect as something which was created by God, as man himself has been created by God.

“So man has dominion over nature, but he uses it wrongly. The Christian is called upon to exhibit this dominion, but exhibit it rightly: treating the thing as having value in itself, exercising dominion without being destructive.

“… what we should have, individually and corporately, is a situation where, on the basis of the work of Christ, Christianity is seen to be not just ‘pie in the sky,’ but something that has in it the possibility of substantial healings now in every area where there are divisions because of the Fall. First of all, my division from God is healed by justification, but then there must be the ‘existential reality’ of this, moment by moment; second, there is the psychological division of man from himself; third, the division of man from nature, and nature from nature. In all of these areas we should expect to see substantial healing.”

Dr. Francis A. Schaeffer, 1970. Pollution and the Death of Man: The Christian View of Ecology. Tyndale House Publishers. Wheaton, Illinois

[bold font added for emphasis; italicized text added by AMG]

“He has shown you, O man, what is good. And what does the LORD require of you? To act justly and to love mercy and to walk humbly with your GOD.” Micah 6:8 NIV

TABLE OF CONTENTS

Chapter 1: Introduction 1

References 10

Chapter 1 Appendix 19

Chapter 2: Research Questions and Framework 20

Conceptual Model: High-Elevation Forest Catchment 20

Conceptual Model: Sulfur Speciation and Distribution 24

Conceptual Model: Sulfur and Oxygen Isotope Composition 25

Dissertation Research Questions 28

References 32

Chapter 2 Appendix 41

Chapter 3: Literature Review 44

Basic Chemistry of Sulfur 44

Aqueous Chemistry of Sulfur 45

Sulfate Chemistry (Hydrolysis and pH) 46

Aqueous-Solid Interface Processes of Sulfur 48

Sulfate and ANC 49

Atmospheric Chemistry of Sulfur 50

Sulfide Mineral Oxidation 52

Biochemistry and Organic Chemistry of Sulfur 55

Stable Isotope Geochemistry of Sulfur and Oxygen 58

References 64

Chapter 4: A HydroGeochemical Analysis of First- and Second-Order Streams of the Great Smoky Mountains: The Influence of land Disturbances and Exposed Bedrock on stream chemistry 88

Abstract 89

Introduction 90
Methods 94
Study Locations 94
Sample Collection 94
Chemical Analyses 96
Data Analysis 96
Results 98
Water Chemistry of Low-Order Steams 98
Mineral Weathering Indices 100
Discussion 102
Stream Water Acidity in Low-Order Streams 102
Influence of Bedrock on Stream Water Chemistry 104
Influence of Land Disturbance on Stream Water Chemistry 107
Conclusions 109
References 111
Chapter 4 Appendix 121
Chapter 5: Conditional Influence of Sulfidic Bedrock on Soil and Stream Water Chemistry in High-Elevation Forest Catchments of the Great Smoky Mountains 134
Abstract 135
Introduction 137
Study Design 141
Study Catchment Selection 141
Methods 144
Sample Collection 144
Analytical Methods 146

Statistical Analyses 147
Results 148
Soil Chemistry – Acidity Parameters 148
Soil Chemistry – Sulfur Species 149
Soil Chemistry by Bedrock Type 150
Stream Water Chemistry 152
Discussion 153
Soil / Bedrock Interactions 154
Soil Sulfur Status – Inorganic Sulfur 156
Soil Sulfur Status – Organic Sulfur 157
Stream Water / Bedrock Interactions 158
Stream Water / Soil Interactions 160
Conclusions 161
References 163
Chapter 5 Appendix 178
Chapter 6: Identifying sulfur sources and cycling mechanisms in high-elevation forest catchments of the Great Smoky Mountains National Park, using stable isotope analysis 189
Abstract 190
Introduction 192
Environmental Setting 197
Study Design 199
Methods 199
Results 202
Surface Water Chemistry 202
Sulfur Isotope Composition 203

Precipitation and Bedrock Endmembers (Isotope Composition) 204
Stream Water Sulfate (Isotope Composition) 206
Soil Sulfur Types (Isotope Composition) 209
Discussion 210
Modern Atmospheric Sulfur Deposition 211
Conditional Influence of Sulfidic Bedrock 214
Conclusions 219
References 221
Chapter 6 Appendix 240
Chapter 7: Summary and Conclusions 257
Revised Conceptual Model 257
Future Studies 258
Appendices 261
Appendix A Detailed Protocols and Analytical Methods 262
Field Work Preparations 263
Sampling Procedures 263
Soil Samples 263
Bedrock Samples 264
Water Samples 264
Laboratory Activities 265
Soil Samples – Analysis and Characterization 266
Bedrock Samples – Analysis and Characterization 270
Water Samples – Analysis and Characterization 271
Stable Isotope Composition Analysis 272
References 274

Appendix B Raw Data – Chapter 4..... 285
Appendix C Raw Data – Chapter 5..... 296
Appendix D Raw Data – Chapter 6 301
Vita..... 307

LIST OF TABLES

Table 1. Summary of stream water chemistry (mean values) for 82 sites sampled between February 2015 and November 2016. 128

Table 2. Statistical analysis of stream water chemistry comparing (a) stream water drainaing catchments overlying sandstone bedrock versus sulfidic bedrock, and (b) stream water draining catchments with versus without natural landslide disturbance areas. Different letters indicate statistically significant differences ($\alpha = 0.05$; Wilcoxon/Kruskal-Wallis rank sums test) 133

Table 3. Description of seven study sites and the characteristics of their associated catchments. 181

Table 4. Soil sample information (numbers, soil classifications, underlying bedrock type). 183

Table 5. Summary of soil chemistry at study sites. Values shown are ranges, in indicated units. 184

Table 6. Soil sulfur concentrations at study sites, by soil profile horizon. Values shown are ranges, as mg sulfur per kg dry soil, or percent where indicated. 185

Table 7. Surface soil chemistry by bedrock type, and statistical comparisons results. 186

Table 8. Subsurface soil chemistry by bedrock type, and statistical comparisons results. 187

Table 9. Surface water chemistry at study sites, and statistical comparisons results. 188

Table 10. Main characteristics of high-elevation forested catchments used in this study. 250

Table 11. Bedrock samples collected throughout the study areas. 252

Table 12. Soil samples collected from the studied catchment sites. Geographic coordinates for each site are the median latitude and longitude of all collected soil cores (World Geodetic System 1984). 253

Table 13. Stream water and bedrock runoff chemistry. 254

Table 14. Sulfur and oxygen isotope composition of bedrock samples. 255

Table 15. Sulfur and oxygen isotope composition of stream water sulfate, soil, rain, throughfall and bedrock runoff. 256

Table 16. Procedures for soil analysis 280

Table 17. Procedures for characterizing the sulfur composition (total, inorganic, and organic) in soil samples 281

Table 18. Procedures for sequential extraction of sulfur-fractions from soil and bedrock samples, and for preparing samples for stable isotope analysis 282

Table 19. Procedures for characterizing the chemical and isotopic composition of water samples 283

Table 20. Sample preparation details for sulfur and sulfate-oxygen isotope composition analysis 284

LIST OF FIGURES

Figure 1. Annual mean throughfall (TF) pH and sulfate concentrations (equivalents per hectare per year) throughout monitoring period 1991 – 2016. Error bars represent one standard error from the mean. Power plant operational changes emplaced in the 2007-2008 time-frame. 19

Figure 2. Conceptual diagram of ecosystem components (phases) that sulfur compounds can enter, occupy or traverse, and pertinent transformation or migration pathways between phases. 41

Figure 3. Conceptual diagram of ecosystem components (phases) and prominent sulfur species in each. 42

Figure 4. Conceptual diagram of the sulfur and oxygen isotope composition of ecosystem components in forested catchments. 43

Figure 5. Location of the Great Smoky Mountains National Park (GRSM), and detailed map of stream sampling sites. Major GRSM watersheds are outlined in black, including the West Prong Little Pigeon River watershed containing the majority of stream sampling sites..... 121

Figure 6. Locations of 82 stream water sites in the central quadrant of the Great Smoky Mountains National Park. The West Prong Little Pigeon River watershed is outlined in black. Five bedrock formations are identified (four predominently sandstone and one sulfidic phyllite)..... 122

Figure 7. Dissolved sodium, calcium, potassium and magnesium versus dissolved silica concentrations (micromoles per liter) in stream water samples. Letters represent the subwatersheds associated with the stream water sites (see text for definitions). Lower case letters represent stream water sites in catchments containing known areas of natural land disturbance. Linear correlation analysis results shown in each panel..... 123

Figure 8. Total dissolved aluminum concentration (micromoles per liter) versus stream water pH. Letters represent the subwatersheds associated with the stream water sites (see text for definitions). Lower case letters represent stream water sites in catchments containing known areas of natural land disturbance. 124

Figure 9. Total stream water acidity (aluminum plus proton equivalents) versus the ratio of anion equivalents to base cation equivalents. Ratios greater than one reflect base cation deficiency which is mitigated by charge-balance from aluminum and protons. Letters represent the subwatersheds associated with the stream water sites (see text for definitions). Lower case letters represent stream water sites in catchments containing known areas of natural land disturbance..... 125

Figure 10. Total dissolved aluminum versus dissolved silica concentrations (micromoles per liter) in stream water. Letters represent the subwatersheds associated with the stream water sites (see text for definitions). Lower case letters represent stream water sites in catchments containing known areas of natural land disturbance..... 126

Figure 11. Sulfate concentrations (micromoles per liter) versus pH (lab-measured) in stream water. Letters represent the subwatersheds associated with the stream water sites (see text for definitions). Lower case letters represent stream water sites in catchments containing known areas of natural land disturbance. 127

Figure 12. Location of the Great Smoky Mountains National Park (GRSM) and detailed map of study locations and major bedrock formations associated with the study areas. Catchments 1, 2 and 3 = sulfidic bedrock; Catchments 4 and 5 = transition zone bedrock; Catchments 6 and 7 = sandstone bedrock (reference sites). 178

Figure 13. Correlation between soil sulfur and soil carbon (molar concentrations), as (A) total and (B) organic forms. Average C:S ratios and regression data are shown for each. 179

Figure 14. Correlations between soil pH and soil organic carbon at Sites 2 and 3 (overlying sulfidic bedrock; top row) and at Sites 6 and 7 (overlying sandstone bedrock; bottom row). Open symbols represent surface soil; filled symbols represent subsurface soil. Coefficients of determination and analysis of variance p-values shown in each panel. Shading represents the 95% confidence interval of the best fit line. 180

Figure 15. Location of the Great Smoky Mountains National Park (GRSM) and detailed map of sampling locations and major bedrock formations associated with the study areas. Sites 1, 2 and 3 = sulfidic bedrock catchments; Sites 4 and 5 = transition zone bedrock catchments; Sites 6 and 7 = sandstone bedrock catchments (reference sites). 240

Figure 16. Concentrations of stream water sulfate relative to the approximate distance from Anakeesta Ridge (Fig. 1). Bedrock runoff data were assigned a distance of 0.05 km to reflect direct contact between water and bedrock. Data were fitted to a three-parameter exponential function [R^2 = 0.92]: sulfate (mg L^{-1}) = 2.0 + 17.3(exp(–1.17*kilometers)) 241

Figure 17. Variations of $\delta^{34}S$ in the samples analyzed for this study. Data are arranged in spatial order: atmospheric samples, surface samples (soil, stream water), bedrock runoff, and bedrock. 242

Figure 18. Variation of $\delta^{34}S$ in stream water sulfate relative to the approximate distance from Anakeesta Ridge. Bedrock runoff data were assigned a distance of 0.05 km to reflect direct contact between water and bedrock. 243

Figure 19. Variation of $\delta^{18}O$ in stream water sulfate relative to the distance from Anakeesta Ridge. Bedrock runoff data were assigned a distance of 0.05 km to reflect direct contact between water and bedrock. 244

Figure 20. Variations of stream water pH and acid neutralizing capacity (ANC) versus $\delta^{34}S$ of stream water sulfate. For comparison, the data for two sulfidic bedrock runoff samples are included. The error bars represent one standard deviation from the mean value. The dashed trend line was added for visual reference. 245

Figure 21. Variations of sulfate concentration versus $\delta^{34}S$ of sulfate in stream water. For comparison, the data for two sulfidic bedrock runoff samples are included. The error bars represent one standard deviation from the mean value. The dashed trend line was added for visual reference. 246

Figure 22. Variations of stream water pH and acid neutralizing capacity (ANC) versus $\delta^{18}O$ of stream water sulfate. For comparison, the data for two sulfidic bedrock runoff samples are included. The error bars represent one standard deviation from the mean value. 247

Figure 23. Variations of sulfate concentration versus $\delta^{18}O$ of stream water sulfate. For comparison, the data for two sulfidic bedrock runoff samples are included. The error bars represent one standard deviation from the mean value. 248

Figure 24. Comparison of $\delta^{34}S$ and $\delta^{18}O$ (‰) of sulfate in precipitation (rain and throughfall) and stream water in the studied sites. Water in direct contact with exposed bedrock (indicated as “R”) represents the sulfidic bedrock endmember for stream water. 249

CHAPTER 1: INTRODUCTION

This dissertation is an extension of a large body of work investigating the environmental issue of acidic air pollutant deposition (AAPD), also known in the vernacular as "acid rain." Mechanistically, it is the continual settling of air-borne gasses and aerosols composed of sulfur and nitrogen species from the atmosphere to ground. The concern with AAPD is the chemical hydrolysis of these sulfur and nitrogen species into acidic compounds (e.g., sulfuric and nitric acids), and the suite of adverse effects which these acidic compounds can induce. This environmental issue is a direct consequence of societal industrialization; the need for massive amounts of energy to power the mechanization of society. Industrial facilities such as coal-fired power plants historically have been efficient point-sources of sulfur-compounds to the atmosphere since the mid- to late-1800s (Schurr and Netschert 1960), As is common with human societal evolution, the invention and development of practical and useful ideas have advanced more quickly than the understanding of their ripple-effects and consequences (adverse or otherwise). Problems with air pollution in general have been written about since the times of ancient Greece (Mosley 2014). Attention to adverse consequences from the burning of carbon-based fuel stocks rose dramatically in the mid-19th century into the early 20th century with incidents like the 1952 Great Smog of London. In the specific case of AAPD, focus on understanding the chemistry involved with acid-forming air pollutants generated by coal-burning began in earnest post-World War II (Mosley 2014).

Understanding the origins, behavior and fate of AAPD is an ongoing goal of environmental agencies, natural resource managers, and academic institutions (Porter et al. 2005; Burns et al. 2011; Fancy and Bennetts 2012; NADP 2013). Attaining a comprehensive understanding of the AAPD problem is challenging because of its scope, both spatial and temporal, and the associated

interdependent and confounding factors (Lischeid et al. 2010). These include multiple chemical pollutants or mixture interference effects, different types of ecosystems affected, disparate sources and formation processes, time-lag between origin and effects, and changes in sources or emission levels over time (Johnson et al. 1979; Brimblecombe et al. 2007). Numerous air pollution and AAPD studies have been conducted, all aimed at learning the relative importance of these factors and at understanding causes, effects and possible mitigation methods.

Chemical species of sulfur (SO_2, sulfate aerosols, volatile organic sulfur compounds) and nitrogen (nitrogen oxides [NO_x], ammonia, volatile organic nitrogen compounds) have both natural (Bates and Lamb 1992; Bates et al. 1992) and anthropogenic sources (Krouse et al. 1991), including electrical discharges in the atmosphere (lightning), volcanic activity, and combustion processes (coal-fired power generation; internal combustion engines). Airborne pollutants are highly mobile, traveling long distances from their point of origin before deposition, making atmospheric pollution a regional issue (Shaw 1982; Driscoll et al., 2001). They can undergo further chemical transformation in the atmosphere (direct photolysis, ozone, hydroxyl radical [OH*], hydrogen peroxide and others) through gas-phase chemical reactions, aqueous phase reactions, or particle-surface catalyzed reactions (Finlayson-Pitts and Pitts, 1986; Chin et al., 1996). These result in sulfuric acid and nitric acid dissolved in meteoric water (clouds, fogs, mists, wetted aerosols, snow and rain; Möller, 2008). Dissociated sulfate and nitrate anions can react with cations present in the same atmospheric aqueous phase. Ammonium, a common counter-ion present in atmospheric water, creates dilute solutions of ammonium sulfate and ammonium nitrate, in addition to the free acids. When the droplets evaporate, aerosols and particles of ammonium sulfate and ammonium nitrate form which are the primary components of dry deposition (Saltzman et al. 1983; Scot et al.,

2012). Chemical reaction pathways and kinetics involved are complex and continue to be studied; however, the end-products of those chemical processes are relevant to acidification in the GRSM.

Once deposited to land surface, atmospheric pollutants interact with biological (bacteria; vegetation) and mineral (soil; rock; surface water) features of the ecosystem. In soil, the effect is to accelerate natural weathering reactions and the consumption of soil buffering capacity, releasing cations, aluminum and iron species, or organic molecules into the soil solution phase (Essington 2015). The reaction products are available to be flushed into drainage water during storm events or as baseflow, thereby influencing the acidity and chemistry of surface water (Cai et al. 2010; Cai et al. 2012; Neff et al. 2009; Deyton et al. 2009). Pertinent geochemical processes between atmospheric pollutants and catchment soil and water are listed below.

- Soil mineral weathering can release aluminum from the mineral crystal structure into soil solution. It can react and re-precipitate as secondary minerals (e.g., alunite, basaluminite, jurbanite, gibbsite) (Adams and Rawajfih, 1977; Courchesne and Hendershot 1990; Flohr et al. 1995; Lauf 1997), or remain in solution as various pH-dependent ion complexes (Cronan and Schofield 1990). Soluble hydrolyzed Al, such as Al^{3+} and $Al(OH)^{2+}$, has been shown to be toxic to aquatic biota at sufficient concentrations (Bacon and Mass 1979; Driscoll et al. 1980).

- Base cations within the interlayer structure of phyllosilicates (clays), or adsorbed on exchange complex sites of soil minerals in general (Essington 2015), can be replaced by Al^{3+} and subsequently released into soil solution (Tomlinson 2003).

- Low-level loss of base cations from soil is a natural phenomenon (i.e., soil cation exchange capacity). The acceleration of this process caused by long-term AAPD out-paces natural

base-cation recharge processes (mineral weathering). The result is a gradual net decrease in the ratio of the exchangeable base cation content to the effective cation exchange capacity (ECEC), also known as the percent base saturation (BS) (Matschonat and Vogt, 1998). As an example, forest soils with a BS of less than 15% have been shown to have insufficient SBC to prevent stream acidification (Reuss 1983; Cronan and Shofield 1990; Sullivan et al. 2008).

- Soil acidity increases the potential for SO_4^{2-} adsorption (Nodvin et al. 1986; Ryan et al. 1989) by electrostatic adsorption to the amphoteric exchange complexes.

- The salting-in effect. Increased anion concentrations (e.g., sulfate) induces the dissolution of cations from the soil matrix for charge-neutrality (Reuss 1980; Reuss 1983; Reuss and Johnson 1985). Soils with sufficient base cation saturation (high acid neutralization capacity [ANC]), the common non-acid cations sodium, potassium, magnesium and/or calcium are released. Soils with low base cation saturation supplement the depleted supply of non-acid cations with potentially toxic aluminum (Bacon and Mass 1979; Driscoll et al. 1980).

- Sulfate can form ion-pairs with dissolved cations such as calcium and aluminum, and at sufficiently high concentrations can be lost from solution as insoluble secondary sulfate minerals (Essington 2015; Appelo and Postma 2005).

Sources of acidity other than atmospheric pollutants have a role in stream chemistry in GRSM. These include:

- Natural soil weathering and loss of base cations from mineral structures (Sverdrup and Warfvinge 1993; Starr et al 2014).

- Biological transformation of nitrogen (Koopmans et al. 1995). Microbial degradation (i.e., mineralization) of nitrogenous organic matter ultimately forms ammonium ions plus protons. Nitrification transforms ammonium into NO_3^- plus protons.

- Oxidation of mineral pyrite (FeS_2) produces SO_4^{2-}, ferrous ions and protons (Flohr et al. 1995).

- Uptake of nutrients through plants root systems releases H^+ ions back into interstitial soil solution (Brady and Weil, 2008) to maintain charge balance.

A number of published studies exists in the literature whose objective was to determine sources and distribution of sulfur species throughout a watershed ecosystem. Rock and Mayer (2009) reported using a combination of hydrometric, chemical and stable isotope data, collected from prudently located sampling sites, to determine the relative influence of geology, land use, agriculture, and AAPD on the composite dissolved-sulfate profile along the flow path of a large watershed in Alberta, Canada. By analyzing both main-stem and tributary water samples for bulk concentrations and isotopic composition of the exported sulfate, and combining those concentration data with flow profiles to estimate mass-flux distribution, the authors were able to conclude that the predominantly agricultural portion of the watershed (the lower half of the watershed) was contributing a sizable flux of sulfate to the main stem river, especially during the irrigation season (mid-April to mid-October). The measured flux was significantly larger than the flux from upstream and atmospheric sources.

Cai et al. (2011) studied the distribution of sulfate in a permanent monitoring station located in a high-elevation catchment in the GRSM (Noland Divide). Their objective was to investigate interactions between anions and cations in incident precipitation and the soil layers in the sub-basin, and to determine the mass distribution of sulfate throughout the soil matrix. The influx of sulfate onto this sub-basin area (originating from regional coal-fired power plants) was thought to be contributing to acidification of the watershed ecosystem (soil and water), and it was hypothesized that the acid-neutralizing capacity (ANC) of those soils were nearly depleted and thus additional sulfate input was controlling the pH of stream water in that sub-basin. Two major conclusions from that study were that sub-basin soil had additional "capacity" for retaining sulfate (although the retention mechanism was assumed to be exclusively mineral adsorption) and that sulfate concentrations in the two streamlets draining the sub-basin varied little over time.

A third example comes from a series of studies conducted at the Hubbard Brook Experimental Forest (HBEF) in White Mountains, New Hampshire (Alewell et al. 1999; Mitchell et al. 2001; Bailey et al. 2004). In each case, a clearer understanding of the dynamics of sulfur processing in forest watersheds was sought through the application of chemical mass balance and stable isotope analytical methods. In each case, sources and sinks of sulfate and organic sulfur species were identified and quantified. A major conclusion from these and associated studies at the HBEF was the importance of the interplay among inorganic sulfur, organic sulfur, biological sulfur, abiotic mechanisms and biotic processes on the control and distribution of sulfur species in forested watersheds.

Mayer et al. (2010) investigated the cause(s) of variations in stream water sulfate concentrations in the Sleepers River watershed (Vermont, USA) during and after a particularly dry summer. The impetus for the study was the observation that sulfate concentrations roughly doubled throughout

the dry period while stream flows decreased, and that during the Fall rewetting period, instead of decreasing by dilution with increased stormflow, the sulfate concentrations continued to increase to nearly four-fold larger than the late Spring levels. A combination of hydrological, chemical and isotopic techniques was used to dissect the contributions to stream water sulfate from AAPD, bedrock weathering and soil. An abrupt shift in sulfur isotope composition coincided with the abnormal increase in sulfate concentration, leading the investigators to speculate on the existence of an unaccounted source of sulfate to the system. The study concluded that secondary sulfide minerals in deeper soil layers, formed under anoxic conditions during the wet (inundated) months, were exposed to oxidizing conditions during the drought months and began to contribute sulfate to the watershed drainage during the post-drought rewetting period. This finding was possible because of stream water sulfur isotope composition measurements.

Long-term air quality and water quality monitoring data collected in the Great Smoky Mountains National Park (GRSM) since 1993 show a strong correspondence between reductions in sulfur emissions from regional coal-fired power plants and measured sulfur deposition on GRSM (Schwartz et al. 2014a; Gonzalez et al. 2015). In the 1980s and 1990s, promulgated air quality regulations led industry to modify operations or to emplace engineering controls to reduce air pollutant emissions. Some East Tennessee power production facilities changed grades or sources of coal feedstocks, and later installed stack scrubbers to remove acid-forming aerosols and gases from air emissions. Publicly available emissions data (www.tva.gov/environment/air/) suggest that those modifications (mostly implemented sometime between 2007 and 2009) have substantially reduced the total mass of acid-forming aerosols and gases of sulfur and nitrogen oxides emanating from at least two large regional power plant facilities. Measurements of pH and sulfate content of precipitation falling onto a permanent monitoring station located in a high-

elevation GRSM catchment, before and after that implementation time-frame (Schwartz et al. 2014b), confirms a striking reduction in proton and sulfate concentrations (Figure 1).

Other studies have focused on the *effects* of acidic air pollutants on components of GRSM ecosystems (Sullivan et al. 2002; Sullivan et al. 2007; Schwartz et al. 2014b; Neff 2010; Jackson 2006). They concluded that degradation of ecosystem function (stream acidity, altered nutrient cycling, and adverse biological effects) appeared to have been the indirect result of AAPD. Requiring additional study is (1) the fate (storage, transformation, transport) of sulfur species in the GRSM over time (both atmospheric and geologic sulfur in native bedrock minerals) and (2) the affect(s) they have had on GRSM ecosystem function.

- Have they accumulated and remained in the GRSM environment?
- Have they passed through the GRSM environment unaltered, and been transported downstream and off-site?
- Have they been transformed into other chemical species and phases?
- Have those transformed forms migrated or remained?

Answers to these types of questions will contribute to a fuller understanding of sulfur's specific role in past/current GRSM stream acidification, potentially allowing prediction of future trends in stream acidification, and developing future studies or monitoring programs to improve the understanding of these processes. This information is critical for GRSM managers to effectively protect and conserve natural resources in the GRSM.

The intent of this dissertation is to apply the methods in these and similar studies to investigate the details of the sulfur cycle in the GRSM. With a combination of historical data review, prudent site selection, collection of new data, and application of stable isotope chemistry, the expected result is clearer understanding of the behavior of sulfur in the GRSM. Results from this study not only can provide information specific to the fate of meteoric sulfur, but can shed light on relative importance or contributions of individual chemical pollutants to the stream acidification problem or to delayed-stream recovery. If it can be shown that one or a few processes are relatively less important to stream acidification, natural resource managers would have an objective, scientific basis for refining the allocation criteria for resources to conserve and manage the natural resources of the GRSM.

References

Adams, F., and Z. Rawajfih (1977). Basaluminite and Alunite: A Possible Cause of Sulfate Retention by Acid Soils1. Soil Sci. Soc. Am. J. 41:686-692. GRef1005

Alewell, Christine, Myron J. Mitchell, Gene E. Likens and H. Roy Krouse (1999). Sources of stream sulfate at the Hubbard Book Experimental Forest: Long-term analyses using stable isotopes. Biogeochemistry 44(3), 281-299. GRef633

Appelo, C.A.J., and D. Postma (2005). Geochemistry, Groundwater and Pollution, 2nd Edition. A.A. Balkema Publishers (a member of Taylor & Francis Group plc); Leiden, The Netherlands.

Bacon, J.R. and Richard P. Maas (1979). Contamination of Great Smoky Mountains Trout Streams by Exposed Anakeesta Formations. Journal of Environmental Quality, 8(4):538-543. GRef553

Bailey, Scott W., Bernhard Mayer and Myron J. Mitchell (2004). Evidence for influence of mineral weathering on stream water sulphate in Vermont and New Hampshire (USA). Hydrological Processes 18(9), 1639-1653. GRef562

Bates, Timothy S. and Brian K. Lamb (1992). Natural sulfur emissions to the atmosphere of the continental United States. Global Biogeochemical Cycles 6(4), 431-435. GRef378

Bates, Timothy S., Brian K. Lamb, A. Guenther, J. Dignon, R.E. Stoiber (1992). Sulfur emissions to the atmosphere from natural sources. GRef379

Brady, N.C. and R.R. Weil (2008). Nature and Properties of Soils. MacMillian Co., New York.

Brimblecombe, P., H. Hara, D. Houle and M. Novák (2007). Acid Rain: Deposition to Recovery. Water, Air & Soil Pollution 1-3, 1-420. GRef595

Burns, D.A., J.A. Lynch, B.J. Cosby, M.E. Fenn, and J.S. Baron, (2011). US EPA Clean Air Markets Division, National Acid Precipitation Assessment Program Report to Congress 2011: An Integrated Assessment, National Science and Technology Council, Washington, DC, 114 p.

Cai, M. J.S. Schwartz, R.B. Robinson, S.E. Moore, and M.A. Kulp (2010). Long-term effects of acidic deposition on water quality in a high-elevation Great Smoky Mountains National Park watershed: Use of an ion input-output budget. Water, Air, & Soil Pollution 209: 143-156.

Cai, Meijun, John S. Schwartz, R. Bruce Robinson, Stephen E. Moore, and Matt A. Kulp (2011). Long-term annual and seasonal patterns of acidic deposition and stream water quality in a Great Smoky Mountains high-elevation watershed. Water, Air, & Soil Pollution, 219(1-4), 547-562. GRef479

Cai, M., A.M. Johnson, J.S. Schwartz, S.E. Moore, and M.A. Kulp (2012). Soil acid-base chemistry of a high-elevation forest watershed in the Great Smoky Mountains National Park watershed: Influences of acid deposition. Water, Air, & Soil Pollution 223: 289-303.

Chin, Mian, Daniel J. Jacob, Geraldine M. Gardner, Michael S. Foreman-Fowler, Peter A. Spiro and Dennis L. Savoie (1996). A global three-dimensional model of tropospheric sulfate. Journal of Geophysical Research – Atmosphere. 101, 18667-188690.

Courchesne, F. and W.H. Hendershot (1990). The role of basic aluminum sulfate minerals in controlling sulfate retention in the mineral horizons of two spodosols. Soil Science, 150(3): 571-578. GRef1004

Cronan, C.S. and C.L. Schofield (1990). Relationships between aqueous aluminum and acid deposition in forested watersheds of North America and Northern Europe. Environmental Science and Technology, 24:1100-1105. GRef654

Deyton, Edwin B., John S. Schwartz, R. Bruce Robinson, Keil J. Neff, Stephen E. Moore and Matt A. Kulp (2009). Characterizing episodic stream acidity during stormflows in the Great Smoky Mountains National Park. Water, Air, and Soil Pollution 196(1-4), 3-18. GRef482

Driscoll, C.T., Baker, J.P., Bisogni, J.J., Schofield, C.L. (1980). Effect of aluminum speciation on fish and dilute acidified waters. Nature 284, 161-164.

Driscoll, Charles T., G.B. Lawrence, A.J. Bulger, T.J. Butler, C.S. Cronan, C. Eagar, K.F. Lambert, Gene E. Likens, J.L. Stoddard, and Kathleen C. Weathers (2001). Acidic deposition in the northeastern United States: Sources and inputs, ecosystem effects, and management strategies. BioScience, 51(3):180-198. GRef1036

Essington, Michael E. (2015). Soil and Water Chemistry: An Integrative Approach (2nd Edition). CRC Press, Boca Raton, Florida.

Fancy, S. G. and R. E. Bennetts (2012). Institutionalizing an effective long-term monitoring program in the US National Park Service. Pages 481-497 in Gitzen et al. (editors). Design and Analysis of Long-term Ecological Monitoring Studies; Cambridge University Press.

Finlayson-Pitts, Barbara J. and James N. Pitts (1986). Atmospheric Chemistry: Fundamentals and Experimental Techniques. John Wiley & Sons, Inc.; New York.

Flohr, Marta J.K., Roberta G. Dillenburg and Geoffrey S. Plumlee (1995). Characterization of secondary mineral formed as the result of weathering of the Anakeesta Formation, Alum Cave, Great Smoky Mountains National Park, Tennessee. U.S. Geological Survey Open-file Report No. 95-477. U.S. Department of the Interior; Reston, Virginia.

Gonzalez, Adrian M., Dr. John S. Schwartz, and Matt Kulp (2015). Geochemistry in a high-elevation watershed responds to reductions in acid-pollutant emissions? 2015 World Environmental & Water Resources Congress (EWRI), Austin, Texas, 17-21 May 2015. Platform presentation 19 May 2015.

Jackson, Karen A. (2006). Effects of water chemistry and watershed characteristics on populations of trout in the Great Smoky Mountains National Park. M.S. Thesis; University of Tennessee, Knoxville.

Johnson, Dale W., J.W. Hornbeck, J.M. Kelly, W.T. Swank and Don E. Todd (1979). Regional patterns of soil sulfate accumulation: relevance to ecosystem sulfur budgets. Conference proceedings of the Second Life Sciences Symposium (Gatlinburg, TN), Potential environmental and health consequences of atmospheric deposition. David S. Shriner, Chester R. Richmond, and Steven E. Lindberg (eds.). Ann Arbor Sciences Publishers, Inc. GRef178

Koopmans, C.J., Lubrecht, W.C. Tietema, A. (1995). Nitrogen transformations in two nitrogen saturated forest ecosystems subjected to an experimental decrease in nitrogen deposition. Plant Soil 175, 205-218.

Krouse, H.R., J.W.B. Stewart, and V.A. Grinenko (1991). Ch. 7 in: Krouse, H.R. and V.A. Grinenko. Stable isotopes: Natural and anthropogenic Sulphur in the environment. SCOPE 43. John Wiley & Sons; New York.

Lischeid, Gunnar, Pavel Kram, and Christina Weyer (2010). Tracing biogeochemical processes in small catchments using non-linear methods. In: Moller, Felix, Cornelia Baessler, Hendrik Schubert, and Stefan Klotz (Eds.). Long-term ecological research. Springer; Netherlands. GRef383

Lauf, Robert J. (1997). Secondary sulfate minerals from Alum Cave Bluff: Microscopy and microanalysis. Report No. ORNL/TM-13471. Metals and Ceramics Division, Oak Ridge National Laboratory, Oak Ridge, TN; July 1997. GRef492

Matschonat, G., Vogt, R. (1998). Significance of the total cation concentration in acid forest soils for the solution composition and the saturation of exchange sites. Geoderma 84, 289-307.

Mayer, Bernhard, James B. Shanley, Scott W. Bailey and Myron J. Mitchell (2010). Identifying sources of stream water sulfate after a summer drought in the Sleepers River watershed (Vermont, USA) using hydrological, chemical, and isotopic techniques. Applied Geochemistry, 25(5), 747-754. GRef289

Mitchell, Myron J., Bernhard Mayer, Scott W. Bailey, J.W. Hornbeck, Christine Alewell, Charles T. Driscoll, and Gene E. Likens (2001). Use of stable isotope ratios for evaluating sulfur sources and losses at the Hubbard Brook Experimental Forest. Water, Air, and Soil Pollution, 130(1-4), 75-86. GRef437

Möller, Detlev (2008). On the History of the Scientific Exploration of Fog, Dew, Rain and Other Atmospheric Water. Die Erde Volume 139 (issue 1-2), 11-44.

Mosley, Stephen (2014). Environmental History of Air Pollution and Protection. In: Agnoletti, Mauro and Simone Neri Serneri (Editors), 2014. The Basic Environmental History. Springer International Publishing, Switzerland. Chapter 5; pp. 143-169.

National Atmospheric Deposition Program (NADP) (2013). National Atmospheric Deposition Program 2012 Annual Summary. NADP Data Report 2013-01. Illinois State Water Survey, University of Illinois at Urbana-Champaign, IL.

Neff, K.J., J.S. Schwartz, T.B. Henry, R.B. Robinson, S.E. Moore, and M.A. Kulp (2009). Physiological stress in native brook trout during episodic stream acidification in the Great Smoky Mountains National Park. Archives of Environmental Contamination and Toxicology 57: 366-376.

Nodvin, S.C., Driscoll, C.T., Likens, G. E. (1986). The effect of pH on sulfate adsorption by a forest soil. Soil Science 142(2), 69-75. GRef152

Porter, Ellen, Tamera Blett, Deborah U. Potter, and Cindy Huber (2005). Protecting resources on Federal lands: Implications of critical loads for atmospheric deposition of nitrogen and sulfur. BioScience 55(7):603-612. GRef451

Reuss, John O. (1980). Simulation of soil nutrient losses resulting from rainfall acidity. Ecological Modeling, 11(1):15-38. GRef822

Reuss, John O. (1983). Implications of the Calcium-Aluminum Exchange System for the Effect of Acid Precipitation on Soils. Journal of Environmental Quality 12(4):591-595. GRef827

Reuss, John O. and D.W. Johnson (1985). Effect of soil processes on the acidification of water by acid deposition. Journal of Environmental Quality, 14(1):26-31. GRef828

Robinson, R. Bruce, Thomas W. Barnett, Glenn R. Harwell, Stephen E. Moore, Matt A. Kulp, and John S. Schwartz (2008). pH and acid anion time trends in different elevation ranges in the Great Smoky Mountains National Park. Journal of Environmental Engineering, 134(9):800-808. GRef1014

Rock, Luc and Bernhard Mayer (2009). Identifying the influence of geology, land use, and anthropogenic activities on riverine sulfate on a watershed scale by combining hydrometric, chemical and isotopic approaches. Chemical Geology, 262(3-4), 121-130. GRef300

Ryan, P. F., G. M. Hornberger, B. J. Cosby, J. N. Galloway, J. R. Webb, and E. B. Rastetter (1989), Changes in the chemical chemistry of stream water in two catchments in the Shenandoah National Park, Virginia, in response to atmospheric deposition of sulfur, Water Resources Research, 25(10), 2091–2099. GRef1006

Saltzman, E.S., G.W. Brass and D.A. Price (1983). The mechanism of sulfate aerosol formation: Chemical and sulfur isotopic evidence. Geophysical Research Letters, 10(7), 513-516. GRef599

Schurr, Sam H. and Bruce C. Netschert (1960). Energy in the American economy, 1850-1975: an economic study of its history and prospects. Resources for the Future. Johns Hopkins Press; Baltimore, Maryland. GRef611

Schwartz, John S., Adrian M. Gonzalez, Matt Aplin, Stephen E. Moore, and Matt A. Kulp (2014a). Great Smoky Mountains National Park 2013 Water Quality Annual Report. Natural Resources Data Series NPS/GRSM/NRDS-2014/XXX.

Schwartz, John S., Meijun Cai, Matt A. Kulp, Stephen E. Moore, Becky Nichols and Charles Parker (2014b). Biological effects of stream water quality on aquatic macroinvertebrates and fish communities within the Great Smoky Mountains National Park. U.S. Department of the Interior, National Park Service (NPS) Natural Resources Report (NRR) No. 778; August 2013. GRef584

Scot, T. Martin, Julie C. Schlenker, Adam Malinowski and Hui-Ming Hung (2012). Crystallization of atmospheric sulfate-nitrate-ammonium particles. Geophysical Research Letters, 30 (issue 21), pp. 6-1 to 6-4.

Shaw, R.W. (1982). Deposition of atmospheric acid from local and distant sources at a rural site in Nova Scotia. Atmospheric Environment (1967), 16(2), 337-348. GRef609

Starr, Mike, Antti Jussi Lindroos and Liisa Ukonmaanaho (2014). Weathering release rates of base cations from soils within a boreal forested catchment: variation and comparison to deposition, litterfall and leaching fluxes. Environmental Earth Sciences 72(12):5101-5111. GRef741

Sullivan, Timothy J., Bernard J. Cosby, J.R. Webb, R.L. Dennis, A.J. Bulger, F.A. Deviney, Jr. (2008). Stream water acid-base chemistry and critical loads of atmospheric sulfur deposition in Shenandoah National Park, Virginia. Environmental Monitoring and Assessment 137, 85-99.

Sullivan, Timothy J., Bernard J. Cosby, Kai U. Snyder, Alan T. Herlihy and B. Jackson (2007). Model-based assessment of the effects of acidic deposition on sensitive watershed resources in the National Forests of North Carolina, Tennessee and South Carolina. Final Report prepared for U.S. Department of Agriculture (USDA) Forest Service, Asheville, North Carolina; October 2007. GRef017

Sullivan, Timothy J., Bernard J. Cosby, James R. Webb, Kai U. Snyder, Alan T. Herlihy, Arthur J. Bulger, Erin H. Gilbert and Deian Moore (2002). Assessment of the effects of acidic deposition on aquatic resources in the Southern Appalachian Mountains. Report prepared for Southern Appalachian Mountains Initiative (SAMI); prepared by E&S Environmental Chemistry, Inc. (Corvallis, Oregon); July 2002. GRef694

Sverdrup, H. and P. Warfvinge (1993). Calculating field weathering rates using a mechanistic geochemical model PROFILE. Applied Geochemistry 8(3):273-283. GRef530

Tomlinson, G.H. (2003). Acidic deposition, nutrient leaching and forest growth. Biogeochemistry 65, 51-81.

Chapter 1 Appendix

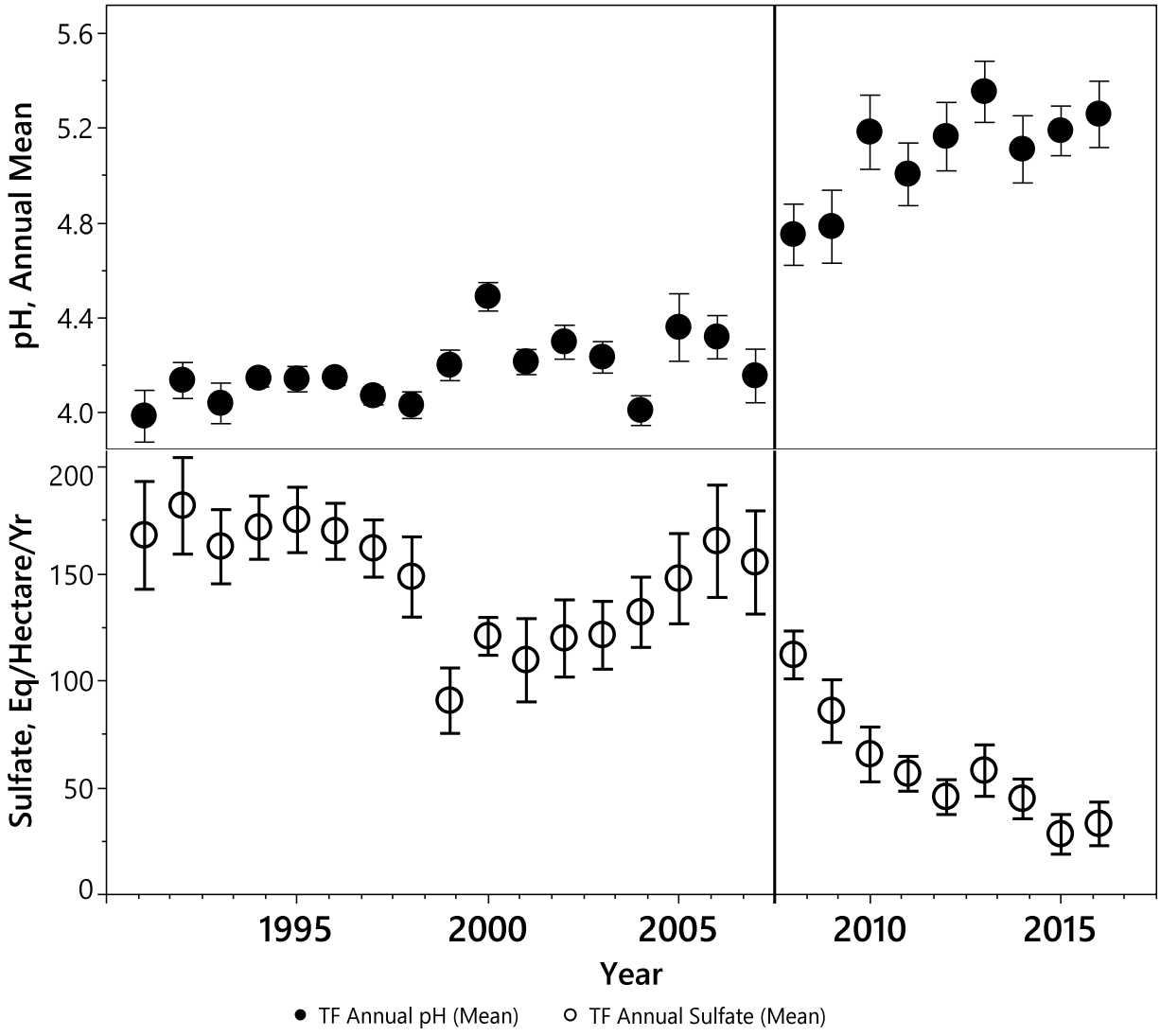

Figure 1. Annual mean throughfall (TF) pH and sulfate concentrations (equivalents per hectare per year) throughout monitoring period 1991 – 2016. Error bars represent one standard error from the mean. Power plant operational changes emplaced in the 2007-2008 time-frame.

CHAPTER 2: RESEARCH QUESTIONS AND FRAMEWORK

The overall objective of this dissertation was to examine the possibility that some ecosystems experience levels of acidification greater than are attributable solely to acidic air pollutant deposition (AAPD). Two observations led to this objective. First was the existence of pockets of extreme stream water and/or soil acidification surrounded by stream water and soil with relatively homogenous and moderate geochemistry. Second was the relative insensitivity of acidified stream water and soil to reductions in known inputs of acidic pollutants (e.g., atmospheric sulfur). The question is what is the cause for these environmental conditions? Specifically, what source(s) add to the acidity and stream water sulfate originating from AAPD, and what source(s) supplement stream water sulfate under conditions of reduced AAPD? The most likely cause was thought to be weathering of bedrock containing reduced-valence sulfur (sulfidic) minerals.

Conceptual Model: High-Elevation Forest Catchment

The assumption underlying this dissertation is that there are two sources of sulfur in GRSM catchments: atmospheric sulfur and geologic sulfur. The dominant form of geologic sulfur in the GRSM is sulfide-rich slate/shale/phyllite bedrock [Hadley and Goldsmith 1963; King 1964]; termed “sulfidic-shale” in this document). A prominent example of this type of bedrock is the Anakeesta Formation, occurring prominently throughout the central ridgeline region of the GRSM. Other formations in the GRSM are described as having minor proportions of sulfidic mineral components, and some formations contain geologic sulfate mineral components (King et al. 1958; King 1964). All can contribute sulfur compounds to catchment soil and water, under appropriate conditions. Sulfur in catchments with negligible sulfidic-shale is presumed to have originated entirely from atmospheric deposition, whereas in catchments underlain by some amount of

sulfidic-shale, sulfur originates from both sources. The mass of sulfur (in all its forms) at any given catchment location is presumed to have originated from various proportions of these two sources.

Figure 2 depicts an idealized high-elevation forest catchment consisting of six major ecosystem phases (that sulfur can enter, occupy or traverse) and relevant pathways by which sulfur compounds can migrate between phases. Ovals represent primary sulfur sources; rectangles represent primary sinks (and secondary sources to other phases). Style and thickness of arrows represents the relative importance of the pathway between phases: dashed lines represent pathways of minor importance or low mass flux; thin solid lines represent pathways of moderate or typical importance; and thick solid lines represent dominant pathways for sulfur species.

At the top of the diagram is the atmosphere, from which atmospheric sulfur pollutants are introduced. Three deposition pathways are depicted between the atmosphere and stream water, soil, and biota (terrestrial vegetation, soil microbes), respectively. Deposition onto stream water (dashed line, left of center) is depicted as a minor pathway because of the relatively small surface area of catchment drainage channels relative to total catchment surface area. Thus, direct interaction between atmospheric deposition and aquatic biota was ignored. Deposition onto soil and terrestrial biota are considered equally important pathways; relative dominance of one or the other locally is a function of proportion land-cover.

Biota is a significant factor in the fate of atmospheric sulfur. The majority of atmospheric sulfur is deposited onto the forest canopy. There, it can undergo chemical transformations, or more commonly, can be transported to the forest floor as throughfall (Figure 2). This pathway has a cyclical component in that a portion of soil sulfur from throughfall can be taken up again by the foliar canopy and recycled. Activity of sulfur transformation and transport in soil is regulated by

soil moisture levels and soil sulfur concentrations (Mitchell and Likens 2011; Edwards 1998), which can vary by season and location in a forest ecosystem (Dail and Fitzgerald 1999). A less-familiar migration pathway for sulfur compounds is as volatile sulfur-compounds (inorganic and organic) from soil back to the atmosphere (Bates and Lamb 1992; Kinsela 2007; Kinsela 2011). Volatilization is a significant source of sulfur-compounds and greenhouse gas to the atmosphere globally (Bates et al. 1992), but for this work, it is considered a minor pathway.

The second prominent source of sulfur to forest catchments, bedrock/regolith, is depicted at the bottom of Figure 2. The most common lithologies responsible for sulfur inputs to catchments are those containing reduced-sulfur minerals (e.g., elemental sulfur, monosulfides (pyrrhotite), disulfides (pyrite), and its analogs; USDA-NRCS 2009). Many are thermodynamically unstable at terrestrial conditions (temperature, moisture, oxidation-reduction state) and prone to chemical weathering. Oxidation is a specific category of weathering (e.g., oxidation via oxygen or ferric iron; Fe^{3+}) for sulfidic minerals, involving complex combinations of abiotic and biologically mediated reactions. For example, oxidation pathways involving ferric-iron are microbiologically catalyzed by sulfur oxidizing bacteria (SOB) (Evangelou and Zhang 1995). Diagram arrows reflect three bedrock weathering scenarios: under the soil mantle, as exposed terrestrial outcrops, or as streambed substrate (boulder, cobble and gravel). Reaction products (e.g. common cations [sodium, potassium, magnesium, calcium; “base cations”], sulfate, dissolved metals [aluminum, iron, manganese], and protons [acidity]) either remain in solution and migrate into the soil solution and ultimately into the drainage channel to be exported from the catchment with stream water, or less commonly recrystallize/precipitate as secondary minerals in the soil matrix. Reaction products in the soil pore water phase are available for additional chemical reaction (weathering of alumino-silicate minerals and release of aluminum and silica), for interaction with solid soil components,

or for transport via subsurface advection (interflow). The transfer of oxidation products from soil water to surface water (or directly to surface water in the streambed substrate scenario) and subsequent discharge out of the catchment completes the sulfur lifecycle in forest catchments. Since GRSM catchments overly some form of bedrock (sulfidic or not) at some depth, the weathering/leaching pathway from bedrock to soil water and stream water was considered important to this work.

The remaining phases depicted in Figure 2 are considered both sink and source phases with respect to sulfur compounds. Stream water and soil water interact through interflow drainage (shallow ground water in hydraulic communication with adjacent streams). Sulfur compounds (inorganic, organic, dissolved and particle-bound) that are introduced into surface soil are either retained in the recalcitrant organic-sulfur matrix, or exported to streams and rivers. Dissolved sulfur compounds in catchment stream water likely have no influence on streambed substrate, or on soil in the riparian corridor since the hydraulic gradient is strongly uni-directional in these steep, forested catchments.

Soil interacts directly and intimately with many species of terrestrial biota, from which they extract sulfate as a necessary nutrient for normal biological function (Anderson 1975). Examples of biota influenced by sulfur biogeochemistry in soil include bushes, trees and grasses (Yang et al. 1996; Wynn et al. 2014), simple terrestrial species like mosses and lichens (Xiao et al. 2010; Xiao et al. 2011; Wadleigh 2003; Batts et al. 2004), and microbial species (bacteria, algae; Denger et al. 2014). In all cases, sulfur found in biological tissues (free sulfate [Cole et al. 1985]; amino acids [Johnson 1984; Brosnan and Brosnan 2006]; and sulfolipids [Harwood and Nicholls 1979]) contributes to soil organic-sulfur through exudates from bacteria and root systems, cell lysis, and

decay of dead organisms. Humification of organic matter creates humic substances containing sulfur-functional groups in their molecular structures (Houle et al. 2014).

Conceptual Model: Sulfur Speciation and Distribution

The forest catchment model was adapted to highlight sulfur species known or expected to exist in the phases (Figure 3). As before, the diagram depicts six major phases in the hypothetical catchment. Atmospheric sulfur in aerated wet deposition (rain, snow) and occult deposition (fog, mist) exists predominantly as sulfate. In dry deposition, sulfur can exist in a number of chemical forms given the heterogeneous nature of aerosol particulates (Saltzman et al. 1983). It is possible for organic-sulfur species to form or even persist on aerosols (Eatough et al. 1986; Smet and Langenhove 1998). Photocatalytic reactions in the atmosphere are known to induce chemical transformations of sulfur species (Jensen et al. 1992), but these pathways are considered low-probability, readily reversible events, ultimately yielding aerosol sulfate or gas-phase oxides of sulfur. In this work, the dominant form of atmospheric sulfur is assumed to be sulfate.

Stream water sulfur species consist predominantly of sulfate with minor amounts of soluble organic-sulfur species (Kertesz 1999) assumed to be associated with the pool of dissolved organic matter/carbon (DOM or DOC) (e.g., soluble fulvic acids), and trace amounts of partially reduced forms such as sulfite and thiosulfate. The bisulfate ion (hydrogen sulfate; HSO_4^-) with a pK_a of 1.99 (Stumm and Morgan 1981) is a minor form of dissolved inorganic sulfur at stream pH conditions (pH > 4) encountered in high-elevation forest catchments. Heterogeneous macro-molecules of fulvic acids and low-molecular weight soluble humic acids can contain sulfur within their amorphous structures (Goh and Greg 1982; Keep et al. 1990; Eriksen et al. 1995). Suspended

solids containing structural or adsorbed sulfur are considered a minor but potentially significant pathway for surface water sulfur.

Sulfur is wide-spread throughout the earth's crust (Murphy and Strongin 2009) but is found in only a few chemical forms (Nayak 2013): reduced inorganic sulfur (as sulfide and disulfide minerals; e.g., pyrite and pyrrhotite), organic sulfur, elemental sulfur, and oxidized sulfur (as secondary sulfate minerals associated with weathered sulfidic formations, and evaporite sulfate minerals). Near-surface and exposed sulfidic-shale bedrock formations are found in many areas of the GRSM (Hadley and Goldsmith 1963; King 1964; Flohr et al. 1995; USDA-NRCS 2009). Biotic sulfur presumably exists in the GRSM in a wide variety of organisms at all trophic levels of biological organization (Yang et al. 1996; Wadleigh 2003; Yun et al. 2010; Wynn et al. 2014). It occurs in very specific chemical structures (Davidson 1980; Markuszewski et al. 1980; Mitchell and Fuller 1988): sulfur-containing amino acids methionine, cysteine, homocysteine, and taurine (Brosnan and Brosnan 2006) and as components of sulfolipids (Harwood and Nicholls 1979). Sulfate ion has very low residence time in cellular fluids because of fast biochemical transformation rates of absorbed sulfate; thus, cellular fluids typically contain very low concentrations of free sulfate (Denger et al. 2014).

Conceptual Model: Sulfur and Oxygen Isotope Composition

Because this study examines the relative importance of atmospheric sulfur and geologic sulfur in high-elevation forest catchments, distinguishing the two was crucial to this work. Analytical methods based on mass spectrometry allow resolution of differences in isotope composition of many elements, including sulfur and oxygen, in environmental media (Sharp 2007). Magnitudes of isotope composition differences can indicate specific geochemical processes that may have

acted on those media, based on equilibrium or kinetically controlled mass preference during the reactions or processes. Over time, the ratios of isotope masses of sulfur or oxygen differentiate in the by-products of the reaction(s) or process(es). If one measures isotope ratios in environmental samples (e.g., water, soil, rock), and if the possible reactions or processes that may have acted on that sample can be constrained, it is possible to infer sources, types and quantities of the original reactant material(s) that likely contributed to the observed environmental composition. This method has been used in numerous studies to identify potential sources of elements observed in environment media (Eriksen 1996; Novák et al. 2003; Novák et al. 2005; Marty et al. 2011; Szynkiewicz et al. 2012; 2011; 2008a; 2008b; Houle et al. 2014). Pertinent aspects of stable isotope geochemistry and their relevance to sulfur isotope composition are reviewed in the Literature Review chapter.

The catchment model was modified to depict the isotope composition of sulfur and oxygen expected in the catchment phases (Figure 4). By-product sulfur compounds in the middle four phases (stream water, soil water, soil and biota) was assumed to originate from either deposition of atmospheric sulfate or geochemical weathering of bedrock minerals. By defining the system with only two endmembers of sulfur, it was feasible to infer the relative contributions of atmospheric and bedrock sulfur to the observed sulfur isotope composition in the four environmental phases. One complication with this approach is the existence of secondary sulfur transformations, specifically microbial reduction of sulfate. Careful interpretation of isotope composition data was required to distinguish these various processes.

In addition, the oxidation mechanism(s) by which sulfide mineral is converted to sulfate can be inferred by evaluating oxygen isotope composition of observed sulfate in the middle four phases (Figure 4). Oxidation mechanisms by which sulfidic bedrock or soil minerals weather incorporate

either atmospheric molecular oxygen or water molecule oxygen (Taylor and Wheeler 1994; Balci et al. 2007; Tichomirowa and Junghans 2009). Each oxygen source has distinct $\delta^{18}O$; atmospheric molecular oxygen has an average $\delta^{18}O$ value of +23.5‰ (Kroopnick and Craig 1972) and water-oxygen has $\delta^{18}O$ values ranging between –25‰ and –5‰ (Dansgaard 1964; Sharp 2007). Sulfide oxidation occurs by a complex set of condition-dependent mechanisms, an example of which is the prevalence of water-oxygen based oxidation under anoxic (dissolved oxygen deficient) conditions, and the prevalence of molecular oxygen based mechanisms under fully oxic (dissolved oxygen saturated) conditions. Sulfate formed from reactions that use water-oxygen will have lower $\delta^{18}O$ than sulfate formed from reactions that use molecular oxygen. Another distinction between these two oxygen sources is fractionations during sulfur-oxygen bond formation. Oxygen isotope enrichment that occurs during sulfur-oxygen bond formation is smaller when water is the source of oxygen (ε = +2.8‰) than when molecular oxygen is the source (ε = –9.8‰) (Balci et al. 2007; Tichomirowa and Junghans 2009). Since each sulfide oxidation mechanism can operate under appropriate environmental conditions, the $\delta^{18}O$ of sulfate in the environment typically will be comprised of mixtures of sulfate molecules formed by multiple reaction mechanisms and incorporating both sources of oxygen. Mixing of sulfate molecules from different sources does not cause isotope fractionations; therefore, the proportions of each oxygen source represented in a given sulfate sample can be quantified using isotope-balance equations (Lloyd 1968; Taylor and Wheeler 1994). Sulfur and oxygen isotope composition ($\delta^{34}S$ and $\delta^{18}O$) of media samples from high-elevation GRSM forest catchments are the key parameters in this dissertation. Isotope compositions were measured in precipitation/throughfall, stream water, soil, and bedrock. Isotope composition of vegetation were not measured; however, this is highly recommended for future studies.

Dissertation Research Questions

This dissertation focuses on sulfur export via stream discharge and sulfur retention in forest catchments of the GRSM. Using a combination of existing data, prudent site selection, analyses of environmental samples at selected sites, geochemistry theory, and stable isotope chemistry, data were collected to infer details of these aspects of the sulfur cycle in the GRSM. In each study, a research question and hypothesis are stated, an experimental study design (including data types to be generated) is outlined, statistical method(s) for data analysis are proposed, experimental outcomes and their corresponding interpretations are described, and the significant contribution(s) to scientific knowledge are explained.

Study 1 – Influence of Land-Surface Disturbances on the Chemistry of Stream Water in Small Catchments of the Great Smoky Mountains: A Hydrogeochemical Analysis

This study examines the extent to which land-surface disturbances in otherwise similar forested catchments lead to significant spatial variability in their stream water chemistry. The objective was to sample water from first- and second-order headwater streams, before mixing of multiple catchment tributaries caused the loss of geochemical resolution and interpretive power of the water chemistry. Results from this survey-level characterization of stream water chemistry were used to select study catchments for subsequent dissertation studies. This survey-level study acknowledges that biogeochemical processes, geologic substrates and differences in precipitation volumes significantly affect the chemistry of discharge water from catchments. Each of these factors were not specifically accounted for or controlled in this study. The assumption was made that these processes occur uniformly throughout GRSM catchments, and that their effects on discharge water

are integrated over time. Differences in water chemistry should be attributable to differences in amount of atmospheric sulfur deposition or to the presence of exposed sulfidic bedrock. Specifically, surface water acid buffering capacity and pH should be lowest, and sulfur concentrations should be highest, at highest elevations or in catchments with land-disturbances that exposed sulfidic bedrock. The acidity parameters should be larger in magnitude, and sulfate concentrations should be smaller, in catchments lower in elevations or in catchments with bedrock that is completely covered/protected by soil.

Study 2 – Conditional Influence of Sulfidic Bedrock on Soil and Stream Water Chemistry in High-Elevation Forest Catchments of the Great Smoky Mountains

The second study addresses the influence of all sulfur sources on the cumulative *quantity* of sulfur species retained by, and exported from, high-elevation forested catchments in the GRSM. Samples of all abiotic ecosystem media from these catchments (soil, bedrock, stream water, precipitation) were characterized with respect to concentrations of sulfur species. To maximize the sulfur content in catchments underlain by negligible bedrock-sulfur, study sites were selected within small high-elevation catchments which are presumed to receive the highest loading of acid-forming sulfur (Weathers et al. 2006). To represent varying amounts of geologic sulfur inputs, sites were chosen to span a range of bedrock compositions (i.e., from negligible sulfur content to predominantly pyrite/pyrrhotite mineral content). Research question #2 asked:

To what extent, if any, does the total sulfur content of ecosystem phases differ between catchments with predominantly atmospheric sulfur input (and minor geologic sources) and catchments with both atmospheric and geologic sulfur inputs?

This study is complementary to Study #1 in that it characterizes a small subset of high-elevation forest catchments with respect to sulfur types and concentrations. The concentrations of various forms of sulfur (inorganic, organic, soil-associated, dissolved) in the abiotic ecosystem phases were compared across catchments and correlated to bedrock type. Given that other water chemistry parameters vary across these catchments as well, some simple geochemical modeling and graphical analysis was done with the stream water data to determine bedrock-type influences on aqueous geochemistry at these sites. These secondary data analyses supplement the primary objective of this study. The null hypothesis for this study is: Concentrations of sulfur species in soil are statistically indistinguishable across high-elevation catchments and independent of bedrock type.

Study 3 – Stable isotope composition evidence for the influence of bedrock sulfur on acidification status of high-elevation catchment stream water and soil

This study addresses the relative influence of sulfur source (atmosphere versus geology) on sulfur species retained by, and exported from, high-elevation GRSM forested catchments. The key aspect of this study was the application of stable isotope geochemistry to discriminate between atmospheric sulfur and geologic sulfur. Samples of all abiotic ecosystem media from these catchments (soil, bedrock, stream water, precipitation) were characterized with respect to stable sulfur and oxygen isotope composition. Atmospheric deposition of sulfur has been modeled as varying in intensity with elevation in the GRSM (Weathers et al. 2006), with the peak ridges receiving the highest loading of acid-forming sulfur. To control for the influence of deposition intensity, study sites were selected within small high-elevation catchments drained by 1st and 2nd order streams, at the headwaters where practicable. To vary geologic sulfur inputs, sites were

chosen to span a range of bedrock compositions, but to be similar in other pertinent factors. Research question #1 asked:

To what extent, if any, does sulfur from geologic sources dominate the sulfur content of ecosystem phases in GRSM catchments with similar inputs of atmospheric sulfur?

This study focuses on the type of sulfur in, and sulfur sources to, high-elevation catchments, thus the need to employ stable isotope geochemistry. The isotope composition of the abiotic ecosystem phases was compared to that of pure endmember phases, atmospheric sulfur (in precipitation) and geologic sulfur (in bedrock samples). Sulfur and oxygen isotope composition of soil (retained sulfur) and discharge water (exported sulfur) was interpreted in terms of proportional contributions from endmember sources. By performing this suite of characterizations in a number of catchments each underlain by different proportions of sulfidic bedrock (i.e., underlain by negligible, partial, and full sulfidic bedrock content), it was possible to determine functional relationships between isotope composition and bedrock composition.

References

Anderson, J.W. (1975). The function of sulphur in plant growth and metabolism. In: K.D. McLachlan (ed.), Sulphur in Australasian agriculture; Sydney University Press, Sydney, Australia. Pp. 87-97.

Balci, Nurgul, Wayne C. Shanks III, Bernhard Mayer and Kevin W. Mandernack (2007). Oxygen and sulfur isotope systematics of sulfate produced by bacterial and abiotic oxidation of pyrite. Geochimica et Cosmochimica Acta, 71(15), 3796-3811. GRef234

Bates, Timothy S. and Brian K. Lamb (1992). Natural sulfur emissions to the atmosphere of the continental United States. Global Biogeochemical Cycles 6(4), 431-435. GRef378

Bates, Timothy S., Brian K. Lamb, A. Guenther, J. Dignon, R.E. Stoiber (1992). Sulfur emissions to the atmosphere from natural sources. GRef379

Batts, Judith E., Lisa J. Calder and Barry D. Batts (2004). Utilizing stable isotope abundances of lichens to monitor environmental change. Chemical Geology 204(3-4), 345-368. GRef342

Brosnan, John T. and Margaret E. Brosnan (2006). The sulfur-containing amino acids: An overview. The Journal of Nutrition 136(6), 1636S-1640S. GRef360

Cole, David E.C., Lesley S. Baldwin, and Linda J. Stirk (1985). Increased renel reabsorption of inorganic sulfate in third-trimester high-risk pregnancies. Obstetrics & Gynecology, 66(4), 485-490. GRef450

Dail, D.B. and John W. Fitzgerald (1999). S cycling in soil and stream sediment: Influence of season and in situ concentrations of carbon, nitrogen and sulfur. Soil Biology and Biochemistry 31(10), 1395-1404. GRef091

Dansgaard, W. (1964). Stable isotopes in precipitation. Tellus 16:436-468.

Davidson, R.M. (1980). Molecular structure of coal. Report No. ICTIS/TR08, IEA Coal Research. London, United Kingdom. 86pp.

Denger, Karin, Michael Weiss, Ann Katrin Felux, Alexander Schneider, Christoph Mayer, Dieter Spiteller, Thomas Huhn, Alasdair M. Cook and David Schleheck (2014). Sulphoglycolysis in Escherichia coli K-12 closes a gap in the biogeochemical sulphur cycle. Nature, advance online publication: http://www.nature.com/nature/journal/v507/n7490/full/nature12947.html#access GRef659

Eatough, Delbert J., Vernon F. White, Lee D. Hansen, Norman L. Eatough, and James L. Cheney (1986). Identification of gas-phase dimethyl sulfate and monoethyl sulfate in the Los Angeles atmosphere. Environmental Science and Technology, 20(9), 867-872. GRef691

Edwards, Pamela J. (1998). Sulfur cycling, retention, and mobility in soils: A review. General technical report NE-250, U.S. Department of Agriculture, Forest Service, Northeastern Research Station. Radnor, PA.

Eriksen, Jørgen, R.D.B. Lefroy and G.J. Blair (1995). Physical protection of soil organic S studied using acetylacetone extraction at various intensities of ultrasonic dispersion. Soil Biology and Biochemistry 27(8), 1005-1010. GRef671

Eriksen Jørgen (1996). Incorporation of S into soil organic matter in the field as determined by the natural abundance of stable S isotopes. Biology and Fertility of Soils, 22(1-2), 149-155.GRef745

Evangelou, V.P. and Y.L. Zhang (1995). A review: Pyrite oxidation mechanisms and acid mine drainage prevention. Critical Reviews in Environmental Science and Technology, 25(2):141-199. GRef219

Flohr, Marta J.K., Roberta G. Dillenburg and Geoffrey S. Plumlee (1995). Characterization of secondary mineral formed as the result of weathering of the Anakeesta Formation, Alum Cave, Great Smoky Mountains National Park, Tennessee. U.S. Geological Survey Open-file Report No. 95-477. U.S. Department of the Interior; Reston, Virginia.

Goh, K.M. and P.E.H. Gregg (1982). Field studies on the fate of radioactive sulphur fertilization applied to pastures. Fertilizer Research 3(4), 337-351. GRef670

Hadley, Jarvis B. and Richard Goldsmith (1963). Geology of the Eastern Great Smoky Mountains North Carolina and Tennessee. Geological survey professional paper 349-B. U.S. Department of the Interior, U.S. Government Printing Office, Washington, D.C.

Harwood, J.L. and R.G. Nicholls (1979). The plant sulpholipid – a major component of the sulphur cycle. Biochemical Society Transactions, 7, 440-447. GRef658

Houle, Daniel, Charles Marty, Louis Duchesne and Christian Gagnon (2014). Humus layer in the main locus of secondary SO_4 production in boreal forests. Geochimica et Cosmochimica Acta 126(1), 18-29. GRef287

Jensen, N.R., J. Hjorth, C. Lohse, H. Skov and G. Restelli (1992). Products and mechanisms of the gas phase reactions of NO3 with CH3SCH3, CD3SCD3, CH3SH and CH3SSCH3. Journal of Atmospheric Chemistry 14(1-4), 95-108. GRef380

Johnson, Dale W. (1984). Sulfur cycling in forests. Biogeochemistry 1(1), 29-43. GRef597

Keep, I., R.G. Mclaren and R.S. Swift (1990). Acetylacetone extraction of soil organic sulphur and fractionation using gel chromatography. Soil Biology and Biochemistry 22(1), 97-104. GRef664

Kertesz, Michael A. (1999). Riding the sulfur cycle – metabolism of sulfonates and sulfate esters in Gram-negative bacteria. FEMS Microbiology Reviews, 24(2), 135-175. GRef717

King, Philip B. (1964). Geology of the Central Great Smoky Mountains Tennessee. Geological Survey Professional Paper No. 349-C. U.S. Department of the Interior, U.S. Government Printing Office, Washington, D.C.

King, P.B., Neuman, R.B., and Hadley, J.B. (1968), Geology of the Great Smoky Mountains National Park, Tennessee and North Carolina: U.S. Geological Survey Professional Paper 587, 23 p., and 1:125,000-scale map.

Kinsela, Andrew Stephen, Jason K. Reynolds and Michael D. Melville (2007). Agricultural acid sulfate soils: A potential source of volatile sulfur compounds? Environmental Chemistry 4(1), 18-25. GRef370

Kinsela, Andrew Stephen, O. Tom Denmead, Bennett C.T. Macdonald, Michael D. Melville, Jason K. Reynolds and Ian White (2011). Field-based measurements of sulfur gas emissions from an agricultural coastal acid sulfate soil, eastern Australia. Soil Research 49(6), 471-480.

Kroopnick, P. and H. Craig (1972). Atmospheric oxygen: Isotopic composition and solubility fractionation. Science 175:54-55. GRef525

Lloyd, R.M. (1968). Oxygen isotope behavior in the sulfate-water system. Journal of Geophysical Research, 73:6099-6209. Ref. in GRef525

Markuszewski, R., C.K. Wei, and T.D. Wheelock (1980). Oxydesulfurization of coal treated with methyl iodide: implications for removal of organic sulfur. CONF-800303-6, Ames Laboratory, Iowa State University, Ames, Iowa. 9pp.

Marty, Charles, Daniel Houle, Christian Gagnon and Louis Duchesne (2011). Isotopic compositions of S, N and C in soils and vegetation of three forest types in Québec, Canada. Applied Geochemistry 26(12), 2181-2190. GRef290

Mitchell, Myron J. and Robert D. Fuller (1988). Models of sulfur dynamics in forest and grassland ecosystems with emphasis on soil processes. Biogeochemistry, 5(1), 133-163. GRef602

Mitchell, Myron J. and Gene E. Likens (2011). Watershed sulfur biogeochemistry: Shift from atmospheric deposition dominance to climatic regulation. Environmental Science & Technology, 45(12), 5267-5271. GRef358

Murphy, Riley and Daniel R. Strongin (2009). Surface reactivity of pyrite and related studies. Surface Science Reports 64(1), 1-45. GRef361

Nayak, Bibhuranjan (2013). Mineral matter and the nature of pyrite in some high-sulfur tertiary coals of Meghalaya, northeast India. Journal of the Geological Society of India, 81(2), 203-214. (February) GRef608

Novák, Martin, James W. Kirchner, Daniela Fottova, Eva Prechova, Iva Jacková, Pavel Kram and Jakub Hruska (2005). Isotopic evidence for processes of sulfur retention/release in 13 forested catchments spanning a strong pollution gradient (Czech Republic, central Europe). Global Biogeochemical Cycles 19(4), GB4012-1 – GB4012-14. GRef183

Novák, Martin, Frantisek Buzek, Anthony F. Harrison, Eva Prechova, Iva Jacková and Daniela Fottova (2003). Similarity between C, N and S stable isotope profiles in European spruce forest soils: Implications for the use of $\delta^{34}S$ as a tracer. Applied Geochemistry 18(5), 765-779. GRef160

Saltzman, E.S., G.W. Brass and D.A. Price (1983). The mechanism of sulfate aerosol formation: Chemical and sulfur isotopic evidence. Geophysical Research Letters, 10(7), 513-516. GRef599

Sharp, Zachary (2007). Principles of Stable Isotope Geochemistry. Pearson – Prentice Hall, Upper Saddle River, New Jersey 07458.

Smet, E. and H. Van Langenhove (1998). Abatement of volatile organic sulfur compounds in odorous emissions from the bio-industry. Biodegradation 9(3-4), 273-284. GRef690

Stumm, Werner and James J. Morgan (1981). Aquatic Chemistry: An introduction emphasizing chemical equilibria in natural waters (2nd Edition). Wiley-Interscience, New York.

Szynkiewicz, Anna, B. Talon Newton, Stacy S. Timmons and David M. Borrok (2012). The sources and budget for dissolved sulfate in a fractured carbonate aquifer, southern Sacramento Mountains, New Mexico, USA. Applied Geochemistry 27(8), 1451-1462. GRef312

Szynkiewicz, Anna, James C. Witcher, Magdalena Modelska, David M. Borrok and Lisa M. Pratt (2011). Anthropogenic sulfate loads in the Rio Grande, New Mexico (USA). Chemical Geology 283(3-4), 194-209. GRef310

Szynkiewicz, Anna, Miguel Rangel Medina, Magdalena Modelska, Rogelio Monreal and Lisa M. Pratt (2008a). Sulfur isotopic study of sulfate in the aquifer of Costa de Hermosillo (Sonora, Mexico) in relation to upward intrusion of saline groundwater, irrigation pumping and land cultivation. Applied Geochemistry 23(9), 2539-2558. GRef394

Szynkiewicz, Anna, Magdalena Modelska, Mariusz Orion Jedrysek and Maria Mastalerz (2008b). The effect of acid rain and altitude on concentration, $\delta^{34}S$, and $\delta^{18}O$ of sulfate in the water from Sudety Mountains, Poland. Chemical Geology 249(1-2), 36-51. GRef395

Taylor, Bruce E., Mark C. Wheeler and Darrell Kirk Nordstrom (1984). Stable isotope geochemistry of acid mine drainage: Experimental oxidation of pyrite. Geochimica et Cosmochimica Acta, 48(12), 2669-23678. GRef526

Taylor, B.E. and Mark C. Wheeler (1994). Sulfur- and Oxygen-Isotope Geochemistry of Acid Mine Drainage in the Western United States. Chapter 30, pp 481-514, in: Alpers, Charles N. and David W. Blowes (eds.). Environmental Geochemistry of Sulfide Oxidation. ACS Symposium Series, Volume 550. American Chemical Society; December 1993. GRef1092

Tichomirowa, Marion and Manuela Junghans (2009). Oxygen isotope evidence for sorption of molecular oxygen to pyrite surface sites and incorporation into sulfate in oxidation experiments. Applied Geochemistry 24(11), 2072-2092. GRef329

USDA-NRCS (2009). Soil survey of Great Smoky Mountains National Park, Tennessee and North Carolina. U.S Department of Agriculture, Natural Resources Conservation Service.

Wadleigh, Moire A. (2003). Lichens and atmospheric sulphur: What stable isotopes reveal. Environmental Pollution 126(3), 345-351. GRef324

Weathers, K.C., S.M. Simkin, G.M. Lovett, and S.E. Lindberg (2006). Empirical modeling of atmospheric deposition in mountainous landscapes. Ecological Applications, 16(4), 1590-1607.

Wynn, P.M., N.J. Loader and I.J. Fairchild (2014). Interrogating trees for isotopic archives of atmospheric sulfur deposition and comparison to speleothem records. Environmental Pollution 187, 98-105. GRef286

Xiao, Hua Yun, Cong Guo Tang, Hong Wei Xiao, Yan Li Wang, Xue Yan Liu, Cong Qiang Liu (2010). Tissue S/N ratios and stable isotopes (d34S and d15N) of epilithic mosses (Haplocladium microphyllum) for showing air pollution in urban cities in Southern China. Environmental Pollution, 158(5), 1726-1732. GRef580

Xiao, Hua Yun, Ren Guo Zhu, Bi Na Lin and Cong Qiang Liu (2011). Sulfur isotopic signatures in rainwater and moss Haplocladium microphyllum indicating atmospheric sulfur sources in Nanchang City (SE China). Science of the Total Environment 409(11), 2127-2132. GRef579

Yang, Wenbo, Ronald J. Spencer and H. Roy Krouse (1996). Stable sulfur isotope hydrogeochemical studies using desert shrubs and tree rings, Death Valley, California, USA. Geochimica et Cosmochimica Act 60(16), 3015-3022. GRef336

Yun, Misuk, Moire A. Wadleigh and Bernhard Mayer (2010). Variations in sulfur isotope ratios in a single lichen thallus: A potential historical archive for sulfur pollution. Environmental Pollution 158(12), 3534-3538. GRef323

Chapter 2 Appendix

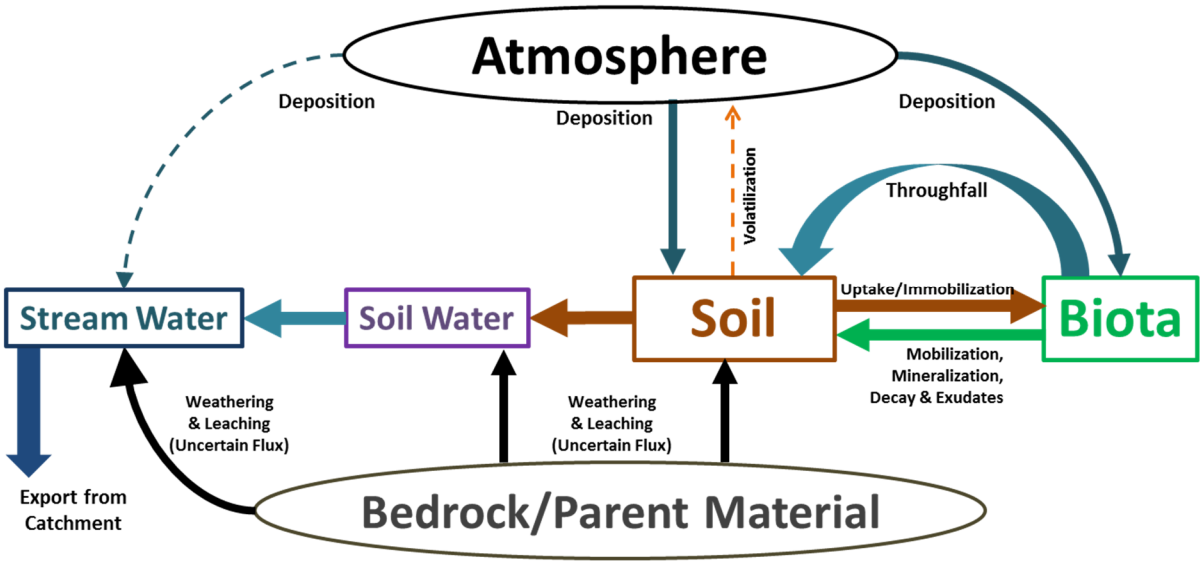

Figure 2. Conceptual diagram of ecosystem components (phases) that sulfur compounds can enter, occupy or traverse, and pertinent transformation or migration pathways between phases.

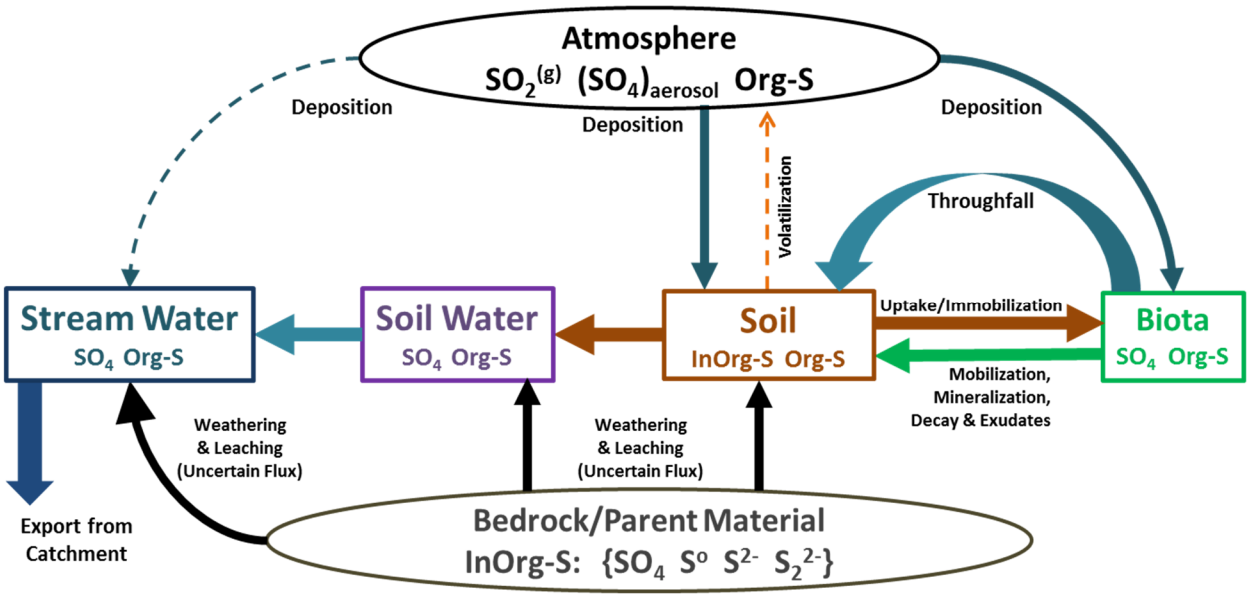

Figure 3. Conceptual diagram of ecosystem components (phases) and prominent sulfur species in each.

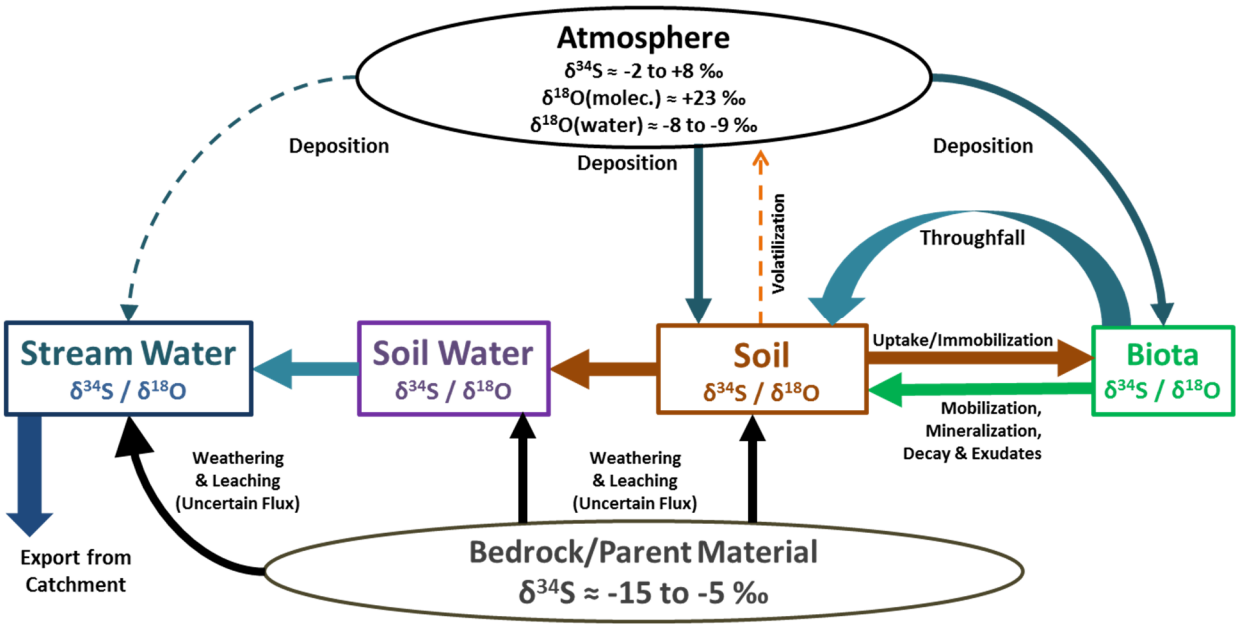

Figure 4. Conceptual diagram of the sulfur and oxygen isotope composition of ecosystem components in forested catchments.

CHAPTER 3: LITERATURE REVIEW

Understanding the origins, behavior and fate of acidic air pollutant deposition (AAPD) is an ongoing goal of environmental agencies, natural resource managers, and academic institutions (Porter et al. 2005; Burns et al. 2011; Fancy and Bennetts 2012; NADP 2013). The objective of this work is to examine the relationship between biogeochemical sulfur cycling and AAPD-induced acidification of stream water and soil in GRSM. The following is an extensive literature review of concepts and theories related to this objective.

Basic Chemistry of Sulfur

Sulfur is a relatively abundant element in nature, by some accounts ranking 10th throughout the known universe and 14th in the Earth's crust (Seal 2006). It is a necessary major nutrient required for biological function (Anderson 1975). Some estimates report an overall mean concentration of ~520 parts per million (ppm) in the biosphere (Goldschmidt 1954) and 270 to 2400 ppm in rock (including igneous and sedimentary) (Bowen 1979). In mature soil, sulfur concentrations vary according to soil type and location/climate where formed; in humid and temperate regions they can range from 100 to 1500 ppm (Lawton 1955). Of the total soil-sulfur phase, ~50 to 500 ppm is in forms that are soluble in water or weak acid (Lawton 1955), but the majority of soil-sulfur in humid to semiarid climates exists as various forms of organic sulfur (Org-S) (Landers et al. 1983; Freney 1967; Kertesz and Mirleau 2004). In drier climates, soil-sulfur has a substantial mineral component in the form of gypsum or epsomite (calcium and magnesium sulfates), and to lesser extents sphalerite (ZnS), chalcopyrite ($CuFeS_2$) and pyrite or marcasite (FeS_2) (Freney 1967). In the aqueous phase, concentrations of soluble sulfur species (predominantly sulfate) average ~3.7 and 905 milligrams per liter (mg L^{-1}) in freshwater and seawater, respectively (Bowen 1979).

Sulfur (atomic number 16) has six electrons in its outer (highest energy) electron orbitals, two in the 3s orbital and four in the 3p orbitals. This allows sulfur to have a wide range of valence states (+6, +4, +3, +2, 0 and -2), the most common ones in the environment being +6 (e.g., S^{6+}; sulfate), +4 (e.g., S^{4+}; sulfite, sulfur dioxide), 0 (S^{0}; elemental sulfur) and -2 (e.g., S^{2-}; sulfide). Oxidation-reduction (redox) reactions transform sulfur compounds from one valence state to another; most of the chemical processes pertinent to this dissertation are redox reactions. These include the combustion (oxidation) of elemental (S^{0}) or organic (S^{2-}) sulfur in coal into gaseous sulfur dioxide (S^{4+}), oxidation of sulfite (S^{4+}) into sulfate (S^{6+}), the oxidation of reduced sulfur minerals (e.g., pyrite; S^{2-}) into sulfate (S^{6+}) (abiotically or biotically), and the reduction of sulfate (S^{6+}) into sulfide (S^{2-}) by sulfate reducing bacteria (SRB). These basic redox reactions involving sulfur can be activated abiotically and biologically, and fall into one of four categories of transformations: immobilization (transformation of sulfate into organic-sulfur; Fitzgerald et al. 1983); mineralization (depolymerization of organic-sulfur into soluble sulfate; Williams 1967); oxidation; and reduction (Edwards 1998). Immobilization and mineralization are enzyme-catalyzed biochemical processes, each mediated by unique families of bacteria, fungi and macrophytes (Fitzgerald et al. 1983; Strickland and Fitzgerald 1984; Edwards 1998).

Aqueous Chemistry of Sulfur

A number of instances in the literature were found of authors attributing increases in dissolved sulfate concentrations to increasing stream “acidity” based on model results (Martinson et al. 2003; Martinson 2004; Martinson and Alveteg 2004; Lawrence 2002). Many report a connection between sulfate desorption and changes in stream chemistry under storm-flow conditions, specifically the well-documented stream water pH and acid-neutralizing capacity (ANC)

depression observed coincident with rising stream gauge (Wigington et al. 1993; Laudon et al. 1999; Laudon et al. 2000; Laudon et al. 2001; Laudon and Hemond 2002; Deyton et al. 2009; Mauney 2009; Neff et al. 2013). There exists in the literature many examples of stream water systems with relatively constant sulfate concentrations while pH and ANC decreased significantly (e.g., Cook et al. 1994; Cai et al. 2011a; Aplin 2014; Robinson et al. 2013; Evans et al. 1995). Detailed review of aqueous sulfur chemistry clarified this confusion and provided plausible explanations for some stream water sulfate resisting large concentration changes (i.e., essentially chemically "buffered").

Sulfate Chemistry (Hydrolysis and pH)

Proton-sulfate dissociation equilibria in aqueous solution are expressed as follows:

$$\mathbf{H_2SO_4 = H^+ + HSO_4^-} \qquad \textbf{and} \qquad \mathbf{HSO_4^- = H^+ + SO_4^{2-}}$$

These two reactions are described by dissociation constants ($pK_{a,1}$ and $pK_{a,2}$, respectively), which have the values of -3.0 and 1.99, respectively (at 25°C; Stumm and Morgan 1981). The implication is that sulfuric acid completely deprotonates at environmentally-relevant pH levels (pH > 3.5). In contrast, atmospheric aqueous phase acidity is generated by a cascade of hydrolysis reactions initiated by the dissolution of precursor SO_2 and SO_3, which are strong Lewis-acid (electron-accepting) molecules:

$$\mathbf{SO_{2(g)} = SO_{2(aq)}} \quad \textbf{and} \quad \mathbf{SO_{3(g)} = SO_{3(aq)}}$$

$$\mathbf{SO_{2(aq)} + H_2O = H_2SO_3 = H^+ + HSO_3^- = 2H^+ + SO_3^-}$$

$$\mathbf{SO_{3(g)} + H_2O = H_2SO_4 = H^+ + HSO_4^- = 2H^+ + SO_4^-}$$

The dissociation constants of the SO_2 sequence of reactions ($pK_{a,1(SO2)}$ and $pK_{a,2(SO2)}$, respectively) are 1.879 and 7.192, respectively (at 25°C; Maaha 1982). This implies that in the range of rainwater pH ($3.5 < pH < 6.5$), the bisulfite (HSO_3^-) species would predominate (ignoring for the moment other reactions such as the oxidation of sulfite to sulfate), and that one proton-mole per mole of $SO_2(g)$ could be formed in the atmospheric aqueous phase. As for the SO_3 component, it rapidly and completely dissolves to form sulfuric acid at terrestrial temperatures (Lovejoy et al. 1996; Loerting and Liedl 2000; Boy et al. 2013), and the dissociation chemistry of sulfuric acid described earlier applies here.

This review of aqueous sulfur oxyanion chemistry makes the case that hydrolysis/proton generation, S^{4+} to S^{6+} oxidation, and sulfate's double-dissociation reactions occur in the atmosphere, long before deposition onto watershed surfaces. The dominant soluble inorganic-sulfur species in precipitation at the moment of impact, and in watershed surface streams at typical pH levels, or even in acidified streams ($pH > 3.5$), is the free hydrated sulfate ion (a small fraction of which will associate with dissolved cations as ion-pairs, depending on the values of ion-pair formation constants). Thus, the sulfate ion in water is merely a charge-balancing spectator-ion for the acidity already in the atmospheric aqueous phase. Free hydrated sulfate ions cannot generate protons directly; therefore, they cannot have a direct influence on stream pH. In fact, under conditions of increasing acidity (e.g., $pH < 3.5$), the proton-sulfate equilibrium will provide weak buffering *against* increasing acidity, by taking up protons and forming bisulfate ions (HSO_4^-). There are examples of studies that arriver at the same conclusion about sulfate's role in acidification (e.g., Evans et al. 1995; Munson and Gherini 1993).

Aqueous-Solid Interface Processes of Sulfur

Negatively charged sulfate participates in *anion* exchange reactions with other anions adsorbed to positively charged surfaces (Stumm and Morgan 1981). It cannot directly exchange with protons; therefore, sulfate cannot directly release adsorbed protons into solution and thus cannot directly influence *stream pH* by this mechanism. Sulfate ions can, however, adsorb to positively charged exchange complexes (PCEC), found as exposed *protonated hydroxyl groups* at the edges of clay-mineral platelets and on the surfaces of hydrous metal oxide (HMO) minerals (Essington 2015). These PCEC are formed by protonation of amphoteric functional groups under low pH (high proton activity) conditions (Stumm and Morgan 1981):

$$\equiv Al\text{-}OH_2^{½+} + H_2O = \mathbf{(H_3O+)} + \equiv Al\text{-}OH^{½-} \qquad pKa \approx 7\text{-}8$$

$$\equiv Fe\text{-}OH_2^{½+} + H_2O = \mathbf{(H_3O+)} + \equiv Fe\text{-}OH^{½-} \qquad pKa \approx 9$$

$$\equiv Fe_3\text{-}OH^{½+} + H_2O = \mathbf{(H_3O+)} + \equiv Fe_3\text{-}O^{½-} \qquad pKa \approx 9$$

The listed dissociation constants imply that at pH values less than the pKa, the protonated form dominates; at stream pH values typically encountered in the GRSM (≈ 4 – 7), these PCECs are available to electrostatically adsorb any anions, including sulfate (Peak et al. 1999; Peak et al. 2001). The structure of outer-sphere (non-specific) adsorption can be envisioned as a three-member complex with a water molecule (i.e., a protonated hydroxyl group) bridging the exchange complex and sulfate ion (Zhang and Sparks 1990; Xue and Harrison 1991).

Functionally, sulfate is a passive, charge-balancing ion on the exchange complex, and any perturbation of the system that disrupts the proton-hydroxyl bond (causing proton release into solution) could simultaneously release the associated sulfate into solution. Unless some other mechanism hinders the released sulfate ions, one would expect stream water concentrations of

previously-adsorbed sulfate to increase as protons are released from these adsorption sites. In cases where aqueous sulfate concentrations remain constant when pH decreases, one might conclude that there was little to no adsorbed sulfate present in the system prior to the perturbation. An alternate adsorption scenario is inner-sphere (specific) chemisorption involving ligand exchange (releasing the entire water molecule, not just the proton) and direct chemical bonding to the mineral surface's metal center (Paul et al. 2007; Zhu et al. 2013).

Sulfate and ANC

The charge-balance definition of ANC (Molot et al. 1989; Munson and Gherini 1993) is:

$$ANC = \{ Ca^{2+} + Mg^{2+} + Na^{+} + K^{+} + NH_4^{+} + Al^{n+} \} - \{ SO_4^{2-} + NO_3^{-} + Cl^{-} + OrgA^{-} \}$$

Sulfate's role in stream water ANC (and indirectly in stream water pH) is related to the "salt effect" (Seip 1980; Church and Turner 1986). This term describes the process by which high concentrations of anions induce cations (ideally, sodium, potassium, magnesium and calcium; base cations) into solution to maintain charge neutrality. In soil-water systems already depleted in available base cations, protons and/or hydrolysable metals (e.g., aluminum) are the next available types of cations to be drawn into solution to charge balance the larger anion concentrations. In this context, higher sulfate concentrations translate to lower ANC, based on ionic charge balance, and (potentially but not necessarily) to lower pH by the induction of protolytic cation species. However, sulfates' role in this water ion balance scenario is as a charge-balancing surrogate for missing bicarbonate ions that would be present in otherwise high-ANC water systems. As such, all anions potentially can induce a salt-effect (e.g., chloride, nitrate, negatively charged organic complexes such as fulvic acids, acetate, tannates, etc.).

Atmospheric Chemistry of Sulfur

The underlying theme of this dissertation, acidic pollutant deposition and watershed acidification, begins with acidic pollutants being created and released into the atmosphere. In the case of sulfur-compounds, combustion of fuel stocks containing residual sulfur is the most common starting point (Schurr and Netschert 1960; Chou 1994). Sulfur is a common impurity in economically recoverable coal (Nayak 2013; Gluskoter and Simon 1968), and exists in coal formations predominantly as reduced inorganic and organic sulfur compounds (Greer 1979) at concentrations ranging between 0.38 and 5.32% (Meyers 1977). Forms and concentrations of sulfur in coal vary by source mine location (Hardman et al. 1998). Combustion is a rapid thermal oxidation of reduced sulfur species (e.g., S^{II-} sulfides and organic-sulfur), transforming them into sulfur species of higher valence states. More than 90% of the total sulfur mass emitted from typical coal-fired power plants consists of sulfur dioxide (S^{4+} sulfur dioxide) (Husar et al. 1978), with the balance found primarily as aerosols of sulfuric acid (Srivastava et al. 2004) and sulfate salts (S^{6+}) (Liebsch and De Pena 1982; Garber et al. 1981). Industrial facilities such as coal-fired power plants historically have been efficient point-sources of sulfur-compounds to the atmosphere since the mid- to late-1800s (Schurr and Netschert 1960), but regulation-driven management (via the 1990 Clean Air Act Amendments; Likens et al. 2001; Chestnut and Mills 2005) has resulted in a substantial decrease in the rate of acidic pollutant emission to the atmosphere and in corresponding reductions in AAPD (Gonzalez et al. 2015; Burns et al. 2008; Rice et al. 2014).

Physical and chemical processes in the atmosphere are far more complex than might be assumed from the relatively low concentrations of pollutants within the dominant oxygen-nitrogen background matrix. Major factors that make atmospheric science complex are the input of solar

radiation (energy), the presence of multiple phases (gas, vapor, liquid, aerosols and fine particulates), and the interactions of multiple pollutant compounds (Finlayson-Pitts and Pitts 1986). In addition, a sizeable proportion of sulfur compounds in the atmosphere originate from natural sources (Bates and Lamb 1992; Bates et al. 1992). These factors influence the mass flux of atmospheric sulfur.

Three general types of chemical interactions occur in the atmosphere: pure gas phase (homogeneous) molecular interactions (e.g., Atkinson and Lloyd 1984); gas-liquid (e.g., Gillani and Wilson, 1983); and gas-solid (heterogeneous) phase interactions (Hulett et al. 1972). Oxidation of air-borne SO_2 occurs by all three, although evidence exists that the gas-phase reactions predominate (Gillani et al. 1981; Boy et al. 2013; Sarwar et al. 2014; Saltzman et al. 1983). They begin with the electronic excitation of SO_2 molecules by the absorption of solar radiation in the ultraviolet (UV) wavelengths 240-330 nm (Finlayson-Pitts and Pitts 1986). These energetically excited species then interact with a number of atmospheric chemical species to complete the oxidation of S^{4+} to S^{6+} (Davis et al. 1979). The kinetic rates for all these chemical reactions are highly sensitive to atmospheric conditions such as temperature (seasonal and diurnal) (Gillani 1978; Richards et al. 1981; Lusis et al. 1978) and humidity (Hegg and Hobbs 1982; Eatough et al. 1984).

Interestingly, the other class of atmospheric pollutants responsible for AAPD and watershed acidification, gas-phase nitrogen oxides (NO_X), plays a major role in the SO_2-oxidation process, generating hydroxyl radicals which are powerful oxidizing agents for the conversion of SO_2 to SO_3 (Hashimoto et al. 1984). This interaction between these two classes of acidic pollutants has important strategy implications for mitigating sources of acidic deposition and watershed acidification (Lonsdale et al. 2012).

A subtle but important distinction to make is that SO_2 is not the acidic pollutant directly; it is the precursor to acidic pollutants. The SO_2 oxidizes rapidly in the atmosphere (Husar et al. 1978; Boy et al. 2013; Sarwar et al. 2014) to form sulfur trioxide (SO_3; S^{6+}). Both sulfur oxides are very water-soluble and hydrolyze upon dissolution to generate protons and their respective counter anions: sulfite (SO_3^{2-}); bisulfite (HSO_3^-); and sulfate (SO_4^{2-}). It is this formation-oxidation-dissolution sequence in the atmosphere that generates the harmful acidity. Although direct deposition of SO_2 does occur (Gillani 1978), the net result is essentially the same after terrestrial processes oxidize and dissolve/hydrolyze the deposited SO_2 into SO_3, SO_3^{2-}, HSO_3^-, and SO_4^{2-} (Overton, Jr. et al. 1979).

Another important atmospheric chemical process to consider is post-formation reactions of atmospheric acids with bases present in the atmosphere. A common example is ammonia (NH_3) and ammonium (NH_4^+) which partially neutralizes acidity due to sulfuric acid, producing particulate aerosols or particulate coatings of ammonium sulfate (McKay 1971; Gong et al. 2013). Base cations such as calcium and magnesium in the atmosphere can do the same. Unlike nitric acid, the resulting salts of sulfuric acid are essentially non-volatile and exist in the atmosphere associated with particulates and aerosols (Roedel 1979). Lastly, organic compounds containing sulfur in various oxidation states have been measured in air samples and power plant plumes, although not in concentrations nearly as high as inorganic (i.e., sulfate) forms (Eatough et al. 1986; Smet and Langenhove 1998).

Sulfide Mineral Oxidation

An important aspects of sulfur biogeochemistry is oxidation of sulfide minerals, and the associated release of acidity, sulfur oxyanions (e.g., sulfate), iron (from the original mineral phases), and trace

metals desorbed from minerals by ion exchange; this is analogous to the acid mine drainage issue (Evangelou and Zhang 1995). Sulfide mineral oxidation is relevant to this dissertation because of the prominence of carbonaceous schist, phyllite and slate, collectively referred to as Anakeesta Formation, in the GRSM (King 1964; USDA-NRCS 2009). The sulfide minerals associated with shale, slate and schist contained in the Anakeesta Formation are estimated to contain up to 1.3 % by weight of sulfur (Hadley and Goldsmith 1963), and are the primary source of native sulfate (NS) in GRSM (Flohr et al. 1995). Oxidation of sulfide minerals in nature is a complex process because of the heterogeneous composition of sulfur minerals in nature, and because of the simultaneous redox reactions of iron and sulfur (Descostes and Vitorge 2004; Paschka et al. 2004). Another complexity in the oxidation of sulfide minerals is the formation of (often short-lived) sulfur-intermediates (Rimstidt and Vaughan 2003; Müller et al. 2013). For example, pyrite (FeS_2) and chalcopyrite ($CuFeS_2$) have been observed to begin their oxidation sequence by being oxidized to iron(II) thiosulfate and an iron(II)/copper(I) thiosulfate mix, respectively. These and other intermediates further oxidize into elemental sulfur and iron(III) and/or copper(II) sulfate, respectively (Steger and Desjardins 1978).

The mechanism(s) and sulfur-proton stoichiometry of pyrite/sulfide oxidation have been thoroughly studied (Salmon 2003; Moses and Herman 1991; Lowson 1982). The oxidation rate of sulfide minerals is known to depend on composition, mechanism, and on environmental and reaction conditions: surface area, pH, presence of iron(III), temperature, etc. (Evangelou 1995 [Chapter 6]). Surface area is a major factor in sulfide oxidation/weathering (Singer and Stumm 1970; Hoffmann et al. 1981; Moses et al. 1987; Moses and Herman 1991). For example, "… it is the belief of most geochemists that framboidal (highly porous, large surface area) and possibly polyframboidal (clusters of framboids) pyrite is the major contributor to the degradation of water

quality and, in general, the cause of environmental pollution during the process of mining [or possibly any process that exposes pyrite to oxic conditions]." (Evangelou 1995).

The initial stage of pyrite oxidation is believed to involve chemisorption of atmospheric or dissolved oxygen onto the pyrite surface, which acts to complete an electrochemical circuit consisting of cathodic ferrous-iron sites and anodic disulfide sites on the pyrite mineral surface (Rimstidt and Vaughan 2003; Tichomirowa and Junghans 2009). The cathodic iron(II) and anodic sulfide sites are heterogeneously distributed on pyrite mineral surfaces, thus the initial pyrite oxidation rate at pH > 5 is first-order with respect to the surface area-to-volume ratio (Moses and Herman 1991). This initial electrochemical redox step is not strongly dependent on initial pH above 5 (Moses et al. 1987). The byproducts of this net 14-electron redox reaction are 16 moles of protons and iron(II), two moles of sulfate, and (often) secondary minerals released from the mineral surface. At typical environmental conditions and oxic redox levels, the iron(II) can be oxidized to iron(III) by reaction with dissolved oxygen. At pH > 5, abiotic oxidation of iron(II) to iron(III) increases rapidly, but dissolved iron(III) concentrations are controlled by saturation index of $Fe(OH)_3$, etc. At this point, molecular O_2 serves its secondary role of regenerating dissolved iron(III) through oxidation of iron(II) (Moses and Herman 1991).

Generation of protons by the initial stage of pyrite oxidation begins to depress the pH of pore water adjacent to the weathering rock. As pH drops to < 4.5, the iron(III) generated by the oxidation of pyritic iron(II) becomes a more efficient oxidant than oxygen itself (Tributsch and Bennett 1981a; 1981b). The rate of pyrite oxidation by iron(III) is faster than the Fe(II) + O_2 → Fe(III) reaction, making the latter reaction the rate-limiting step at this stage of pyrite oxidation (Singer and Stumm 1970). As the pore water pH drops below 3, the Fe(II) + O_2 → Fe(III) reaction becomes extremely slow ($t_{½}$ = 100 days). However, at such low pH, the conversion of iron(II) to iron(III) is quite

efficiently catalyzed by microbial species. Acidophilic biotic oxidation of iron(II) is extremely rapid and not rate limiting (Evangelou 1995). Organisms capable of catalyzing this biotic oxidation include the well-known *Acidithiobacillus ferrooxidans*, an acidophilic chemolithotrophic organism that is ubiquitous in geologic environments containing pyrite (Mustin et al. 1992; Salmon 2003; Pisapia et al. 2007). Reaction products resulting from pyrite oxidation can include a wide variety of secondary minerals of iron (Nordstrom 1982; Peacor et al. 1999a; Peacor et al. 1999b), aluminum (Bigham and Nordstrom 2000; Rouse et al. 2001), and others (Flohr et al. 1995). These secondary minerals persist in the watershed environment (soil, stream water, stream sediment) or participate in further biogeochemical transformations. Thus, the oxidation of mineral sulfide is a complex, pH-dependent combination of abiotic sulfide oxidation by molecular oxygen, abiotic iron(II) oxidation to iron(III) by molecular oxygen, abiotic sulfide oxidation by iron(III), and microbiologically catalyzed iron(II) oxidation (Melton et al. 2014; Roden 2008).

Biochemistry and Organic Chemistry of Sulfur

The majority (> 90%) of total sulfur mass retained in temperate-climate watersheds is comprised of soil organic sulfur (soil-OrgS) (Kertesz and Mirleau 2004; Likens et al. 2002; Landers et al. 1983), which exists in many different chemical functional-group forms (Davidson 1980; Markuszewski et al. 1980; Mitchell and Fuller 1988):

- Aliphatic or aromatic thiols (mercaptans, thio-phenols): R-C-SH, Ar-SH
- Aliphatic, aromatic or mixed sulfides (thio-ethers): R-C-S-C-R, Ar-S-Ar
- Aliphatic, aromatic or mixed disulfides: R-C-S-S-C-R, R-S-S-Ar, Ar-C-S-S-Ar
- Aliphatic or aromatic sulfonates (C-sulfonates): R-C-SO_3
- Aliphatic or aromatic sulfate esters (O-sulfonates): R-C-O-SO_3

- Aliphatic or aromatic sulfamates (N-sulfonates): R-C-NH-SO_3
- Heterocyclic compounds of the thiophene type (e.g., dibenzothiophene),

where the symbols are: Ar aromatic organic structures, C carbon atoms, O oxygen atoms, R aliphatic organic structures, and S sulfur. There is a complex and elaborate sequence of biogeochemical reactions that operate in the cycling of sulfur in forest watersheds (Edwards 1998). The major biotic and organic components of the sulfur cycle are summarized here.

Soil-OrgS compounds are rapidly synthesized by microbial or cellular metabolism acting on available sulfate ions in the surrounding environment (Fitzgerald et al. 1982; Fitzgerald et al. 1983; Fitzgerald et al. 1985; Stanko-Golden et al. 1994). This is called immobilization of free sulfate, and is a major mechanism for "retention" of sulfate in forested watersheds (Edwards 1998).

Mobilization is the depolymerization of larger S-containing organic molecules into smaller S-containing organic molecules that are more labile and mobile (Edwards 1998). Mineralization is the enzymatic or microbial (metabolic) conversion of small, labile low-molecular weight S-containing organic molecules into sulfate (Edwards 1998). Sulfur functional groups with an O (O-sulfonate: -C-O-SO_3) or N (N-sulfonate: -C-N-SO_3) between the sulfate and carbon backbone are quite labile; easily mineralized back into soluble/mobile sulfate for sulfate-deficient soils by specific microbe species (Vidyalakshmi et al. 2009; Schroth et al. 2007). In contrast, sulfur functional groups with a direct carbon-sulfur bond are more resistant to mineralization. The combination of sulfur mobilization and mineralization can explain the excess sulfate exported from watersheds in amounts exceeding net inputs from the atmosphere (Mitchell et al. 2001).

Immobilization and mobilization/mineralization occur simultaneously in soils, given that microbial species responsible for each of these processes exist in soils (Maynard et al. 1983).

When plant and animal tissues decay, their organic sulfur components (e.g., plant sulfolipids [Harwood and Nicholls 1979] and amino acids [Johnson 1984; Brosnan and Brosnan 2006]) are released and accumulate in the soil. These sulfur-containing materials are initial substrates for the sulfur transformation processes. The net loss or gain of sulfate in a forested watershed (that is, which transformation process dominates at any given time and location) is dependent on the concentrations of substrates available to each particular microbial population: available sulfate ions for immobilizing bacteria, and available O-sulfonate or N-sulfonate compounds for mobilizing/mineralizing bacteria (Strickland and Fitzgerald 1984).

Biotic oxidation of sulfur species occurs as reduced-valence forms of sulfur are taken up by specific microbe species and metabolized into higher valence sulfur compounds. This includes conversion of elemental sulfur (S^0), hydrogen sulfide (H_2S; S^{2-}), sulfite (SO_3^{2-}; S^{4+}) and thiosulfate ($S_2O_3^{2-}$; mixed valence sulfur) into sulfate (SO_4^{2-}) by chemoautotrophic and photosynthetic bacteria (Ehrlich 1990). Members of the genus *Thiobacillus* (obligate chemolithotrophic, non-photosynthetic) are the most common aerobic microbial organisms involved in the oxidation of elemental sulfur to sulfates (Ehrlich 1990). Heterotrophic bacteria and fungi and some actinomycetes also are reported to oxidize sulfur compounds, as do green and purple bacteria (Photolithotrophs) of genera *Chlorbium* and *Chromatium*. *Rhodopseudomonas* (Ehrlich 1990).

Sulfate in soil is incorporated into the cellular and structural components of plants (Harwood and Nicholls 1979) and microorganisms (Denger et al. 2014) by assimilatory sulfate reduction. The first step in that process is the transport of sulfate ion from the soil solution through the microbial cell membrane or into the root system of macrophyte species (Davidian and Kopriva 2010). Once inside the cytoplasmic environment, a series of biochemical reactions involving various enzymes and cellular structures sequentially reduce the free sulfate ion to APS (adenosine-5'-

phosphosulfate), PAPS (3'-phosphoadensosine-5'-phosphosulfate), sulfite, sulfide and finally cysteine (Kertesz 1999; Davidian and Kopriva 2010). Intra-cellular cysteine is the initial building block for all biological structures and compounds containing sulfur: methionine, proteins, gamma-glutamylcysteine, glutathione, and sulfolipids (Leustek and Saito 1999).

In contrast, sulfate can be reduced to hydrogen sulfide (H_2S) by sulfate reducing bacteria (SRB) in a process called dissimilatory sulfate reduction (Ehrlich 1990), a process that is favorable under alkaline and anaerobic soil conditions. The predominant SRB genera in soil are *Desulfovibrio*, *Desulfatomaculum* and *Desulfomonas*. *Desulfovibrio desulfuricans* is the most common, non-spore forming obligate anaerobe that rapidly reduces sulfates in waterlogged soils. All SRB excrete an enzyme called "desulfurase" or "bisulfate reductase" (Ehrlich 1990). Rate of sulfate reduction is enhanced by high water levels, temperature, and organic substrate concentrations. Generally, H_2S oxidizes quickly under aerobic conditions such as are predominant in GRSM forests; accumulation of H_2S is not expected in GRSM surface soil.

Stable Isotope Geochemistry of Sulfur and Oxygen

Almost all chemical elements exist as a mixture of two or more stable isotopes (non-radioactive atoms with characteristic number of protons but different number of neutrons). While individual atoms of a given element are characterized by whole-number atomic mass units, the established molar mass of an element, shown for instance on the periodic table of elements, is a weighted-average mass of the element's stable atomic isotopes. For instance, the atomic molar mass of sulfur (32.066) is the weighted-average of four stable sulfur isotopes (and their relative abundance): ^{32}S (95.039579), ^{33}S (0.7486512), ^{34}S (4.1971987), and ^{36}S (0.0145921). Isotopic composition of a given element is described as the mass ratio (R) of given pairs of isotopes, typically the ratio of a

less abundant isotope to the most abundant isotope. In the case of sulfur, it is the ratio of ^{34}S (the heavier, rarer isotope) to ^{32}S (the lighter, most abundant isotope). In general, R-values of stable isotopes ($^{34}S/^{32}S$ and $^{18}O/^{16}O$) differ systematically in different media and from different sources, the result of various kinetic fractionation processes (Sharp 2007). The method for comparing isotopic compositions was defined early in the developmental history of stable isotope geochemistry, not using absolute R-values, but by the establishment of element-specific standard isotope R values to serve as an agreed-upon baseline from which all other isotope ratios measurements are compared. The ratio of isotope abundance in a given material is quantified by the "delta value," essentially the difference between a sample's R value and the standard's R value, normalized to the standard's R value. It is calculated as:

$$\delta = 1000\left(\frac{R_{sample} - R_{standard}}{R_{standard}}\right)$$

The delta value for an element is denoted by the heavier (less abundant) isotope: $\delta^{34}S$ for sulfur, $\delta^{18}O$ for oxygen, etc. Since the sulfur isotope composition in numerous meteorite samples has been shown to be remarkably constant, the sulfur isotope composition standard is the R-value measured from the troilite mineral in a meteorite sample associated with the Barringer Crater ("Meteor Crater") located in central Arizona. It was assigned the $\delta^{34}S$ value of 0 ‰ ("per mil"), and all other sulfur isotope composition measurements are reported relative to this baseline composition. Isotope compositions characterized by enrichment in the heavier/rarer ^{34}S isotope are described by larger R-values relative to the standard material. By definition, such materials would have positive (greater than 0 ‰) $\delta^{34}S$ values. Conversely, isotope compositions with relatively lower amounts of the heavier/rarer ^{34}S isotope are described by smaller R values relative to the standard material. Such materials would have negative $\delta^{34}S$ values. In many cases, these differences in stable isotope

ratios effectively act as a source-specific signature or fingerprint (Migaszewski et al. 2013; Heidel et al. 2013). For decades, stable isotope geochemistry has been a valuable chemical "probe," distinguishing among pollutant sources (through unique isotope compositions) or biogeochemical processes acting on those pollutants (e.g., Pichlmayer et al. 1998).

The slight differences in atomic masses of isotopes of a given element are sufficient to cause selectivity in how those isotopes behave during chemical reactions or physical processes (e.g., magma melt solidification, water evaporation, adsorption, microbiological transformation). Non-random, non-probabilistic selectivity for the lower mass over the higher mass isotope creates two pools of "reaction product" over time: one with a slight concentration of the lower-mass isotope in the "reaction product's" isotope composition, and one with a slight depletion of the lower-mass isotope in its isotope composition (or conversely, a correspondingly slight concentration of the *higher*-mass isotope in its isotope composition). This systematic segregation of isotope masses is termed isotopic fractionation (Seal 2006). The effect is measured as shifts in the baseline ratio of lower-mass ("light") isotope to higher-mass ("heavy") isotope counts in its isotope composition, and this shift in isotope composition is quantified by a few different parameters: the "big delta" (Δ) value, the fractionation factor (α), or the epsilon (ε) (Sharp 2007).

Fractionation of stable sulfur isotopes is known to occur in many other natural and anthropogenic processes. Examples (along with reported fractionation values for the process) include:

- Initial combustion of sulfur-contaminated fuel stocks (Derda et al. 2007): +0.6 to 2.4 ‰ (Yaofa et al. 2008)
- Oxidation of SO_2 to SO_3 and sulfate (Saltzman et al. 1983; Leung et al. 2001; Harris et al. 2012): -5.1 to +12.4 ‰ (Krouse et al. 1991);

- Adsorption of sulfate to mineral surfaces (van Stempvoor et al. 1990): 0 to +1 ‰;
- Uptake of sulfate by microbes and terrestrial vascular plants (Xiao et al. 2010; Novák et al. 2005; Zhang et al. 1998): +1 to +2 ‰ (Krouse et al. 1991);
- Oxidation of sulfide minerals to sulfate (Taylor et al. 1984; Müller et al. 2013; Heidel et al. 2013): 0 to +5 ‰ (Thode 1991);
- Microbial assimilatory sulfate reduction (Canfield 2001; Butler et al. 2004; Stam et al. 2011): -4.5 to +0.5 ‰ (Kaplan 1983); and
- Microbial dissimilatory sulfate reduction (Canfield 2001): -20 to -45 ‰.

A relevant example is the reduction of sulfate to sulfide leading to the formation of sulfidic (reduced-valence sulfur) minerals in rock formations. Absorption of the light sulfur isotope (^{32}S) takes slightly less metabolic energy than absorption of heavier sulfur isotopes (e.g., ^{34}S), and this simple biophysical preference results in ^{32}S being statistically slightly more likely to be absorbed into the bacterium than heavier sulfur isotopes. With the mass-ratios of sulfur isotopes within the bacterium now slightly shifted to proportionally higher amounts of the lighter ^{32}S isotope, the resulting reduced-valence sulfur by-product will have a net isotopic composition that is "lighter" (i.e., more negative) relative to the sulfur isotope composition of the ambient sulfate. This is the process responsible for biogenic pyritic sulfur minerals having strongly negative $\delta^{34}S$ values (Sharp 2007). If isotopic fractionation did not occur, biochemical reactions responsible for uptake and enzymatic reduction of sulfate would process sulfate-sulfur in the same mass-ratio of sulfur isotopes as the available pool of ambient sulfate: ~95.04% ^{32}S, ~4.20% ^{34}S and ~0.76% as the other sulfur isotopes (Sharp 2007). That is, all isotopes of sulfate-sulfur would have equal probability of being absorbed and transformed. Also, reduced-valence sulfur byproduct (e.g., elemental sulfur or sulfide) would have the same isotopic composition as the ambient sulfate.

The oxygen isotope composition of sulfate in GRSM stream water and soil not as effective of a source tracer as sulfur isotope composition. Numerous processes influence the $\delta^{18}O$ of sulfate, but processes related to sulfide oxidation are most relevant to ambient terrestrial and aquatic environments. Sulfide oxidation reaction pathways exist that use molecular oxygen and other pathways exist that use water-bound oxygen (Taylor and Wheeler 1994; Balci et al. 2007; Tichomirowa and Junghans 2009). This is significant to sulfate formation because the $\delta^{18}O$ of meteoric water-oxygen (–25‰ to –5‰; Sharp 2007) is significantly lower than the $\delta^{18}O$ of atmospheric oxygen (+23.5‰; Kroopnick and Craig 1972). Sulfate formed from reactions that use water-oxygen will have lower $\delta^{18}O$ than sulfate formed from reactions that use molecular oxygen. Another distinction between these two oxygen sources is fractionations during sulfur-oxygen bond formation. Oxygen isotope enrichment that occurs during sulfur-oxygen bond formation is smaller when water is the source of oxygen (ε = +2.8‰) than when atmospheric molecular oxygen is the source (ε = –9.8‰) (Balci et al. 2007; Tichomirowa and Junghans 2009). Since each sulfide oxidation mechanism can operate under appropriate environmental conditions, the $\delta^{18}O$ of sulfate in the environment will be comprised of mixtures of sulfate molecules formed by multiple reaction mechanisms and incorporating both sources of oxygen. Mixing of sulfate molecules from different sources does not cause isotope fractionations; therefore, the proportions of each oxygen source represented in a given sulfate sample can be quantified using isotope-balance equations (Lloyd 1968; Taylor and Wheeler 1994).

It is important to understand the relative influence of sulfur sources on specific aspects of the sulfur cycle in GRSM catchments. The two main sources of sulfate in the GRSM are atmospherically deposited sulfate and native (geologic) reduced-valence sulfur species (e.g., elemental sulfur, sulfide and disulfide). The ability to distinguish these two sources is possible by measuring the

isotope mass-ratios of sulfur in environmental samples. This analytical tool can be applied to many forms of environment sulfur, including sulfur species in soils (e.g., organic-S as thio-esters, thio-ethers, and aliphatic sulfides; Rossete et al. 2008; Rossete et al. 2012), in macrophyte vegetation like lichens and mosses (Xiao et al. 2010; Xiao et al. 2011), and in components of woody vegetation such as tree rings (Yang et al. 1996; Wynn et al. 2014). This is an extremely useful tool for understanding the "source-migration-transformation-disposition" lifecycle of sulfur in environmental media of forested catchments.

References

Anderson, J.W. (1975). The function of sulphur in plant growth and metabolism. In: K.D. McLachlan (ed.), Sulphur in Australasian agriculture; Sydney University Press, Sydney, Australia. Pp. 87-97.

Aplin, Matthew W. (2014). Chemical Flux During Event Storm Water Flows in the Great Smoky Mountains National Park: Comparison of Two Streams Varying by Drainage Area and Elevation. Master of Science thesis, Department of Civil and Environmental Engineering, University of Tennessee; pp.62.

Atkinson, R. and A.C. Lloyd (1984). Evaluation of kinetics and mechanistic data for modeling of photochemical smog. Journal of Physical and Chemical Reference Data, 13, 315.

Balci, Nurgul, Wayne C. Shanks III, Bernhard Mayer and Kevin W. Mandernack (2007). Oxygen and sulfur isotope systematics of sulfate produced by bacterial and abiotic oxidation of pyrite. Geochimica et Cosmochimica Acta, 71(15), 3796-3811. GRef234

Bates, Timothy S. and Brian K. Lamb (1992). Natural sulfur emissions to the atmosphere of the continental United States. Global Biogeochemical Cycles, 6(4), 431-435. GRef378

Bates, Timothy S., Brian K. Lamb, A. Guenther, J. Dignon, R.E. Stoiber (1992). Sulfur emissions to the atmosphere from natural sources. Journal of Atmospheric Chemistry, 14(1-4), 315-337. GRef379

Bigham, J.M. and Darrell Kirk Nordstrom (2000). Iron and aluminum hydroxysulfates from acid sulfate waters. Reviews in Mineralogy and Geochemistry 40(1), 351-403. GRef582

Bowen, H.J.M. (1979). Environmental Chemistry of the Elements. Academic Press, London, England.

Boy, M., D. Morgensen, S. Smolander, L. Zhou, T. Nieminen, P. Paasonen, C. Plass-Dülmer, M. Sipilä, T. Petäjä, L. Mauldin, H. Berresheim, and M. Kulmala (2013). Oxidation of SO2 by stabilized Criegee intermediate (sCI) radicals as a crucial source for atmospheric sulfuric acid concentrations. Atmospheric Chemistry and Physics, 13, 3865-3879. GRef626

Brosnan, John T. and Margaret E. Brosnan (2006). The sulfur-containing amino acids: An overview. The Journal of Nutrition, 136(6), 1636S-1640S. GRef360

Burns, D.A., J.A. Lynch, B.J. Cosby, M.E. Fenn, and J.S. Baron, (2011). US EPA Clean Air Markets Division, National Acid Precipitation Assessment Program Report to Congress 2011: An Integrated Assessment, National Science and Technology Council, Washington, DC, 114 p.

Burns, Douglas A., Karen Riva-Murray, Robert W. Bode, and Sophia Passy (2008). Changes in stream chemistry and biology in response to reduced levels of acid deposition during 1987-2003 in the Neversink River Basin, Catskill Mountains. Ecological Indicators, 8(3), 191-203. GRef433

Butler, Ian B., Michael E. Böttcher, David Rickard, and Anthony Oldroyd (2004). Sulfur isotope partitioning during experimental formation of pyrite via the polysulfide and hydrogen sulfide pathways: Implications for the interpretation of sedimentary and hydrothermal pyrite isotope records. Earth and Planetary Science Letters, 288(3-4), 495-509. GRef340

Cai, Meijun, Amy M. Johnson, John S. Schwartz, Stephen E. Moore, Matt A. Kulp (2011a). Response of soil water chemistry to simulated changes in acid deposition in the Great Smoky Mountains. Journal of Environmental Engineering, 137(7), 617-628. GRef592

Cai, Meijun, John S. Schwartz, R. Bruce Robinson, Stephen E. Moore, and Matt A. Kulp (2011b). Long-term annual and seasonal patterns of acidic deposition and stream water quality in a Great Smoky Mountains high-elevation watershed. Water, Air, and Soil Pollution, 219(1-4), 547-562. GRef479

Canfield, Donald E. (2001). Isotope fractionation by natural populations of sulfate-reducing bacteria. Geochimica et Cosmochimica Acta, 65(7), 1117-1124. GRef214

Chestnut, Lauraine G. and David M. Mills (2005). A fresh look at the benefits and costs of the U.S. acid rain program. Journal of Environmental Management, 77(3), 252-266. GRef612

Chou, Mei-in Melissa (1994). Low temperature perchloroethylene extraction of sulfur from Illinois coal. Report No. 1994-1, Illinois State Geological Survey, Champaign, IL. GRef607

Church, M. Robbins and Robert S. Turner (Editors.) (1986). Factors affecting the long-term response of surface waters to acidic deposition: State of the Science (Volume II). ORNL-M-152. Environmental Research Laboratory, Office of Research and Development; U.S. Environmental Protection Agency; Corvallis, Oregon. GRef(nnn)

Cook, Robert B., J.W. Elwood, R.R. Turner, M.A. Bogle, Patrick J. Mulholland, A.V. Palumbo (1994). Acid-base chemistry of high-elevation streams in the Great Smoky Mountains. Water, Air, and Soil Pollution, 72, 331-356. GRef559

Davidian, Jean Claude and Stanislav Kopriva (2010). Regulation of Sulfate Uptake and Assimilation-the Same or Not the Same? Molecular Plant, 3(2), 314-325. GRef739

Davidson, R.M. (1980). Molecular structure of coal. Report No. ICTIS/TR08, IEA Coal Research. London, United Kingdom. 86pp.

Davis, D.D., A.R. Ravishankara and S. Fischer (1979). SO_2 oxidation via the hydroxyl radical: atmospheric fate of HSO_X radicals. Geophysical Research Letters, 6(2), 113-116. GRef718

Denger, Karin, Michael Weiss, Ann Katrin Felux, Alexander Schneider, Christoph Mayer, Dieter Spiteller, Thomas Huhn, Alasdair M. Cook and David Schleheck (2014). Sulphoglycolysis in Escherichia coli K-12 closes a gap in the biogeochemical sulphur cycle. Nature, advance online publication: http://www.nature.com/nature/journal/v507/n7490/full/nature12947.html#access GRef659

Derda, Malorzata, Andrzej Grzegorz Chmielewski and Janusz Licki (2007). Sulphur isotope compositions of components of coal and S-isotope fractionation during its combustion and flue gas desulphurization. Isotopes in Environmental and Health Studies, 43(1), 57-63. GRef642

Descostes, Michael, P. Vitorge and C. Beaucaire (2004). Pyrite dissolution in acidic media. Geochimica et Cosmochimica Acta, 68(22), 4559-4569. GRef226

Deyton, Edwin B., John S. Schwartz, R. Bruce Robinson, Keil J. Neff, Stephen E. Moore and Matt A. Kulp (2009). Characterizing episodic stream acidity during stormflows in the Great Smoky Mountains National Park. Water, Air, and Soil Pollution, 196(1-4), 3-18. GRef482

Eatough, D.J., R.J. Arthur, N.L. Eatough, M.W. Hill, N.F. Mangelson, B.E. Richter, L.D. Hansen, and J.A. Cooper (1984). Rapid conversion of SO2(g) to sulfate in a fog bank. Environmental Science and Technology, 18, 855.

Eatough, Delbert J., Vernon F. White, Lee D. Hansen, Norman L. Eatough, and James L. Cheney (1986). Identification of gas-phase dimethyl sulfate and monoethyl sulfate in the Los Angeles atmosphere. Environmental Science and Technology, 20(9), 867-872. GRef691

Edwards, Pamela J. (1998). Sulfur cycling, retention, and mobility in soils: A review. General technical report NE-250, U.S. Department of Agriculture, Forest Service, Northeastern Research Station. Radnor, PA.

Ehrlich, Henry Lutz (1990). Geomicrobiology (2nd Edition). Marcel Dekker, Inc., New York, N.Y. Chapter 17

Essington, Michael E. (2015). Soil and Water Chemistry: An Integrative Approach (2nd Edition). CRC Press, Boca Raton, Florida.

Evangelou, V.P. (1995). Pyrite oxidation and its control. Taylor & Francis Group, CRC Press; Boca Raton, Florida; pp.293. GRef710

Evangelou, V.P. and Y.L. Zhang (1995). A review: Pyrite oxidation mechanisms and acid mine drainage prevention. Critical Reviews in Environmental Science and Technology, 25(2):141-199. GRef219

Evans, Christopher D., T.D. Davies, and P.J. Wigington, Jr. (1995). Assessing the contribution of individual dissolved ions to depressions in acid neutralizing capacity of streams in the Adirondack and Catskill Mountains, New York. Water, Air, and Soil Pollution, 85(2), 425-432.

Fancy, S. G. and R. E. Bennetts (2012). Institutionalizing an effective long-term monitoring program in the US National Park Service. Pages 481-497 in Gitzen et al. (editors). Design and Analysis of Long-term Ecological Monitoring Studies; Cambridge University Press.

Finlayson-Pitts, Barbara J. and James N. Pitts (1986). Atmospheric Chemistry: Fundamentals and Experimental Techniques. John Wiley & Sons, Inc.; New York.

Fitzgerald, John W., Jaru T. Ash, Timothy C. Strickland, and Wayne T. Swank (1983). Formation of organic sulfur in forest soils: a biologically mediated process. Canadian Journal of Forest Research, 13(6), 1077-1082. GRef605

Fitzgerald, John W., Timothy C. Strickland, and Jaru T. Ash (1985). Isolation and partial characterization of forest floor and soil organic sulfur. Biogeochemistry, 1(2), 155-167. GRef119

Fitzgerald, John W., Timothy C. Strickland, and Wayne T. Swank (1982). Metabolic fate of inorganic sulfate in soil samples from undisturbed and managed forest ecosystems. Soil Biology and Biochemistry, 14, 529-536. GRef373

Flohr, Marta J.K., Roberta G. Dillenburg and Geoffrey S. Plumlee (1995). Characterization of secondary mineral formed as the result of weathering of the Anakeesta Formation, Alum Cave, Great Smoky Mountains National Park, Tennessee. U.S. Geological Survey Open-file Report No. 95-477. U.S. Department of the Interior; Reston, Virginia.

Freney, J.R. (1967). Sulfur-containing organics. In: A.D. McLaren and G.H. Petersen (eds.), Soil Biochemistry. Marcel Dekker, New York; pp. 229-259.

Garber, Robert W., Joseph Forrest, and Leonard Newman (1981). Conversion rates in power plant plumes based on filter pack data: The oil-fired Northport plume. Atmospheric Environment (1967), 15(10-11), 2283-2292. GRef619

Gillani, N.V. (1978). Project MISTT: Mesoscale plume modeling of the dispersion, transformation and ground removal of SO2. Atmospheric Environment, 12, 569. GRef615

Gillani, N.V., S. Kohli, and W.E. Wilson (1981). Gas-to-particle conversion of sulfur in power plant plumes: I. Parameterization of the conversion rate for dry, moderately polluted ambient conditions. Atmospheric Environment, 15(10-11), 2293-2313. GRef618

Gillani, Noor V. and William E. Wilson (1983). Gas-to-particle conversion of sulfur in power plant plumes: II. Observations of liquid-phase conversions. Atmospheric Environment (1967), 17(9), 1739-1752. GRef617

Gluskoter, Harold J. and Jack A. Simon (1968). Sulfur in Illinois Coals. Illinois State Geological Survey Circular 432. Department of Registration and Education; Urbana, Illinois.

Goldschmidt, V.M. (1954). Geochemistry. Clarendon Press, Oxford, England; pp. 621-642.

Gong, Longwen, Rafal Lewicki, Robert J. Griffin, Frank K. Tittel, Chantelle R. Lonsdale, Robin G. Stevens, Jeffrey R. Pierce, Quentin G.J. Malloy, Severin A. Travis, Loliya M. Bobmanuel, Barry L. Lefer and James H. Flynn (2013). Role of atmospheric ammonia in particulate matter formation in Houston during summertime. Atmospheric Environment 77, 893-900. GRef716

Gonzalez, Adrian M., Dr. John S. Schwartz, and Matt Kulp (2015). Geochemistry in a high-elevation watershed responds to reductions in acid-pollutant emissions? 2015 World

Environmental & Water Resources Congress (EWRI), Austin, Texas, 17-21 May 2015. Platform presentation 19 May 2015.

Greer, R.T. (1979). Organic and inorganic sulfur in coal. Scanning Electron Microscopy, 1, 477-486.

Hadley, Jarvis B. and Richard Goldsmith (1963). Geology of the Eastern Great Smoky Mountains North Carolina and Tennessee. Geological survey professional paper 349-B. U.S. Department of the Interior, U.S. Government Printing Office, Washington, D.C.

Hardman, R., R. Stacy and E. Dismukes (1998). Estimating Sulfuric Acid Aerosol Emissions from Coal-Fired Power Plants. Presented at: *DOE-FETC Conference on Formation, Distribution, Impact and Fate of Sulfur Trioxide in Utility Flue Gas Streams*, Pittsburgh, PA, March 1998.

Harris, E., B. Sinha, P. Hoppe, J.N. Crowley, S. Ono, and S. Foley (2012). Sulfur isotope fractionation during oxidation of sulfur dioxide: gas-phase oxidation by OH radicals and aqueous oxidation by H_2O_2, O_3 and iron catalysis. Atmospheric Chemistry and Physics, 12(1), 407-423. GRef574

Harwood, J.L. and R.G. Nicholls (1979). The plant sulpholipid – a major component of the sulphur cycle. Biochemical Society Transactions, 7, 440-447. GRef658

Hashimoto, S. G. Inoue, and H. Akimoto (1984). Infrared spectroscopic detection of the $HOSO_2$ radical in argon matrix at 11°K. Chemical Physics Letters, 107(2), 198-202. GRef714

Hegg, Dean A. and Peter V. Hobbs (1982). Measurements of sulfate production in natural clouds. Atmospheric Environment (1967), 16(11), 2663-2668. GRef713

Heidel, Claudia, Marion Tichomirowa and Manuela Junghans (2013). Oxygen and sulfur isotope investigations of the oxidation of sulfide mixtures containing pyrite, galena, and sphalerite. Chemical Geology, 342(1), 29-43. GRef321

Hoffmann, Michael R., Bruce C. Faust, Fern A. Panda, Hong H. Koo and Henry M. Tsuchiya (1981). Kinetics of the removal of iron pyrite from coal by microbial catalysis. Applied and Environmental Microbiology 42(2), 259-271. GRef711

Hulett, L.D., T.A. Carlson, B.R. Fish and J.L. Durham (1972). Studies of sulfur compounds adsorbed on smoke particles and other solids by photoelectron spectroscopy. In: Gleb Mamantov and W.D. Shults, Determination of Air Quality. Springer U.S.; pp. 179-187. GRef620

Husar, R.B., D.E. Patterson, J.D. Husar, N.V. Gillani, and W.E. Wilson, Jr. (1978). Sulfur budget of a power plant plume. Atmospheric Environment (1967), 12(1-3), 549-568. GRef613

Johnson, Dale W. (1984). Sulfur cycling in forests. Biogeochemistry 1(1), 29-43. GRef597

Kaplan I.R. (1983). Stable isotopes of sulfur, nitrogen and deuterium in Recent marine environments. In: Stable Isotopes in Sedimentary Geology, Vol. 10 (ed. M.A. Arthur, T.F. Anderson, I.R. Kaplan, J. Veizer, and L.S. Land), pp. 2.1 – 2.108. Columbia, SC: SEMP Short Course.

Kertesz, Michael A. (1999). Riding the sulfur cycle – metabolism of sulfonates and sulfate esters in Gram-negative bacteria. FEMS Microbiology Reviews, 24(2), 135-175. GRef717

Kertesz, Michael A. and Pascal Mirleau (2004). The role of soil microbes in plant soil nutrition. Journal of Experimental Botany, 55(404), 1939-1945. GRef622

King, Philip B. (1964). Geology of the Central Great Smoky Mountains Tennessee. Geological Survey Professional Paper No. 349-C. U.S. Department of the Interior, U.S. Government Printing Office, Washington, D.C.

Krouse, H.R., J.W.B. Stewart, and V.A. Grinenko (1991). Ch. 7 in: Krouse, H.R. and V.A. Grinenko. Stable isotopes: Natural and anthropogenic Sulphur in the environment. SCOPE 43. John Wiley & Sons; New York.

Landers, D.H., Mark B. David, and Myron J. Mitchell (1983). Analysis of organic and inorganic sulfur constituents in sediments, soils and water. International Journal of Environmental Analytical Chemistry, 14(4):245-256. GRef218

Laudon, Hjalmar, Stephan Köhler and Kevin H. Bishop (1999). Natural acidity or anthropogenic acidification in the Spring flood of northern Sweden. Science of the Total Environment 234(1-3), 63-73. GRef422

Laudon, Hjalmar, Olle Westling and Kevin H. Bishop (2000). Cause of pH decline in stream water during Spring melt runoff in northern Sweden. Canadian Journal of Fisheries and Aquatic Sciences 57(9), 1888-1900. GRef426

Laudon, Hjalmar, Olle Westling, Stephan Löfgren and Kevin H. Bishop (2001). Modeling preindustrial ANC and pH during the Spring flood in northern Sweden. Biogeochemistry 54(2), 171-195. GRef424

Laudon, Hjalmar and Harry F. Hemond (2002). Recovery of streams from episodic acidification in northern Sweden. Environmental Science and Technology 36(5), 921-928. GRef466

Lawrence, G.B. (2002). Persistent episodic acidification of streams linked to acid rain effects on soil. Atmospheric Environment, 36, 1589-1598. GRef650

Lawton, K. (1955). Chemical composition in soils. In: F.E. Bear (ed.), Chemistry of the Soil. Reinholt, New York; pp. 53-84.

Leung, Fok Yan, A.J. Colussi, and M.R. Hoffmann (2001). Sulfur isotopic fractionation in the gas-phase oxidation of sulfur dioxide initiated by hydroxyl radicals. The Journal of Physical Chemistry A, 105(34), 8073-8076. GRef628

Leustek, Thomas and Kazuki Saito (1999). Sulfate transport and assimilation in plants. Plant Physiology, 120(3), 637-644. GRef740

Liebsch, Edward J. and Rosa G. De Peña (1982). Sulfate aerosol production in coal-fired power plant plumes. Atmospheric Environment (1967) 16(6), 1323-1331. GRef706

Likens, Gene E., Thomas J. Butler, and Donald C. Buso (2001). Long- and short-term changes in sulfate deposition: Effects of the 1990 Clean Air Act Amendments. Biogeochemistry, 52(1), 1-11. GRef593

Likens, Gene E., Charles T. Driscoll, Donald C. Buso, Myron J. Mitchell, Gary M. Lovett, Scott W. Bailey, T.G. Siccama, W.A. Reiners and Christine Alewell (2002). The biogeochemistry of sulfur at Hubbard Brook. Biogeochemistry 60(3), 235-316. GRef632

Lischeld, Gunnar, Pavel Kram, and Christina Weyer (2010). Tracing biogeochemical processes in small catchments using non-linear methods. In: Moller, Felix, Cornelia Baessler, Hendrik

Schubert, and Stefan Klotz (Eds.). Long-term ecological research. Springer; Netherlands. GRef383

Lloyd, R.M. (1968). Oxygen isotope behavior in the sulfate-water system. Journal of Geophysical Research, 73:6099-6209. Ref. in GRef525

Loerting, Thomas and Klaus R. Liedl (2000). Toward elimination of discrepancies between theory and experiment: The rate constant of the atmospheric conversion of SO_3 to H_2SO_3. Proceedings of the National Academy of Sciences of the United States of America (PNAS), 97(16), 8874-8878. GRef707

Lonsdale, Chantelle R., R.G. Stevens, C.A. Brock, P.A. Makar, E.M. Knipping and J.R. Pierce (2012). The effect of coal-fired power-plant SO2 and NOx control technologies on aerosol nucleation in the source plumes. Atmospheric Chemistry and Physics 12(23), 11519-11531. GRef715

Lovejoy, Edward R., David R. Hanson and L. Gregory Huey (1996). Kinetics and products of the gas-phase reaction of SO3 with water. The Journal of Physical Chemistry 100(51), 19911-19916. GRef627

Lowson, Richard T. (1982). Aqueous oxidation of pyrite by molecular oxygen. Chemical Reviews 82(5), 461-497. GRef709

Lusis, M.A., K.G. Anlauf, L.A. Barrie, and H.A. Wiebe (1978). Plume chemistry studies at a northern Alberta power plant. Atmospheric Environment (1967), 12(12), 2429-2437. GRef705

Maaha, Howard G. (1982). Sulfur dioxide/water equilibria between 0° and 50°C. An examination of data at low concentrations. In: David R. Schryer (ed.), Geophysical Monograph Series Volume 26: "Heterogeneous Atmospheric Chemistry," American Geophysical Union, Washington, D.C.; pg. 187-195. GRef708

Markuszewski, R., C.K. Wei, and T.D. Wheelock (1980). Oxydesulfurization of coal treated with methyl iodide: implications for removal of organic sulfur. CONF-800303-6, Ames Laboratory, Iowa State University, Ames, Iowa. 9pp.

Martinson, Liisa, Mattias Alveteg, and Per Warfvinge (2003). Parameterization and evaluation of sulfate adsorption in a dynamic soil chemistry model. Environmental Pollution, 124(1), 119-125. GRef257

Martinson, Liisa (2004). Recovery from acidification: policy oriented dynamic modeling. Ph.D. dissertation; Lund Institute of Technology, Department of Chemical Engineering, Lund University. GRef186

Martinson, Liisa and Mattias Alveteg (2004). The importance of including the pH dependence of sulfate adsorption in a dynamic soil chemistry model. Water, Air, and Soil Pollution, 154(1-4), 349-356. GRef149

Mauney, John Leland III (2009). Characterizing episodic stream acidification using a concentration-duration-frequency methodology in watersheds of the Great Smoky Mountains National Park. Master's thesis, University of Tennessee, 2009.

Maynard, D.G., Y.P. Kalra, and F.G. Radford (1987). Extraction and Determination of Sulfur in Organic Horizons of Forest Soils. Soil Science Society of America Journal, 51(3):801-806. GRef730

Maynard, D.G., J.W.B. Stewart and J.R. Bettany (1983). Sulfur and nitrogen mineralization in soils compared using two incubation techniques. Soil Biology and Biochemistry 15(3), 251-256. GRef687

McKay, H.A.C. (1971). The Atmospheric Oxidation of Sulfur Dioxide in Water Droplets in Presence of Ammonia. Atmospheric Environment (1967), 5, 7-14. GRef712

Melton, Emily D., Elizabeth D. Swanner, Sebastian Behrens, Caroline Schmidt and Andreaas Kappler (2014). The interplay of microbially and abiotic reactions in the biogeochemical Fe cycle. Nature Reviews Microbiology – Advanced online publication.

http://www.nature.com/nrmicro/journal/vaop/ncurrent/full/nrmicro3347.html GRef704

Meyers, R.A. (1977). Coal desulfurization. Marcel Dekker, New York, New York. 254pp.

Migaszewski, Zdzisław M., Agnieszka Gałuszka, Artur Michalik, Sabina Dołęgowska, Andrzej Migaszewski, Stanisław Hałas and Andrzej Trembaczowski (2013). The use of stable sulfur, oxygen and hydrogen isotope ratios as geochemical tracers of sulfates in the Podwisniowka acid drainage area (South-Central Poland). Aquatic Geochemistry 19(4), 261-280. GRef388

Mitchell, Myron J. and Robert D. Fuller (1988). Models of sulfur dynamics in forest and grassland ecosystems with emphasis on soil processes. Biogeochemistry, 5(1), 133-163. GRef602

Mitchell, Myron J., Bernhard Mayer, Scott W. Bailey, J.W. Hornbeck, Christine Alewell, Charles T. Driscoll, and Gene E. Likens (2001). Use of stable isotope ratios for evaluating sulfur sources and losses at the Hubbard Brook Experimental Forest. Water, Air, and Soil Pollution, 130(1-4), 75-86. GRef437

Molot, Lewis A., P.J. Dillon, and B.D. LaZerte (1989). Factors affecting alkalinity concentrations of stream water during snowmelt in Central Ontario. Canadian Journal of Fisheries and Aquatic Sciences, 46(10), 1658-1666. GRef630

Moses, Carl O., Darrell Kirk Nordstrom, Janet S. Herman and Aaron L. Mills (1987). Aqueous pyrite oxidation by dissolved oxygen and by ferric ion. Geochimica et Cosmochimica Acta 51(6), 1561-1571. GRef527

Moses, Carl O. and Janet S. Herman (1991). Pyrite oxidation at circumneutral pH. Geochimica et Cosmochimica Acta 55(2), 471-482. GRef528

Müller, Inigo A., Benjamin Brunner and Max Coleman (2013). Isotopic evidence of the pivotal role of sulfite oxidation in shaping the oxygen isotope signature of sulfate. Chemical Geology, 354, 186-202. GRef322

Munson, R.K. and S.A. Gherini (1993). Analysis of the mineral acid-base components of acid-neutralizing capacity in Adirondack lakes. Water Resources Research, 29(4), 881-890. GRef631

Mustin, C., J. Berthelin, P. Marion, P. de Donato (1992). Corrosion and electrochemical oxidation of a pyrite by thiobacillus ferrooxidans. Applied and Environmental Microbiology 58(4), 1175-1182. GRef224

National Atmospheric Deposition Program (NADP) (2013). National Atmospheric Deposition Program 2012 Annual Summary. NADP Data Report 2013-01. Illinois State Water Survey, University of Illinois at Urbana-Champaign, IL.

Nayak, Bibhuranjan (2013). Mineral matter and the nature of pyrite in some high-sulfur tertiary coals of Meghalaya, northeast India. Journal of the Geological Society of India, 81(2), 203-214. (February) GRef608

Neff, Kiel J., John S. Schwartz, Stephen E. Moore and Matt A. Kulp (2013). Influence of basin characteristics on baseflow and stormflow chemistry in the Great Smoky Mountains National Park, USA. Hydrological Processes 27(14), 2061-2074. GRef484

Nordstrom, Darrell Kirk (1982). Aqueous pyrite oxidation and the consequent formation of secondary iron minerals. In: J.A. Kittrick, D.S. Fanning and L.R. Hossner (Eds), Acid Sulfate Weathering. Special Publication 10: Soil Science Society of America (publisher) (ISBN: 978-0-89118-905-3; pg. 37-56. GRef446

Novák, Martin, James W. Kirchner, Daniela Fottova, Eva Prechova, Iva Jacková, Pavel Kram and Jakub Hruska (2005). Isotopic evidence for processes of sulfur retention/release in 13 forested catchments spanning a strong pollution gradient (Czech Republic, central Europe). Global Biogeochemical Cycles 19(4), GB4012-1 – GB4012-14. GRef183

Overton, John H., Jr., Viney P. Aneja and Jack L. Durham (1979). Production of sulfate in rain and raindrops in polluted atmospheres. Atmospheric Environment (1967) 13(3), 355-367. GRef624

Paschka, Michael G. and David Adam Dzombak (2004). Use of dissolved sulfur species to measure pyrite dissolution in water at pH 3 and 6. Environmental Engineering Science 21(4), 411-420. GRef396

Paul, Kristian W., James D. Kubicki and Donald L. Sparks (2007). Sulphate adsorption at the Fe (hydr)oxide-H2O interface: Comparison of cluster and periodic slab DFT predictions. European Journal of Soil Science, 58(4), 978-988. GRef216

Peacor, Donald R., Roland C. Rouse, T. Dennis Coskren and Eric J. Essene (1999a). Destinezite ("diadochite"), $Fe_2(PO_4)(OH)•6H_2O$; its crystal structure and role as a soil mineral at Alum Cave Bluff, Tennessee. Clays and Clay Minerals 47(1), 1-11. GRef493

Peacor, Donald R., Roland C. Rouse, Eric J. Essene and Robert J. Lauf (1999b). Coskrenite-(Ce), $(Ce,Nd,La)_2(SO_4)_2(C_2O_4)•8H_2O$, A New Rare-Earth Oxalate Mineral from Alum Cave Bluff, Tennessee: Characterization and Crystal Structure. The Canadian Mineralogist 37(6), 1453-1462. GRef511

Peak, D.; Elzinga, E. J.; Sparks, D.L. (2001). Understanding sulfate adsorption mechanisms on iron(III) oxides and hydroxides: Results from ATR-FTIR spectroscopy. In Heavy Metals Release in Soils; Sparks, D. L., Selim, H. M., Eds.; CRC Press: Boca Raton, FL, 2001; pp 167-190. GRef262

Peak, D.; Ford, R. G.; Sparks, D. L. (1999). An in-situ ATR-FTIR investigation of sulfate bonding mechanisms on goethite. J. Colloid and Interface Science 218(1), 289-299. GRef167

Pichlmayer, Friedrich, Wolfgang Schöner, Petra Seibert, Willibald Stichler, and Dietmar Wagenbach (1998). Stable isotope analysis for characterization of pollutants at high elevation alpine sites. Atmospheric Environment, 32(23):4075-4085. GRef334

Pissapia, Céline, M. Chaussidon and B. Humbert (2007). O and S isotopic composition of dissolved and attached oxidation products of pyrite by Acidithiobacillus ferrooxidans: Comparison with abiotic oxidations. Geochimica et Cosmochimica Acta 71(10), 2474-2490. GRef330

Porter, Ellen, Tamera Blett, Deborah U. Potter, and Cindy Huber (2005). Protecting resources on Federal lands: Implications of critical loads for atmospheric deposition of nitrogen and sulfur. BioScience 55(7):603-612. GRef451

Rice, Karen C., Todd M. Scanlon, Jason A. Lynch, and Bernard J. Cosby (2014). Decreased atmospheric sulfur deposition across the Southeastern U.S.: When will watersheds release stored sulfate? Environmental Science and Technology, 48(17), 10071-10078. GRef356

Richards, L. Willard, Jerry A. Anderson, Donald L. Blumenthal, Alan A. Brandt, J. Alexander McDonald, and Nan Waters (1981). The chemistry, aerosol physics and optical properties of a western coal-fired power plant plume. Atmospheric Environment (1967), 15(10-11), 2111-2134.

Rimstidt, J. Donald and David J. Vaughan (2003). Pyrite oxidation: A state-of-the-art assessment of the reaction mechanism. Geochimica et Cosmochimica Acta 67(5), 873-880. GRef391

Robison, Andrew L., Todd M. Scanlon, Bernard J. Cosby, James R. Webb, and James N. Galloway (2013). Roles of sulfate adsorption and base cation supply in controlling the chemical response of streams of western Virginia to reduced acid deposition. Biogeochemistry, 116(1-3), 119-130. GRef384

Roden, Eric E. (2008). Microbiological controls on geochemical kinetics 2: Case study on microbiological oxidation of metal sulfide minerals and future prospects. Chapter 9 in: Brantley, Susan L., James D. Kubicki and Art F. White (eds.), 2008. Kinetics of Water-Rock Interaction. Springer Science, New York.

Roedel, W. (1979). Measurement of sulfuric acid saturation vapor pressure; implications for aerosol formation by heteromolecular nucleation. Journal of Aerosol Science, 10(4), 375-386.

Rossete, Alexssandra Luiza Rodrigues Molina, José Albertino Bendassolli, and Paulo Cesar Ocheuze Trivelin (2008). Organic sulfur oxidation to sulfate in soil samples for total sulfur determination by turbidimetry. Revista Brasileira de Ciência do Solo, 32(6), 2547-2553.GRef662

Rossete, Alexssandra Luiza Rodrigues Molina, and José Albertino Bendassolli (2012). Isotope determination of sulfur by mass spectrometry in soil samples. Revista Brasileira de Ciéncia do Solo, 36(6):1787-1793. GRef556

Rouse, Roland C., Donald R. Peacor, Eric J. Essene, Thomas Dennis Coskren and Robert J. Lauf (2001). The new minerals levinsonite and zugshunstite: Coexisting oxalates with different structures and differentiation of LREE and HREE. Geochimica et Cosmochimica Acta 65(7), 1101-1115. GRef688

Salmon, Sally Ursula (2003). Geochemical modeling of acid mine drainage in mill tailings: quantification of kinetic processes from laboratory to field scale. Ph.D. Dissertation, Tekniska Högskolan, Stockholm, Sweden; pp.61. GRef702

Saltzman, E.S., G.W. Brass and D.A. Price (1983). The mechanism of sulfate aerosol formation: Chemical and sulfur isotopic evidence. Geophysical Research Letters, 10(7), 513-516. GRef599

Sarwar, Golam, Heather Simon, Kathleen Fahey, Rohit Mathur, Wendy S. Goliff and William R. Stockwell (2014). Impact of sulfur dioxide oxidation by stabilized criegee intermediate on sulfate. Atmospheric Environment 85(1), 204-214. GRef625

Schroth, Andrew W., Benjamin C. Bostick, Margaret Graham, James M. Kaste, Myron J. Mitchell and Andrew J. Friedland (2007). Sulfur species behavior in soil organic matter during decomposition. Journal of Geophysical Research: Biogeosciences 112, G04011-G0420. GRef697

Schurr, Sam H. and Bruce C. Netschert (1960). Energy in the American economy, 1850-1975: an economic study of its history and prospects. Resources for the Future. Johns Hopkins Press; Baltimore, Maryland. GRef611

Seal, Robert R., II (2006). Sulfur isotope geochemistry of sulfide minerals. Reviews in Mineralogy & Geochemistry, 61, 633-677. GRef557

Seip, H. M. (1980). Acidification of freshwater--sources and mechanisms. pp. 358-365. IN Ecological Impact of Acid Precipitation (D. Drablos and A. Tollan, eds.). Johs. Grefslie Trykkeri A/S, Mysen, Norway.

Sharp, Zachary (2007). Principles of Stable Isotope Geochemistry. Pearson – Prentice Hall, Upper Saddle River, New Jersey 07458.

Singer, Philip C. and Werner Stumm, 1970. Acidic mine drainage: The rate-determining step. Science 167(3921), 1121-1123. GRef689

Smet, E. and H. Van Langenhove (1998). Abatement of volatile organic sulfur compounds in odorous emissions from the bio-industry. Biodegradation 9(3-4), 273-284. GRef690

Srivastava, R.K., C.A. Miller, C. Erickson and R. Jambhekar (2004). Emissions of sulfur trioxide from coal-fired power plants. Journal of the Air & Waste Management Association 54(6), 750-762. GRef698

Stam, Marjolijn C., Paul R.D. Mason, Anniet M. Laverman, and Celine Pallud (2011). 34S/32S fractionation by sulfate-reducing microbial communities in estuarine sediments. Geochimica et Cosmochimica Act, 75(14), 3903-3914. GRef399

Stanko-Golden, K.M., Wayne T. Swank, and John W. Fitzgerald (1994). Factors affecting sulfate adsorption, organic sulfur formation, and mobilization in forest and grassland spodosols. Biology and Fertility of Soils, 17(4), 289-396. GRef606

Steger, H.F. and L.E. Desjardins (1978). Oxidation of sulfide minerals: 4. Pyrite, chalcopyrite and pyrrhotite. Chemical Geology 23(1-4), 225-237. GRef564

Strickland, Timothy C. and John W. Fitzgerald (1984). Formation and mineralization of organic sulfur in forest soils. Biogeochemistry, 1(1), 79-95. GRef122

Stumm, Werner and James J. Morgan (1981). Aquatic Chemistry: An introduction emphasizing chemical equilibria in natural waters (2nd Edition). Wiley-Interscience, New York.

Taylor, Bruce E., Mark C. Wheeler and Darrell Kirk Nordstrom (1984). Stable isotope geochemistry of acid mine drainage: Experimental oxidation of pyrite. Geochimica et Cosmochimica Acta, 48(12), 2669-23678. GRef526

Taylor, B.E. and Mark C. Wheeler (1994). Sulfur- and Oxygen-Isotope Geochemistry of Acid Mine Drainage in the Western United States. Chapter 30, pp 481-514, in: Alpers, Charles N. and

David W. Blowes (eds.). Environmental Geochemistry of Sulfide Oxidation. ACS Symposium Series, Volume 550. American Chemical Society; December 1993. GRef1092

Thode, H.G. (1991). Sulphur isotopes in nature and the environment: An overview. Ch.1 in: Krouse, H.R. and V.A. Grinenko. Stable isotopes: Natural and anthropogenic Sulphur in the environment. SCOPE 43. John Wiley & Sons; New York.

Tichomirowa, Marion and Manuela Junghans (2009). Oxygen isotope evidence for sorption of molecular oxygen to pyrite surface sites and incorporation into sulfate in oxidation experiments. Applied Geochemistry 24(11), 2072-2092. GRef329

Tributsch H. and Bennett J. C. (1981a). Semiconductor-electrochemical aspects of bacterial leaching. I. Oxidation of metal sulphides with large energy gaps. Journal of Chemical Technology and Biotechnology, 32, 565–577.

Tributsch H. and Bennett J. C. (1981b). Semiconductor-electrochemical aspects of bacterial leaching. II. Survey of rate-controlling sulphide properties. Journal of Chemical Technology and Biotechnology, 32, 627–635.

USDA-NRCS (2009). Soil survey of Great Smoky Mountains National Park, Tennessee and North Carolina. U.S Department of Agriculture, Natural Resources Conservation Service.

Van Stempvoort, D.R., E.J. Reardon, and P. Fritz (1990). Fractionation of sulfur and oxygen isotopes in sulfate by soil sorption. Geochimica et Cosmochimica Acta, 54, 2817-2826. GRef157

Vidyalakshmi, R., R. Paranthaman, and R. Bhakyaraj (2009). Sulfur oxidizing bacteria and pulse nutrition: A review. World Journal of Agriculture Sciences, 5(3), 270-278.

Wigington, Parker J., J.P. Baker, D.R. DeWalle, W.A. Kretser, P.S. Murdoch, H.A. Simonin, J. van Sickle, M.K. McDowell, D.V. Peck and W.R. Barchet (1993). Episodic acidification of streams in the northeastern United States: chemical and biological results of the episodic response project. Episodic project final report; U.S. Environmental Protection Agency (EPA), Corvallis, Oregon. Report number EPA/600/R-93/190. GRef543

Williams, C.H. (1967). Some factors affecting the mineralization of organic sulfur in soils. Plant and Soil Science, 26(2), 205-223. GRef623

Wynn, P.M., N.J. Loader and I.J. Fairchild (2014). Interrogating trees for isotopic archives of atmospheric sulfur deposition and comparison to speleothem records. Environmental Pollution 187, 98-105. GRef286

Xiao, Hua Yun, Cong Guo Tang, Hong Wei Xiao, Yan Li Wang, Xue Yan Liu, Cong Qiang Liu (2010). Tissue S/N ratios and stable isotopes ($\delta^{34}S$ and $\delta^{15}N$) of epilithic mosses (Haplocladium microphyllum) for showing air pollution in urban cities in Southern China. Environmental Pollution, 158(5), 1726-1732. GRef580

Xiao, Hua Yun, Ren Guo Zhu, Bi Na Lin and Cong Qiang Liu (2011). Sulfur isotopic signatures in rainwater and moss Haplocladium microphyllum indicating atmospheric sulfur sources in Nanchang City (SE China). Science of the Total Environment 409(11), 2127-2132. GRef579

Xue, Dongsen and Robert B. Harrison (1991). Sulfate, aluminum, iron, and pH relationships in four Pacific-Northwest forest subsoil horizons. Soil Science Society of America Journal, 55, 837-840. GRef161

Yang, Wenbo, Ronald J. Spencer and H. Roy Krouse (1996). Stable sulfur isotope hydrogeochemical studies using desert shrubs and tree rings, Death Valley, California, USA. Geochimica et Cosmochimica Act 60(16), 3015-3022. GRef336

Yaofa, Jiang, Erika R. Elswick, and Maria Mastalerz (2008). Progression in sulfur isotopic compositions from coal to fly ash: Examples from single-source combustion in Indiana. International Journal of Coal Geology, 73, 273-284. GRef782

Zhang, Peng Chu and Donald L. Sparks (1990). Kinetics and mechanisms of sulfate adsorption/desorption on goethite using pressure-jump relaxation. Soil Science Society of America Journal, 54, 1266-1273. GRef162

Zhang, Yimin, Myron J. Mitchell, Martin Christ, Gene E. Likens and H. Roy Krouse (1998). Stable sulfur isotope biogeochemistry of the Hubbard Brook Experimental Forest, New Hampshire. Biogeochemistry, 41(3), 259-275. GRef335

Zhu, Mengqiang, Paul Northrup, Chenyang Shi, Simon J.L. Billinge, Donald L. Sparks, and Glenn A. Waychunas (2013). Structure of sulfate adsorption complexes on ferrihydrite. Environmental Science and Technology Letters, 1(1), 97-101. GRef165

CHAPTER 4: A HYDROGEOCHEMICAL ANALYSIS OF FIRST- AND SECOND-ORDER STREAMS OF THE GREAT SMOKY MOUNTAINS: THE INFLUENCE OF LAND DISTURBANCES AND EXPOSED BEDROCK ON STREAM CHEMISTRY

Abstract

Extensive datasets of stream water chemistry in the Great Smoky Mountains National Park (GRSM) have been compiled from monitoring programs beginning in the 1980s, but until recently, stream water sampling strategies have been biased toward 3rd-order to 5th-order streams and rivers. Detailed hydrogeochemical analyses of water chemistry of low-order streams in small GRSM catchments is a significant knowledge gap. In addition, clarification is needed of the relationship between bedrock type and the water chemistry of first- and second-order streams, and of the role of exposed bedrock resulting from natural land disturbances. Water from 69 first-order streams and 13 second-order streams, located between 441 and 1750 meters a.m.s.l, was analyzed for chemical parameters related to acidification. Data were used to characterize variability in water chemistry throughout the study area, to identify sandstone and sulfidic bedrock weathering processes responsible for observed stream water chemistry, and to evaluate the influence of land disturbance (i.e., exposed bedrock) on stream water chemistry. Based on our data, it is concluded that weathering of exposed sulfidic bedrock was responsible for highly acidified stream water observed at specific locations, and weathering of minerals associated with sandstone bedrock at all other study locations was the primary process responsible for the "baseline" stream water chemistry observed at the majority of sites. Water chemistry (e.g., acidity and inorganic ions) of the sampled first- and second-order streams varied spatially within the study area, but sites generally clustered into three groups based on similar water chemistry. Indicators of specific weathering reactions were found in the water chemistry data, and differences in weathering indices among the stream water sites were related to underlying bedrock type and the existence of known areas of natural land disturbances that have exposed fresh (highly reactive) surfaces of bedrock directly to the atmosphere.

Introduction

The effects of atmospheric deposition on water quality in the Great Smoky Mountains National Park (GRSM) have been studied for several decades (Johnson and Lindburg 1992; Cook et al. 1994; NPS 2015). A long-term monitoring program at the GRSM includes a Park-wide water chemistry survey consisting of periodic collection and chemical analysis of stream water grab-samples. Sampling frequency and number of Park-wide stream sites has changed over the years, but monitoring sites prior to 2014 were biased toward mid-elevation, 3rd to 5th order streams and rivers (Odom 2003). To date, results from this monitoring program show improvements in the water chemistry of many GRSM streams impacted by acidification. However, water quality trends vary throughout the GRSM due to differences in watershed factors such as elevation, drainage area, surficial and bedrock geology, forest composition, etc. (Schwartz et al. 2014; Schwartz et al. 2016). Water chemistry in high-order (e.g., $\geq$ 3rd order) streams and rivers reflects the integration and comingling of upstream tributaries, and a large amount of small-scale geochemical resolution is lost by sampling only high-order streams and rivers. Thus, the pre-2014 GRSM monitoring data are appropriate for assessing basin- and watershed-scale spatial relationships in water quality, but not for understanding inter-relationships of biogeochemical processes at small spatial scales (e.g., headwater catchments drained by 1st and 2nd order streams).

In general, water chemistry at a given location within the landscape reflects the surface and subsurface geophysical attributes and biogeochemical processes occurring upgradient of that pour-point (Billett and Cresser 1992; Weyer et al. 2014; Grathwohl et al. 2013). From the chemistry of stream water in small catchments, it is possible to infer details of the geochemical processes that occur during the interaction of water with soil, bedrock minerals, vegetation, etc. This has been

demonstrated by investigators (Weyer et al. 2014; Grathwohl et al. 2013) who have analogized small forested catchments as “chemical reactors” in which material/nutrient inputs are acted upon by catchment-specific biogeochemical processes, and stream water with a chemistry profile characteristic of the catchment is exported. Weyer et al. (2014) analyzed a large dataset of soil solution, groundwater, and stream water chemistry, associated with a 420-hectare drainage area, using a non-linear form of Principle Components Analysis. They determined that 89% of the variance in their dataset could be explained by three principle components, which they ascribed to three groupings of biogeochemical processes: (1) oxidation-reduction reactions; (2) acid-induced soil-formation processes; and (3) mineral weathering reactions. The GRSM monitoring program includes one permanent field site at the outlet of a small (17.2-hectare) headwaters catchment. The high-elevation field station (~1700 meters above mean sea level) is located where precipitation volumes and atmospheric deposition fluxes were known to be greatest in the GRSM (Lindberg and Owens 1992; Shubzda et al. 1995; Weathers et al. 2006). Since 1993, this small-catchment field station has provided bi-weekly data used to monitor trends in atmospheric deposition and acidification of water and soil (Schwartz et al. 2014; Cai et al. 2010; Cai et al. 2011; Cai et al. 2012). The robust long-term monitoring dataset that has been generated from this field station represents only one small-catchment system in the GRSM. **Thus, detailed hydrogeochemical analyses of water chemistry of low-order streams in small GRSM catchments is a significant knowledge gap.**

The weathering of bedrock has been shown to be a prominent factor in determining stream water chemistry (Matschullat et al. 1992; Deviney et al. 2006). In the GRSM, two major bedrock types generally dominate the GRSM geology. Much of the GRSM overlies sandstone and siltstone conglomerate of the Thunderhead and Copperhill Formations (Hadley and Goldsmith 1963; King

1964). Some weathering reactions involving sulfur-deficient alumino-silicate minerals are acid-buffering processes, in theory (Nesbitt et al. 1997; LeComte et al. 2005). In practice, however, their reaction rates are too slow (e.g., 0.6 to 22 x 10^{-7} mol m^{-2} yr^{-1}; White and Brantley 2003) to provide significant buffering against atmospheric acidity (Brantley 2008; Brantley et al. 2014). The steep catchments at the higher elevations of the GRSM are well-drained, hydrologically "flashy" systems that limit contact-time between soil water and minerals in soil or bedrock. At such short time-scales, the only significant acidity-buffering mechanisms are ion exchange reactions, and the specific soil components that are involved in those ion exchange reactions differ as a function of soil pH (Sumner 2000; Essington 2015). Other areas of the GRSM are underlain by thick units of phyllite and carbonaceous (graphitic) shale containing sulfidic minerals (i.e., pyrite; pyrrhotite; other metal monosulfide and disulfide minerals) (Southworth et al. 2005). Sulfidic bedrock formations are prominent at the higher elevations of the central and northeastern sectors of the GRSM; the pertinent example of this bedrock type in the GRSM is the Anakeesta Formation (Hadley and Goldsmith 1963; King 1964; Southworth et al. 2005; Thornberry-Ehrlich 2008). Weathering of sulfidic minerals in soil or bedrock primarily consists of oxidation of pyrite and formation of acidity, sulfate and iron, which are transported to the stream water channel.

A GRSM study that explicitly included sulfidic bedrock as a study variable was reported by Neff et al. (2013). They designed a three-factor block-design study looking at elevation ("high" > 975 meters, and "low" < 975 meters), drainage area ("large" = 10 to 20 km^2 and "small" = 1 to 10 km^2), and sulfidic bedrock content (>10% coverage or 0% [absent]). Measurements were made during both baseflow and stormflow conditions. They found that pH and ANC in stream water from catchments with > 10% sulfidic bedrock was lower than from catchments with no sulfidic bedrock, but only weak evidence that exposed sulfidic bedrock was exacerbating the degradation

of stream water chemistry. They could not propose definitive conclusions regarding the role of exposed bedrock on stream water chemistry because (i) drainage areas of selected sites were too large and integrated too many smaller catchment streams and (ii) several of the studied basin factors were inter-correlated. **Thus, clarification of the relationship between bedrock type and the water chemistry of first- and second-order streams is needed.**

At some locations, slate/shale type geology and shallow soil mantels provide ideal conditions for landslides and debris slides (Ryan 1989) which exposes large areas of sulfidic phyllite/shale/slate bedrock to atmospheric climate conditions. Landslides and debris slides at higher elevations in the GRSM, where the steepest catchment slopes and thinner soil profiles are found, are suspected of being the source of acute stream acidification and acute toxicity to stream biota (e.g., Huckabee et al. 1975; Maas 1976; Bacon and Maas 1979). Streams in catchments overlying sulfidic bedrock are hypothesized to have distinct water chemistry relative to streams overlying sandstone, but the exact nature of the differences in stream water chemistry has only been speculated to this point. **Thus, the detailed geochemistry of first- and second-order streams that are impacted by exposed sulfidic bedrock in high-elevation small-catchment systems needs further investigation.**

This study was designed to meet three objectives. The first was to generally characterize water chemistry (e.g., acidity and inorganic ions) of first- and second-order stream water of the GRSM. The second was to identify indicators of specific weathering reactions responsible for the observed stream water chemistry in GRSM catchments overlying different bedrock types. The third objective was to determine if water chemistry of streams overlying sulfidic bedrock is substantially modified by the presence of disturbed sulfidic bedrock (in the form of natural landslides).

Methods

Study Locations

This study focused on first- and second-order streams flowing from drainage areas < 50 hectares. Stream water was sampled from 82 sites throughout the north-central sector of GRSM (Figure 5), primarily within the West Prong Little Pigeon River (WPLPR) watershed along the Route 441 corridor on the Tennessee side (Figure 6). Five sub-watersheds feed into the WPLPR: Walker Camp Prong (WCP) from its headwaters at the base of Mt. Kephart to its confluence with Road Prong (RP); RP from its headwaters (at the Clingman's Dome access road) to its confluence with WCP; Alum Cave Creek (ACC) from its confluence with Styx Branch to its confluence with WCP; creeks draining into WCP from the southwest-facing slopes of Mt. LeConte (MtLC); and lower WPLPR (LWPLPR) beginning at the confluence of the WCP and RP rivers and ending at the GRSM boundary, near the NPS headquarters. A few sites were located in two drainage areas adjoining WPLPR, on the North Carolina side of the State-Line ridge: the headwaters of the Oconoluftee River (Beech Flats Prong; BFP) and the headwaters of Noland Creek (NDW). These seven sub-watersheds were chosen based on site access, the wide elevation span represented, and their association with two major geologic bedrock types: (1) sandstone/siltstone (Roaring Fork (RFK), Elkmont (ELK), Thunderhead (THD) and Copperhill (COP) Formations) and (2) sulfidic graphitic phyllite/shale (the Anakeesta (ANK) Formation) (King et al. 1958; King et al. 1968).

Sample Collection

Water was sampled from 69 first-order streams and 13 second-order streams, spanning elevations near the outlet of WPLPR (441 meters above mean sea level; a.m.s.l), to the peaks west of

Newfound Gap (approximately 1750 meters a.m.s.l). Stream sampling sites were distributed among the seven sub-watersheds as follows: ACC (7 sites); BFP (3 sites); NDW (2 sites); MtLC (3 sites); LWPLPR (13 sites); RP (30 sites); and WCP (24 sites sampled). ArcGIS layers of known land-disturbance areas in the GRSM (natural land disturbances and exposed bedrock scars) provided by NPS (ESRI 2017) were compared to stream site coordinates. Eleven of the 82 sites were identified as potentially influenced by land-disturbances: one in the ACC sub-watershed, three in the RP sub-watershed, and seven in the WCP sub-watershed (five of which were in catchments draining Anakeesta Ridge) (Figure 6).

A total of 282 water samples were collected under baseflow conditions from among the 82 sampling sites. Stream sites were sampled on at least one field visit (in duplicate) within the 21-month study period between February 2015 and November 2016. Thirteen sites were sampled more than twice as a check on water chemistry variability; the most frequently visited site was sampled 12 times. Grab samples were collected in acid-rinsed polyethylene containers. At each site, sample containers were rinsed twice with ambient stream water, submerged to fill, and capped while submerged to prevent trapping air with the sample. Ambient water temperature was measured using a digital thermometer with stainless-steel thermistor probe (± 0.1 °C). On a select number of visits, field pH, conductivity and temperature were recorded using portable pH meter/probe and a combination conductivity and temperature probe (Thermo Scientific, Beverly, MA). Water samples were transported back to the laboratory and stored at ~6 °C until analyzed. Geographic coordinates of sample locations were recorded using a Garmin® geographic positioning system (GPS) receiver based on the WGS 1984 coordinate system; later these point coordinates were transposed into Projected Coordinate System UTM Zone 17N (North American Datum; NAD 1983) for use in ArcMap® /ArcGIS® 10.5 (ESRI, Redlands, CA).

Chemical Analyses

Water samples were analyzed for chemical parameters using standard laboratory practices (Standard Methods 1999). Within 6-12 hours of sampling, water samples were returned to laboratory for analysis (unfiltered) for pH, specific conductance, and acid neutralizing capacity (ANC; titration with 0.01 M hydrochloric acid) on an automated titration system (Mantech PC-Titrate® system; Guelph, Ontario, Canada). Within one week of sampling, water samples were filtered through 0.45 micrometer (µm) hydrophilic filter-cartridges directly into low-density polyethylene (LDPE) vials in preparation for (1) ion chromatography (IC) using a Thermo-Dionex 2100/1100 dual column system with background conductivity suppression (Thermo-Element, Florida, USA), and (2) inductively coupled argon plasma (iCAP) optical emission spectroscopy (OES) using an iCAP DUO 7400 (Thermo-Scientific, Florida, USA). Unpreserved filtered samples were analyzed by IC for chloride, nitrate, and sulfate. Portions of filtered water were acidified (pH < 2) with trace metal-grade nitric acid and analyzed by iCAP-OES for a suite of elements (sodium, potassium, magnesium, calcium, aluminum, iron, manganese, and silica). Analytical precision was better than ± 0.02 milligrams per liter (mg L^{-1}) and quantitation limit was 0.02 mg L^{-1} for both IC and iCAP-OES.

Data Analysis

To facilitate comparing analytical results of dissolved ionic species to uncharged (i.e., silica) or multi-valence (i.e., aluminum and iron) dissolved species, concentration data are presented in units of micromoles per liter (µmol L^{-1}). To convert into micro-equivalents per liter (µeq L^{-1}), multiply by the appropriate ionic charge. Statistical analyses used the non-parametric Wilcoxon/Kruskal-Wallis rank sums test ($\alpha = 0.05$), followed by the Steel-Dwass method for all-pairs testing (which

controls the family-wise Type I error rate), or the Mann-Whitney U-test method for pair-wise testing (without Type I error control) for tests with only two treatment levels (e.g., with/without land disturbance; sandstone/sulfidic bedrock types). The significance criterion was set at the 5% Type-1 error probability ($\alpha = 0.05$). JMP® Pro 12 was used for all statistical testing.

HYDROGEOCHEMICAL ANALYSIS

Two sets of graphical analyses were done to explore causal relationships between water chemistry and geochemical processes in catchments. For graphical analysis, water chemistry and catchment parameter data were compiled and plotted using JMP® Pro 12. First, indications of silicate mineral weathering were evaluated based on correlations between concentrations of base cations versus dissolved silica. Second, indications of sulfidic mineral weathering were evaluated by examining the relationship between sulfate and pH, and the behavior of total aluminum in stream water samples. Three aspects of aluminum geochemistry were examined graphically. First, the solubility of total dissolved aluminum was plotted as a function of pH. Second, the contribution of total dissolved aluminum to stream water acidity was evaluated by plotting aluminum and proton equivalents versus the ratio of anion equivalents (sulfate, nitrate, chloride) to sum of base cation equivalents (calcium, magnesium, sodium and potassium). Because dissolved aluminum can exist as several ion-pair species in natural water (e.g., monomeric, labile, nonlabile, colloidal; Driscoll 1985), the exact distribution of equivalents is difficult to estimate. For this survey-level study, aluminum was assigned charge equivalence of one, the assumed net charge equivalence of all aqueous aluminum species existing in any given water sample. Ratios greater than one reflect excess anionic species requiring charge-balancing counterions, in the form of acidity. Lastly, the relationship between dissolved aluminum and dissolved silica concentrations was examined for

indications of aluminum solubility limits and secondary alumino-silicate mineral formation following bedrock weathering.

BEDROCK INFLUENCE ON STREAM WATER CHEMISTRY

Two statistical data analyses were performed to examine the influence of bedrock type on stream water. First, sites were segregated by corresponding underlying bedrock formation, and statistical testing was done comparing pooled sandstone bedrock formations (RFK, ELK, THD and COP) and sulfidic bedrock formation (ANK). Second, sites were segregated into those without (no) and with (yes) known natural land disturbances within their corresponding catchment. Lastly, a comparative evaluation of each chemical parameter was done to identify differences between catchments overlying sulfidic bedrock with and without known areas of natural land disturbances. The significance criterion was set at the 5% Type-1 error probability ($\alpha = 0.05$).

Results

Water Chemistry of Low-Order Steams

Conductivity, pH, ANC, and concentrations of dissolved ions and silica varied widely among water samples. Sample pH (lab-measured) ranged between 4.3 and 7.3; the median was 5.7. Water pH within the ranges 6.0–5.5, 5.5–5.0, 5.0–4.5 and < 4.5 was measured in 68, 40, 35 and 37 individual samples, respectively. Stream ANC concentrations ranged between –71 and +527 µeq L^{-1}; the median was +6 µeq L^{-1}. ANC between 0 and 20 µeq L^{-1}, and < 0 µeq L^{-1} was measured in 108 and 100 individual samples, respectively. Specific conductivity ranged from 9.0 to 75.5 µS cm^{-1} (micro-siemens per centimeter); the median was 18 µS cm^{-1}. Sulfate concentrations ranged between 2.9 and 98.0 µmol L^{-1}; the median was 25.4 µmol L^{-1}. Concentration ranges of other ions were as follows: nitrate (1.2 to 55.1 µmol L^{-1}), sodium (9.7 to 120 µmol L^{-1}), potassium (1.3 to

31.4 µmol L^{-1}), magnesium (1.4 to 91.8 µmol L^{-1}), and calcium (7.1 to 213 µmol L^{-1}). Concentration ranges of metals associated with mineral weathering were as follows: aluminum (< 0.3 to 22.7 µmol L^{-1}), iron (< 0.3 to 4.9 µmol L^{-1}, with one outlier result of 21.5 µmol L^{-1}), manganese (< 0.3 to 2.2 µmol L^{-1}), and silica (28 to 248 µmol L^{-1}).

Water chemistry of stream water from the 82 sites is summarized as site mean values in Table 1. Stream water with mean pH > 6 and mean ANC > 50 µeq L^{-1} were found at 36 and 15 sites, respectively. Stream sites with mean pH ≥ 6.0 were found in all sub-watersheds except ACC. LWPLPR sub-watershed had stream water with the highest pH (6.0 to 7.2) and ANC (29 to 522 µeq L^{-1}); eight of the 13 LWPLPR stream sites had pH > 6.8 and ANC > 175 µeq L^{-1}. In contrast, mean pH ≤ 5 was found in stream water from ACC (five sites), RP (six sites) and WCP (six sites) sub-watersheds. Mean ANC ≤ 0 µeq L^{-1} was found in stream water from ACC (five sites), RP (10 sites) and WCP (10 sites). Mean sulfate concentrations were highest within WCP sub-watershed; stream water from four catchments draining the southern slope of Anakeesta Ridge (Figure 5) had the highest mean sulfate concentrations, ranging from 63 to 74 µmol L^{-1}. Sixteen sites within sub-watersheds LWPLPR, RP and WCP had mean sulfate concentrations ≤ 10 µmol L^{-1}. The remaining 62 sites had mean sulfate concentrations in the range of 10 to 40 µmol L^{-1}. Mean total dissolved aluminum concentrations > 10 µmol L^{-1} were found within sub-watersheds with the lowest pH and ANC: ACC (3 sites); RP (4 sites); and WCP (3 sites). Aluminum concentrations greater than the current aquatic life ambient water quality criterion for chronic effects (0.087 mg L^{-1} = 3.2 µmol L^{-1}; USEPA 1988) were found in 24 sites (seven of which were found in the WCP sub-watershed). None of the stream sites exceeded the current acute toxicological effects criterion for aluminum (0.75 mg L^{-1} = 27.8 µmol L^{-1}; USEPA 1988). Mean total dissolved iron concentrations > 1.0 µmol L^{-1} generally were found in sub-watersheds where dissolved aluminum concentrations were

highest: ACC (2 sites); RP (4 sites); and WCP (3 sites). Dissolved silica concentrations generally increased with increasing water pH. Stream water with mean silica concentrations > 100 µmol L^{-1} and pH > 6.4 were found in sub-watersheds BFP (3 sites) and LWPLPR (10 sites). Conversely, stream water with mean silica concentrations < 50 µmol L^{-1} and pH < 5.1 were found within ACC (6 sites); MtLC (1 site); RP (1 site); and WCP (5 sites).

Mineral Weathering Indices

Figure 7 is a composite of graphs for sodium, calcium, magnesium and potassium (clock-wise from top-left) plotted versus dissolved silica. Sodium showed the strongest linear relationship to dissolved silica among all stream water sites (r^2 = 0.857 and approximately 1:2 slope [0.51]). The other three cations showed weak direct relationships with silica that were not statistically significant. Figure 8 depicts a non-linear, inverse relationship between total dissolved aluminum (in µmol L^{-1}) and pH in which aluminum solubility increases beginning at water pH < 5.5. Stream water with pH < 4.7 had the highest total aluminum concentrations (8 to 23 µmol L^{-1}), and stream water with pH > 5.5 had total dissolved aluminum at or below detection. Figure 9 shows the plot of measured equivalents of acid cations aluminum and hydronium versus the concentration ratios of anion to base cation concentrations (both in µmol L^{-1}). The subset of stream water with anion:cation ratios greater than one are predominantly those associated with the WCP sub-watershed and Anakeesta Ridge, and specifically with sites downgradient of known areas of land disturbances. Some sites within the WCP sub-watershed plotted to the left of the reference line at 1, suggesting that assuming net ionic charge of dissolved aluminum species was 1 was not valid.

The relationship between aluminum and dissolved silica in GRSM stream water samples is depicted in Figure 10. Concentrations of aluminum (in µM) were at or below detection limit when

silica concentrations were greater than 110 µM. At the time of sampling, conditions were such that aluminum solubility may have been controlled by stability of secondary aluminum minerals (e.g., lower order aluminum silicates, kaolinite, aluminum hydroxides, gibbsite, etc.) (Appelo and Postma 2005). Stream water from sites in the WCP sub-watershed had high total aluminum and relatively low silica concentrations. In contrast, stream water from sites in the LWPLPR sub-watershed had low to non-detectable aluminum concentrations and the highest silica concentrations. Excess silica at these low-elevation sites suggests high rates of soil/bedrock mineral weathering, and the non-linear covariance of aluminum and silica is consistent with the complexity of aluminum geochemistry in natural waters (Nordstrom 1982; Driscoll 1985; Stumm and Morgan 1991; Jones et al. 2011).

Sulfate concentrations did not correlate to stream water pH in this study (Figure 11). Concentrations between 2 and 45 µmol L^{-1} were measured in stream water samples with pH spanning three pH units (4.3 to 7.3). A small number of stream water samples plot as a distinct cluster with relatively low pH (4.3 to 5.0) and relatively high sulfate concentrations (54 to 98 µmol L^{-1}). These samples were collected at sites within the WCP sub-watershed, from catchments on the south and southeastern slopes of Anakeesta Ridge (Figure 6) and containing known areas of land disturbance (i.e., exposed sulfidic bedrock). Some sites overlying sulfidic bedrock ("W") had sulfate concentrations < 45 µmol L^{-1} (Figure 11). Exclusive of the sites associated with Anakeesta Ridge (Figure 6), the lack of systematic correspondence between stream water sulfate and pH (and by association, ANC) suggests that local, site-specific factors can modify the influence of sulfidic bedrock on stream water sulfate concentrations. Flum and Nodvin (1995) reported the results of the GRSM synoptic monitoring program, for which stream water was collected from numerous monitoring sites situated at a range of elevations throughout the GRSM. Sulfate data did not exhibit

definitive elevational trends across the entire GRSM, but they did show elevated stream water sulfate concentrations from sites overlying Anakeesta Formation bedrock at the 1300- to 1500-meter elevation band.

Bedrock and Land Disturbances

Statistical analysis of stream water data, based on bedrock type (sandstone versus sulfidic bedrock), found significant differences in mean concentrations of all chemical parameters ($p < 0.04$; most were significantly different at $p < 0.0001$) except calcium and total dissolved iron (Table 2). Stream water overlying sandstone had higher levels of pH, ANC, sodium, potassium and dissolved silica; stream water overlying sulfidic bedrock had higher levels of all other chemical parameters (notably: sulfate, total aluminum, iron and manganese). Statistical analysis of stream water data, based on presence/absence of land disturbance (exposed versus protected/unexposed bedrock), found significant differences in all chemical parameters ($p < 0.009$) except chloride (Table 2). Sites within catchments with known areas of natural land disturbances had stream water with higher levels of sulfate (by factor of 2), magnesium, and total aluminum, iron and manganese. Catchments without known land disturbance areas had stream water with higher levels of pH, ANC, nitrate, calcium, sodium, potassium and silica.

Discussion

Stream Water Acidity in Low-Order Streams

Stream water data revealed that approximately 1/3 of the study sites had acidified stream water (e.g., pH < 5.5 and ANC < 0 $\mu eq\ L^{-1}$; the approximate pH and ANC of air-equilibrated distilled water), and that the locations of those sites appeared to be randomly distributed spatially

throughout the study area. Stream water with pH < 5.5 was found in 40% of samples and at 38% of sites, and stream water with ANC < 0 µeq L^{-1} was found in 35% of samples and at 30% of sites. Sites with acidified stream water did not appear to be correlated to site elevation or to sub-watershed (Table 1). For example, sites located within a relatively narrow elevation band (1050 to 1650 meters a.m.s.l) had stream water with pH values spanning the entire range of measured pH (4.3 to 7) and ANC (–71 to +527 µeq L^{-1}). Conversely, no acidified stream water was found in low-elevation catchments in sub-watershed LWPLPR (elevations < 900 meters a.m.s.l) or in high-elevation catchments in sub-watersheds BFP (elevations 1490 to 1560 meters a.m.s.l) or NDW (elevation 1670 meters a.m.s.l). The "patchy" distribution of sites with acidified stream water is illustrated by examples of pairs of spatially adjacent catchments drained by streams having different water acidity.

Sites:	RtS6	RtS7	WtM11	WtGrass1	WtX1	WtA1	WtA6	WtA3
pH (std. units)	6.3	4.6	6.4	5.0	5.5	4.5	6.3	5.0
ANC (µeq L^{-1})	+46	–26	+128	–8	+1	–37	+41	–12

These observations suggest that ubiquitous atmospheric deposition in the GRSM (Weathers et al. 2006) was not the primary cause of stream water acidification in all cases, and that site-specific factors had a stronger influence on stream water chemistry at small spatial scales such as headwater sub-catchments.

The small variance in measured sulfate concentrations at the study sites overlying sandstone suggests that GRSM catchments not influenced by sulfidic bedrock discharge very consistent, base-flow sulfate concentration of approximately 10 to 14 µmol L^{-1}. This is consistent with sulfate concentrations (median 17 µmol L^{-1}; range < 42 µmol L^{-1} [N = 7,383]) measured in GRSM stream water collected throughout the GRSM for monitoring programs since the early 1990s (STORET

2016). The rates of atmospheric deposition of sulfate have been decreasing in the U.S. since the 1970s (NADP 2013), and precipitation and throughfall monitoring data from the GRSM have confirmed that atmospheric deposition of acidity and sulfate has decreased dramatically since the early 2000s (STORET 2016). However, stream water pH, ANC and sulfate concentrations generally have not responded to the decreasing deposition inputs to the GRSM catchments (Robinson et al. 2008; Gonzalez et al. 2015; Schwartz et al. 2016). The concentrations of sulfate in stream water have remained relatively constant due in part to absorption and assimilation of sulfate inputs by soil organic matter and microbial biomass in the forest floor (Autry and Fitzgerald 1991; Eriksen 1996; Giesler et al. 2005). Thus, the catchment soil acts as a large sulfate buffer, and likely releases a consistent amount of sulfate to the soil solution and stream water in response to dynamic changes in nutrient requirements by forest vegetation. Based on a fairly homogenous assemblage of forest vegetation within catchments of the GRSM, it is reasonable to expect sulfate concentrations to be fairly consistent in stream water from GRSM catchments that are not influenced by sulfidic bedrock or episodic storm-induced acidification (Hooper and Christophersen 1992; Lawrence 2002; Deyton et al. 2009; Neff et al. 2013).

Influence of Bedrock on Stream Water Chemistry

SANDSTONE BEDROCK

Stream water overlying sandstone had statistically higher concentrations of sodium, potassium and silica ($p < 0.004$) than stream water overlying sulfidic bedrock. Calcium concentrations in stream water overlying both bedrock types were not statistically different from each other ($p = 0.455$). Weathering of soil and bedrock minerals releases constituents of the original material, which depending on the extent of reaction can result in dissolved constituents and solid-phase secondary minerals (from incongruent dissolution) (Appelo and Postma 2005). In general, byproducts of

weathering of non-sulfidic rock include dissolved aluminum species and silica from crystal lattices, base cations from interlayer or lattice substitution sites, and trace elements associated with mineral heterogeneity in the solid-solution or structural impurities in the mineral crystal lattices (Essington 2015). Depending on the composition of the original material and the stoichiometry of weathering reactions, weathering byproducts may be found in corresponding molar ratios. The stream water data from sites overlying sandstone indicates the stream water chemistry at those sites is most directly influenced by weathering sandstone bedrock minerals.

Dissolved silica in stream water is evidence for silicate mineral dissolution (White and Brantley 2003; Farmer et al. 2005; Johnson-Maynard et al. 2005). Silica concentrations have an upper bound based on water pH, alkalinity and the presence of reactive metals such as aluminum and iron (Nesbitt et al. 1997; Appelo and Postma 2005). These factors determine the saturation indices of potential silicate minerals that may form (e.g., phytolith [Farmer et al. 2005], amorphous silica; kaolinite and halloysite if dissolved aluminum is present [Burns 1989; Appelo and Postma 2005], and jarosite if dissolved iron is present [Jamieson et al. 2005]). The positive linear correlation between sodium and dissolved silica concentrations was interpreted as evidence of ubiquitous silicate mineral weathering across all study catchments. The data were checked for indications of other sources of sodium (independent of silica). The absence of a marine source of sodium was confirmed by a lack of correlation with chloride ion (data not shown). Ignoring other catchment processes that can act as sinks or sources of dissolved silica (Taylor and Velbel 1991), a simplistic interpretation of the strong correlation ($r^2 = 0.86$) and nearly 1:2 slope (m = 0.51) observed in the sodium-silica plot (Figure 7) is the incongruent weathering reaction of sodium-rich plagioclase feldspar type minerals (e.g., albite) to kaolinite (Appelo and Postma 2005):

$$2\,Na(AlSi_3)O_8 + 2H^+ + 9\,H_2O \rightarrow Al_2Si_2O_5 + 2\,Na^+ + 4\,Si(OH)_4^\circ$$

The corresponding weathering reaction of a calcium-rich plagioclase endmember (e.g., anorthite) would yield a 1:1 molar ratio of calcium to dissolved silica (regression slope = 1), and a potassium-rich feldspar endmember (e.g., microcline) would yield a 1:2 molar ratio of potassium to dissolved silica (regression slope = 0.5) (Appelo and Postma 2005). Since the slopes of the potassium-silica and calcium-silica plots are lower than stoichiometric ideal, the mineral chemistry of parent material and soil in the catchments may be more similar to the sodium-rich albite endmember. If stream flow could be measured, the flux of sodium and silica leaving the catchments could be calculated, and (since sodium as a by-product of mineral weathering is rarely reincorporated into secondary minerals) weathering rates of feldspar type minerals in the catchments could be estimated (Johnson-Maynard et al. 2005).

SULFIDIC BEDROCK

Stream water acidification was not restricted to sites underlying sulfidic bedrock. Examples of stream water across the entire range of measured pH were found at sites overlying sulfidic or sandstone bedrock. This is expected given that the GRSM has historically received high loads of acidic pollutants via atmospheric deposition (Weathers et al. 2006; Cai et al. 2011). Catchment acidification is accelerated by the interaction between four factors: (1) the rate of atmospheric deposition, (2) the physical and biogeochemical characteristics of soil in the catchment, (3) the composition and reactivity of bedrock minerals, and (4) the size of the catchment (drainage area and tree canopy area) (Matschullat et al. 1992). Factor #1 determines the rate of external inputs of acid (protons) and ions into the catchment. To some extent, Factor #3 can contribute to catchment acidification if bedrock minerals such as sulfides weather to produce acidity byproducts (e.g., protons, aluminum, sulfate). Factors #2 and #4 (and in some scenarios, Factor #3) can act as acidification modulators by neutralizing acid inputs or dilution of inputs by large drainage areas.

Statistical analysis of this study's stream water data showed that pH and ANC were significantly lower ($p < 0.001$) at sites overlying sulfidic bedrock (mean pH 5.5 and mean ANC 5.8 µeq L^{-1}) than at sites overlying sandstone (mean pH 6.0 and mean ANC 61.6 µeq L^{-1}) (Table 2). Sulfidic bedrock accounted for an 0.5-unit decrease in mean pH and a 55.8 µeq L^{-1} decrease in mean ANC, suggesting that underlying sulfidic bedrock has some level of influence on stream water acidity in the GRSM. Total aluminum, sulfate, base cations, and dissolved silica in stream water showed similar responses to bedrock type (Table 2). Statistical analysis showed that stream water overlying sulfidic bedrock had statistically higher concentrations of total aluminum, sulfate, and magnesium ($p < 0.022$) than stream water overlying sandstone. These differences in pH, ANC, and aluminum and sulfate concentrations are consistent with oxidation of sulfide minerals in the Anakeesta Formation bedrock (e.g., Huckabee et al. 1975; Maas 1976; Bacon and Maas 1979)

Influence of Land Disturbance on Stream Water Chemistry

A separate statistical analysis, based on presence/absence of known areas of land disturbance (Table 2), showed that stream water pH and ANC were statistically lower ($p < 0.001$) at sites in catchments containing known areas of land disturbances (mean pH 4.7 and mean ANC –29.3 µeq L^{-1}) than at sites in catchments without land disturbance (mean pH 5.9 and mean ANC +35.6 µeq L^{-1}). Land disturbance accounted for a 1.2-unit decrease in mean pH and a 64.9 µeq L^{-1} decrease in mean ANC. Thus, land disturbance (i.e., exposed bedrock) appeared to affect stream water acidity more effectively than undisturbed, soil-protected sulfidic bedrock. It is notable that of the 12 sites that were downgradient of known areas of land disturbance (exposed bedrock), seven were located in catchments that overly sulfidic bedrock and five were in catchments that overly sandstone (Table 1). A statistical comparison of the two types of exposed bedrock showed that

stream water pH and ANC was significantly lower ($p < 0.0001$) at sites downgradient of exposed sulfidic bedrock (mean pH 4.6 and ANC –34.2 µeq L^{-1}) than at sites downgradient of exposed sandstone (mean pH 5.1 and mean ANC –5.5 µeq L^{-1}). Thus, observed differences in stream water pH and ANC attributable to presence/absence of land disturbance (ΔpH = –1.2 units and ΔANC = –64.9 µeq L^{-1}) would be even larger if the statistical comparison was between stream water in catchments without land disturbance and stream water downgradient of exposed *sulfidic* bedrock.

Influence of Spatial Scale on Geochemical Interpretation

Several investigators have attempted to systematically describe or classify spatially variability of stream water chemistry based on catchment characteristics and bedrock weathering. Examples of such classifications for the Southern Appalachian region include work by Flum and Nodvin (1995), who introduced the "water quality districts" concept to help organize observed spatial differences in stream water chemistry in the GRSM. They assigned each of the 45 watersheds of the GRSM (Parker et al. 1990) to one of six districts defined primarily by geologic substrate. Sullivan et al. (2007) used a five-class "geologic sensitivity classification" scheme and a "landscape sensitivity classification" scheme, based on composition and weathering properties of rock types underlying their 909 study sites, to organize observed stream water chemistry data. Their scheme was an extension of a three-class system developed by Peper et al. (1995). The difference between regional studies (e.g., Kaufmann et al. 1991; Johnson and Lindburg 1992; Odom et al. 2003), and this study is spatial scale. Whereas such broad-scale regional studies assess the aggregate water chemistry of high-order stream and river systems, geochemical details at the catchment and sub-catchment scale have been preserved in this study by focusing on first- and second-order streams. The advantage of this approach was demonstrated by Weyer et al. (2014)

who analyzed a large dataset of soil solution, groundwater, and stream water chemistry, and determined that 89% of the variance in their water chemistry could be ascribed to three types of biogeochemical processes: (1) oxidation-reduction reactions; (2) acid-induced soil-formation processes; and (3) mineral weathering reactions. Their study catchment (420 hectares) was over an order of magnitude larger than the catchment areas associated with our study, yet they were able to distinguish geochemical details from their analysis. Our relatively limited dataset of only stream water chemistry was sufficient for discerning causal relationships between geochemical processes and stream water chemistry because the drainage areas of the study catchments were < 30 hectares.

Conclusions

Based on our data, it is concluded that weathering of exposed sulfidic bedrock was responsible for highly acidified stream water observed at specific locations, and weathering of minerals associated with sandstone bedrock at all other study locations was the primary process responsible for the "baseline" stream water chemistry observed at the majority of sites. Water chemistry (e.g., acidity and inorganic ions) of the sampled first- and second-order streams varied spatially within the study area, but sites generally clustered into three groups based on similar water chemistry. Indicators of specific weathering reactions were found in the water chemistry data, and differences in weathering indices among the stream water sites were related to underlying bedrock type and the existence of known areas of natural land disturbances that have exposed fresh (highly reactive) surfaces of bedrock directly to the atmosphere.

Significant differences in water chemistry were found between streams in catchments with and without known areas of natural land disturbances (i.e., exposed bedrock scars). Natural land

disturbances in the GRSM tend to occur in high-elevation, steep-slope catchments associated with sulfidic slate/shale bedrock of the Anakeesta Formation. The sulfidic mineral content in the freshly exposed bedrock weathers rapidly upon exposure to the atmosphere, generating oxidation byproducts (acidity, iron and aluminum, sulfate, etc.) which were evident in the stream water samples collected from those catchments. In stream water from catchments without known natural land disturbances, the water chemistry signature (i.e., the combination of pH, ANC, conductivity (surrogate for total dissolved ions), sulfate and metals concentrations) was similar to that in stream water monitoring samples collected in the GRSM since the early 1990s. The water chemistry signature of stream water in undisturbed catchments is consistent with interactions between atmospheric deposition, precipitation and catchment hydrology, and soil minerals and organic matter. Most notably, the water chemistry signature of stream water in undisturbed catchments overlying sulfidic bedrock was similar to that of stream water in catchments overlying sandstone. The influence of sulfidic mineral weathering on stream water chemistry is manifested primarily and most strongly in catchments with known land disturbances (i.e., exposed bedrock).

References

Appelo, C.A.J., and D. Postma (2005). Geochemistry, Groundwater and Pollution, 2nd Edition. A.A. Balkema Publishers (a member of Taylor & Francis Group plc); Leiden, The Netherlands.

Autry, Andrew R. and John W. Fitzgerald (1991). Organosulfur formation in forest soils: Site comparison of kinetic parameters. Soil Biology and Biochemistry, 23(7), 689-693. GRef

Bacon, J.R. and Richard P. Maas (1979). Contamination of Great Smoky Mountains Trout Streams by Exposed Anakeesta Formations. Journal of Environmental Quality, 8(4):538-543. GRef553

Billett, M.F. and M.S. Cresser (1992). Predicting stream-water quality using catchment and soil chemical characteristics. Environmental Pollution 77(2-3):263-268. GRef681

Brantley, Susan L. (2008). Kinetics of mineral dissolution. Chapter 5 in: Susan L. Brantley, James D. Kubicki, and Art F. White (2008). Kinetics of Water-Rock Interaction. Springer, New York. Pp. 151-210. GRef009

Brantley, Susan L., M.I. Lebedeva, and Ekaterina Bazilevskaya (2014). Relating Weathering Fronts for Acid Neutralization and Oxidation to pCO_2 and pO_2. Chapter 6 in: Holland, Heinrich D. and Karl K. Turekian (2014). Treatise on Geochemistry, Second Edition. Elsevier, Oxford, United Kingdom. Pp. 151-210. GRef1063

Burns, Douglas A. (1989). Speciation and equilibrium relations of soluble aluminum in a headwater stream at base flow and during rain events. Water Resources Research, 25(7):1653-1665. GRef520

Cai, M. J.S. Schwartz, R.B. Robinson, S.E. Moore, and M.A. Kulp (2010). Long-term effects of acidic deposition on water quality in a high-elevation Great Smoky Mountains National Park watershed: Use of an ion input-output budget. Water, Air, & Soil Pollution 209:143-156.

Cai, Meijun, John S. Schwartz, R. Bruce Robinson, Stephen E. Moore, and Matt A. Kulp (2011). Long-term annual and seasonal patterns of acidic deposition and stream water quality in a Great Smoky Mountains high-elevation watershed. Water, Air, & Soil Pollution, 219(1-4), 547-562. GRef479

Cai, M., A.M. Johnson, J.S. Schwartz, S.E. Moore, and M.A. Kulp (2012). Soil acid-base chemistry of a high-elevation forest watershed in the Great Smoky Mountains National Park watershed: Influences of acid deposition. Water, Air, & Soil Pollution 223:289-303.

Cook, Robert B., J.W. Elwood, R.R. Turner, M.A. Bogle, Patrick J. Mulholland, A.V. Palumbo (1994). Acid-base chemistry of high-elevation streams in the Great Smoky Mountains. Water, Air, and Soil Pollution 72:331-356. GRef559

Deviney, Frank A., Karen C. Rice, and George M. Hornberger (2006). Time series and recurrence interval models to predict the vulnerability of streams to episodic acidification in Shenandoah National Park, Virginia. Water Resources Research, 42(9), W09405. GRef1097

Deyton, Edwin B., John S. Schwartz, R. Bruce Robinson, Keil J. Neff, Stephen E. Moore and Matt A. Kulp (2009). Characterizing episodic stream acidity during stormflows in the Great Smoky Mountains National Park. Water, Air, and Soil Pollution, 196(1-4), 3-18. GRef482

Driscoll, Charles T. (1985). Aluminum in acidic stream waters: Chemistry, transport, and effects. Environmental Health Perspectives 63:93-104. GRef923

Environmental Systems Research Institute (ESRI). (2017). ArcGIS Online. Redlands, CA. Found online at: www.esri.com/software/arcgis/arcgisonline

Eriksen, Jørgen (1996). Incorporation of S into soil organic matter in the field as determined by the natural abundance of stable S isotopes. Biology and Fertility of Soils, 22(1-2), 149-155.GRef745

Essington, Michael E. (2015). Soil and Water Chemistry: An Integrative Approach (2nd Edition). CRC Press, Boca Raton, Florida.

Farmer, V.C., E. Delbos, and J.D. Miller (2005). The role of phytolith formation and dissolution in controlling concentrations of silica in soil solutions and streams. Geoderma, 127(1-2):71-79. GRef041

Flum, T. and Stephen C. Nodvin (1995). Factors affecting stream water chemistry in the Great Smoky Mountains, USA. Water, Air, and Soil Pollution, 85(3):1707-1712. GRef100

Giesler, Reiner, Carl Magnus Mörth, Elin Mellqvist, and Peter Torssander (2005). The humus layer determines SO_4^{2-} isotope values in the mineral soil. Biogeochemistry, 74(1):3-20. GRef1055

Gonzalez, Adrian M., Dr. John S. Schwartz, and Matt Kulp (2015). Geochemistry in a high-elevation watershed responds to reductions in acid-pollutant emissions? 2015 World Environmental & Water Resources Congress (EWRI), Austin, Texas, 17-21 May 2015. Platform presentation 19 May 2015.

Gonzalez, Adrian Miguel (2018). Biogeochemistry of Sulfur in Small Forested Catchments of the Great Smoky Mountains National Park. Ph.D. Dissertation. University of Tennessee, Knoxville; in progress.

Grathwohl Peter, Hermann Rügner, Thomas Wöhling, Karsten Osenbrück, Marc Schwientek, Sebastian Gayler, Ute Wollschläger, Benny Selle, Marion Pause, Jens-Olaf Delfs, Matthias Grzeschik, Ulrich Weller, Martin Ivanov, Olaf A. Cirpka, Ulrich Maier, Bertram Kuch, Wolfgang Nowak, Volker Wulfmeyer, Kirsten Warrach-Sagi, Thilo Streck, Sabine Attinger, Lars Bilke, Peter Dietrich, Jan H. Fleckenstein, Thomas Kalbacher, Olaf Kolditz, Karsten Rink, Luis Samaniego, Hans-Jörg Vogel, Ulrike Werban and Georg Teutsch, 2013. Catchments as reactors: a comprehensive approach for water fluxes and solute turnover. Environmental Earth Sciences 69(2):317-333. GRef416

Hadley, Jarvis B. and Richard Goldsmith (1963). Geology of the Eastern Great Smoky Mountains North Carolina and Tennessee. Geological survey professional paper 349-B. U.S. Department of the Interior, U.S. Government Printing Office, Washington, D.C.

Hooper, Richard P. and Nils Christophersen (1992). Predicting episodic stream acidification in the southeastern United States: Combining a long-term acidification model and the end-member mixing concept. Water Resources Research, 28(7), 1983-1990. GRef956

Huckabee, John W., C. Phillip Goodyear, and Ronald D. Jones (1975). Acid Rock in the Great Smokies: Unanticipated Impact on Aquatic Biota of Road Construction in Regions of Sulfide Mineralization. Transactions of the American Fisheries Society, 104(4):677-684. GRef816

Jamieson, Heather E., Clare Robinson, Charles N. Alpers, D. Kirk Nordstrom, Alexei Poustovetov, and Heather A. Lowers (2005). The composition of coexisting jarosite-group minerals and water from the Richmond Mine, Iron Mountain, California. U.S. Geological Survey (USGS) Staff Published Research. Paper 475. GRef993b

Johnson, Dale W. and Steven E. Lindberg (ed.) (1992). Atmospheric deposition and forest nutrient cycling: A synthesis of the Integrated Forest Study. Springer-Verlag, New York, NY. GRef1018

Johnson-Maynard, J.L., R.C. Graham, P.J. Shouse, and S.A. Quideau (2005). Base cation and silicon biogeochemistry under pine and scrub oak monocultures: implications for weathering rates. Geoderma, 126(3-4):353-365. GRef054

Jones, Adele M., Richard N. Collins, and T. David Waite (2011). Mineral species control of aluminum solubility in sulfate-rich acidic waters. Geochimica et Cosmochimica Acta, 75(4):965-977. GRef241

Kaufmann, Philip R., Alan T. Herlihy, Mark E. Mitch, Jay J. Messer, and W. Scott Overton (1991). Stream chemistry in the eastern United States: 1. Synoptic survey design, acid-base status, and regional patterns. Water Resources Research, 27(4):611-627. GRef1002

King, P.B., Hadley, J.B., Neuman, R.B., and Hamilton, W.B. (1958), Stratigraphy of the Ocoee Series, Great Smoky Mountains, Tennessee and North Carolina: Geological Society of America Bulletin, v. 69, no. 8, p. 947-966.

King, Philip B. (1964). Geology of the Central Great Smoky Mountains Tennessee. Geological Survey Professional Paper No. 349-C. U.S. Department of the Interior, U.S. Government Printing Office, Washington, D.C.

King, P.B., Neuman, R.B., and Hadley, J.B. (1968), Geology of the Great Smoky Mountains National Park, Tennessee and North Carolina: U.S. Geological Survey Professional Paper 587, 23 p., and 1:125,000-scale map.

Lawrence, G.B. (2002). Persistent episodic acidification of streams linked to acid rain effects on soil. Atmospheric Environment, 36, 1589-1598. GRef650

LeComte, Karina L., Andrea I. Pasquini, and Pedro J. Depetris (2005). Mineral Weathering in a Semiarid Mountain River: Its assessment through PHREEQC inverse modeling. Aquatic Geochemistry, 11(2):173-194. GRef778

Lindberg, Steven E. and J.G. Owens (1992). Throughfall studies of deposition to forest edges and gaps in montane ecosystems. Biogeochemistry, 19(3):173-194. GRef1026

Maas, Richard P. (1976). Characterization of water chemistry of Anakeesta pyrite affected streams in the Great Smoky Mountains National Park. Master's thesis: Western North Carolina University.

Matschullat, J., H. Andreae, D. Lessmann, V. Malessa, and U. Siewers (1992). Catchment acidification – from the top down. Environmental Pollution, 77(2-3), 143-150. GRef685

National Atmospheric Deposition Program (NADP) (2013). National Atmospheric Deposition Program 2012 Annual Summary. NADP Data Report 2013-01. Illinois State Water Survey, University of Illinois at Urbana-Champaign, IL.

National Parks Service (NPS) (2015). Webpage "Program Brief: Inventory and Monitoring." U.S. Department of the Interior website URL: https://science.nature.nps.gov/im/ (accessed July 28, 2017).

Neff, Keil J., John S. Schwartz, Stephen E. Moore, and Matt A. Kulp (2013). Influence of basin characteristics on baseflow and stormflow chemistry in the Great Smoky Mountains National Park. Hydrological Processes 27:2061-2074. GRef484

Nesbitt, H. Wayne, Christopher M. Fedo, and Grant M. Young (1997). Quartz and feldspar stability, steady and non-steady-state weathering, and petrogenesis of siliciclastic sands and muds. The Journal of Geology, 105, 173-191.

Nordstrom, Darrell Kirk (1982). The effect of sulfate on aluminum concentrations in natural waters: some stability relations in the system Al2O3-SO3-H2O at 298 K. Geochimica et Cosmochimica Acta, 46(4):681-692. GRef240

Odom, Kenneth Ray (2003). Assessment and Redesign of the Synoptic Water Quality Monitoring Network in the Great Smoky Mountains National Park. Ph.D. Dissertation. University of Tennessee, Knoxville. http://trace.tennessee.edu/utk_graddiss/2193

Parker, Charles R. and David W. Pipes (1990). Watersheds of the Great Smoky Mountains National Park: A Geographic Information System Analysis. Research/Resources Management Report SER-91/01. Uplands Field Research Laboratory, GSMNP, Gatlinburg, TN 37738; November 1990.

Peper, J.D., A.E. Grosz, T.H. Kress, T.K. Collins, G.B. Kappesser, and C.M. Huber (1995). Acid deposition sensitivity map of the Southern Appalachian Assessment Area: Virginia, North Carolina, South Carolina, Tennessee, Georgia, and Alabama. U.S. Geological Survey On-line Digital Data Series Open-File Report 95-810.

Robinson, R. Bruce, Thomas W. Barnett, Glenn R. Harwell, Stephen E. Moore, Matt A. Kulp, and John S. Schwartz (2008). pH and acid anion time trends in different elevation ranges in the Great Smoky Mountains National Park. Journal of Environmental Engineering, 134(9):800-808. GRef1014

Ryan, Patrick T. (1989). "Debris Slides and Flows on Anakeesta Ridge within the Great Smoky Mountains National Park, Tennessee, U.S.A. " Master's Thesis, University of Tennessee, 1989. http://trace.tennessee.edu/utk_gradthes/2493 GRef857

Schwartz, John S., Meijun Cai, Matt A. Kulp, Stephen E. Moore, Becky Nichols and Charles Parker (2014). Biological effects of stream water quality on aquatic macroinvertebrates and fish communities within the Great Smoky Mountains National Park. U.S. Department of the Interior, National Park Service (NPS) Natural Resources Report (NRR) No. 778; August 2013. GRef584

Schwartz, John S., Adrian M. Gonzalez and Matt A. Kulp (2016). Geochemistry in a High-Elevation Watershed Responds to Reductions in Acid-Pollutant Emissions. Abstract No. presented at 2016 Fall Meeting, American Geophysical Union (AGU), San Francisco, Calif., USA; 12-16 Dec.

Shubzda, J., Steven E. Lindberg, C.T. Garten, and S.C. Nodvin (1995). Elevational trends in the fluxes of sulphur and nitrogen in throughfall in the Southern Appalachian Mountains: Some surprising results. Water, Air and Soil Pollution, 85(4):2265-2270. GRef487

Silsbee, David G. and Gary L. Larson (1982). Water quality of streams in the Great Smoky Mountains National Park. Hydrobiologia 89(2):97-115. GRef098

Southworth, Scott, Art Schultz, and Danielle Denenny (2004). Generalized Geologic map of Bedrock Lithologies and Surficial Deposits in the Great Smoky Mountains National Park region, Tennessee and North Carolina. U.S. Geological Survey Open File Report 2004-1410, scale 1:100,000.

Southworth, Scott, Art Schultz and Danielle Denenny (2005). Geologic map of the Great Smoky Mountains National Park Region, Tennessee and North Carolina. U.S. Geological Survey Open-File Report 2005-1225. Online at: http://pubs.usgs.gov/of/2005/1225/OF2005-1225_map.pdf

Standard Methods (1999). Standard Methods for the Examination of Water and Wastewater, 20th edition. Editors: Lenore S. Clescerl (WEF, chair), Arnold E. Greenberg (APHA), and Andrew D. Eaton (AWWA). Published jointly by: American Public Health Association (APHA), American Water Works Association (AWWA), and Water Environment Federation (WEF). Washington, D.C.

STORET (STOrage and RETrieval) Data Warehouse (2016). U.S. Environmental Protection Agency Web site. http://www.epa.gov/storet. Accessed August 8, 2016.

Stumm, Werner and James J. Morgan (1981). Aquatic Chemistry: An introduction emphasizing chemical equilibria in natural waters (2nd Edition). Wiley-Interscience, New York.

Sullivan, Timothy J., James R. Webb, Kai U. Snyder, Alan T. Herlihy, and Bernard J. Cosby (2007). Spatial distribution of acid-sensitive and acid-impacted streams in relation to watershed features in the Southern Appalachian Mountains. Water, Air, and Soil Pollution, 182(1):57-71. GRef017

Sumner, Malcolm E. (ed.) (2000). Handbook of Soil Science. CRC Press, Boca Raton, Florida.

Taylor, Allan B., and Michael Anthony Velbel (1991). Geochemical mass balances and weathering rates in forested watersheds of the southern Blue Ridge. II. Effects of botanical uptake terms. Geoderma, 51(1):29-50. GRef049

Thornberry-Ehrlich, Trista (2008). Great Smoky Mountains National Park Geologic Resource Evaluation Report. National Resource Report NPS/NRPC/GRD/NRR-2008/048. National Park Service, Denver, Colorado; NPS D-626, September 2008.

USEPA (1988). Ambient Water Quality Criteria for Aluminum. Report No. EPA 440/5-86/008. Office of Research and Development Environmental Research Laboratory, Duluth, MN. August, 1988.

Weathers, Kathleen C., Samuel M. Simkin, Gary M. Lovett and Steven E. Lindberg (2006). Empirical modeling of atmospheric deposition in mountainous landscapes. Ecological Applications 16(4):1590-1607. GRef522

Weyer, Christina, Stefan Peiffer, Kerstin Schulze, Werner Borken and Gunnar Lischeid (2014). Catchments as heterogeneous and multi-species reactors: An integral approach for identifying biogeochemical hot-spots at the catchment scale. Journal of Hydrology 519(Part B):1560-1571. GRef983

White, Art F. and Susan L. Brantley (2003). The effect of time on the weathering of silicate minerals: why do weathering rates differ in the laboratory and field? Chemical Geology, 202(3-4):479-506. GRef779

Winston, R.B. (2000). Graphical User Interface for MODFLOW, Version 4: U.S. Geological Survey Open-File Report 00-315, 27 p.

Chapter 4 Appendix

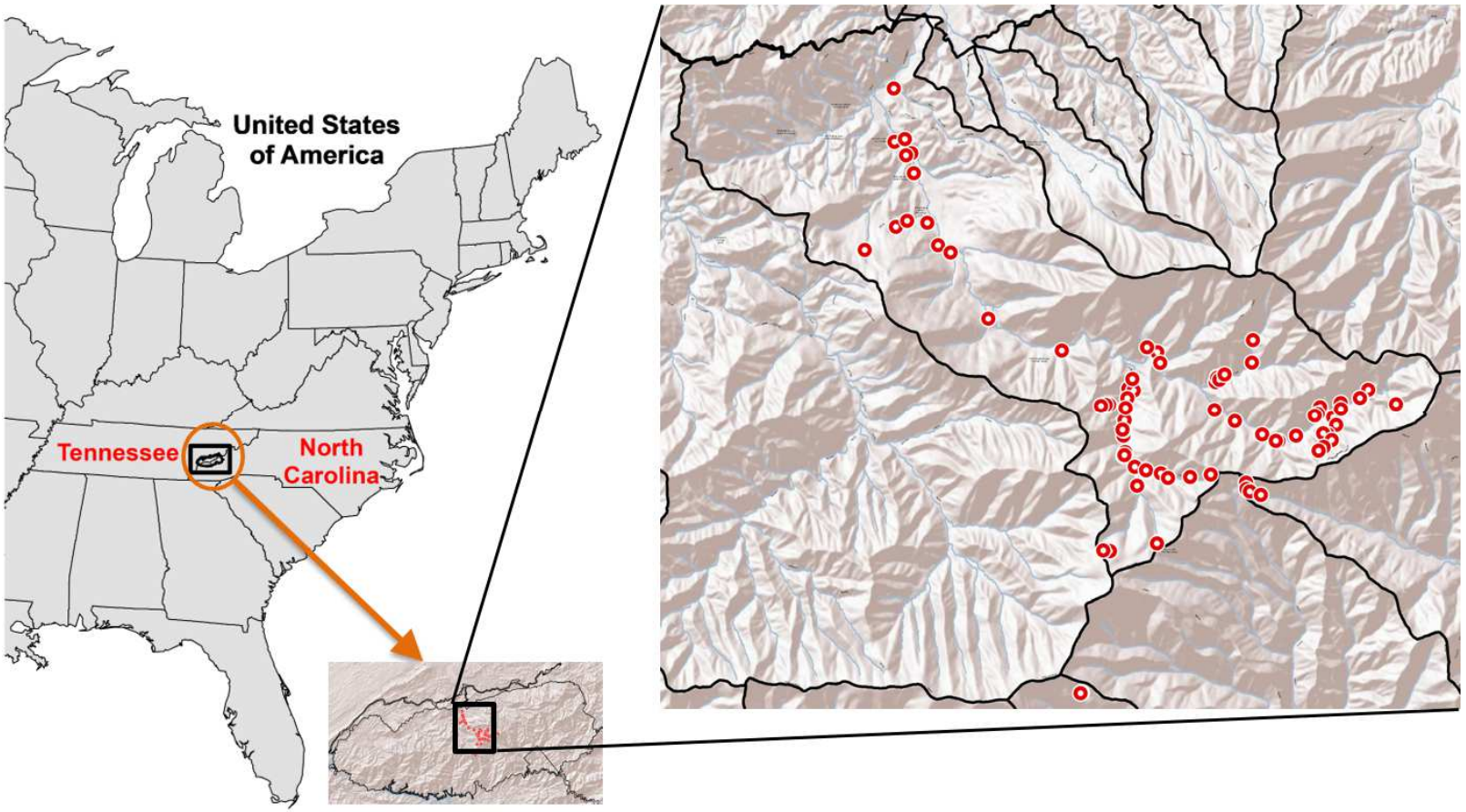

Figure 5. Location of the Great Smoky Mountains National Park (GRSM), and detailed map of stream sampling sites. Major GRSM watersheds are outlined in black, including the West Prong Little Pigeon River watershed containing the majority of stream sampling sites.

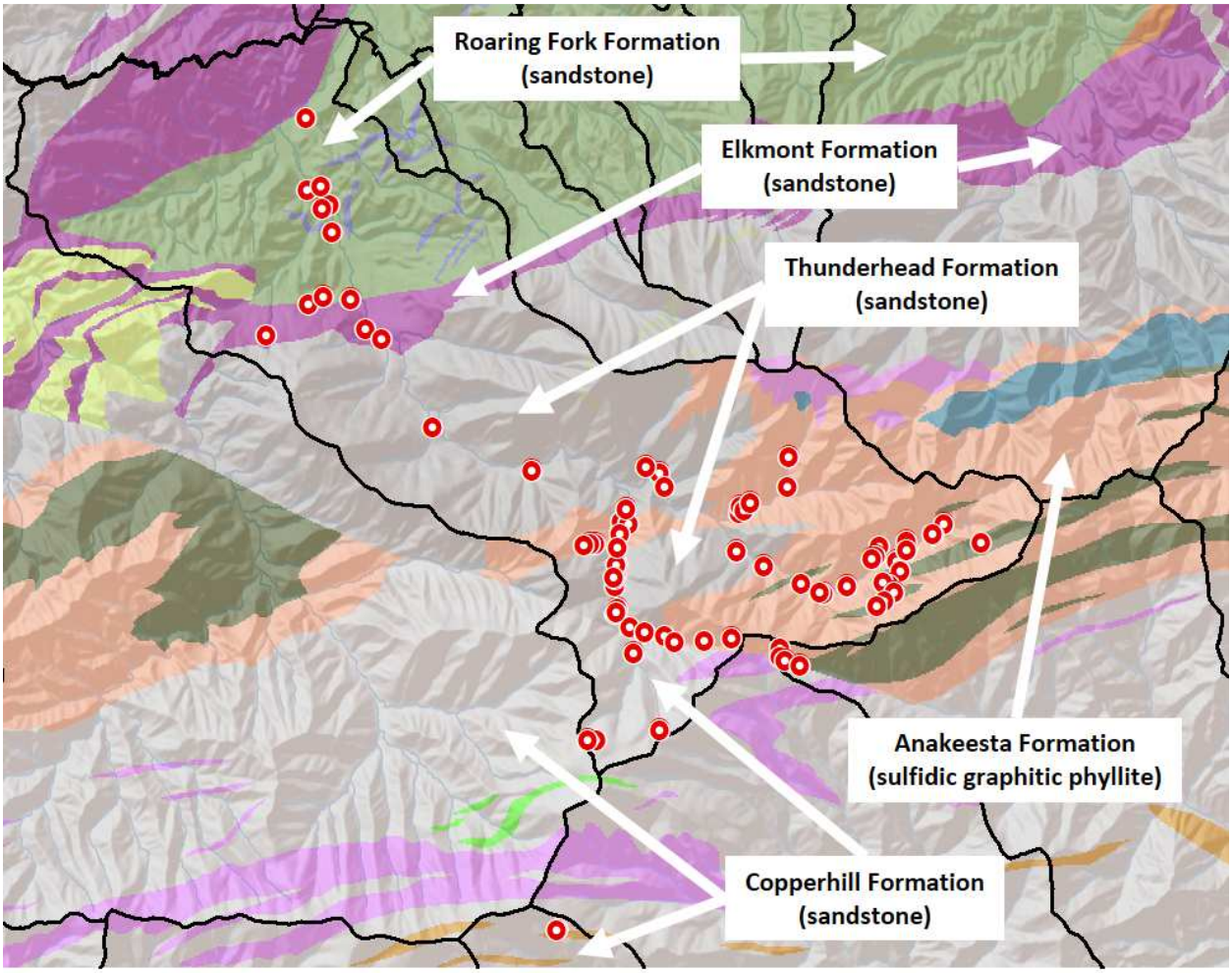

Figure 6. Locations of 82 stream water sites in the central quadrant of the Great Smoky Mountains National Park. The West Prong Little Pigeon River watershed is outlined in black. Five bedrock formations are identified (four predominantly sandstone and one sulfidic phyllite).

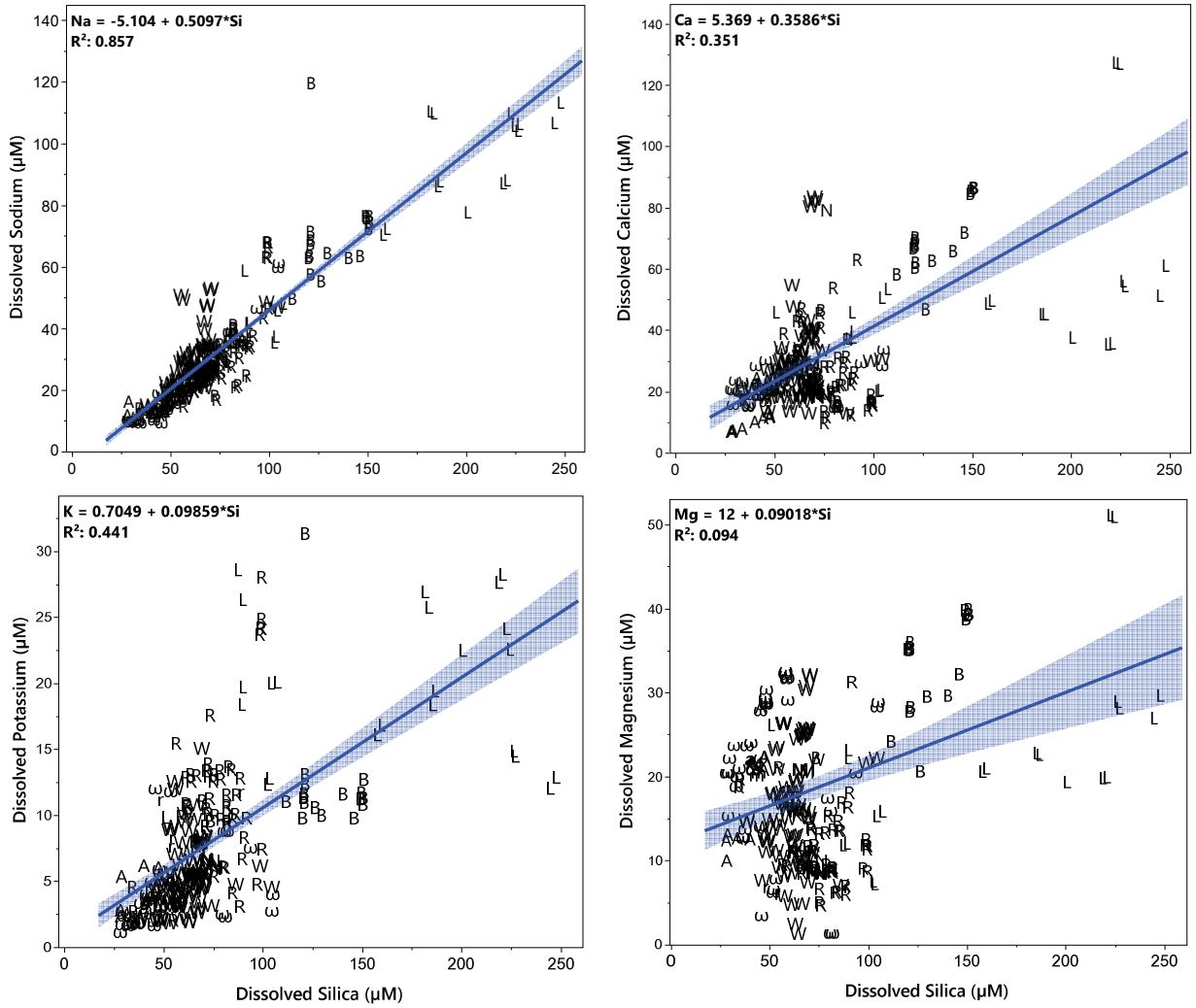

Figure 7. Dissolved sodium, calcium, potassium and magnesium versus dissolved silica concentrations (micromoles per liter) in stream water samples. Letters represent the sub-watersheds associated with the stream water sites (see text for definitions). Lower case letters represent stream water sites in catchments containing known areas of natural land disturbance. Linear correlation analysis results shown in each panel.

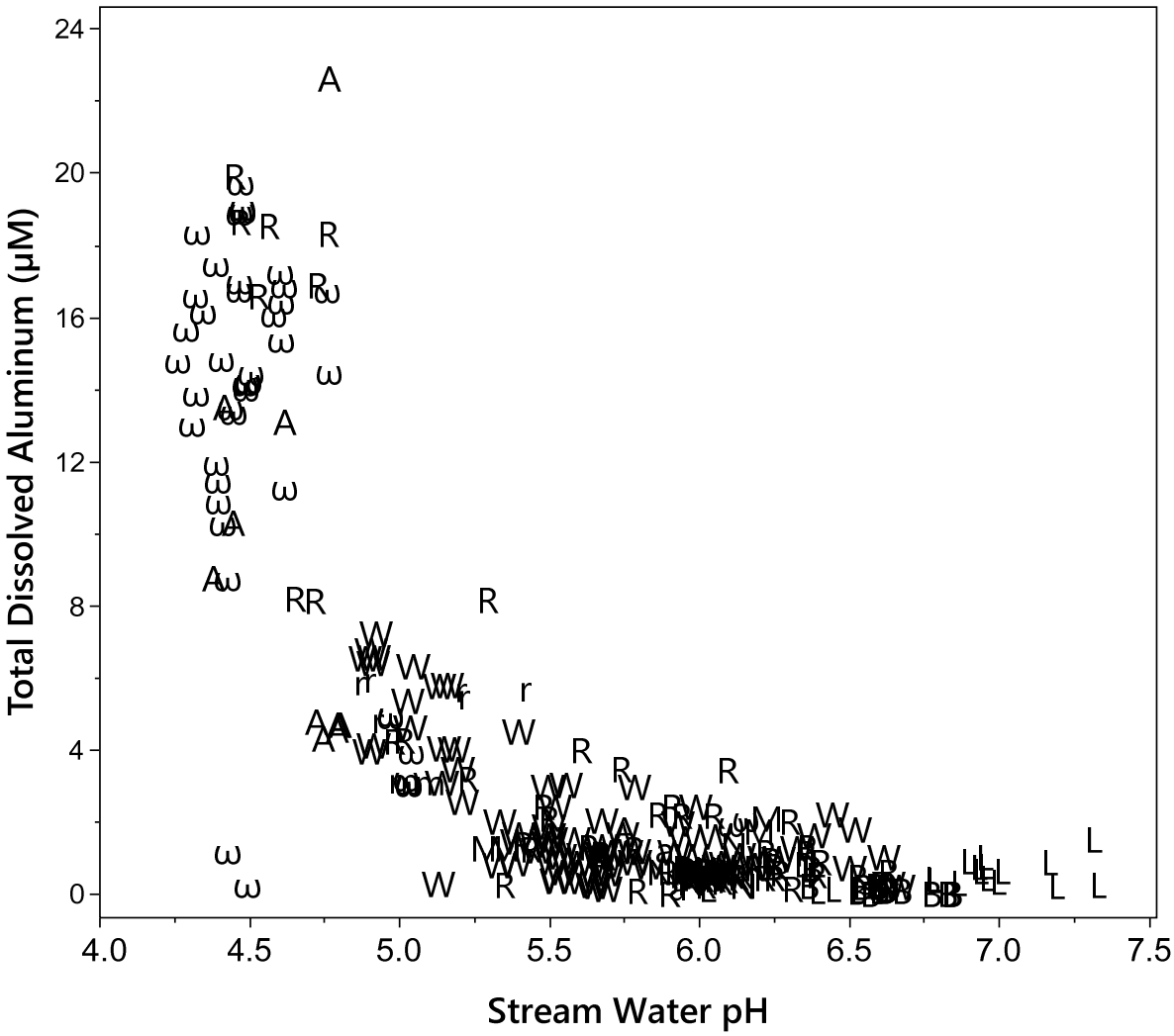

Figure 8. Total dissolved aluminum concentration (micromoles per liter) versus stream water pH. Letters represent the sub-watersheds associated with the stream water sites (see text for definitions). Lower case letters represent stream water sites in catchments containing known areas of natural land disturbance.

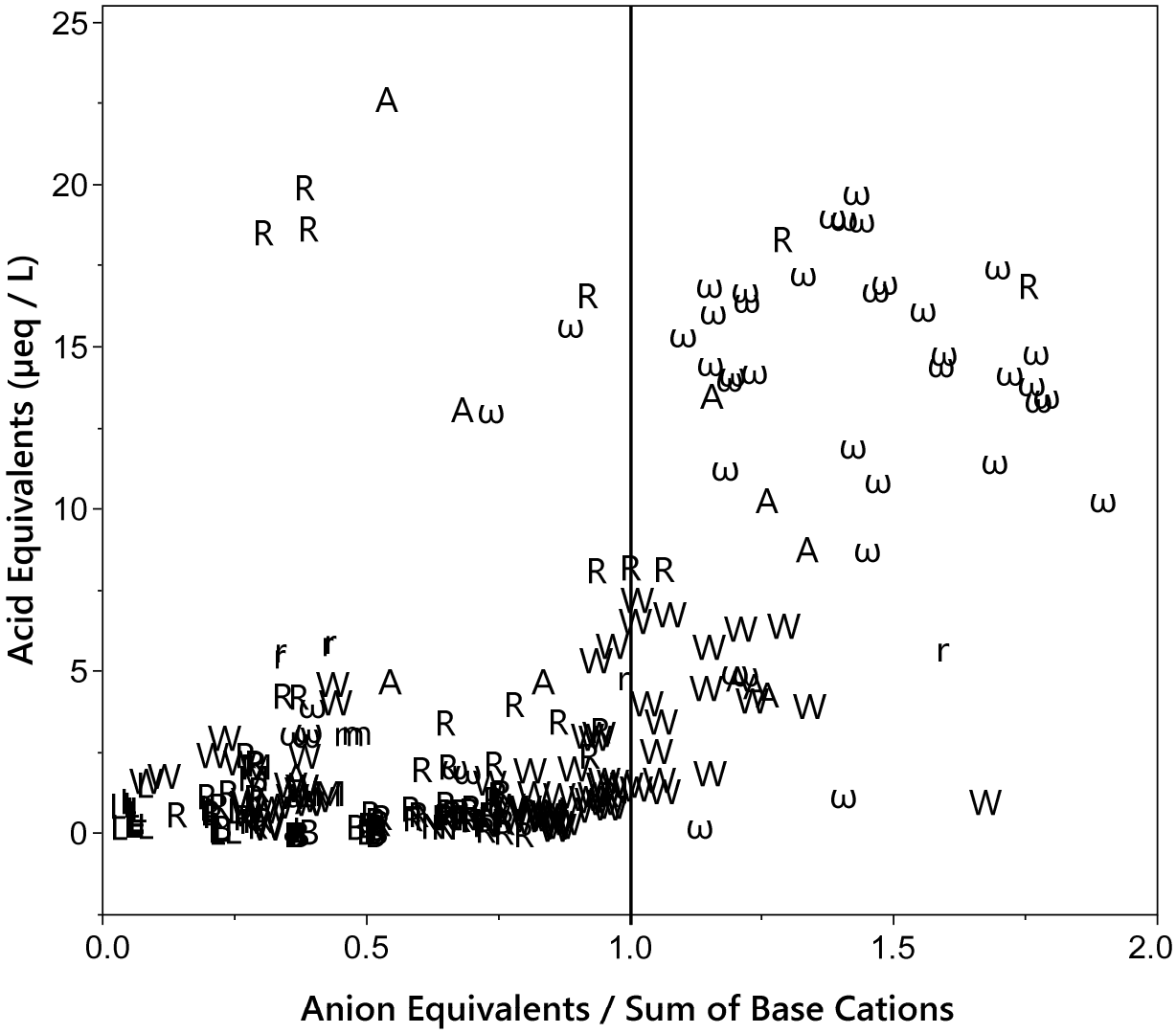

Figure 9. Total stream water acidity (aluminum plus proton equivalents) versus the ratio of anion equivalents to base cation equivalents. Ratios greater than one reflect base cation deficiency which is mitigated by charge-balance from aluminum and protons. Letters represent the sub-watersheds associated with the stream water sites (see text for definitions). Lower case letters represent stream water sites in catchments containing known areas of natural land disturbance.

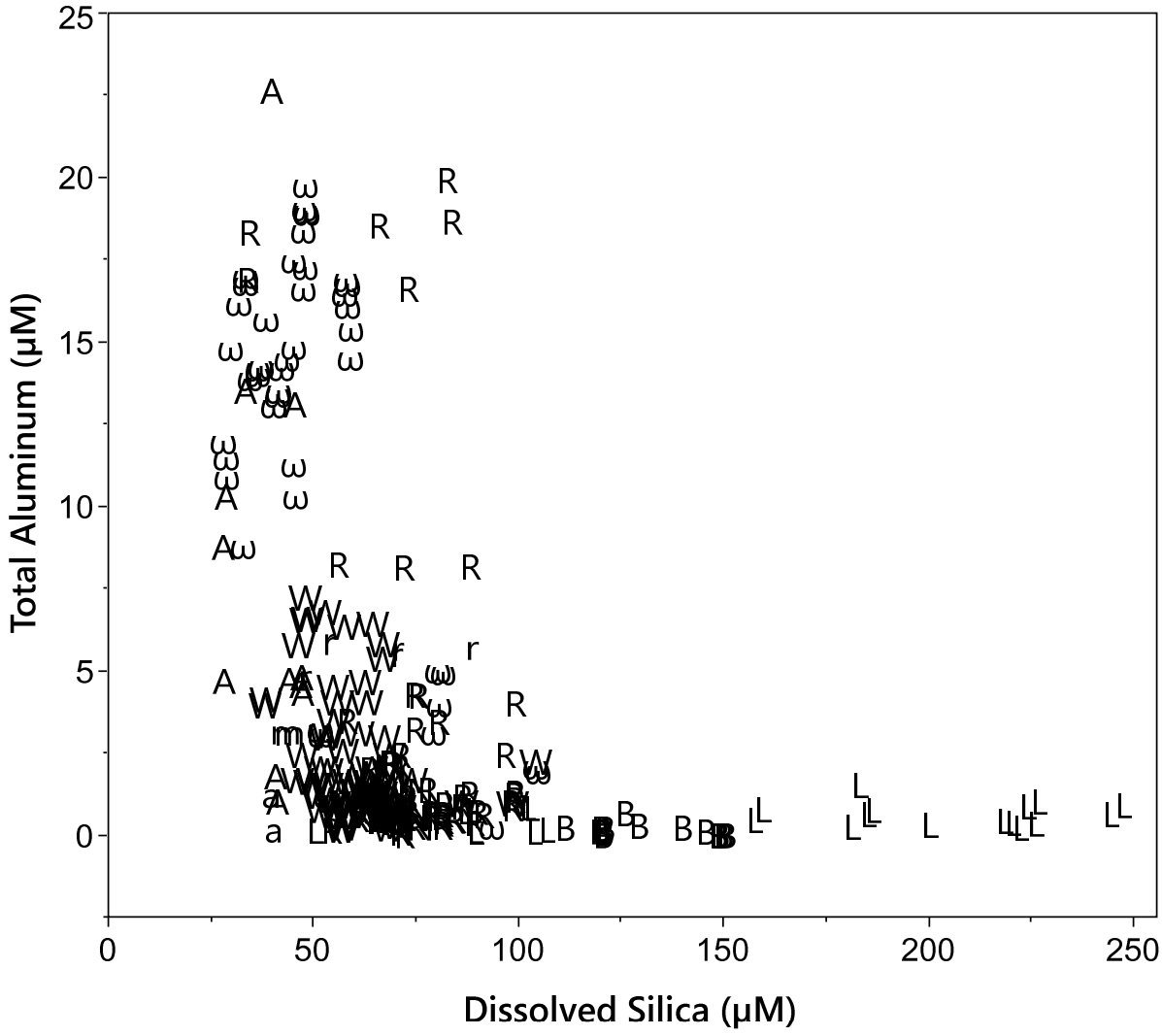

Figure 10. Total dissolved aluminum versus dissolved silica concentrations (micromoles per liter) in stream water. Letters represent the sub-watersheds associated with the stream water sites (see text for definitions). Lower case letters represent stream water sites in catchments containing known areas of natural land disturbance.

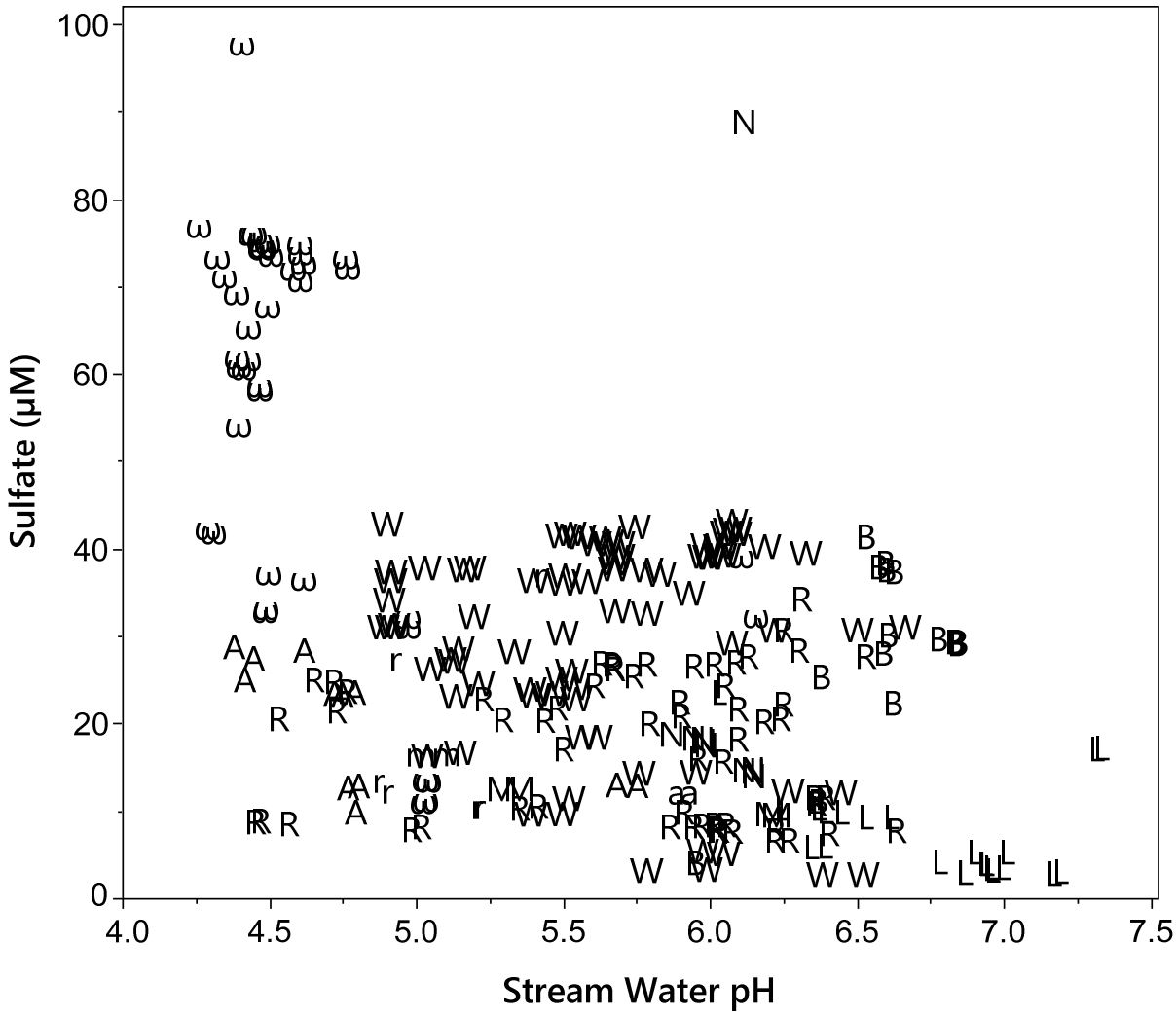

Figure 11. Sulfate concentrations (micromoles per liter) versus pH (lab-measured) in stream water. Letters represent the sub-watersheds associated with the stream water sites (see text for definitions). Lower case letters represent stream water sites in catchments containing known areas of natural land disturbance.

Table 1. Summary of stream water chemistry (mean values) for 82 sites sampled between February 2015 and November 2016.

Site Code	Elevation	Land	Bedrock	Cond.	pH	ANC [2]	Anions (µmol L^{-1}) [3]			Total dissolved metals (µmol L^{-1})							
	meters	Disturbance	Type [1]	µS/cm		µeq L^{-1}	Cl	NO3	SO4	Na	K	Mg	Ca	Al	Fe	Mn	Si
ACC – Alum Cave Creek sites																	
ACtP1-1	1190	no	S	22	4.7	-28	8.8	7.0	17.8	13.2	4.8	12.0	8.2	12.6	7.9	1.1	32.4
ACtP1-2	1211	no	S	19	4.8	-19	16.2	48.6	23.6	16.1	5.4	21.9	12.6	4.6	< 0.3	0.7	47.4
ACtP1-3	1207	no	S	23	4.4	-49	8.9	4.9	27.1	11.7	2.3	12.6	7.6	11.1	2.8	0.6	30.9
ACtP2-1	1198	no	S	20	4.8	-17	5.2	19.1	10.1	12.0	3.5	21.3	11.6	4.7	< 0.3	0.5	44.3
ACtP3-1	1208	no	S	30	4.6	-33	4.7	13.3	28.6	12.8	4.1	28.3	18.1	13.1	< 0.3	1.2	45.7
ACtSTYX1	1273	no	S	16	5.7	4	4.6	10.6	13.1	14.7	3.5	21.6	23.7	1.4	< 0.3	< 0.3	41.2
ACtSTYX2	1356	**yes**	S	16	5.9	8	4.2	10.4	12.3	13.4	3.2	22.2	23.4	0.7	< 0.3	< 0.3	40.3
BFP – Beech Flats Prong sites																	
BFP1	1556	no	S	27	6.7	134	13.0	48.3	24.9	70.9	11.2	35.8	78.6	< 0.3	< 0.3	< 0.3	146
BFP1b	1511	no	S	25	6.6	96	17.2	55.1	28.2	63.2	11.7	29.7	66.2	< 0.3	< 0.3	< 0.3	140
BFP2	1492	no	S	29	6.6	91	16.3	48.7	32.5	66.0	13.2	31.0	63.5	< 0.3	< 0.3	< 0.3	116
NDW – Noland Creek Headwaters Sites																	
NDNE	1670	no	Q	11	6.0	9	10.2	19.0	18.3	29.0	6.6	8.8	19.3	0.5	< 0.3	< 0.3	71.7
NDSW	1670	no	Q	11	6.1	16	9.0	20.6	29.5	30.4	6.2	8.9	30.8	0.6	< 0.3	< 0.3	76.1
MtLC – Sites on streams draining from Mt. LeConte																	
WtBEAR1	1119	no	Q	19	5.3	2	5.8	19.3	12.7	22.4	4.8	20.9	24.4	1.3	< 0.3	< 0.3	65.5
WtCOLE1	1105	no	Q	18	6.2	26	4.7	14.7	9.8	26.1	8.1	20.7	29.3	1.9	< 0.3	< 0.3	69.1
WtTROUT1	1125	**yes**	Q	20	5.1	12	4.0	11.7	16.7	14.7	4.1	20.4	21.7	3.1	< 0.3	0.6	44.0

Table 1 continued

Site Code	Elevation	Land	Bedrock	Cond.	pH	ANC [2]	Anions (µmol L^{-1}) [3]			Total dissolved metals (µmol L^{-1})							
	meters	Disturbance	Type [1]	µS/cm		µeq L^{-1}	Cl	NO3	SO4	Na	K	Mg	Ca	Al	Fe	Mn	Si
LWPLPR – Lower West Prong Little Pigeon River sites																	
WLPtBULL1	474	no	Q	26	6.9	202	5.0	1.2	4.1	87.1	18.9	22.8	45.4	0.7	0.4	< 0.3	186
WLPtCT1-1	866	no	Q	22	6.0	27	4.5	14.7	23.7	22.1	9.9	26.2	46.3	< 0.3	< 0.3	< 0.3	50.8
WLPtCRITT1	609	no	Q	25	6.6	57	5.5	23.8	9.4	47.2	20.1	15.7	52.3	< 0.3	< 0.3	< 0.3	106
FlintRockBr1	785	no	Q	14	6.4	31	3.7	5.1	6.1	36.8	12.6	7.4	45.4	0.8	< 0.3	< 0.3	103
WLPtHick1	613	no	Q	21	6.3	34	11.6	9.4	10.4	50.6	23.5	12.0	41.8	0.8	< 0.3	< 0.3	88.4
WLPtHusk1	492	no	Q	51	7.2	437	6.3	2.6	3.1	108	23.4	51.1	127	0.6	0.7	< 0.3	224
WLPtHusk2	629	no	Q	30	7.0	216	7.2	0.8	3.7	106	14.7	28.6	55.4	0.7	< 0.3	< 0.3	227
HuskeyGAP1	588	no	Q	28	7.0	201	6.1	n.d.	5.4	110	12.5	28.4	56.4	0.8	< 0.3	< 0.3	246
WLPtSteep1	760	no	Q	22	6.4	29	7.9	12.6	10.1	40.6	23.1	22.8	38.9	< 0.3	< 0.3	< 0.3	89.8
WLPtSugar1	476	no	Q	25	7.0	191	5.0	3.3	3.5	71.6	16.5	20.9	49.4	0.6	0.5	< 0.3	159
WLPt13	547	no	Q	75	7.3	522	15.5	7.4	17.3	110	26.4	69.6	212	0.9	0.5	< 0.3	183
WLPt14	467	no	Q	24	6.9	178	4.9	1.2	3.1	77.9	22.5	19.4	37.9	0.3	< 0.3	< 0.3	201
WLPt15	475	no	Q	25	6.8	190	4.6	1.1	4.3	87.9	28.0	20.0	35.8	0.4	< 0.3	< 0.3	220

Table 1 continued

Site Code	Elevation	Land	Bedrock	Cond.	pH	ANC [2]	Anions (µmol L^{-1}) [3]			Total dissolved metals (µmol L^{-1})							
	meters	Disturbance	Type [1]	µS/cm		µeq L^{-1}	Cl	NO3	SO4	Na	K	Mg	Ca	Al	Fe	Mn	Si
RP – Road Prong sites																	
ChTt1-1	1231	no	S	14	5.8	13	11.1	32.2	20.6	27.4	10.4	11.6	23.6	< 0.3	< 0.3	< 0.3	72.0
ChTt2-1	1244	no	S	16	6.0	17	12.3	18.6	25.4	20.6	10.8	11.1	33.5	0.7	< 0.3	< 0.3	61.8
RtCHT1-1	1286	no	S	17	6.1	27	9.2	26.1	27.4	25.7	9.2	14.0	36.4	0.5	< 0.3	< 0.3	70.9
RtM10-1	1139	no	S	15	6.2	29	6.5	23.3	15.2	33.3	10.7	15.3	33.5	0.8	< 0.3	< 0.3	85.8
RtM1-1	1322	**yes**	Q	18	4.9	-15	6.6	14.8	17.9	22.2	9.1	6.5	24.2	5.6	< 0.3	0.4	52.1
RtM11-1	1121	no	S	16	6.4	34	7.1	26.8	14.9	36.0	8.3	23.9	43.9	0.5	< 0.3	< 0.3	90.7
RtM11-2	1153	no	S	17	6.2	20	9.4	39.5	20.4	34.4	8.4	18.1	26.4	0.7	0.3	< 0.3	90.4
RtM1-2	1330	**yes**	Q	18	5.4	-3	53.4	28.9	37.2	24.6	11.8	7.0	24.0	5.7	0.8	0.3	88.9
RtM12-1	1094	no	Q	14	6.3	31	8.8	26.1	34.4	19.7	2.1	21.2	39.2	< 0.3	< 0.3	< 0.3	54.7
RtM13-1	1271	no	Q	12	5.7	5	10.4	32.8	25.6	19.9	10.0	9.4	30.2	3.4	< 0.3	< 0.3	58.6
RtM14-2	1617	no	Q	14	5.6	2	30.1	20.2	24.6	53.3	17.1	10.1	16.7	2.4	0.3	< 0.3	96.6
RtM2-1	1327	no	Q	16	5.0	-12	4.9	6.0	8.2	29.6	11.3	4.9	12.9	4.3	< 0.3	< 0.3	75.5
RtM3-1	1367	no	Q	18	6.4	27	4.8	11.6	11.7	25.8	12.2	9.2	43.3	0.8	< 0.3	< 0.3	73.0
RtM4-1	1412	no	Q	26	4.6	-37	30.2	20.7	13.2	19.2	10.6	10.4	20.7	18.4	1.5	0.7	67.1
RtM4-2	1420	no	Q	21	4.8	-18	30.8	36.8	23.8	12.0	2.8	19.7	17.5	18.3	1.1	1.1	34.8
RtM5-1	1418	**yes**	Q	17	5.2	-8	5.1	10.0	10.6	25.7	7.7	10.7	26.4	5.6	0.6	< 0.3	70.7
RtM6-1	1518	no	S	16	6.2	15	7.6	15.7	6.8	36.7	5.2	15.1	40.3	0.5	< 0.3	< 0.3	82.2
RtM7-1	1335	no	Q	13	5.9	8	3.8	7.9	8.4	25.3	8.0	9.2	22.9	2.2	< 0.3	< 0.3	69.1
RtM9-1	1151	no	S	14	6.0	10	7.1	18.8	17.3	26.9	12.3	11.5	27.7	2.3	< 0.3	< 0.3	70.6

Table 1 continued

Site Code	Elevation	Land	Bedrock	Cond.	pH	ANC [2]	Anions (µmol L^{-1}) [3]			Total dissolved metals (µmol L^{-1})							
	meters	Disturbance	Type [1]	µS/cm		µeq L^{-1}	Cl	NO3	SO4	Na	K	Mg	Ca	Al	Fe	Mn	Si
RtMOC1	1752	no	Q	9	5.2	-7	7.4	8.4	23.0	26.6	5.4	6.7	9.9	3.2	0.5	0.3	75.2
RtMOC2	1728	no	Q	10	6.0	16	15.1	19.7	11.2	36.1	10.0	9.6	17.3	0.7	< 0.3	< 0.3	79.8
RtS10-1	1235	no	Q	19	4.5	-35	9.3	33.9	20.7	17.1	17.6	8.9	19.6	16.6	1.8	< 0.3	73.4
RtS1-1	1436	no	S	13	6.0	11	2.8	9.7	8.5	22.9	7.9	10.1	25.3	0.4	< 0.3	< 0.3	65.9
RtS6-1	1215	no	Q	16	6.3	41	6.4	19.1	19.8	24.6	11.4	15.7	44.0	1.7	< 0.3	< 0.3	63.2
RtS6-2	1221	no	Q	18	6.4	51	10.6	26.2	29.3	24.8	13.0	17.0	45.4	0.6	< 0.3	< 0.3	62.6
RtS7-1	1241	no	Q	21	4.6	-33	8.2	18.7	16.9	20.3	14.3	9.1	21.1	13.4	1.2	< 0.3	61.4
RtS7-2	1250	no	Q	19	4.7	-20	10.3	27.0	25.0	18.4	13.9	9.4	20.9	8.1	0.5	0.3	72.4
RtS8-1	1178	no	S	15	6.3	33	7.2	22.5	14.1	33.6	9.8	13.8	31.4	0.9	< 0.3	< 0.3	84.2
RtTOM1	1710	no	Q	20	5.4	48	6.7	10.4	10.6	32.6	13.3	13.2	28.4	0.8	< 0.3	< 0.3	76.7
RtTOM2	1383	no	Q	12	6.1	15	9.6	15.8	18.3	27.8	6.1	8.8	21.9	3.4	0.3	< 0.3	80.9
WCP – Walker Camp Prong sites																	
WtA1-1	1404	**yes**	S	29	4.5	-39	12.2	12.0	74.1	14.9	4.0	25.3	22.9	16.4	0.9	1.8	46.9
WtA1-2	1427	**yes**	S	31	4.5	-35	23.9	17.4	67.9	47.2	7.6	20.6	30.1	< 0.3	< 0.3	< 0.3	93.7
WtA2-1	1465	no	S	19	4.9	-15	11.6	23.8	40.3	15.3	2.3	14.8	21.4	4.0	< 0.3	0.6	38.5
WtA3-1	1369	**yes**	S	40	4.3	-59	9.3	10.4	63.7	14.4	3.4	24.4	22.9	15.0	1.5	1.1	39.6
WtA3-2	1393	**yes**	S	31	4.5	-37	12.4	11.9	67.4	16.6	3.8	24.4	25.6	14.4	1.8	1.2	45.1
WtA4-1	1358	no	S	17	5.0	-8	11.4	11.3	30.4	29.1	3.1	11.7	19.0	5.9	< 0.3	0.4	58.2
WtA5-1	1354	**yes**	S	20	5.0	-12	10.4	18.9	30.4	33.3	3.8	14.9	19.8	7.4	2.7	0.3	68.9
WtA6-1	1312	no	S	20	6.3	41	20.1	17.2	18.5	44.3	5.2	17.1	24.7	1.4	< 0.3	< 0.3	96.5

Table 1 continued

Site Code	Elevation	Land	Bedrock	Cond.	pH	ANC [2]	Anions (µmol L^{-1}) [3]			Total dissolved metals (µmol L^{-1})							
	meters	Disturbance	Type [1]	µS/cm		µeq L^{-1}	Cl	NO3	SO4	Na	K	Mg	Ca	Al	Fe	Mn	Si
WtGRASS1	1210	**yes**	S	16	5.0	-8	3.6	4.2	11.3	16.7	5.6	6.6	21.2	3.1	< 0.3	0.7	52.1
WtK1	1438	no	S	13	5.5	3	2.6	8.4	11.6	17.7	3.8	13.2	20.6	2.4	< 0.3	< 0.3	47.4
WtK1b	1431	no	S	17	5.8	10	9.7	19.4	37.4	22.2	4.3	18.1	27.5	1.0	< 0.3	< 0.3	51.9
WtK2	1556	no	S	14	6.1	11	6.9	19.2	29.4	21.0	3.2	14.3	26.3	0.6	< 0.3	< 0.3	55.1
WtM10-1	1269	no	S	15	6.0	30	5.1	15.4	5.4	28.1	4.6	15.2	25.1	0.9	< 0.3	< 0.3	69.8
WtM1-1	1386	no	S	17	5.5	2	10.0	20.4	34.1	27.0	6.0	18.9	31.9	1.5	< 0.3	< 0.3	58.0
WtM11-1	1234	no	Q	20	6.5	128	6.7	4.4	2.9	27.4	6.8	15.6	51.5	1.7	< 0.3	< 0.3	59.2
WtM1-2	1403	no	S	17	5.6	1	10.4	30.8	40.3	28.4	3.6	24.5	29.0	0.5	< 0.3	< 0.3	56.0
WtM2-2	1426	no	S	17	5.8	9	9.2	20.6	30.2	28.4	6.4	26.4	30.0	1.7	< 0.3	< 0.3	58.6
WtM2-4	1467	no	S	20	6.0	10	12.7	46.8	39.8	34.5	5.4	25.0	37.4	0.6	< 0.3	< 0.3	67.0
WtM6N-2	1456	no	S	18	5.8	4	11.3	35.9	38.0	28.3	6.5	18.3	32.6	1.5	< 0.3	< 0.3	63.2
WtM6S-2	1464	no	S	14	5.4	-3	8.2	23.4	20.8	26.2	6.4	9.9	21.0	1.4	< 0.3	< 0.3	66.6
WtM6S-2b	1464	no	S	13	5.1	-9	8.4	15.7	25.7	17.7	4.8	7.1	15.0	4.4	< 0.3	< 0.3	57.5
WtM7-1	1285	no	S	11	5.9	17	4.5	6.4	3.4	22.1	4.0	10.0	17.1	2.7	0.5	< 0.3	68.1
WtM8-1	1283	no	S	36	6.6	91	13.1	11.9	31.0	50.4	8.2	31.4	82.4	0.6	< 0.3	< 0.3	69.5
WtX1-1	1404	no	S	11	5.5	1	10.1	22.1	24.6	27.5	3.5	14.5	20.0	0.5	< 0.3	< 0.3	66.4

(1) Bedrock Type: “S” – sulfidic bedrock (Anakeesta Formation); “Q” – sandstone/siltstone conglomerate
(2) ANC = acid-neutralizing capacity in units of microequivalents per liter
(3) Anion and metals concentrations in units of micromoles per liter

Table 2. Statistical analysis of stream water chemistry comparing (a) stream water draining catchments overlying sandstone bedrock versus sulfidic bedrock, and (b) stream water draining catchments with versus without natural landslide disturbance areas. Different letters indicate statistically significant differences ($\alpha = 0.05$; Wilcoxon/Kruskal-Wallis rank sums test)

Chemical Parameter (units) *	Bedrock Classification			Catchments with Disturbance Areas		
	Sandstone	Sulfidic	p value	No	Yes	p value
pH (lab) (std. units)	6.0 ± 0.8 (82) A	5.5 ± 0.7 (200) B	< 0.0001	5.9 ± 0.6 (223) A	4.7 ± 0.4 (59) B	< 0.0001
ANC ($\mu mol_C\ L^{-1}$)	61.6 ± 118 (82) A	5.8 ± 43 (200) B	< 0.0001	35.6 ± 81 (223) A	– 29.3 ± 23 (59) B	< 0.0001
Conductivity ($\mu S\ cm^{-1}$)	20.0 ± 12 (82) A	21.1 ± 7.8 (200) B	0.0398	19.1 ± 8.5 (223) A	27.2 ± 8.5 (59) B	< 0.0001
Chloride ($\mu mol\ L^{-1}$)	9.6 ± 10 (82) A	11.7 ± 7.0 (184) B	< 0.0001	**11.0 ± 8.4 (209) A**	**11.1 ± 7.9 (57) A**	**0.7310**
Nitrate ($\mu mol\ L^{-1}$)	14.0 ± 9.4 (82) A	22.4 ± 14 (184) B	< 0.0001	21.6 ± 14 (209) A	13.1 ± 7.0 (57) B	< 0.0001
Sulfate ($\mu mol\ L^{-1}$)	14.0 ± 11 (82) A	35.3 ± 20 (184) B	< 0.0001	22.5 ± 13 (209) A	51.5 ± 25 (57) B	< 0.0001
Calcium ($\mu mol\ L^{-1}$)	**37.2 ± 35 (82) A**	**30.4 ± 18 (197) A**	**0.4552**	34.9 ± 26 (220) A	23.2 ± 4.6 (59) B	0.0012
Magnesium ($\mu mol\ L^{-1}$)	15.8 ± 12 (82) A	20.0 ± 11 (197) B	< 0.0001	18.3 ± 12 (220) A	20.5 ± 8.9 (59) B	0.0085
Sodium ($\mu mol\ L^{-1}$)	40.5 ± 28 (82) A	30.3 ± 18 (197) B	0.0032	37.0 ± 23 (220) A	19.8 ± 11 (59) B	< 0.0001
Potassium ($\mu mol\ L^{-1}$)	12.0 ± 6.5 (82) A	6.5 ± 4.6 (197) B	< 0.0001	9.1 ± 6.1 (220) A	4.4 ± 2.7 (59) B	< 0.0001
Total Aluminum ($\mu mol\ L^{-1}$)	2.9 ± 4.7 (82) A	4.7 ± 6.1 (197) B	0.0211	2.2 ± 3.7 (220) A	11.4 ± 6.3 (59) B	< 0.0001
Total Iron ($\mu mol\ L^{-1}$)	**0.3 ± 0.4 (82) A**	**0.6 ± 1.8 (197) A**	**0.5851**	0.3 ± 1.5 (220) A	1.3 ± 1.3 (59) B	< 0.0001
Total Manganese ($\mu mol\ L^{-1}$)	0.1 ± 0.2 (82) A	0.4 ± 0.6 (197) B	0.0005	0.1 ± 0.2 (220) A	1.0 ± 0.7 (59) B	< 0.0001
Silica ($\mu mol\ L^{-1}$)	96.0 ± 55 (82) A	66.8 ± 27 (197) B	< 0.0001	81.8 ± 41 (220) A	51.7 ± 18 (59) B	< 0.0001

* Some chemical parameters were not analyzed in a few samples; thus, number of samples do not always sum to 282 (the total number of samples collected). Units: $\mu mol_C\ L^{-1}$ = micromoles of charge per liter; $\mu mol\ L^{-1}$ = micromoles per liter

Note: Samples from sites RtM4 and RtS7 (overlying sandstone) had chemistry consistent with land disturbance in sulfidic bedrock catchments, but GIS analysis did not confirm this. It is possible that unidentified areas of sulfidic bedrock and land disturbance exist in those two catchments.

CHAPTER 5: CONDITIONAL INFLUENCE OF SULFIDIC BEDROCK ON SOIL AND STREAM WATER CHEMISTRY IN HIGH-ELEVATION FOREST CATCHMENTS OF THE GREAT SMOKY MOUNTAINS

Abstract

Multi-decade monitoring of acidification effects in the Great Smoky Mountains National Park (GRSM) has shown recent evidence of decreased acidic deposition. There is interest in knowing if forest catchments will recover from their current acidification status, and if biogeochemical processes exist in these ecosystems that will delay or prevent recovery. Sulfidic bedrock and acid-sulfate soil exists in the GRSM, but the extent to which sulfide mineral weathering affects the already acid-sensitive forest ecosystems is still unclear. Seven high-elevation sites were characterized to evaluate whether soil and stream water overlying sulfidic bedrock is experiencing additional acidification, above that attributable to atmospheric deposition. Soil and water chemistry (including pH, sulfate, metals, and cations) in three catchments overlying sulfidic bedrock were statistically compared to two overlying sandstone and two overlying a bedrock transition zone. Soil pH_{water} was ≤ 5 or ≤ 4 in 92% and 18% of samples, respectively, but was not statistically different among the study sites. In each catchment, > 90% of the sulfate mass was found in subsurface soil samples, and > 90% of the soil sulfate mass was found in the strongly adsorbed (phosphate-extractable) form. Strongly adsorbed sulfate in two of the three sulfidic bedrock catchments (moderate topographic slopes and containing exposed sulfidic bedrock) was statistically larger than in the third sulfidic bedrock catchment (with no known exposed bedrock) or the other bedrock types. Stream water from the two sites adjacent to exposed sulfidic bedrock outcrops had the lowest pH and acid-neutralizing capacity, the highest sulfate concentrations, as well as the highest metals and cations concentrations. However, stream water chemistry at the third sulfidic bedrock site was statistically different from that at the other two sulfidic bedrock sites, and more similar to the stream water chemistry at the transition zone and sandstone bedrock sites. This suggests that potential exacerbation of soil and stream water acidification by sulfidic bedrock is

more likely if bedrock is physically exposed to direct precipitation and atmospheric climate. The soil mantel's moderating effect on the geochemistry of high-elevation catchment ecosystems, even if overlying potentially acidifying sulfidic bedrock, is an important finding that GRSM resource managers and ecosystem modelers can use. The correspondence between adsorbed sulfate concentrations in subsurface soil and stream water sulfate concentrations at each site suggests that dissolved sulfate exported from GRSM catchments originates from subsurface soil under baseflow conditions. Other results show the soil organic phase to be the locus of sulfur retention in high-elevation forest catchments. Thus, the most influential factors determining sulfur geochemistry in high-elevation forest catchments appear to be (1) exposed sulfidic bedrock outcrops and landslide scars, and (2) the cycling of throughfall sulfate through the soil organic matter phase. Additional studies are needed to confirm the importance of soil depth and vegetation type/density on these two sulfur biogeochemical processes in the GRSM.

Introduction

Emission of acid-forming sulfur and nitrogen compounds to the atmosphere has been an environmental issue since the mid- to late-1800s; Schurr and Netschert 1960). Oxidation and hydrolysis of airborne sulfur and nitrogen oxides and aerosols form sulfuric acid, nitric acid, and sulfate, nitrate and ammonium salts (Overton et al. 1979). This material is transported onto tree foliage and soil as acidic precipitation. The acidity and associated ion species in this material disrupt normal ecological functions (Galloway et al. 1983; Turner et al. 1992; Herlihy et al. 1996; Neff et al. 2009; Schwartz et al. 2014) and contributes to soil and stream water acidification (Driscoll et al. 2001).

Adverse effects from acidic precipitation include the accelerated loss of acid-buffering components and simultaneous buildup of acidity in soil and stream water (i.e., acidification). These effects have been observed in a variety of terrestrial ecosystems such as agriculture land and public national parks under the stewardship of the National Park Service (NPS). The Great Smoky Mountains National Park (GRSM) which straddles the border between Tennessee and North Carolina, USA (Figure 12) is one such national park. It contains more than 2,200 square kilometers of predominantly forest ecosystems, ~4,700 kilometers of streams/rivers, and some of the richest, most diverse assemblages of flora and fauna in the USA (NPS 2017). The GRSM and surrounding region have geologically old, highly weathered soils whose acidity-buffering components have been depleted over time (Omernik and Powers 1982). Deficiencies in acidity-buffering components have made GRSM soil and stream water susceptible to further acidification (Cook et al. 1994; Robinson et al. 2008; Cai et al. 2010; Cai et al. 2011; Cai et al 2012), and have made

GRSM flora and fauna susceptible to biological and ecological dysfunction (Sullivan et al. 2002; Sullivan et al. 2007; Neff et al. 2009; Schwartz et al. 2014; Baldigo et al. 2017).

In regions of the world where sulfur emissions to the atmosphere have been regulated (e.g., the 1990 Clean Air Act Amendments in the USA; Likens et al. 2001; Chestnut and Mills 2005; Burns et al. 2006), lower emission rates of sulfur dioxides and sulfur aerosols have resulted in lower concentrations of these sulfur pollutants in the atmosphere, and in less mass of acidity and sulfate being deposited onto terrestrial ecosystems (Burns et al. 2008; Vestreng et al. 2007; Smith et al. 2011; Klimont et al. 2013). Coal-burning power plants in the vicinity of the GRSM have achieved similar reductions in sulfur emissions since the late 1990s and early 2000s (TVA 2017). As a result, rain and throughfall (TF) water falling on the GRSM has experienced substantial decreases in dissolved sulfate concentrations and increases in pH and acid-neutralizing capacity (ANC) (Gonzalez et al. 2015).

Based on the connection between deposition of acidic pollutants and acidification of soil and water, environmental resource stakeholders and scientists hypothesized that reductions in deposition inputs should result in soil/stream water "recovery" (i.e., either slowing the rate of continued ecosystem acidification, or allowing ecosystems containing sources of acid-buffering components to reverse the acidification process). Underlying this hypothesis are two key assumption. First, that soil and stream water acidification is reversible (e.g., Rice et al. 2014), and second, that deposition of acidic pollutants is the sole cause of observed soil and stream water acidification. In some regions, acidification reversal has been reported, but in regions such as the buffer-capacity poor GRSM (Omernik and Powers 1982), recovery from acidification is not clearly evident (Gonzalez et al. 2015). GRSM stakeholders and scientists have been interested in learning (1) if, when, and how quickly soil and stream water acidification will reverse, (2) what is the critical mass below

which acidified soil/stream water will begin reversal, and (3) subsequently how quickly can impacted flora and fauna reestablish normal biological function (Chen et al. 2004; Zhai et al. 2008; Zhou et al. 2015; Fakhraei et al. 2016). If either of the two stated assumptions are invalid, reversal of acidification might not be possible. The first assumption would be invalid if there are insufficient or no sources of acid-buffering components in soil or water to ameliorate existing acidity. The second assumption would be invalid if there are geochemical conditions or processes in GRSM forest catchments that can delay or prevent recovery of acidified soil and stream water.

With regard to the first assumption, many weathering reactions involving alumino-silicate minerals in forest ecosystems are acid-buffering processes, but their reaction rates are too slow (e.g., 0.6 to 22 x 10^{-7} mol m^{-2} yr^{-1}; White and Brantley 2003) to provide significant buffering against atmospheric acidity (Brantley 2008; Brantley et al. 2014). The steep catchments of the GRSM are well-drained systems that do not allow for long contact-time between soil water and soil minerals. On short time-scales, the significant proton-consuming reactions are primarily ion exchange reactions, and the efficacy of soil components involved in the exchange reactions is dependent on soil pH.

With regard to the second assumption, weathering of reduced sulfur minerals (e.g., sulfide) releases sulfate, protons and metals such as aluminum and iron to forest soil and stream water. Sulfidic bedrock formations exist in the central and northeastern sectors of the GRSM (Figure 12) (Hadley and Goldsmith 1963; King 1964; Southworth et al. 2005; Thornberry-Ehrlich 2008). At those locations, slate/shale type geology and shallow soil mantels provide ideal conditions for landslides and debris slides (Ryan 1989) which exposes large areas of sulfidic phyllite/shale/slate bedrock to the atmosphere and to direct precipitation. Landslides and debris slides at the higher elevations in the GRSM, where the steepest catchment slopes are found, have been the source of

localized acute stream acidification and acute toxicity to stream biota (e.g., Huckabee et al. 1975; Maas 1976; Bacon and Maas 1979). This process has the potential of delaying or preventing acidification recovery at locations in the GRSM where this geology exists.

A review of the literature showed that soil geochemistry studies in the GRSM are not as common as surface water chemistry studies. The one example of GRSM soil characterization was a Master's Degree thesis by Grell (2010) for which 25 sites among eight acid-sensitive watersheds were sampled. The objectives of the study were to characterize dominant soil types in the GRSM, characterize soil for evidence of acidification, and identify correlations between soil geochemistry and watershed characteristics. Of particular interest were: the presence or absence of sulfidic bedrock, bulk soil properties, forest type, and catchment slope and aspect. Soil cores were sampled at the A-horizon and B/C-horizon, and soil samples were characterized for a suite of soil geochemistry parameters, including pH and total phosphate-extractable sulfate. The data were analyzed for statistical differences in soil geochemistry among the eight watersheds based the physical watershed characteristics. The major findings reported were (1) measured soil pH was less than 5.0 in all but two A-horizon samples and two B/C-horizon samples, (2) unexposed sulfidic bedrock was not a factor in determining soil properties, (3) significant differences in soil geochemistry were found in adjacent watersheds, and (4) most of the soil samples showed evidence of long-term exposure to acidic deposition. Grell's (2010) soil sampling locations were widely dispersed throughout the GRSM, and their selection apparently did not consider potential differences in deposition loads. Stream water associated with the soil samples was not sampled and characterized, and the soil data were used to develop multivariate empirical predictive models for particular soil parameters based on other soil parameters. Thus, the focus of that study was not on geochemical mechanisms responsible for the observed soil characteristics.

The objective of this study was to evaluate the sensitivity of GRSM catchments, that are currently affected by acidic air pollutant deposition (AAPD), to further acidification by a non-atmospheric source: underlying sulfidic bedrock. Soil and stream water in high-elevation forest catchments was characterized with respect to acidification chemistry and sulfur species concentrations. Critical to this study was selecting study sites within a relatively narrow elevation band (to minimize elevation effects) at the highest elevations practicable (which presumably have been chronically exposed the highest rates of AAPD; e.g., Weathers et al. 2006). Headwaters and first-order stream drainage areas were targeted to simplify the interpretation of stream water chemistry results. Understanding how non-AAPD sources exacerbate acidification in GRSM catchments can provide information useful for further refinements to acidification and critical loads models (Chen et al. 2004; Zhai et al. 2008; Zhou et al. 2015; Fakhraei et al. 2016). Also, results from this study should bring resolution to the speculation that soil and stream water in the GRSM are impacted by bedrock only as exposed scars and outcrops.

Study Design

Study Catchment Selection

It was hypothesized that two catchment factors control the extent to which sulfidic bedrock can affect the acidification status of soil and stream water: (1) bedrock exposure (i.e., outcrops and landslide/disturbance scars), and (2) contact (or "residence") time of catchment water from precipitation to discharged from the outlet. The first factor was hypothesized to increase catchment water acidification. The second factor was selected to reflect the combined effects of catchment slope (i.e., steeper slopes cause shorter water/soil/bedrock contact times), total soil depth (i.e., shallow soil mantles have smaller water holding capacity and cause shorter water/soil/bedrock

contact time), and soil organic matter content (i.e., catchments with thick surface soil horizons [O-plus A-] have large water holding capacity and cause longer water/soil/bedrock contact time). Vegetation type and soil biogeochemistry are known to be tightly coupled catchment factors (Johnson-Maynard et al. 2005; Burke et al. 2009; Chandra et al. 2016) but this factor was not controlled in this study.

For clarity in describing the role of spatial scales in this study, the following terms are defined, ordered by decreasing drainage area (in hectares): basin (> 5000), watershed (500-5000), sub-watershed (50-500), catchment (5-50), sub-catchment and headwaters drainage area (< 5). Study areas were selected from the catchment to headwaters spatial scales (< 50 hectares) to minimize loss of geochemical information that occurs when samples are collected further downgradient in the landscape or drainage system. For brevity, however, all study areas are referred to as catchments.

Bedrock type was the primary independent variable in this study, and sites associated with sulfidic or non-sulfidic bedrock were required. Headwater drainage areas or small catchments with first-order streams were identified based on the following criteria. Much of the GRSM is underlain by sandstone and siltstone conglomerate of the Thunderhead and Copperhill Formations (Hadley and Goldsmith 1963; King 1964) (Figure 12). Thus, the reference scenario was defined as the chemical composition of soil and stream water from high-elevation catchments overlying sandstone bedrock. Other areas of the GRSM are underlain by thick units of phyllite and carbonaceous (graphitic) shale containing sulfidic minerals (i.e., pyrite; pyrrhotite; other metal monosulfide and disulfide minerals) (Southworth et al. 2005). The experimental scenario in this study was defined as the chemical composition of soil and stream water from high-elevation catchments overlying

sulfidic bedrock. The pertinent example of this bedrock type is the Anakeesta Formation which is prominent at the higher elevations of central GRSM (Figure 12).

For this study, three sets of catchments were identified (Figure 12): three catchments overlying only sulfidic bedrock (Sites 1, 2 and 3), two catchments overlying only sandstone (Sites 6 and 7), and two catchments (Sites 4 and 5) overlying a bedrock transition zone along the seam between sulfidic and sandstone bedrock formations. From each of these catchments, soil from multiple locations was sampled to account for intra-catchment variance in soil chemistry. It was assumed that bedrock's influence on soil acidification would vary within the soil profile, with greater influence on deeper soil nearer the bedrock. Thus, at each soil sampling location, samples were collected from surface soil (O- and A-horizons) and subsurface soil (B-, and where possible, C-horizons). Stream water was collected from locations adjacent to the soil sampling sites, representing baseflow water draining through the catchment soil in that vicinity.

Two sets of metrics used in this study to quantify "sensitivity to additional acidification." For soil they were adsorbed sulfate, organic sulfur, total sulfur, base saturation (ratio of exchangeable base cations to cation exchange capacity), and extractable aluminum. For stream water, they were pH, ANC, base cations and dissolved aluminum, sulfate and dissolved silica. The primary hypothesis for soil was that soil from catchments overlying sulfidic bedrock should have lower pH and extractable base cations concentrations, and larger concentrations of sulfur species and extractable aluminum, relative to soil overlying sandstone bedrock. For stream water, it was that stream water from sulfidic bedrock catchments should have the lowest pH and ANC and the highest concentrations of sulfate, aluminum, iron, and base cations. It was assumed that soil and stream water in all high-elevation GRSM catchments have been equally and ubiquitously affected by long-term AFPD. Further, a secondary hypothesis for soil was that the effects on soil chemistry

from underlying sulfidic bedrock would be stronger in subsurface soil (closer to bedrock) and with exposed bedrock outcrops or landslides.

Methods

Sample Collection

The seven high-elevation study catchments described previously were selected along the State Boundary Ridge in the central GRSM (Figure 12). Physical catchment characteristics, bedrock classification, and general soil characteristics are summarized in Table 3. Drainage area is a factor in determining water chemistry of catchment streams, and drainage areas of the selected catchments ranged between 2.2 hectares and 28 hectares. The approach to Site 1 catchment was from its outlet, and access to pour points higher up into the catchment (to reduce the effective drainage area) was hindered by thick undergrowth of rhododendron and landslide debris. This required stream water sampling at the catchment outlet, and prevented soil collection from Site 1. The approach to Sites 4, 5 and 6 was from the top drainage divide; access to pour points further downgradient (to increase the effective drainage area) was hindered by steep gradients and unsafe conditions. The climate at the GRSM study areas is classified as perhumid mesothermal (Busing 2005), with annual air temperature ranging between -2 and 17 °C (Johnson et al. 1991; van Miegroet et al. 2001), annual stream water temperature at Site #7 ranging between 2 and 13 °C, and annual rainfall at Site #7 averaged 181 cm between 1991 and 2016 (unpublished data).

From April through August 2016, 50 soil samples were collected from 23 locations within six of the seven catchments (Site 1 excluded; Table 4). All soil samples were stored at ~4 to 6 °C until analyzed. Three to six soil cores were collected from each catchment using 4-inch diameter

stainless steel blade augers and soil scoops. Sampling depths varied as indicated in Table 4, but depths were based on soil profile descriptions of the USDA-NRCS (2017). From each core, at least two samples were taken, one from the surface and one from the subsurface soil horizons. At Sites 2 through 5, a second subsurface sample (C-horizon) was collected from further down the core.

Soil profiles varied with respect to total depth and horizon thickness. For instance, Site 2 (sulfidic phyllite bedrock type) soil cores were located in open drainage areas with sparse vegetation (grasses and some trees with trucks < 6 inches in diameter) and numerous exposed bedrock outcrops. Soil depths at those sites were mixed; some being less than 30 cm to bedrock and a few having recognizable C-horizons. All soil profiles lacked recognizable O-horizons, and only two cores had a recognizable A-horizon. Residence time for water in Site 2 catchment is expected to be relatively long although the stream channel in this catchment is known to go dry during the summer dry season. Site 3 (sulfidic phyllite bedrock type) had thin soil profiles located in the steep (~30° to 40°) slope of a long, narrow (~30 to 40 meters from ridge to ridge) V-shape catchment. The ground cover consisted of grasses and low-lying shrubs including nettle (Urtica species), but where vegetation cover was sparse, there was evidence of erosion and exposed rock. Residence time for water in the Site 3 catchment, and consequently contact time between water and soil/bedrock, is expected to be small. Indistinct soil horizons, such as were found in many of the soil cores, have been reported previously by McCracken et al. (1962). In contrast, Sites 6 and 7 (overlying sandstone bedrock) had thick O/A- and A/B-horizons; C-horizon soil was not reached. It should be noted that the soil class fHD (frigid Humic Dystrudepts) appeared to be correlated with sulfidic bedrock type in Sites 1 – 5 (Table 4).

Stream water was sampled from each catchment within 20 meters of all soil cores, resulting in 46 stream water data points. All stream water sites were sampled on at least three separate occasions

as a check on water chemistry variability. The two streamlets comprising the NDW catchment were sampled once in November 2016 (N = 5 for each streamlet) and the average of each set was calculated. This small (N = 2) NDW dataset was supplemented with 2016 monitoring data collected at the same NDW two field sites (Schwartz et al. 2017). Grab samples were collected in acid-rinsed polyethylene containers, which were rinsed twice with ambient stream water before submerging to fill and cap. Ambient water temperature was measured using a digital thermometer with stainless-steel thermistor probe (± 0.1 °C). On a select number of visits, water pH, conductivity and temperature were measured in the field using portable pH meter/probe (Orion Corp., Massachusetts, USA) and a combination conductivity and temperature probe (Thermo Scientific, Beverly, MA). Water samples were transported back to the laboratory and stored at ~4 to 6 °C until analyzed.

Analytical Methods

Soil samples were press-sieved through a 2-mm screen. Portions were taken immediately for soil pH and soil moisture analysis. Air-dried samples were analyzed for total and organic sulfur concentrations. Analyses requiring extraction with aqueous salt solutions were done with 5 grams of soil and 50 mL of extractant solution in 60-mL polyethylene conical centrifuge tubes. Soil residue were separated from leachate by centrifugation and filtration through 0.45 µm mixed cellulose membrane. Soil pH measurements based on water were used in this analysis because that is the basis used in evaluating acid sulfate soil (ASSoil) status (Kittrick et al. 1982; SA-EPA 2007; Sullivan et al. 2009; Jayalath 2012), which will be discussed later. Soil was characterized for the following geochemical parameters. Soil pH (1:1 slurry in water and 0.01M calcium chloride) (Thomas 1996) and moisture content (Or and Wraith 2000); grain size composition (Kettler et al.

2001); cation exchange capacity (CEC unbuffered) and exchangeable base cations (EBC) (Sumner and Miller 1996); exchangeable acidity (EA = CEC – EBC); base saturation (%BS = EBC/CEC); anion exchange capacity (AEC) (Zelanzny et al. 1996); total soil sulfur (TS) and total organic sulfur (TOS) (Tabatabai et al. 1988; Rossete et al. 2008); weakly associated (chloride-extractable) soil sulfate (Bloem et al. 2002; Maynard et al. 1987), and strongly bound (phosphate-extractable) soil sulfate (Ensminger 1954; Sahrawat et al. 2009). For all methods, extracted anions and ammonium concentrations were quantified by ion chromatography (IC) using a Dionex 2100/1100 dual column system with background suppression; extracted metals concentrations were quantified by inductively coupled argon plasma optical emission spectrometry (iCAP-OES) using a Thermo-Elemental iCAP DUO 7400.

Surface water was analyzed for the following water quality parameters. Portions of unfiltered water samples were analyzed for general water quality parameters (pH, specific conductance and ANC) using an automated titration system (Mantech PC-Titrate® system). Sample portions were filtered through 0.45 micrometer (µm) membrane filters and analyzed for dissolved anions and cations by IC. Sample portions were filtered through 0.45 µm membrane filters and preserved with ultra-pure (trace metals grade) nitric acid to a final concentration of 1% by volume (pH < 2) and analyzed for dissolved trace metals by iCAP-OES.

Statistical Analyses

Normality in soil data distribution was not assumed for any of the soil parameters. Thus, soil data were tested using the non-parametric Wilcoxon/Kruskal-Wallis rank sums test ($\alpha = 0.05$), followed by the Steel-Dwass method for all-pairs testing (which controls the family-wise Type I error rate). The Mann-Whitney U-test method for pair-wise testing (without Type I error control) was also run

for comparison. Normality in stream water chemistry data was assumed for this study. Stream data were tested for statistical differences among catchments using a one-way analysis of variance test ($\alpha = 0.05$), followed by the Tukey's HSD test (which controls the overall error rate). Pearson correlation analyses ($\alpha = 0.05$) were run between select pairs of soil geochemical parameters to evaluate inter-relatedness and covariance. All statistical and graphical analyses of soil geochemistry data were done in JMP® Pro 13.

Results

Soil and water chemistry results (ranges) were organized by individual site or by sites grouped by bedrock type. Data from O- and A-horizon soil were grouped as surface soil; data from B- and C-horizon soil were grouped as subsurface soil.

Soil Chemistry – Acidity Parameters

Site 4 (a transition zone catchment located on the North Carolina side of the ridgeline; see Figure 12) had anomalous soil chemistry results which warranted closer examination. It was found that soil from one of the four cores (core #3; designated as 4b in Table 5) showed markedly distinct values of surface and subsurface soil pH, surface soil CEC and EA, %BS, and surface soil carbon. Contrary to theory and to other soil results, the core #3 soil pH (both water and chloride basis) was higher in surface soil than in subsurface soil, and the magnitudes of soil pH in core #3 were substantially higher than other Site 4 cores. Lastly, contrary to the pattern exhibited by all other sites, the core #3 soil %BS was lower in surface soil than in subsurface soil, and surface soil organic carbon concentration was higher than surface soil total carbon. Results associated with core #3 from Site 4 were not weighted heavily in statistical analysis or data interpretations.

Soil pH_{water} of surface and subsurface soil from the six catchments ranged between 3.46 and 4.88, and between 3.95 and 5.26, respectively (Table 5). Soil pH_{CaCl2} of the same sets of soil samples ranged between 2.73 and 3.98, and between 3.32 and 4.50, respectively. No statistically significant differences ($p > 0.05$) in soil pH_{water} or pH_{CaCl2} were found among the sites. For all soil samples, $pH_{CaCl2} < pH_{water}$ (e.g., Brennan and Bolland 1998; Minasny et al. 2011). Soil pH_{water} data were emphasized in this discussion because it is one of the parameters used for defining/identifying acid sulfate soils (ASSoil) (Sullivan et al. 2009; Sullivan et al. 2010; Jayalath 2012). Of the 50 soil samples, nine had $pH_{water} < 4.00$, the criterion pH for ASSoil, and another 5 had pH_{water} between 4.00 and 4.05 (within measurement error of the ASSoil criterion pH). Only four of these 14 samples were from catchments overlying sulfidic bedrock. Twelve of the 14 soils with $pH < 4.05$ were from the A+O horizon, which suggests that soil organic matter is controlling the surface soil pH at these sites. Results similar to those found for soil pH_{water} were found for soil pH_{CaCl2}.

Except for pH, soil chemistry values were larger in surface soil than in subsurface soil at all sites (Table 5). Soil AEC values were too small to provide sufficient resolution for determining significant differences. Soil CEC, EBC, exchangeable acidity (covariant with exchangeable aluminum), and %BS (covariant with EBC) all covaried with soil organic carbon concentrations. As discussed later, soil organic matter appeared to be an important factor in GRSM soil chemistry at these sites.

Soil Chemistry – Sulfur Species

Concentrations of sulfur species in soil from transition zone Site 4 core #3 were generally in the lower end of the range of all measured values (designated as 4b in Table 6), but were not distinct outliers, unlike the acidity chemistry data from that soil core. For consistency with the previous

analysis, sulfur species results associated with core #3 from Site 4 were not weighted heavily in statistical analysis or data interpretations.

Soils had wide ranges of sulfur species concentrations (Table 6). At all sites, soil organic sulfur content was larger in surface soil (594 – 2099 mg S kg^{-1} soil) than subsurface soil (47 – 888 mg S kg^{-1} soil). That corresponds to soil organic matter content being larger in surface soil (9.6% - 29.4% soil organic carbon) than in subsurface soil (1.2% - 14.6% soil organic carbon) (Table 5), and the predominance of soil sulfur existing in organic forms (62% - 104% in surface soil; 17% - 100% in subsurface soil) (Table 6). In contrast, total extractable sulfate concentrations were larger in the subsurface soil (7.6 – 131 mg S kg^{-1} soil) than in surface soil (5.4 – 28.1 mg S kg^{-1} soil). The observed soil sulfate distribution was expected given that subsurface soil had higher proportion of mineral content than surface soil (inferred based on measured soil organic carbon; Table 5) and thus presumably smaller concentrations of sulfate binding sites (Stumm and Morgan 1981; Appelo and Postma 2005; Essington 2015). Concentrations of weakly-associated sulfate were small and relatively uniform throughout the soil profiles at all sites: 0.8 – 8.9 mg S kg^{-1} surface soil, and 0.8 – 9.6 mg S kg^{-1} subsurface soil. At most sites, the majority of adsorbed sulfate in soils existed as phosphate-extractable sulfate, in both surface and subsurface soil (28% - 94% and 61% - 98% of total extractable sulfate, respectively). Surface soil from Site 7 (sandstone bedrock catchment) was the exception where majority of adsorbed sulfate found to exist in the weakly-associated chloride-extractable form (46% - 72%; Table 6).

Soil Chemistry by Bedrock Type

To provide higher statistical power for non-parametric tests, the same data for surface and subsurface soil were organized and analyzed statistically by bedrock type (Tables 7 and 8,

respectively). Sites 2 and 3, 4 and 5, and 6 and 7 were paired to represent soil from sulfidic, transition zone and sandstone bedrock catchments, respectively. Each table shows the overall non-parametric chi-squared p-value for each soil chemistry parameter, followed by the median value from each subset of data. Different letters indicate statistically significant differences ($p < 0.05$); capital letters indicate marginal differences ($0.05 < p < 0.10$) (identified to support discussion of patterns and trends in results). Of primary interest were the comparisons between sulfidic bedrock (Sites 2 and 3) and sandstone bedrock (Sites 6 and 7).

For surface soil (Table 7), statistically significant differences were found among the bedrock types for soil chemistry parameters pH_{water}, EA, %BS, CEC, exchangeable aluminum (covariant with EA), and strongly adsorbed (phosphate-extractable) sulfate. Soil overlying sandstone bedrock contained the statistically lowest median values of pH_{water}, %BS, and extractable sulfate. The same set of soils contained the statistically highest median values of EA and aluminum, and CEC. Marginal differences (not statistically significant at $\alpha = 0.05$) were found for weakly adsorbed (chloride-extractable) sulfate and total extractable sulfate (covariant with phosphate-extractable sulfate). Non-significant differences in surface soil for the following were notable: (1) soil pH_{CaCl2} results (lowest in sandstone catchment soil) were consistent with soil pH_{water} results (also lowest in sandstone catchment soil), and (2) surface soil overlying sandstone had the largest concentrations of total and organic carbon, and total and organic sulfur (Table 7). Except for extractable sulfate, surface soils from sulfidic and transition zone sites had generally similar soil chemistry.

For subsurface soil (Table 8), pH (both water and $CaCl_2$ basis), CEC, and weakly adsorbed (chloride-extractable) sulfate were similar among the three bedrock types. Statistically significant differences were found among the bedrock types for some soil chemistry parameters. Subsurface

soil overlying sandstone contained the statistically lowest median values of total and phosphate-extractable sulfate. The same set of sites contained the statistically highest median values of %BS, total carbon, total organic sulfur (covariant with total carbon), and total sulfur (covariant with organic sulfur) in subsurface soil (Table 8). Marginal differences ($0.05 < p < 0.10$) were found for EA (highest in sandstone catchment soil) and total organic carbon (highest in sulfidic bedrock soil; consistent with subsurface total carbon results). Non-significant differences in subsurface soil for the following were notable: EBC (highest in subsurface soil overlying sulfidic bedrock) was consistent with %BS (also highest over sulfidic bedrock); and EA and aluminum concentrations were consistent with each other (largest in subsurface soil overlying sandstone). Subsurface soil overlying sandstone had largest concentrations of total and organic carbon and total and organic sulfur (Table 8). Except for extractable sulfate, subsurface soils from sulfidic and transition zone catchments had generally similar soil chemistry. Though not as definitive as for surface soil, subsurface soil overlying sandstone bedrock showed the greatest effects from acidification. Unlike surface soil, concentrations of extractable sulfate were higher (not statistically) in subsurface soil overlying sulfidic and transition zone bedrock than overlying sandstone. With respect to subsurface soil sulfate content, transition zone and sulfidic bedrock sites were more similar to each other than to sandstone sites. As was the case for surface soil, subsurface soil sulfate content and soil acidification did not appear to correlate.

Stream Water Chemistry

Stream water chemistry results from individual catchments (Table 9) are presented as ranges, and statistically significant differences based on non-parametric statistical tests are indicated by different letters. The ANC, sulfate, and sum of base cations (SBC) are shown in micromoles of

charge per liter ($\mu mol_C\ L^{-1}$); dissolved metals (aluminum, iron, manganese) and silica are shown in micromoles per liter ($\mu mol\ L^{-1}$). As was found for several soil chemistry parameters (Tables 7 and 8), stream water from transition zone catchment Site 4 had markedly larger values of pH (in both field measured and lab measured [pH_{Lab}]), ANC, SBC, and dissolved silica (Table 9). As such, results from Site 4 were not weighted heavily in statistical analysis or data interpretations.

Stream water pH measured in the field was not significantly different than pH_{Lab} (Table 9) ($p < 0.001$). Stream water pH_{Lab} ranged from 4.26 to 6.18 across all samples (excluding Site 4). Concentrations of SBC were statistically indistinguishable among the Sites (excluding Site 4). Stream water from Sites 1 and 2 (sulfidic bedrock catchments) had statistically lower stream water pH_{Lab} (4.26 – 4.77) than the other five sites (5.30 – 6.18), including Site 3 (the third sulfidic bedrock catchment). Stream water from Sites 1 and 2 had statistically lowest ANC values (-62 – -22 versus -5 – +19 $\mu eq\ L^{-1}$), and statistically highest concentrations of sulfate (54.3 – 77.1 versus 8.1 – 42.7 $\mu mol\ L^{-1}$), total aluminum (0.3 – 18.8 versus < 0.1 – 8.2 $\mu mol\ L^{-1}$), total iron (< 0.1 – 9.9 versus < 0.1 – 2.2 $\mu mol\ L^{-1}$), and total manganese (< 0.1 – 4.3 versus < 0.1 – 0.8 $\mu mol\ L^{-1}$). Thus, water chemistry data from Sites 1 and 2 were found to be similar to each other, but statistically different from all other sites (including Site 3).

Discussion

Having accurate understanding of fundamental transformation mechanisms and typical compositions of sulfur in GRSM forest soil is critical if more complex scenarios, such as the influence of atmospheric sulfur on soil sulfur content and processing, are to be modeled accurately.

Soil / Bedrock Interactions

Bedrock composition is one factor in soil development that shapes soil characteristics that potentially ameliorate or exacerbate catchment acidification. The primary hypothesis in this study was that some GRSM soils, that are poorly buffered due to naturally base cation-poor geology and historical climate (e.g., high precipitation causing high rates of base cation flushing), may be further acidified by oxidative weathering of local sulfidic bedrock. However, analytical results for the subset of soil geochemistry parameters relevant to acidification showed little evidence that sulfidic bedrock had exacerbated soil acidification or increased the total soil sulfur load. Geochemical evidence of susceptibility to acidification was much clearer in surface soils overlying sandstone bedrock than in surface soils overlying sulfidic bedrock, based on soil pH and exchangeable acidity and aluminum results (Table 7). Differences in subsurface soil pH relative to underlying bedrock were not distinct, but differences in other subsurface soil chemistry parameters did show higher susceptibility to acidification of catchments overlying sandstone (Table 8). Soil pH measured in this study (i.e., > 90% of samples pH_{water} < 5) are in the range where the following soil pH buffer systems are active: dissolution/precipitation of aluminum and iron oxides, ion exchange reactions, and protonation/deprotonation of soil organic functional groups (Sumner 2000; Essington 2015). The consistently low soil pH data across all GRSM catchments is consistent with the generally low neutralizing potential of GRSM soil and bedrock minerals (low in sandstone bedrock; absent in sulfidic bedrock).

Strongly adsorbed (phosphate-extractable) sulfate was the only soil chemistry parameter apparently affected by sulfidic bedrock. Their concentrations were significantly higher in both surface soil (Table 7) and subsurface soil (Table 8) overlying sulfidic bedrock as compared to soil

overlying sandstone. In all catchments, subsurface soil had higher concentrations of strongly adsorbed sulfate than surface soil (Table 6). This is consistent with the existence of a large source of sulfate generated by sulfide oxidation in the underlying bedrock. Total soil sulfur content (primarily soil organic sulfur; Table 6) was not significantly larger in soils overlying sulfidic bedrock relative to soil overlying sandstone. A number of interrelated environmental factors may explain the lack of differences in soil organic sulfur relative to underlying bedrock. For example, based on qualitative observations during sampling, vegetation type was different and vegetation density appeared to be lower at the sulfidic bedrock catchment sites. Thus, relatively lower annual inputs of organic matter to the forest floor may be a limiting factor in sulfidic bedrock catchments ability to efficiently sequester/immobilize additional (lithogenic) sulfur into soil organic sulfur.

At the sites examined, GRSM surface soil overlying sandstone showed the clearest effects from acidification with respect to soil pH and ion-exchange chemistry. In contrast, surface soil overlying sulfidic bedrock had the statistically higher concentrations of phosphate-extractable sulfate than did surface soil overlying transition zone or sandstone bedrock. Thus, soil sulfate content and soil acidification did not correlate in sampled surface soil. Though not as definitive as for surface soil, subsurface soil overlying sandstone bedrock showed the greatest effects from acidification, also because of inherently low neutralizing potential. Unlike surface soil, concentrations of extractable sulfate were higher (though not statistically) in subsurface soil overlying sulfidic and transition zone bedrock than overlying sandstone. With respect to subsurface soil sulfate content, transition zone and sulfidic bedrock sites were more similar to each other than to sandstone sites. Subsurface soil sulfate content and soil acidification did not appear to correlate.

Soil Sulfur Status – Inorganic Sulfur

Concentrations of soil sulfate (0.8 to 9.6 mg-S kg^{-1} chloride-extractable and 2.8 to 126 mg-S kg^{-1} phosphate-extractable) indicate that strongly adsorbed sulfate represents 78% to 93% of total soil sulfate pool at these sampled sites. Concentrations of strongly adsorbed sulfate were statistically larger in soil overlying sulfidic bedrock than in soil overlying sandstone bedrock. In catchments overlying sulfidic and transition zone bedrock, approximately 5x-10x more mass of total sulfate was found in subsurface soil than in surface soil (Table 6). Subsurface soil appears to be the primary source of dissolved sulfate exported from these GRSM catchments during baseflow conditions by throughflow water flushing the B- and C-horizons. The concept of stream water sulfate originating from the subsurface soil horizons is consistent with other studies reporting changes in stream water sulfate concentrations with changing water table levels (i.e., before and after storm events). Mayer et al. (2010) investigated the causes of variations in stream water sulfate concentrations in the Sleepers River watershed (Vermont, USA) during and after a particularly dry summer. It was found that under anoxic soil conditions during the wet (inundated) months, microbial sulfate reduction was generating sulfidic minerals in deeper soil layers. They also found that the newly precipitated sulfidic minerals were re-oxidizing to sulfate (secondary sulfate) when soil conditions became aerobic during the drought months. It was concluded that secondary sulfate had dissolved into the soil solution phase during the post-drought, soil-rewetting period, and contributed to the increase in stream water sulfate exported from the watershed. Similar results have been found in studies of acid sulfate soil (ASSoil) (Kittrick et al. 1982; SA-EPA 2007; Sullivan et al. 2009; Sullivan et al. 2010; Jayalath 2012). ASSoils containing substantial amounts of pyrite-type minerals can be kept in pseudo-steady-state under anoxic conditions (i.e., sulfidic or potential ASSoil), but rapidly oxidize when exposed to air or oxygenated water and form sulfuric

acid (i.e., sulfuric or actual ASSoil). Except for degree or scale, the net effects from actual ASSoil are similar to the effects of atmospheric sulfur deposition: mobilization of acidity and sulfate to the soil solution phase, and ultimately to the catchment's stream water. Studies have shown that weathering of native sulfidic minerals can acidify forest catchment stream water to an equal or greater extent than atmospheric deposition (Baur and Feger 1992; Bailey et al. 2004; Mitchell and Likens 2011).

Soil Sulfur Status – Organic Sulfur

In the study catchments, organic matter is a major sink for sulfur inputs. It is well-documented that soil organic sulfur comprises >90% of total soil sulfur in most temperate climate surface soils (e.g., Autry et al. 1990), and a similarly high percentage in most subsurface soil. In this study, the percentage of total soil sulfur found as organic sulfur was marginally (but not statistically significantly) higher in surface soil than in subsurface soil at each site (Table 6).

A strong correlation between soil carbon and soil sulfur in the study catchments was found (Figure 13). With data from all catchments and soil profile horizons combined, 90% ($p < 0.0001$) of the variability in total soil sulfur (moles S kg^{-1} soil) was explained by total carbon content (moles C kg^{-1} soil) (Figure 13A). Comparing molar concentrations of soil organic carbon and soil organic sulfur (Figure 13A), 85% ($p < 0.0001$) of the variability in soil organic sulfur was explained by soil organic carbon.

Carbon-to-sulfur ratio (C:S molar basis) has been reported to have ecological relevance to sulfur cycling by soil micro-organisms in forest ecosystems (Jez 2008). Net immobilization tends to occur when soil C:S > 400, and net mobilization/mineralization tends to occur when soil C:S < 200 (Freney 1967). Overall average C:S (molar basis) were 356 for total C:S, and 471 for organic

C:S. Individual soil samples had C:S (total basis) ranging from 78 to 696 (10 samples < 200; 21 > 400), and C:S (organic basis) ranging from 167 to 826 (2 samples < 200; 27 > 400). The values measured in this study are higher than other soil C:S ratios reported in the literature (e.g., C:S range 96 to 194 Fitzgerald et al. 1985; 62.5 to 185 Tipping et al. 2016). These ratios are heavily biased toward values > 400, and there were no statistically significant correlations between C:S value and soil horizon, bedrock type or site. The C:S ratios found in this study suggests there is net retention of sulfur occurring in these catchments. This is consistent with net retention of sulfur calculated using monitoring data collected from the Noland Divide (NDW) environmental monitoring station (Cai et al. 2011).

Stream Water / Bedrock Interactions

Despite Sites 1 – 3 all overlying sulfidic bedrock, stream water chemistry at Site 3 was consistently more similar to transition zone and sandstone bedrock Sites 5, 6 and 7 than to Sites 1 and 2 (Table 9). Site 3 soil locations had thin soil profiles and steep slopes (short water/soil/bedrock contact time) whereas Site 2 had thin soil but less steep slopes; Site 1 soil was inaccessible. Additional confounding factors are drainage area, dominant vegetation, soil classification, and area contribution from disturbed soil/exposed bedrock areas (Table 3). To examine the contribution of disturbed soil/exposed bedrock to stream water chemistry, an extreme case of surface water/sulfidic bedrock contact was quantified. During baseflow conditions, water flowing on the surface of a large sulfidic bedrock slab at Site 2 was sampled and analyzed for chemistry parameters. That surface water source represents a direct water/bedrock contact scenario without modification by soil interactions, and the corresponding analytical results them to have extremely acidified water chemistry (Table 9). Note that in addition to direct influence of sulfide bedrock

weathering, these results also reflect the effects of evaporative concentration of dissolved solutes on the exposed bedrock surface.

Stable isotope composition of dissolved sulfate in stream water and in a sample of water flowing over the surface of sulfidic bedrock outcrops (rock-face) was measured for a complementary study at these same sites (Gonzalez et al. 2018). Sulfur isotope composition ("$\delta^{34}S$") has units of parts per thousand (per mil; ‰), and is quantified as the difference in isotope ratios ($R = {}^{34}S/{}^{32}S$) between the sample and the established sulfur isotope reference material, Vienna Canon Diablo Troilite, normalized to the isotope ratios in the reference material: $\delta^{34}S_{sample} = 1000\ (R_{sample} / R_{standard} - 1)$. For context, the magnitudes and signs of $\delta^{34}S$ values generally indicate oxidation states of sulfur in the original sample, with increasingly negative values associated with reduced sulfur (e.g., sulfidic bedrock) and increasingly positive values associated with lithospheric sulfate (e.g., marine and evaporite mineral sulfate) (Sharp 2007). The sulfur isotope composition of dissolved sulfate in the water samples are summarized below as mean values (and number of replicates):

Site	1	2	3	4	5	6	7	2
Sample	stream	stream	stream	stream	stream	stream	stream	rock-face
$\delta^{34}S$, ‰	– 1.9	+ 1.4	+ 6.2	+ 4.0	+ 6.9	+ 7.2	+ 7.8	– 7.6
N samples	3	2	3	2	1	1	8	1

Sites 1 and 2 had stream water sulfate with $\delta^{34}S$ values that were much lower than those from the other sites, including Site 3 (the third sulfidic bedrock catchment). The rock-surface water sample from Site 2 had the most negative $\delta^{34}S$ value, which is consistent with the source of that sulfur being oxidation of sulfide-mineral rich bedrock. If one considers the rock-face $\delta^{34}S$ as the lower endmember and the $\delta^{34}S$ value of sandstone bedrock Site 7 as the upper endmember, it can be argued that the $\delta^{34}S$ of sulfate in stream water from the three sulfidic bedrock catchments were

comprised of mixtures of these two source endmembers. Approximate proportions of each component can be calculated for each site from a simple two-component mixing model:

$\delta^{34}S(\text{stream water}) = X(\delta^{34}S\text{-sulfidic bedrock}) + (1 - X)(\delta^{34}S\text{-soil})$

- Site 1: 63% bedrock // 27% soil
- Site 2: 42% bedrock // 58% soil
- Site 3: 10% bedrock // 90% soil

Based on both water chemistry results and stable isotope analysis, exposure of bedrock (as natural outcrops or landslide-type disturbance events) is the condition under which sulfidic bedrock appears to exert its most direct influence on stream water chemistry. This same conclusion has been reported for abandoned copper mines within the GRSM boundaries and offsite to the south (in North Carolina, USA), and for GRSM areas north and southwest of the seven study sites (Hammarstrom et al. 2003, Hammarstrom et al. 2005, and citations therein), where water in direct contact with exposed rock substrate had generally acidic chemistry: pH < 5, ANC < 0 $\mu mol_C\ L^{-1}$, aluminum > 0.2 mg L^{-1}, and sulfate concentrations > 5 mg L^{-1}.

Stream Water / Soil Interactions

Stream water acidity and soil acidity results from this study were not correlated. Surface water pH and ANC were statistically smaller from catchments overlying sulfidic bedrock, but soil pH was statistically smallest in catchments overlying sandstone. Oxidation of sulfidic bedrock appeared to control stream water acidity, but the lack of acid neutralizing capacity of sandstone bedrock appeared to control the soil acidity. This is consistent with Elwood et al. (1991) that found dissolved sulfate and stream water ANC were weakly inversely related when sum of base cations (SBC) concentrations were below roughly 100 $\mu mol_C\ L^{-1}$ but not so at higher SBC concentrations.

The pH of the soil solution is known to be buffered by ion-exchange reactions at the surfaces of soil mineral solids, and potentially by dissociation and complexation reactions between aluminum and organic matter functional groups (Sumner 2000; Essington 2015). Organic matter was thought to be a major factor explaining soil pH results in this study. Correlations between soil pH_{water} and soil organic carbon (%) provide evidence for soil pH buffering mechanisms (Figure 14). The soil pH_{water} and pH_{CaCl2} (left column and right column, respectively) were plotted against soil organic carbon, distinguished by bedrock type (sulfidic top row; sandstone bottom row) and soil horizon (surface soil = open symbols; subsurface soil = filled symbols). Soil pH was found to be inversely related to soil organic carbon in all four scenarios, but the relationship between soil pH_{CaCl2} and organic carbon in soil overlying sulfidic bedrock was not statistically significant ($p = 0.4738$). The inverse relationship between soil pH and soil carbon content has been reported by others (e.g., Stanko and Fitzgerald 1990).

Conclusions

The objective of this study was to further the understanding of acidification in high-elevation GRSM catchments by focusing on biogeochemical processes operating at small spatial scales (first-order stream catchments and headwaters drainage areas). It was hypothesized that the geochemistry of soil and stream water influenced by atmospheric acidic deposition (used as the study's reference scenario) would be significantly altered at locations overlying sulfidic bedrock. Characterization data for soil samples in this study were similar to those reported by Grell (2010) for soil collected from eight catchments across a wider area of the GRSM.

Based on this study's results, neither direct atmospheric acidic deposition nor sulfidic bedrock was the single dominant factor determining soil or stream water geochemistry in the study catchments.

First, sulfate concentrations in GRSM stream water were consistently larger than in GRSM precipitation, indicative of additional sulfate sources (e.g., sulfidic bedrock weathering; mineralization of organic sulfur). Two catchments nearest known areas of exposed sulfidic bedrock had statistically higher adsorbed sulfate concentrations than the third catchment overlying sulfidic bedrock, or than any of the catchments overlying sandstone bedrock. Several stream water chemistry parameters (pH, ANC, sulfate, aluminum and iron, and dissolved silica) were significantly altered in the two catchments nearest the known areas of exposed sulfidic bedrock, but not in the third catchment overlying sulfidic bedrock, nor in the catchments overlying sandstone bedrock. Sites 1 and 2 were located at the base of the prominent sulfidic phyllite and shale mountain peak (Anakeesta Ridge) in the central GRSM, a ridge associated with numerous landslide scars of exposed sulfidic bedrock. In contrast, the Site 3 catchment (also overlying sulfidic bedrock) is not known to have exposed bedrock, and the soil profile depth at the sampling locations was observed to be relatively thin. Its stream water chemistry generally was similar to that of the transition zone and sandstone catchment sites, not to Sites 1 and 2. These results suggest that during baseflow conditions, stream water from Sites 1 and 2 might be comprised of drainage water from two intra-catchment sources: subsurface soil throughflow and water that had been in direct contact with exposed bedrock. The soil mantel's moderating role in stream water chemistry of high-elevation catchment ecosystems, even if overlying potentially acidifying sulfidic bedrock, is an important finding for GRSM resource managers and ecosystem acidification modelers. These factors need further study to confirm their role in determining soil and stream water chemistry. Such studies would contribute to the growing understanding of the acidification and sulfur biogeochemistry in the GRSM.

References

Appelo, C.A.J., and D. Postma (2005). Geochemistry, Groundwater and Pollution, 2nd Edition. A.A. Balkema Publishers (a member of Taylor & Francis Group plc); Leiden, The Netherlands.

Autry, Andrew R., John W. Fitzgerald, and Penny R. Caldwell (1990). Sulfur fractions and retention mechanisms in forest soils. Canadian Journal of Forest Research, 20(3):337-342. GRef120

Bacon, J.R. and Richard P. Maas (1979). Contamination of Great Smoky Mountains Trout Streams by Exposed Anakeesta Formations. Journal of Environmental Quality, 8(4):538-543. GRef553

Bailey, Scott W., Bernhard Mayer and Myron J. Mitchell (2004). Evidence for influence of mineral weathering on stream water sulphate in Vermont and New Hampshire (USA). Hydrological Processes 18(9), 1639-1653. GRef562

Baldigo, Barry P., Matt A. Kulp, and John S. Schwartz (2017). Relationships between fish assemblages and acid-base chemistry in streams of the Great Smoky Mountains National Park. Ecological Indicators (in press).

Baur, S. and K.H. Feger (1992). Importance of natural soil processes relative to atmospheric deposition in the mobility of aluminum in forested watersheds of the Black Forest. Environmental Pollution, 77(2-3):99-105. GRef676

Bloem, E., S. Haneklaus, and E. Schnug (2002). Optimization of a method for soil sulphur extraction. Communications in Soil Science and Plant Analysis, 33(1-2):41-51. GRef792

Brantley, Susan L. (2008). Kinetics of mineral dissolution. Chapter 5 in: Susan L. Brantley, James D. Kubicki, and Art F. White (2008). Kinetics of Water-Rock Interaction. Springer, New York. Pp. 151-210. GRef009

Brantley, Susan L., M.I. Lebedeva, and Ekaterina Bazilevskaya (2014). Relating Weathering Fronts for Acid Neutralization and Oxidation to pCO_2 and pO_2. Chapter 6 in: Holland, Heinrich D. and Karl K. Turekian (2014). Treatise on Geochemistry, Second Edition. Elsevier, Oxford, United Kingdom. Pp. 151-210. GRef1063

Brennan, R.F. and M.D.A. Bolland, 1998. Relationship between pH measured in water and calcium chloride for soils of Southwestern Australia. Communications in Soil Science and Plant Analysis, 29(17-18):2683-2689. GRef1050

Burke, D. J., López-Gutiérrez, J. C., Smemo, K. A., & Chan, C. R. (2009). Vegetation and Soil Environment Influence the Spatial Distribution of Root-Associated Fungi in a Mature Beech-Maple Forest. Applied and Environmental Microbiology, 75(24), 7639–7648. http://doi.org/10.1128/AEM.01648-09

Burns, Douglas A., Karen Riva-Murray, Robert W. Bode, and Sophia Passy (2008). Changes in stream chemistry and biology in response to reduced levels of acid deposition during 1987-2003 in the Neversink River Basin, Catskill Mountains. Ecological Indicators 8(3):191-203. GRef433

Burns, Douglas A., Michael R. McHale, Charles T. Driscoll, and Karen M. Roy (2006). Response of surface water chemistry to reduced levels of acid precipitation: comparison of trends in two regions of New York, USA. Hydrological Processes, 20(7):1611-1627. GRef629

Busing, R.T. (2005). NPP (Net Primary Production) Temperate Forest: Great Smoky Mountains, Tennessee, USA, 1978–1992. Oak Ridge National Laboratory Distributed Active Archive Center, Oak Ridge, Tennessee

Cai, M., A.M. Johnson, J.S. Schwartz, S.E. Moore, and M.A. Kulp (2012). Soil acid-base chemistry of a high-elevation forest watershed in the Great Smoky Mountains National Park watershed: Influences of acid deposition. Water, Air, & Soil Pollution 223:289-303. GRef590

Cai, Meijun, Amy M. Johnson, John S. Schwartz, Stephen E. Moore, Matt A. Kulp (2011). Response of soil water chemistry to simulated changes in acid deposition in the Great Smoky Mountains. GRef592

Cai, M. J.S. Schwartz, R.B. Robinson, S.E. Moore, and M.A. Kulp (2010). Long-term effects of acidic deposition on water quality in a high-elevation Great Smoky Mountains National Park watershed: Use of an ion input-output budget. Water, Air, & Soil Pollution 209:143-156. GRef591

Chandra, L. R., Gupta, S., Pande, V., & Singh, N. (2016). Impact of forest vegetation on soil characteristics: a correlation between soil biological and physico-chemical properties. 3 Biotech, 6(2), 188. http://doi.org/10.1007/s13205-016-0510-y

Chen, Limin, Charles T. Driscoll, Solomon Gbondo-Tugbawa, Myron J. Mitchell, and Peter S. Murdoch (2004). The application of an integrated biogeochemical model (PnET-BGC) to five forested watersheds in the Adirondack and Catskill regions of New York. Hydrological Processes, 18(14):2631-2650. GRef726

Chestnut, Lauraine G. and David M. Mills (2005). A fresh look at the benefits and costs of the U.S. acid rain program. Journal of Environmental Management, 77(3), 252-266. GRef612

Claff, S.R., L.A. Sullivan, E.D. Burton, and R.T. Bush (2010). A sequential extraction procedure for acid sulfate soils: Partitioning of iron. Geoderma, 155, 224-230. GRef838

Cook, Robert B., J.W. Elwood, R.R. Turner, M.A. Bogle, Patrick J. Mulholland, A.V. Palumbo (1994). Acid-base chemistry of high-elevation streams in the Great Smoky Mountains. Water, Air, and Soil Pollution 72:331-356. GRef559

Driscoll, Charles T., G.B. Lawrence, A.J. Bulger, T.J. Butler, C.S. Cronan, C. Eagar, K.F. Lambert, Gene E. Likens, J.L. Stoddard, and Kathleen C. Weathers (2001). Acidic deposition in the northeastern United States: Sources and inputs, ecosystem effects, and management strategies. BioScience, 51(3):180-198. GRef1036

Elwood J.W., Sale M.J., Kaufmann P.R., Cada G.F. (1991) The Southern Blue Ridge Province. In: Charles D.F. (eds.) Acidic Deposition and Aquatic Ecosystems. Springer, New York, NY

Ensminger, L.E. (1954). Some factors affecting the adsorption of sulfate by Alabama soils. Soil Science Society of America Journal, 18(3), 259-264. GRef844

Essington, Michael E. (2015). Soil and Water Chemistry: An Integrative Approach (2nd Edition). CRC Press, Boca Raton, Florida.

Fakhraei, Habibollah, Charles T. Driscoll, James R. Renfro, Matt A. Kulp, Tamara F. Blett, Patricia F. Brewer, and John S. Schwartz (2016). Critical loads and exceedances for nitrogen and sulfur atmospheric deposition in Great Smoky Mountains National Park, United States. Ecosphere, 7(10), e01466. pp. 1-28 GRef1047

Fitzgerald, John W., Timothy C. Strickland, and Jaru T. Ash (1985). Isolation and partial characterization of forest floor and soil organic sulfur. Biogeochemistry, 1(2), 155-167. GRef119

Freney, J.R. (1967). Sulfur-containing organics. In: A.D. McLaren and G.H. Petersen (eds.), Soil Biochemistry. Marcel Dekker, New York; pp. 229-259.

Galloway, James N., Stephen A. Norton, and M. Robbins Church (1983). Freshwater acidification from atmospheric deposition of sulfuric acid: A conceptual model. Environmental Science and Technology, 17(11):541A-545A. GRef196

Gonzalez, Adrian M., Anna Szynkiewicz, John S. Schwartz, Michael E. Essington and Matt A. Kulp (2018). Identifying sulfur sources and cycling mechanisms in high-elevation forest catchments of the Great Smoky Mountains National Park, USA, using stable isotope composition analysis. In manuscript.

Gonzalez, Adrian M., John S. Schwartz, and Matt Kulp (2015). Geochemistry in a high-elevation watershed responds to reductions in acid-pollutant emissions? 2015 World Environmental & Water Resources Congress (EWRI), Austin, Texas, 17-21 May 2015. Platform presentation 19 May 2015.

Grell, Mary Ann Elizabeth (2010). Soil chemistry characterization of acid sensitive watershed in the Great Smoky Mountains National Park. Master of Science Thesis, University of Tennessee, Knoxville; December 2010.

Hadley, Jarvis B. and Richard Goldsmith (1963). Geology of the Eastern Great Smoky Mountains North Carolina and Tennessee. Geological survey professional paper 349-B. U.S. Department of the Interior, U.S. Government Printing Office, Washington, D.C.

Hammarstrom, Jane M., Robert R. Seal, Allen, L. Meier, and John C. Jackson (2003). Weathering of sulfidic shale and copper mine waste: secondary minerals and metal cycling in Great Smoky Mountains National Park, Tennessee, and North Carolina, USA. Environmental Geology, 45(1):35-57. GRef490

Hammarstrom, Jane M., Robert R. Seal, Allen L. Meier, and J.M. Kornfeld (2005). Secondary sulfate minerals associated with acid drainage in the eastern US: recycling of metals and acidity in surficial environments. Chemical Geology, 215(1-4):407-431. GRef486

Herlihy, A.T., P.R. Kaufmann, J.L. Stoddard, K.N. Eshleman, and A.J. Bulger (1996). Effects of Acidic Deposition on Aquatic Resources in the Southern Appalachians with a Special Focus on Class I Wilderness Areas. Prepared for the Southern Appalachian Mountains Initiative (SAMI).

Holmgren, George G.S. (1967). A rapid citrate-dithionite extractable iron procedure. Soil Science Society of America Proceedings, 31(2), 210-211. GRef839

Huckabee, John W., C. Phillip Goodyear, and Ronald D. Jones (1975). Acid Rock in the Great Smokies: Unanticipated Impact on Aquatic Biota of Road Construction in Regions of Sulfide Mineralization. Transactions of the American Fisheries Society, 104(4):677-684. GRef816

Jayalath, Nilmini (2012). Laboratory protocols for acid sulfate soils. CSIRO Land and Water Science Report 01/12; June 2012.

URL: https://publications.csiro.au/rpr/download?pid=csiro:EP124374&dsid=DS3. Accessed on 19 September 2017.

Jez, Joseph (Editor) (2008). Sulfur: A Missing Link between Soils, Crops, and Nutrition. American Society of Agronomy, Inc., Crop Science Society of America, Inc. and Soil Science Society of America, Inc.; Agronomy Monograph 50.

Johnson, Dale W., H. Van Miegroet, S.E. Lindberg and D.E. Todd (1991). Nutrient cycling in red spruce forest of the Great Smoky Mountains. Canadian Journal of Forest Research, 21, 769–787.

Johnson-Maynard, J.L., R.C. Graham, P.J. Shouse, and S.A. Quideau (2005). Base cation and silicon biogeochemistry under pine and scrub oak monocultures: implications for weathering rates. Geoderma, 126(3-4):353-365. GRerf054

Kettler, T.A., J.W. Doran and T.L. Gilbert (2001). Simplified Method for Soil Particle-Size Determination to Accompany Soil-Quality Analyses. Soil Science Society of America Journal, 65(3), 849-852. GRef836

King, Philip B. (1964). Geology of the Central Great Smoky Mountains Tennessee. Geological Survey Professional Paper No. 349-C. U.S. Department of the Interior, U.S. Government Printing Office, Washington, D.C.

Kittrick, J.A., D.S. Fanning, and L.R. Hosner (eds.), 1982. Acid Sulfate Weathering. Soil Science Society of America; Madison, WI.

Klimont, Z., S.J. Smith and J. Cofala (2013). The last decade of global anthropogenic sulfur dioxide: 2000-2011 emissions. Environmental Research Letters 8 (1): no.014003.

DOI:10.1088/1748-9326/8/1/014003. GRef1048

Likens, Gene E., Thomas J. Butler, and Donald C. Buso (2001). Long- and short-term changes in sulfate deposition: Effects of the 1990 Clean Air Act Amendments. Biogeochemistry, 52(1), 1-11. GRef593

Loeppert, Richard H. and William P. Inskeep (1996). Iron. Chapter 23, 639-664. In: D.L. Sparks (ed.), Methods of Soil Analysis, Part 3, Chemical Methods. Soil Science Society of America. Book Series 5. ASA and SSSA, Madison, WI.

Maas, Richard P. (1976). Characterization of water chemistry of Anakeesta pyrite affected streams in the Great Smoky Mountains National Park. Master's thesis: Western North Carolina University.

Mayer, Bernhard, James B. Shanley, Scott W. Bailey and Myron J. Mitchell (2010). Identifying sources of stream water sulfate after a summer drought in the Sleepers River watershed (Vermont, USA) using hydrological, chemical, and isotopic techniques. Applied Geochemistry, 25(5), 747-754. GRef289

Maynard D.G., Y.P. Kalra and F.G. Radford (1987). Extraction and Determination of Sulfur in Organic Horizons of Forest Soils. Soil Science Society of America Journal, 51(3), 801-806. GRef730

McCracken, R.J., R.E. Shanks, and E.E.C. Clebsch (1962). Soil Morphology and Genesis at Higher Elevations of the Great Smoky Mountains. Soil Science Society of America Journal, 26(4):384-388. GRef1003

Minasny, B., A.B. McBratney, D.M. Brough, and D. Jacquire (2011). Models relating soil pH measurements in water and calcium chloride that incorporate electrolyte concentration. European Journal of Soil Science, 62(5):728-732. GRef1051

Mitchell, Myron J. and Gene E. Likens (2011). Watershed sulfur biogeochemistry: Shift from atmospheric deposition dominance to climatic regulation. Environmental Science & Technology, 45(12), 5267-5271. GRef358

National Parks Service (NPS) (2017). Webpage "World Heritage Sites in the United States: Great Smoky Mountains National Park." U.S. Department of the Interior website URL: https://www.nps.gov/nr/travel/worldheritagesites/Great_Smoky_Mountains_National_Park.htm Accessed on 23 August 2017).

Neff, Kiel J., John S. Schwartz, Theodore B. Henry, R. Bruce Robinson, Stephen E. Moore, and Matt A. Kulp (2009). Physiological Stress in Native Southern Brook Trout During Episodic Stream Acidification in the Great Smoky Mountains National Park. Archives of Environmental Contamination and Toxicology 57(2):366-376. GRef0-in_que

Omernik, James M. and C.F. Powers (1982). Total alkalinity of surface waters: A national map. U.S. Environmental Protection Agency. Corvallis Environmental Research Laboratory, Corvallis, Oregon.

Or, Dani and Jon M. Wraith (2000). Soil Water Content and Water Potential Relationships. Chapter 3, pp. A53-A63. In: Handbook of Soil Science. Malcolm E. Sumner (Editor-in-Chief), CRC Press, New York, N.Y.

Overton, John H., Jr., Viney P. Aneja and Jack L. Durham (1979). Production of sulfate in rain and raindrops in polluted atmospheres. Atmospheric Environment (1967) 13(3), 355-367.

Rice, Karen C., Todd M. Scanlon, Jason A. Lynch, and Bernard J. Cosby (2014). Decreased Atmospheric Sulfur Deposition across the Southeastern U.S.: When Will Watersheds Release Stored Sulfate? Environmental Science and Technology, 48(17):10071-10078. GRef356

Robinson, R. Bruce, Thomas W. Barnett, Glenn R. Harwell, Stephen E. Moore, Matt A. Kulp, and John S. Schwartz (2008). pH and acid anion time trends in different elevation ranges in the Great Smoky Mountains National Park. Journal of Environmental Engineering, 134(9):800-808. GRef1014

Rossete, Alexssandra Luiza Rodrigues Molina, José Albertino Bendassolli, and Paulo Cesar Ocheuze Trivelin (2008). Organic sulfur oxidation to sulfate in soil samples for total sulfur determination by turbidimetry. Revista Brasileira de Ciência do Solo, 32(6), 2547-2553.GRef662

Ryan, Patrick T. (1989). "Debris Slides and Flows on Anakeesta Ridge within the Great Smoky Mountains National Park, Tennessee, U.S.A. " Master's Thesis, University of Tennessee, 1989. http://trace.tennessee.edu/utk_gradthes/2493 GRef857

Sahrawat, Kanwar L., K.V.S. Murthy, and S.P. Wani (2009). Comparative evaluation of Ca chloride and Ca phosphate for extractable sulfur in soils with a wide range in pH. Journal of Plant Nutrition and Soil Science, 172(3), 404-407. GRef729

Schurr, Sam H. and Bruce C. Netschert (1960). Energy in the American economy, 1850-1975: an economic study of its history and prospects. Resources for the Future. Johns Hopkins Press; Baltimore, Maryland. GRef611

Schwartz, John S., Meijun Cai, Matt A. Kulp, Stephen E. Moore, Becky Nichols and Charles Parker (2014). Biological effects of stream water quality on aquatic macroinvertebrates and fish

communities within the Great Smoky Mountains National Park. U.S. Department of the Interior, National Park Service (NPS) Natural Resources Report (NRR) No. 778; August 2013. GRef584

Schwartz, John S., Adrian M. Gonzalez, Andrew Veenemen, Matt A. Kulp (2017). Great Smoky Mountains National Park Monitoring Program Annual Report of 2016 Activities. Prepared for the National Parks Service, U.S. Department of the Interior.

Sharp, Zachary (2007). Principles of Stable Isotope Geochemistry. Pearson – Prentice Hall, Upper Saddle River, New Jersey 07458.

Smith S.J., J. van Aardenne, Z. Klimont, R.J. Andres, A. Volke, and Arias S. Delgado (2011). Anthropogenic sulfur dioxide emissions: 1850-2005. Atmospheric Chemistry and Physics 11 (3): 1101-1116. GRef1043

South Australia Environmental Protection Agency (SA-EPA) (2007). Acid sulfate soil material guideline – November 2007. South Australia Environmental Protection Agency. URL: www.epa.sa.gov.au/files/8371_guide_sc_acid.pdf. Accessed on 21 September 2017.

Southworth, Scott, Art Schultz, and Danielle Denenny (2004). Generalized Geologic map of Bedrock Lithologies and Surficial Deposits in the Great Smoky Mountains National Park region, Tennessee and North Carolina. U.S. Geological Survey Open File Report 2004-1410, scale 1:100,000.

Southworth, Scott, Art Schultz and Danielle Denenny (2005). Geologic map of the Great Smoky Mountains National Park Region, Tennessee and North Carolina. U.S. Geological Survey Open-File Report 2005-1225. Online at: http://pubs.usgs.gov/of/2005/1225/OF2005-1225_map.pdf

Stanko, Karen M. and John W. Fitzgerald (1990). Sulfur transformations in forest soils collected along an elevational gradient. Soil Biology and Biochemistry, 22(2):213-216. GRef126

Stumm, Werner and James J. Morgan (1981). Aquatic Chemistry: An introduction emphasizing chemical equilibria in natural waters (2nd Edition). Wiley-Interscience, New York.

Sullivan, Timothy J., Bernard J. Cosby, James R. Webb, Kai U. Snyder, Alan T. Herlihy, Arthur J. Bulger, Erin H. Gilbert and Deian Moore (2002). Assessment of the effects of acidic deposition on aquatic resources in the Southern Appalachian Mountains. Report prepared for Southern Appalachian Mountains Initiative (SAMI); prepared by E&S Environmental Chemistry, Inc. (Corvallis, Oregon); July 2002. GRef694

Sullivan, Timothy J., Bernard J. Cosby, Kai U. Snyder, Alan T. Herlihy and B. Jackson (2007). Model-based assessment of the effects of acidic deposition on sensitive watershed resources in the National Forests of North Carolina, Tennessee and South Carolina. Final Report prepared for U.S. Department of Agriculture (USDA) Forest Service, Asheville, North Carolina; October 2007. GRef017

Sullivan, Leigh A., R.W. Fitzpatrick, R.T. Bush, E.D. Burton, P. Shand, and N.J. Ward (2010). The classification of acid sulfate soil materials: further modifications. Southern Cross GeoScience Technical Report No. 310. Southern Cross University, Lismore, NSW, Australia; April 2010. URL: https://www.nrcs.usda.gov/Internet/FSE_DOCUMENTS/nrcs142p2_051509.pdf. Accessed on 19 September 2017.

Sullivan, Leigh A., R.W. Fitzpatrick, R.T. Bush, E.D. Burton, P. Shand, and N.J. Ward (2009). Modifications to the classification of acid sulfate soil materials. Southern Cross GeoScience; 2009.

Sumner, Malcolm E. (ed.) (2000). Handbook of Soil Science. CRC Press, Boca Raton, Florida.

Sumner, M.E. and W.P. Miller (1996). Cation Exchange Capacity and Exchange Coefficients. Chapter 40, p.1201-1229. In: In: D.L. Sparks (ed.), Methods of Soil Analysis, Part 3, Chemical Methods. Soil Science Society of America. Book Series 5. ASA and SSSA, Madison, WI.

Tabatabai, M. Ali, N.T. Basta and H.J. Pirela (1988). Determination of total sulfur in soils and plant materials by ion chromatography. Communications in Soil Science and Plant Analysis, 19(15), 1701-1714. GRef845

Tennessee Valley Authority (TVA) (2017). Environmental stewardship URL: https://www.tva.gov/Environment/Environmental-Stewardship/Air-Quality/Sulfur-Dioxide. Accessed on 10 August 2017.

Thomas, G.W. (1996). Soil pH and soil acidity. Chapter 16, p.475-490. In: In: D.L. Sparks (ed.), Methods of Soil Analysis, Part 3, Chemical Methods. Soil Science Society of America. Book Series 5. ASA and SSSA, Madison, WI.

Thornberry-Ehrlich, Trista (2008). Great Smoky Mountains National Park Geologic Resource Evaluation Report. National Resource Report NPS/NRPC/GRD/NRR-2008/048. National Park Service, Denver, Colorado; NPS D-626, September 2008.

Tipping, Edward, Cayman J. Somerville, and Jörg Luster (2016). The C:N:P:S stoichiometry of soil organic matter. Biogeochemistry, 130(1):117-131. GRef1054

Turner, R.S., P.F. Ryan, D.R. Marmorek, K.W. Thornton, T.J. Sullivan, J.P. Baker, S.W. Christensen, and M.J. Sale (1992). Sensitivity to change for low-ANC eastern US lakes and

streams and brook trout populations under alternative sulfate deposition scenarios. Environmental Pollution, 77(2-3):269-277. GRef680

USDA-NRCS (2009). Soil survey of Great Smoky Mountains National Park, Tennessee and North Carolina. U.S Department of Agriculture, Natural Resources Conservation Service.

van Miegroet, H., I.F. Creed, N.S. Nicholas, D.G. Tarboton, K.L. Webster, J. Shubzda, B. Robinson, J. Smoot, D.W. Johnson, S.E. Lindberg, G. Lovett, S. Nodvin, and S. Moore (2001). Is There Synchronicity in Nitrogen Input and Output Fluxes at the Noland Divide Watershed, a Small N-Saturated Forested Catchment in the Great Smoky Mountains National Park? The Scientific World Journal, (1):480-492.

Vestreng, V., G. Myhre., H. Fagerli, S. Reis, and L. Tarrasón (2007). Twenty-five years of continuous sulphur dioxide emission reduction in Europe. Atmospheric Chemistry and Physics, 7:3663-3681. URL: https://doi.org/10.5194/acp-7-3663-2007. Accessed on 19 September 2017. GRef1042

Weathers, Kathleen C., Samuel M. Simkin, Gary M. Lovett and Steven E. Lindberg (2006). Empirical modeling of atmospheric deposition in mountainous landscapes. Ecological Applications 16(4):1590-1607. GRef522

White, Art F. and Susan L. Brantley (2003). The effect of time on the weathering of silicate minerals: why do weathering rates differ in the laboratory and field? Chemical Geology, 202(3-4):479-506. GRef779

Zhai, Jing, Charles T. Driscoll, Timothy J. Sullivan, and Bernard J. Cosby (2008). Regional application of the PnET-BGC model to assess historical acidification of Adirondack lakes. Water Resources Research, 44(1):W01421. GRef727

Zhou, Qingtao, Charles T. Driscoll, Stephen E. Moore, Matt A. Kulp, James R. Renfro, John S. Schwartz, Meijun Cai, and Jason A. Lynch (2015). Developing Critical Loads of Nitrate and Sulfate Deposition to Watersheds of the Great Smoky Mountains National Park, USA. Water, Air, & Soil Pollution, 226(8):1-16. GRef908

Zelazny, Lucian W., Liming He, and An Vanwormhoudt (1996). Charge Analysis of Soils and Anion Exchange. Chapter 41, p.1231-1253. In: D.L. Sparks (ed.), Methods of Soil Analysis, Part 3, Chemical Methods. Soil Science Society of America. Book Series 5. ASA and SSSA, Madison, WI.

Chapter 5 Appendix

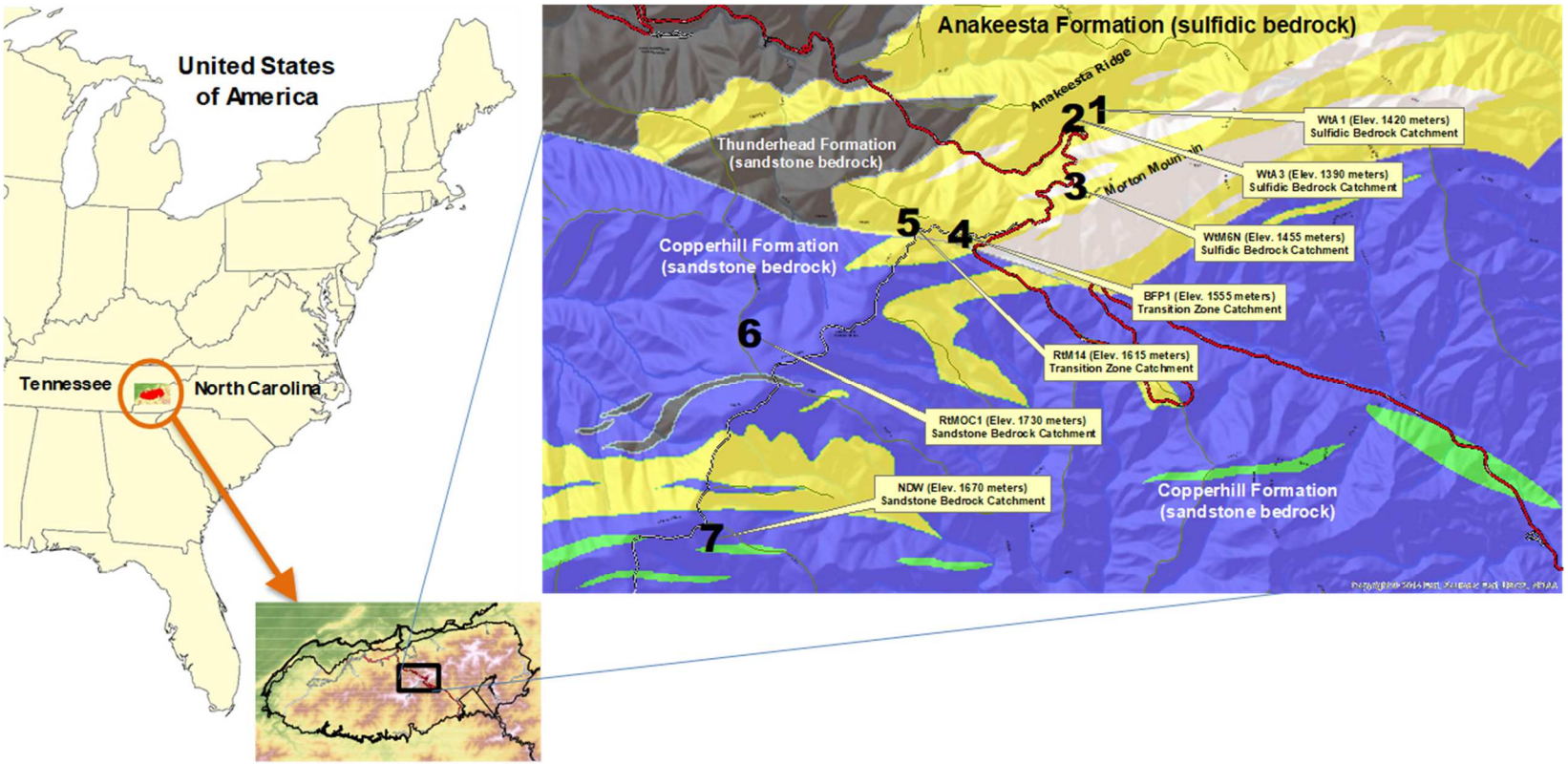

Figure 12. Location of the Great Smoky Mountains National Park (GRSM) and detailed map of study locations and major bedrock formations associated with the study areas. Catchments 1, 2 and 3 = sulfidic bedrock; Catchments 4 and 5 = transition zone bedrock; Catchments 6 and 7 = sandstone bedrock (reference sites).

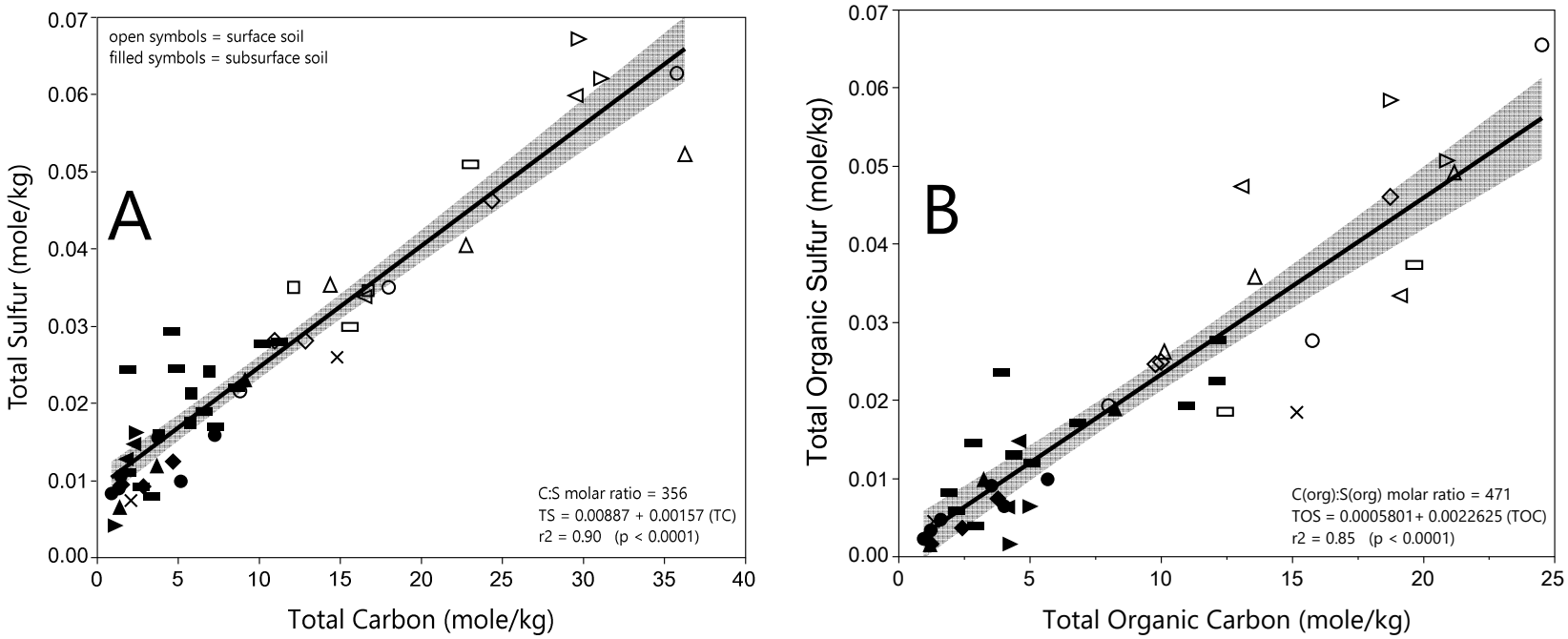

Figure 13. Correlation between soil sulfur and soil carbon (molar concentrations), as (A) total and (B) organic forms. Average C:S ratios and regression data are shown for each.

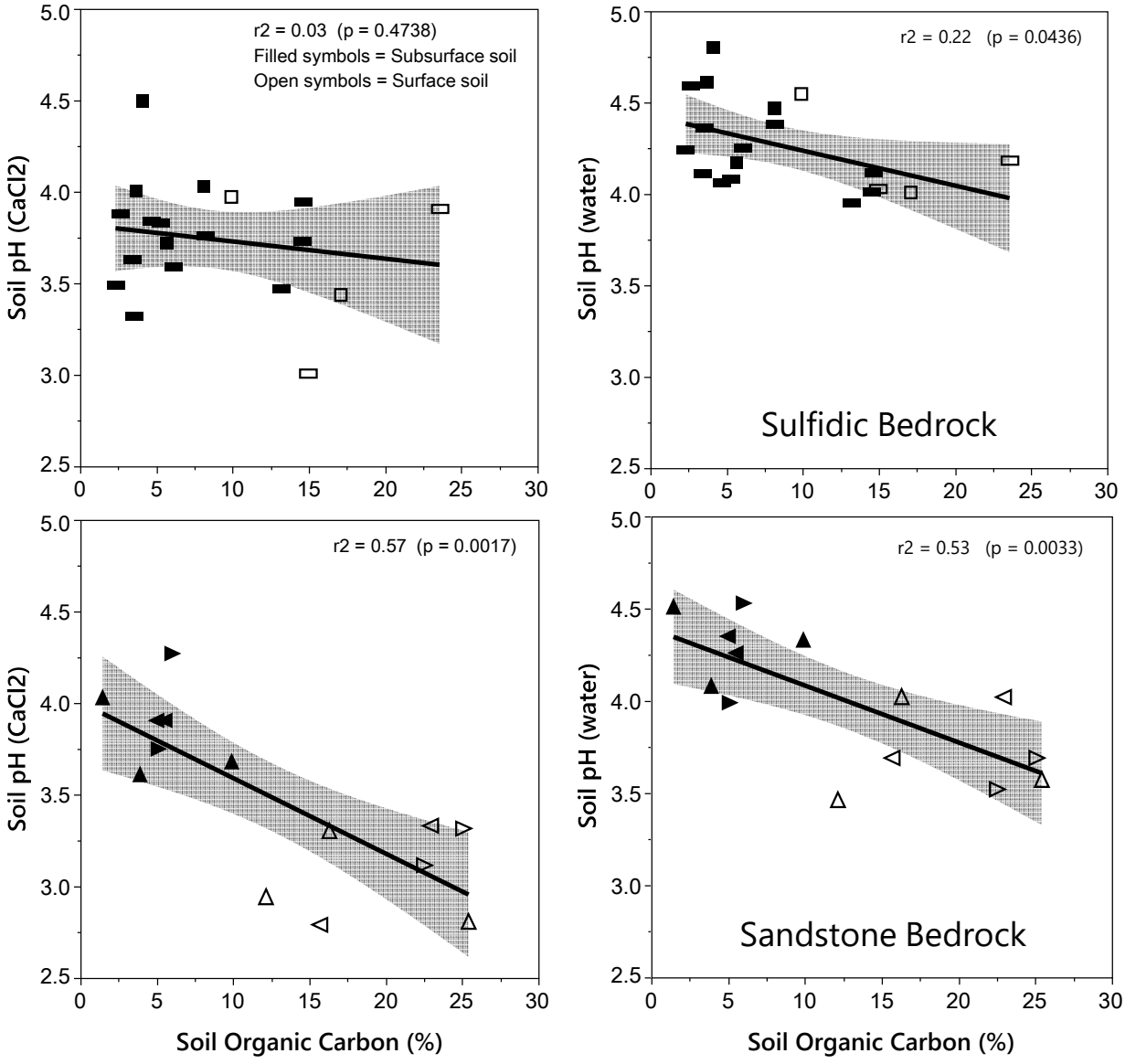

Figure 14. Correlations between soil pH and soil organic carbon at Sites 2 and 3 (overlying sulfidic bedrock; top row) and at Sites 6 and 7 (overlying sandstone bedrock; bottom row). Open symbols represent surface soil; filled symbols represent subsurface soil. Coefficients of determination and analysis of variance p-values shown in each panel. Shading represents the 95% confidence interval of the best fit line.

Table 3. Description of seven study sites and the characteristics of their associated catchments.

Catchment Characteristic	Site/Catchment Number						
	1	2	3	4	5	6	7
Latitude / Longitude (Decimal Degrees)	35.627 -83.415	35.626 -83.420	35.616 -83.417	35.609 -83.438	35.611 -83.448	35.594 -83.475	35.565 -83.480
Drainage Source	Anakeesta Ridge	Anakeesta Ridge	Morton Mountain	Indian Gap	Mount Mingus	Sugarland Mountain	Mount Love
Drainage Area (hectares)	28.0	14.2	7.0	4.0	2.2	5.0	17.4
Catchment Elevation Span (meters above mean sea-level)	1410 - 1820	1390 - 1710	1485 - 1670	1545 - 1585	1600 - 1695	1720 -1805	1680 – 1920
Prominent Bedrock Type	Sulfidic	Sulfidic	Sulfidic	Transition	Transition	Sandstone	Sandstone
Bedrock Classification*	(43;Za) with (Qdf) influence	(43;Za) with (Qdf) influence	(43;Za) with minor (45;Zag)	(43;Za) bordering (51;Zch)	(43;Za) bordering (51;Zch)	(51;Zch)	(51;Zch) with minor (52;Zchs)
Soil Classification **	RtF / SL / LrF	RtF / SL	BpF / LrF	LrF	LrF / LrD	BpF	BpF/SsE/OcF/OwF
Mean Soil Thickness (meters) †	0.9 to 1.1	0.9 to 1.1	0.5 to 1.0	0.9 to 1.1	0.9 to 1.1	0.5 to 1.0	> 2.0
Bulk Density (gram cm^{-3}) †	0.29 - 1.68	0.29 - 1.68	0.29 - 1.68	0.37 - 1.68	0.37 - 1.68	0.29 - 1.68	0.54 - 1.55
Surface Organic Carbon (%)†	10 to 15%	10 to 15%	5 to 15%	10 to 15%	10 to 15%	5 to 90%	8 to 31%
Local Slope (° from horizonal)	13.5°	18.7°	39.0°	29.6°	25.0°	17.7°	25.5°
Local Aspect (° from north)	170°	170°	315°	180°	225°	355°	135°
Dominant Vegetation ***	Northern hardwood	Northern hardwood	Mixed	Mixed	Mixed	Spruce/fir	Spruce/fir

Table 3 continued

* Bedrock lithology and deposit map unit codes (text taken from Southworth et al. 2004; 2005):
(1) Code 43 or Za: Anakeesta formation; dark-gray to black slate and phyllite, medium- to coarse-grained feldspathic sandstone, and arkosic conglomerate, thin- to thick-bedded with dolomite beds.
(2) Code Qdf: Debris flows; scars, tracks, and deposits from modern and historic storms with high rainfall (e.g., exposed sulfidic bedrock "scars").
(3) Code 45 or Zag: Metagraywacke; light-gray, coarse-grained to conglomeratic metagraywacke interbedded with metasiltstone.
(4) Code 51 or Zch: Copperhill formation; Massive to coarse-grained metagraywacke and metaconglomerate interbedded with locally sulfidic quartz-garnet-muscovite phyllite and schist.
(5) Code 52 or Zchs: Quartz-muscovite schist; quartz-muscovite and phyllite interbedded with metagraywacke. Phyllite locally graphitic and sulfidic. Schist contains porphyroblasts of garnet, kyanite, or staurolite, corresponding to metamorphic grade.

** Soil classification codes (descriptions taken from USDA-NRCS 2017):
(1) Code RtF: Rock outcrop-Luftee complex, 30 to 95 percent slopes, very rocky
Rock outcrop: exposed bedrock; Luftee: loamy-skeletal, isotic, frigid Humic Dystrudepts
(2) Code SL: slide area [disturbed soil, commonly associated with exposed bedrock]
(3) Code LrF: Luftee-Anakeesta complex, 30 to 95% slopes, very rocky (50% Luftee soil; 30% Anakeesta soil; 20% other)
Luftee: loamy-skeletal, isotic, frigid Humic Dystrudepts; Anakeesta: same as Luftee
(4) Code BpF: Breakneck-Pullback complex, 30 to 94 percent slopes, very rocky
Breakneck: fine-loamy, isotic, frigid Typic Humudepts; Pullback: loamy, isotic, frigid Lithic Humudepts
(5) Code LrD: same as LrF except 15 to 30 percent slopes
(6) Code SsE: Spivey-Santeetlah complex, 30 to 50 percent slopes, very stony
Spivey: loamy-skeletal, isotic, mesic Typic Humudepts; Santeetlah: fine-loamy, isotic, mesic Typic Humudepts
(7) Code: OcF: Oconaluftee-Heintooga Rubble land complex, 30 to 95 percent slopes, stony
Oconoluftee: fine-loamy, isotic, frigid Typic Humudepts; Heintooga: loamy-skeletal, isotic, frigid Typic Humudepts
(8) Code OwF: Oconoluftee-Guyot-Cataloochee complex, 50 to 95 percent slopes, stony, windswept
Oconoluftee: fine-loamy, isotic, frigid Typic Humudepts; Guyot and Cataloochee: same as Oconoluftee

*** Vegetation Type: Spruce/fir refers to red spruce and Fraser fir. Northern hardwoods refer to such trees as northern red oak, black cherry, yellow birch, sugar maple, beech, and serviceberry. Mixed refers to both spruce/fir and Northern hardwoods.

† Source: USDA-NRCS 2017. Soil Survey Staff, Natural Resources Conservation Service, United States Department of Agriculture. Official Soil Series Descriptions. Available online: https://websoilsurvey.nrcs.usda.gov/app/ [Accessed November 4, 2017].

Table 4. Soil sample information (numbers, soil classifications, underlying bedrock type).

Site No.	Site Code	Bedrock Type [1]	Soil Class [2]	Elevation meters	Counts (Sample Depth; centimeters)				
					Cores	O	A	B	C
1	WtA1	sulfidic phyllite	fHD, outcrops	1427 m	n/a	n/a	n/a	n/a	n/a
2	WtA3	sulfidic phyllite	fHD, outcrops	1397 m	6	0	2 (5-15)	8 (5-30)	3 (25-45)
3	WtM6N	sulfidic phyllite	fTH, fLH fHD	1486 m	3	0	2 (5-15)	3 (5-25)	1 (15-25)
4	BFP1 [3]	transition (sulfidic)	fHD	1560 m	4	0	4 (5-15)	5 (5-45)	2 (25-70)
5	RtM14	transition (sulfidic)	fHD	1625 m	3	0	2 (5-15)	3 (15-35)	1 (15-25)
6	RtMOC	sandstone	fTH, fLH	1740 m	3	0	3 (5-15)	3 (20-30)	0
7	NDW	sandstone	fTH, fLH mTH	1722 m	4	4 (5-15)	0	4 (25-35)	0

(1) Estimated from National Park Service bedrock geology GIS layer; parentheses indicate the prominent bedrock composition based on a “bedrock type” ArcGIS® layer.

(2) fHD – frigid Humic Dystrudepts; fLH – frigid Lithic Humudepts; fTH – frigid Typic Humudepts; mTH – mesic Typic Humudepts;
SOURCE: USDA-NRCS 2017. Soil Survey Staff, Natural Resources Conservation Service, United States Department of Agriculture. Official Soil Series Descriptions.

(3) Many of the soil chemistry results from core #3 (column 4b) at Site 4 differed significantly from the other three cores at Site 4. These data were weighed less heavily in subsequent data interpretations.

Table 5. Summary of soil chemistry at study sites. Values shown are ranges, in indicated units.

Soil Chemistry Parameter	Soil Profile Horizon	Site Number (and Associated Bedrock Type)						
		Sulfidic		Transition			Sandstone	
		2 (1)	3	4	4b (2)	5	6	7
pH (water-basis)	O - A	4.03 – 4.19	4.01 – 4.55	3.66 – 4.88	6.02	3.91 – 4.11	3.46 – 4.02	3.52 – 4.02
	B - C	3.95 – 4.59	4.17 – 4.80	4.05 – 5.26	5.79	4.39 – 4.67	4.08 – 4.51	3.99 – 4.53
pH ($CaCl_2$-basis)	O - A	3.01 – 3.91	3.44 – 3.98	2.73 – 3.95	5.15	3.14 – 3.53	2.81 – 3.30	2.79 – 3.33
	B - C	3.32 – 3.95	3.72 – 4.50	3.48 – 4.27	4.73	3.79 – 4.19	3.61 – 4.03	3.75 – 4.27
Cation Exchange Capacity (CEC) $cmol_C$ / kg soil	O - A	13.9 – 15.4	10.5 – 13.0	14.9 – 25.3	40.5	14.6 – 23.8	17.4 – 24.6	14.9 – 23.7
	B - C	4.4 – 12.1	3.1 – 10.3	3.1 – 12.4	6.9	4.6 – 9.7	6.7 – 15.6	7.5 – 13.3
Anion Exchange Capacity (AEC) $cmol_C$ / kg soil	O - A	0.2 – 0.7	0.0 – 0.0	0.4 – 2.2	0.4	0.0 – 0.1	0.0 – 0.3	0.8 – 1.3
	B - C	0.0 – 0.2	0.0 – 0.0	0.1 – 0.2	0.0	0.0 – 0.0	0.0 – 0.0	0.0 – 0.0
Exch. Base Cations (EBC) $cmol_C$ / kg soil	O - A	2.8 – 6.4	2.2 – 4.9	7.1 – 15.5	8.4	1.6 – 1.8	2.2 – 3.2	1.2 – 1.9
	B - C	0.5 – 2.6	0.6 – 1.2	0.5 – 1.9	4.6	0.3 – 0.7	0.9 – 1.4	0.4 – 0.6
Exchangeable Acidity (EA) $cmol_C$ / kg soil	O - A	7.6 – 12.7	8.1 – 8.3	2.5 – 18.3	32.1	13.0 – 22.2	15.1 – 21.4	13.0 – 22.4
	B - C	3.7 – 9.9	2.5 – 9.1	1.6 – 11.4	2.3	4.3 – 9.0	5.8 – 14.2	7.0 – 12.9
Base Cation Saturation (BCS)	O - A	18 – 46%	21. – 38%	28 – 86%	21%	7 – 11%	10 – 13%	5 – 13%
	B - C	7 – 25%	12 – 19%	5 – 48%	67%	7 – 8%	9 – 13%	3 – 7%
Total Carbon (TC)	O - A	19 – 28%	15 – 20%	11 – 43%	18%	13 – 29%	17 – 44%	20 – 37%
	B - C	2 – 14%	5 – 8%	1 – 9%	3%	2 – 6	2 – 11%	1 – 3%
Total Organic Carbon (TOC)	O - A	15 – 24%	10 – 17%	10 – 29%	18%	12 – 23	12 – 25%	16 – 25%
	B - C	2 – 15%	4 – 8%	1 – 7%	2%	2 – 5%	1 – 10%	5 – 6%

(1) Soil profiles in Site 2 overlying Anakeesta Formation (sulfidic phyllite/shale) bedrock generally lacked an O-horizon or distinct A-horizon. Most surface soil samples had characteristics of a A/B transition.

(2) Many of the soil chemistry results from core #3 (column 4b) were different from the results from the other three cores. These data were weighed less heavily in subsequent data interpretations.

Table 6. Soil sulfur concentrations at study sites, by soil profile horizon. Values shown are ranges, as mg sulfur per kg dry soil, or percent where indicated.

Soil Sulfur Type	Soil Profile Horizon	Site Number (and Associated Bedrock Type)						
		Sulfidic		Transition			Sandstone	
		2 (1)	3	4	4b (2)	5	6	7
Total Sulfur (TS)	O - A	959 – 1634	1110 – 1123	690 – 2010	830	899 – 1480	1130 – 1672	1082 – 2153
	B - C	254 – 937	504 – 772	264 – 506	235	294 – 397	206 – 736	131 – 517
Sulfate (weak) chloride-extractable	O - A	3.7 – 4.8	1.9 – 2.2	2.6 – 4.3	5.8	0.8 – 1.4	1.6 – 2.9	5.4 – 8.9
	B - C	2.3 – 9.6	1.3 – 2.7	2.4 – 4.9	3.6	2.1 – 2.7	0.8 – 3.8	2.8 – 4.4
Sulfate (strong) phosphate-extractable	O - A	21.0 – 23.3	8.4 – 16.0	2.8 – 14.4	3.7	7.9 – 13.4	3.7 – 5.8	3.5 – 10.0
	B - C	22.2 – 84.3	26.3 – 111	14.6 – 126	7.9	42.4 – 112	6.0 – 6.8	7.3 – 32.3
Total Extractable Sulfate ($TESO_4$) (weak+strong)	O - A	24.7 – 28.1	10.6 – 18.0	5.4 – 18.7	9.5	8.8 – 14.2	6.6 – 7.4	9.9 – 18.3
	B - C	26.3 – 90.1	27.6 – 114	17.0 – 131	11.4	44.5 – 115	7.6 – 9.8	10.1 – 36.0
Percentage of $TESO_4$ that is phosphate-extractable	O - A	83%, 85%	80%, 89%	52 – 77%	39%	85 – 94%	56 – 78%	28 – 54%
	B - C	76 – 95%	93 – 98%	80 – 97%	69%	95 – 98%	61 – 89%	72 – 90%
Total Organic Sulfur (TOS)	O - A	594 – 1197	no data	617 – 2099	590	788 – 1475	838 – 1573	1069 – 1872
	B - C	125 – 888		71 – 316	142	50 – 235	47 – 605	49 – 472
Percentage of TS that is Organic Sulfur	O - A	62 – 73%	no data	79 – 104%	71%	88 – 100%	74 – 94%	79 – 99%
	B - C	49 – 99%		27 – 65%	61%	17 – 59%	23 – 83%	37 – 100%

(1) Soil profiles in catchment #2 overlying Anakeesta Formation (sulfidic phyllite/shale) bedrock generally lacked an O-horizon or distinct A-horizon. Most surface soil samples had characteristics of a A/B transition.

(2) Many of the soil chemistry results from core #3 (column 4b) were different from the results from the other three cores. These data were weighed less heavily in subsequent data interpretations.

Table 7. Surface soil chemistry by bedrock type, and statistical comparisons results.

Surface Soil Chemistry Parameter [1]	χ^2 p-value [2]	Bedrock Type		
		Sulfidic Sites 2 & 3	Transition Sites 4 & 5	Sandstone Sites 6 & 7
pH (water-basis)	0.0304	4.11 a [3]	4.10 a	3.69 b
pH ($CaCl_2$-basis)	0.1412	3.68 a	3.42 a	3.11 a
Exchangeable Base Cations ($cmol_C\ kg^{-1}$ soil)	0.1383	3.83 a	4.42 ab	1.86 b
Exchangeable Acidity ($cmol_C\ kg^{-1}$ soil)	0.0302	8.18 a	13.7 ab	19.8 b
Base Cation Saturation (%)	0.0461	29.4 a	19.5 ab	9.98 b
Cation Exchange Capacity ($cmol_C\ kg^{-1}$ soil)	0.0278	13.4 a	17.1 b	22.0 b
Exchangeable Aluminum ($cmol_C\ kg^{-1}$ soil)	0.0506	2.57 a	2.71 ab	3.87 b
Total Organic Carbon (%)	0.4470	16.0 a	15.4 a	22.5 a
Total Carbon (%)	0.2127	19.4 a	18.5 a	35.4 a
Extractable Sulfate (weak) (mg-S kg^{-1} soil)	0.1731	2.92 aA	2.02 a	5.45 A
Extractable Sulfate (strong) (mg-S kg^{-1} soil)	0.0192	18.5 a	8.05 ab	5.41 b
Extractable Sulfate (total) (mg-S kg^{-1} soil)	0.0985	21.3 A	9.53 a	9.85 a
Total Organic Sulfur (mg-S kg^{-1} soil)	0.2425	896 a	841 a	1,517 a
Total Sulfur (mg-S kg^{-1} soil)	0.1441	1116 a	1010 a	1,672 a

(1) weak = chloride-extractable soil sulfate; strong = phosphate-extractable soil sulfate; total = total extractable soil sulfate (weak + strong)

(2) Chi-squared probability that medians are not different; based on overall Wilcoxon/Krustal-Wallis (rank sum) test ($\alpha = 0.05$)

(3) Statistical probability result from Steel-Dwass (all pairs) or Wilcoxon pair-wise tests ($\alpha = 0.05$). Analysis excludes data for core #3 of Site 4. Same letters indicate no statistical difference. Capital letter indicates $0.05 < p < 0.10$ (marginally non-significant) versus treatments with lower case (same) letter.

Table 8. Subsurface soil chemistry by bedrock type, and statistical comparisons results.

Subsurface Soil Chemistry Parameter [1]	χ^2 p-value [2]	Bedrock Type		
		Sulfidic Sites 2 & 3	Transition Sites 4 & 5	Sandstone Sites 6 & 7
pH (water-basis)	0.1453	4.24 a [3]	4.55 a	4.33 a
pH ($CaCl_2$-basis)	0.2864	3.76 a	4.04 a	3.91 a
Exchangeable Base Cations ($cmol_C\ kg^{-1}$ soil)	0.1648	1.16 a	0.65 a	0.62 a
Exchangeable Acidity ($cmol_C\ kg^{-1}$ soil)	0.0633	6.68 a	5.30 a	8.82 A
Base Cation Saturation (%)	0.0325	15.7 a	8.36 ab	6.94 b
Cation Exchange Capacity ($cmol_C\ kg^{-1}$ soil)	0.0947	7.84 a	5.78 a	9.71 a
Exchangeable Aluminum ($cmol_C\ kg^{-1}$ soil)	0.2732	1.76 a	1.31 a	2.10 a
Total Organic Carbon (%)	0.0743	5.27 a	2.92 a	5.10 a
Total Carbon (%)	0.0262	6.91 a	3.44 b	2.75 b
Extractable Sulfate (weak) ($mg\text{-}S\ kg^{-1}$ soil)	0.5851	3.23 a	2.90 a	3.45 a
Extractable Sulfate (strong) ($mg\text{-}S\ kg^{-1}$ soil)	0.0023	35.2 a	54.9 a	7.28 b
Extractable Sulfate (total) ($mg\text{-}S\ kg^{-1}$ soil)	0.0020	39.7 a	57.3 ab	10.1 b
Total Organic Sulfur ($mg\text{-}S\ kg^{-1}$ soil)	0.0150	465 a	150 b	204 Ab
Total Sulfur ($mg\text{-}S\ kg^{-1}$ soil)	0.0074	681 a	314 b	407 b

1) weak = chloride-extractable soil sulfate; strong = phosphate-extractable soil sulfate; total = total extractable soil sulfate (weak + strong)

2) Non-parametric Chi-squared probability that medians are not different; based on overall Wilcoxon/Krustal-Wallis (rank sum) test ($\alpha = 0.05$)

3) Statistical probability result from Steel-Dwass (all pairs) or Wilcoxon pair-wise tests ($\alpha = 0.05$). Analysis excludes data for core #3 of Site 4. Same letters indicate no statistical difference. Capital letter indicates $0.05 < p < 0.10$ (marginally non-significant) versus treatments with lower case (same) letter.

Table 9. Surface water chemistry at study sites, and statistical comparisons results.

Water Chemistry Parameter	Site Number (and Associated Bedrock Type) [1]							
	Sulfidic Bedrock			Transition Zone		Sandstone Bedrock		Rock-Face
	1	2	3	4	5	6	7	Site 2
pH (field) (std. units)	a 4.46 – 4.90	a 4.38 – 4.90	bc 5.11 – 6.73	**e** 6.45 – 7.12	b 5.06 – 5.80	cd 5.26 – 5.50	d 5.80 – 6.30	no data
pH (lab) (std. units)	a 4.39 – 4.50	a 4.26 – 4.77	bc 5.40 – 6.10	**e** 6.59 – 6.83	b 5.30 – 5.69	cd 5.50 – 6.05	d 5.68 – 6.18	3.61, 3.64
ANC: Acid Neutralizing Capacity ($\mu mol_C\ L^{-1}$) [2]	a -46 – -35	a -62 – -22	b -5 – +13	**c** 87 – 148	b -4 – +5	b 7 – 19	b 1 – 19	-270, -260 [3]
Sulfate ($\mu mol_C\ L^{-1}$)	**a** 65.5 – 75.0	**a** 54.3 – 77.1	b 22.3 – 42.7	bc 22.5 – 38.7	d 20.5 – 26.8	d 8.1 – 17.3	d 12.7 – 24.9	465, 1020
Sum of Base Cations ($\mu mol_C\ L^{-1}$)	a 54.4 – 106	a 45.3 – 88.1	a 52.7 – 106	**b** 167 – 213	a 57.4 – 120	a 67.0 – 77.4	a 50.4 – 91.7	143, 810
Total Dissolved Aluminum ($\mu mol\ L^{-1}$)	**a** 0.3 – 18.8	**ab** 8.8 – 17.0	c 0.8 – 4.5	c < 0.1 – 0.3	bc 1.1 – 8.2	c 0.4 – 2.1	c 0.4 – 3.4	47, 27
Total Dissolved Iron ($\mu mol\ L^{-1}$)	**a** < 0.1 – 6.8	**a** 1.5 – 9.9	b < 0.1 – 0.5	b < 0.1	b 0.2 – 2.2	b < 0.1	b < 0.1 – 0.4	26, 142
Total Dissolved Manganese ($\mu mol\ L^{-1}$)	**a** < 0.1 – 4.3	**ab** 1.6 – 2.9	b < 0.1 – 0.5	b < 0.1	b 0.1 – 0.8	b 0.2 – 0.4	b < 0.1 – 0.1	2.7, 33
Dissolved Silica ($\mu mol\ L^{-1}$)	a 45.4 – 93.7	b 28.3 – 59.3	b 46.3 – 74.1	**d** 121 – 150	c 88.4 – 99.7	bc 71.3 – 81.8	b 55.5 – 78.6	49, 133

(1) Statistical comparison results from Tukey's HSD all-pairs test ($\alpha = 0.05$). Same letters indicate no statistical difference. Bold font indicates stream water with largest values.

(2) Units: $\mu mol_C\ L^{-1}$ – micromoles of charge per liter; $\mu mol\ L^{-1}$ – micromoles per liter

(3) Estimated acid-neutralizing capacity value, based on pH and inverse sigmoidal functional model between pH and ANC.

CHAPTER 6: IDENTIFYING SULFUR SOURCES AND CYCLING MECHANISMS IN HIGH-ELEVATION FOREST CATCHMENTS OF THE GREAT SMOKY MOUNTAINS NATIONAL PARK, USING STABLE ISOTOPE ANALYSIS

Abstract

Understanding how sulfur is cycled within the Great Smoky Mountains National Park (GRSM) is of interest for assessing ecosystem recovery from acidification caused by acid deposition. Two main sulfur sources, atmospheric deposition and sulfidic bedrock, may influence the sulfur biogeochemistry in high-elevation forested catchments. It was hypothesized that stream water chemistry, and the sulfur ($\delta^{34}S$) and oxygen ($\delta^{18}O$) isotope compositions of stream water sulfate and soil sulfur would reflect atmospheric sulfate in the absence of significant sulfur/sulfate inputs from other sources (e.g., sulfidic bedrock). Seven high-elevation catchments (1390 to 1730 meters above sea level), representing three bedrock types, were selected to be studied. Stream water and soil were characterized with respect to water quality and sulfur chemistry, respectively, and the $\delta^{34}S$ and $\delta^{18}O$ of precipitation, bedrock, stream water, and soil were measured. Sulfate in precipitation (the atmospheric sulfur endmember) had $\delta^{34}S$ and $\delta^{18}O$ of +1.3‰ and +7.3‰, respectively in rain, and +3.8 to +4.5‰ and +9.4 to +11.0‰, respectively in foliage drip water (throughfall). The $\delta^{34}S$ of sulfidic phyllite/shale bedrock endmember (–9.9 to –2.8‰), and of water directly contacting sulfidic bedrock (–7.9 to –7.5‰), was significantly lower than that of sandstone bedrock (+1.7 to +2.9‰). The $\delta^{34}S$ of soil-associated sulfate ranged from +1.3 to +8.1‰. Stream water from two of three catchments overlying sulfidic bedrock was statistically significantly different from the other five catchments with respect to $\delta^{34}S$, sulfate, pH, acid-neutralizing capacity, and metal concentrations. Catchments overlying sandstone bedrock had the lowest $\delta^{18}O$ and highest $\delta^{34}S$ of stream water sulfate relative to low $\delta^{18}O$ and negative $\delta^{34}S$ in sulfidic-rich catchments. Statistically significant differences among the catchments were not found for $\delta^{34}S$ of total sulfur in surface soil, but subsurface soil from the sulfidic bedrock catchments had the lowest $\delta^{34}S$ of total sulfur and mineral-bound sulfate. The isotope results showed that (1) modern

atmospheric sulfur is the primary factor controlling sulfur cycling in high-elevation catchments overlying sandstone bedrock, (2) atmospheric sulfate undergoes substantial cycling in soil (via microbial immobilization/assimilation and adsorption/desorption), and (3) sulfidic bedrock decreases the $\delta^{34}S$ and pH of stream water sulfate, soil sulfate and total soil sulfur only if the bedrock is exposed to the atmosphere. To our knowledge, this is the first report of $\delta^{34}S$ and $\delta^{18}O$ of organic sulfur and mineral-bound sulfate in GRSM soil, the first characterization of sulfur types in GRSM bedrock, and the first comparison of $\delta^{34}S$ and $\delta^{18}O$ of stream water sulfate and bedrock sulfur in the GRSM.

Introduction

Sulfur in terrestrial ecosystems originates from natural (e.g., sulfidic and evaporite bedrock, sea spray aerosols) and anthropogenic sources (e.g., combustion of sulfur-containing fuels and coal; Smith et al. 2011). The transformation of atmospheric sulfur oxides into sulfuric acid (Overton et al. 1979) and its deposition onto land have contributed to adverse ecological effects (Galloway et al. 1983; Turner et al. 1992; Neff et al. 2009; Schwartz et al. 2014) and to the acidification of soil and stream water (Driscoll et al. 2001). Much has been learned about ecosystem responses to atmospheric deposition, but it continues to be the focus of two broad areas of research. First is mass transport and loading rates of atmospheric sulfur (Likens et al. 2002; Porter et al. 2005; Weathers et al. 2006; Zhou et al. 2015), including inter-relationships between emission sources, weather patterns, and distances between sources and deposition locations (e.g. Isil et al. 2017). Second is the geochemical and biological effects of atmospheric sulfur deposition (Novák et al. 2000; Sullivan et al. 2002; Novák et al. 2003; Novák et al. 2005; Neff et al. 2013; Neff et al. 2009). Effects from the deposition of acidic air pollutants are of concern to policy makers and resource managers of public lands in the United States (U.S.) (NPS 2015; Sullivan et al. 2007), such as the Great Smoky Mountains National Park (GRSM). The GRSM is located on the border between Tennessee and North Carolina, U.S. (Figure 15). It contains more than 800 square-miles of some of the richest, most divers assemblages of flora and fauna in the U.S. (NPS 2017). Coal-fired power plants, industry, and a network of highways and population centers have developed around the GRSM region, creating significant sources of acidic air pollutants (Schwartz et al. 2014; Cai et al. 2010; Cai et al. 2012). Much of the GRSM region has characteristically low acid-neutralizing capacity (ANC) (Omernik and Powers 1982; Herlihy et al. 1993; Robison et al. 2013), making GRSM stream water and soil susceptible to acidification.

World-wide, sulfur oxides emissions to the atmosphere have been decreasing (Dostalova et al. 2004). In the U.S., air quality regulations promulgated by the federal government between 1970 and 1990 required industry to mitigate sulfur emissions to the atmosphere (Likens et al. 2001; Burns et al. 2011). In the region surrounding the GRSM, facility modifications and increased use of low-sulfur fuel/coal by power generators have caused significant and sustained reductions in total sulfur emissions to the atmosphere (TVA 2017). In years since these actions, chemical analyses of open-field rain and throughfall (forest canopy drip water) collected at a high-elevation GRSM monitoring station have shown a rapid and sustained increase in pH and ANC, and decrease in sulfate concentrations in precipitation over GRSM. However, data from stream water sampled concurrently at the same monitoring station have not shown comparable changes in stream water pH, ANC or sulfate concentrations (Gonzalez et al. 2015; Schwartz et al. 2016).

Decreases in precipitation sulfate and acidity also have been observed in Europe (Novák et al. 2000; Novák et al. 2003; Novák et al. 2005), but expected changes in soil (e.g., Balík et al. 2009) and stream water (e.g., Marnette et al. 1993) chemistry have not always followed. A desire to explore reasons for these observations led us to develop this study. There is still much uncertainty in our understanding of stream water and soil acidification and sulfur geochemistry in the GRSM. One is the degree and efficiency with which geochemical conditions and processes (Edwards 1998) in the GRSM delay or prevent stream water and soil from responding to decreases in atmospheric sulfur deposition. Plausible geochemical processes that release sulfate into the catchment include (1) desorption of mineral-bound sulfate from soil (Robison et al. 2013; Mayer et al. 2001), (2) dissolution of sulfate-bearing secondary minerals from bedrock or soil (Hammarstrom et al. 2005; Bigham and Nordstrom 2000; Flohr et al. 1995), (3) oxidation of sulfide minerals in soil and bedrock (Heidel et al. 2013; Chandra and Gerson 2010), and (4) mineralization of organic sulfur

species previously formed by microbial assimilatory reduction of sulfate (Fitzgerald et al. 1983; David and Mitchell 1987; Ghani et al. 1993). Previous research in the GRSM has not determined the extent to which these geochemical processes contribute to stream water and soil acidification or the inventory of sulfur in catchments. More information is needed on the forms and amounts of sulfur that currently exist in GRSM forested catchments (after decades of high rates of atmospheric sulfur deposition), and on how sulfur from natural sources contributes to the cycling of sulfur in these systems.

Modeling and field research to understand and predict recovery of forested ecosystems from acidification have been ongoing. Utility of critical loads models (e.g., PnET-BGC; Chen et al. 2004; Zhai et al. 2008; Zhou et al. 2015; Fakhraei et al. 2016) depend on accurate understanding of quantities and rates of all inputs, and major biogeochemical processes affecting those inputs. Field research related to atmospheric deposition in the GRSM has been ongoing, beginning with the inception of broad-scale monitoring programs for determining the status of terrestrial and aquatic biota, air quality, and stream water quality (e.g., the Integrated Forest Study [Johnson and Lindberg 1992] and the NPS Natural Resource Inventory and Monitoring program [NPS 2015]). Examples of focused research questions studied by GRSM investigators follow.

A symposium abstract submitted by Cook et al. (1987) briefly summarizes a study in which sulfur isotope composition measurements were made to examine sulfur sources and transport in two GRSM watersheds (one high-elevation catchment overlying sandstone bedrock, and the other overlying sulfidic bedrock). Precipitation, bedrock, soil, soil water and stream water were characterized, and results appear to identify shifts in sulfur isotope composition of stream water due to soil cycling of atmospheric sulfur and the presence of bedrock sulfidic minerals. They concluded that 80% and 30% – 40% of atmospheric sulfate were being retained by the two

watersheds, respectively. This 30-year old abstract is the only report found of sulfur isotope composition measurements in the GRSM. The study apparently did not include measurements of oxygen isotope composition or speciation of sulfur in bedrock and soil samples.

Cai et al. (2011) studied sulfate dynamics at the Noland Divide monitoring station located in a high-elevation catchment in the GRSM. They investigated interactions between anions and cations in incident precipitation and the soil layers in the sub-basin, and determined the mass distribution of sulfate throughout the soil matrix. Influx of sulfate was thought to be contributing to acidification of the watershed ecosystem (soil and water). It was hypothesized that the soil's acid-neutralizing capacity (ANC) was nearly depleted, and that additional sulfate input was controlling stream water pH. Two major conclusions from that study were that sub-basin soil had additional "capacity" for retaining sulfate (although the retention mechanism was assumed to be exclusively mineral adsorption), and that sulfate concentrations in the two streamlets draining the sub-basin varied little over time. Measurements of soil organic sulfur, bedrock sulfur content, or stable isotope composition were not part of the study.

Neff et al. (2013) examined the influence of sulfidic geology on stream acidification. They found that drainage basins overlying bedrock with >10% sulfidic content had lower stream water pH and calcium concentrations than basins without sulfidic bedrock. Similar differences in stream water chemistry, based on >10% or <10% sulfidic bedrock, were found for ANC, sulfate, nitrate, and magnesium during baseflow, and for dissolved aluminum during stormflow. However, the presence/absence of sulfidic bedrock was not as strong of a factor in determining stream chemistry as were topographic, pedological, and vegetative basin factors. Their study did produce some evidence of changes in stream water chemistry due to sulfidic bedrock. They recommended further study and use of sulfur isotopes.

A related study by Grell (2010) used the same eight study areas (Neff et al. 2013) to examine soil geochemistry in relation to eight watershed characteristics. A combination of soil sampling and chemical analysis, and GIS data analysis, was used to examine which factors were determining the observed soil chemistry. Significant differences among the watersheds with respect to soil chemistry parameters were not found based on soil type. Significant differences were found based on the sulfidic bedrock factor for some soil chemistry parameters, but notably not for chloride-extractable and phosphate-extractable soil sulfate. Stream water, bedrock and precipitation were not included in the study, and stable isotopes were not used.

Stable isotope tracers are useful environmental tracers to answer such questions. For example, differences in $\delta^{34}S$ and $\delta^{18}O$ have been used extensively to identify sources of sulfate in rivers and groundwater, to study sulfate immobilization and organosulfur mineralization in soil, and the reaction mechanisms of pyrite oxidation (Houle et al. 2014; Szynkiewicz et al. 2012; 2011; 2008a; 2008b; Marty et al. 2011; Rock and Mayer 2009; Novák et al. 2005; Novák et al. 2003; Fuller et al. 1986). Variations in stream water sulfate concentrations during and after a particularly dry summer were investigated by Mayer et al. (2010) using a combination of hydrological, chemical and isotopic techniques. Sulfate concentrations roughly doubled throughout the dry period while stream flows decreased, but during the Fall rewetting period, instead of decreasing by dilution with increased stormflow, sulfate concentrations continued to increase to nearly four-fold larger than the late Spring levels. An abrupt decrease in $\delta^{34}S$ coinciding with the unexpected increase in sulfate concentration lead investigators to conclude that biogenic sulfide was formed via microbial sulfate reduction in deeper soil layers during high-water table periods, which later was oxidized to sulfate during the drought months, and finally flushed into stream water during the post-drought rewetting

period. This finding was possible only by measuring the $\delta^{34}S$ of bedrock, soil and stream water sulfate over the study period.

The objective of this study was to measure the chemical composition and $\delta^{34}S$ and $\delta^{18}O$ of stream water sulfate and soil sulfur from several high-elevation GRSM catchments overlying bedrock types differing in sulfur contents but with similar sulfate loading from atmospheric deposition, and to compare these data sets to isotope compositions in known endmember sulfur sources (i.e., precipitation, bedrock, soil). The prime assumptions in this study were (1) that GRSM soil and stream water acidification due to atmospheric deposition was ubiquitous throughout the study area (the "reference" condition), and (2) that effects from sulfidic bedrock on stream water and soil could be quantified relative to the reference condition. Results from this study address uncertainties in the role of sulfidic bedrock weathering in soil and stream water acidification, and can contribute to refinements in critical loads models of forested watersheds (Chen et al. 2004; Zhai et al. 2008; Zhou et al. 2015; Fakhraei et al. 2016).

Environmental Setting

An example of sulfide-rich bedrock in the GRSM is the Precambrian Anakeesta Formation (Figure 15) in the Ocoee Series (Hadley and Goldsmith 1963; King 1964; Southworth et al. 2005; Thornberry-Ehrlich 2008), described as a pyritic carbonaceous phyllite (Espenshade 1963) and black mica schist with abundant graphite and pyrrhotite (Mohr 1973). Oxidative weathering of the sulfide minerals generates sulfuric acid, iron, aluminum and mineral-bound trace metals, and common cations and dissolved silica from the mineral lattice structure (Flohr et al. 1995). This process has been documented to have adverse environmental effects in the GRSM (Huckabee et al. 1975; Mathews and Morgan 1982). The other predominant GRSM geologic formation in the

study area is the non-sulfidic Thunderhead and Copperhill Formations comprised of sandstone/siltstone conglomerate (King 1964; Southworth et al. 2005). It is possible that such non-sulfidic bedrock can have minor components comprised of soluble sulfate-bearing secondary minerals or primary sulfate-bearing evaporite minerals (e.g., gypsum, anhydrite).

Sulfur inputs into GRSM catchments can vary spatially based on variability in bedrock sulfur content and on elevational variability in acidic deposition loading (Weathers et al. 2006). Seven study catchments were selected from areas along the State-boundary ridgeline in GRSM, between 1390 and 1730 meters above mean sea level (Figure 15). This high-elevation band was selected to reflect the highest levels of atmospheric deposition loading in the GRSM, but also to minimize potential variation in atmospheric deposition loading across the study sites. Three locations (Sites 1, 2 and 3) were selected to represent catchments that overlie sulfidic phyllite/shale bedrock. Sites 1 and 2 were located on the south-facing slopes of Anakeesta Ridge, whereas Site 3 was located on the northwest-facing slope of the State-line ridge unconnected to Anakeesta Ridge. Additionally, two locations (Sites 6 and 7) were selected to represent catchments that overlie sandstone/siltstone bedrock (containing minimal amounts of sulfur-bearing minerals). Finally, two locations (Sites 4 and 5) were selected in a transition zone between these two bedrock types. An important feature in the study area is a prominent ridge line (Anakeesta Ridge; Figure 15) comprised of sulfidic bedrock of the Anakeesta Formation. References to distance in this study are relative to this feature; sites are numbered nearest (Site 1) to furthest (Site 7) from this feature. Pertinent environmental characteristics of the seven study sites are summarized in Table 10.

Study Design

The $\delta^{34}S$ and $\delta^{18}O$ of two distinctive sulfur/sulfate endmembers were measured in this study: bedrock (sulfide and sulfate minerals) and atmosphere (sulfate). The $\delta^{34}S$ and $\delta^{18}O$ of stream water sulfate and soil sulfur species from the three sets of catchments were compared to the isotope composition of two predominant endmembers. Four types of sulfur were extracted from bedrock samples and analyzed to examine potential weathering reactions/sources responsible for the isotope composition of soil and stream water at the sites. Three types of soil sulfur (total sulfur, mineral-bound sulfate, and organic sulfur) also were extracted and analyzed to examine the concentrations and proportional distribution of soil sulfur species, and to assess the possible origins of soil sulfur species based on isotope composition. Chemical analyses of stream water from the seven sites were used to compliment isotope composition results.

Methods

Stream water (175 mL grab samples) was collected from each site in November 2016 for chemical analysis. Larger volumes (>10 liters) of stream water were collected for isotope analysis from the same locations. Rain water was captured at Site 7 during one storm event in July 2016. Throughfall (drip water through the forest canopy) was collected under foliage at Site 7 in March and May 2017. Water flowing over the exposed surfaces of sulfidic bedrock was collected under drought conditions in March and June 2016. Two samples were collected downstream of Site 4 (the site of severe stream water acidification caused by the use of sulfidic bedrock rubble for road construction; Huckabee et al. 1975) and one sample was collected at the base of a bedrock scar at Site 2. All water samples were stored at 4-6 °C until analyzed.

Portions of all water samples and soil extract liquids containing dissolved sulfate were filtered (0.45 µm) and analyzed for pH, ANC by automated titration, major anions by ion chromatography, and major cations and trace metals by ICP-OES in the Department of Civil/Environmental Engineering's Water Quality Laboratory at the University of Tennessee, Knoxville, TN, USA. The remaining portions of the samples were acidified to pH < 3 with ultrapure hydrochloric acid followed by addition of 10% (w/v) barium chloride solution (1 mL $BaCl_2$ solution per 100 mL sample) to precipitate the dissolved sulfate as barium sulfate ($BaSO_4$) (Mayer and Krouse 2004; Kendall and Caldwell 1998).

Twelve bedrock samples representative of prominent GRSM rock types were collected throughout the study area (Table 11). Each was subjected to a sulfur sequential extraction method to extract four types of sulfur (elemental sulfur (ES), acid-volatile sulfide (AVS), acid-soluble sulfate (ASS), and chromium-reducible sulfide (CRS)) (Tuttle et al. 1986; Fauville et al. 2004). Extracted sulfur was converted to silver sulfide (Ag_2S), or $BaSO_4$ in the case of acid-soluble sulfates, for quantitative estimates and isotope composition analysis using methods previously described by Mayer and Krouse (2004) and Kendall and Caldwell (1998).

A total of 50 soil samples from 23 cores within six of the seven sites were collected between April and August 2016 (Table 12). Soil from Site 1 was inaccessible due to debris slides and thick vegetation. Three to six soil cores (~65 centimeters maximum depth) were taken from each site. Soil samples were collected from the surface and B-horizon, and where possible from the C-horizon. Not all soil profiles were identifiable or complete; most soil overlying sulfidic phyllite/shale bedrock lacked a distinct A-horizon, and soil overlying sandstone bedrock had thick O- and A-horizons. Wet soil was analyzed for pH as 1:1 suspensions with water or 0.01M calcium chloride.

Total soil sulfur and three types of soil sulfur were extracted from air-dried soil for quantitative estimates and isotope composition analysis. Weakly-bound sulfate, consisting of both dissolved sulfate in the soil solution and sulfate held non-specifically (electrostatically) to mineral surface sites, was extracted with 1M ammonium chloride (Bloem et al. 2002; Maynard et al. 1987). Strongly-bound sulfate, chemically coordinated to exchange complex sites by ligand-exchange reactions, was extracted with potassium or calcium dihydrogen phosphate (500 mg-P L^{-1}) (Ensminger 1954; Sahrawat et al. 2009). Soil organic sulfur was extracted from soil residue remaining after phosphate-treatment, by oxidation with sodium bicarbonate and silver oxide mixture at 550 °C followed by dissolution in hydrochloric acid (Tabatabai et al. 1988; Rossete et al. 2008). Soil total sulfur was extracted from untreated soil by same method as soil organic sulfur.

The $BaSO_4$ and Ag_2S obtained from water and bedrock/soil samples were analyzed using a Delta Plus XL isotope ratio mass spectrometer (IRMS) located in the Department of Earth and Planetary Sciences at the University of Tennessee, Knoxville, TN, USA. For analysis, < 1 milligram of sample was combined with catalyst in the crucible cups. Isotope results are reported in the standard δ notation, in parts per thousand (‰): $\delta_{sample} = 1000 ((R_{sample} / R_{standard}) - 1)$. $BaSO_4$ and Ag_2S samples for $\delta^{34}S$ analysis were mixed with vanadium pentoxide (V_2O_5) in tin cups. Sulfur was converted to sulfur dioxide (SO_2) by combustion at 1150°C in a Costech Elemental Analyzer and analyzed for $\delta^{34}S$. $BaSO_4$ samples for $\delta^{18}O$ analysis were mixed with sodium fluoride in silver cups. Oxygen released from $BaSO_4$ was converted to carbon monoxide by combustion in a Thermo Scientific TC/EA High Temperature Conversion Elemental Analyzer and analyzed for $\delta^{18}O$ value. Laboratory standards were run in conjunction with field samples: for $\delta^{18}O$ (UTK-Gyp1 [+16.83 ‰], SC-1std [-2.52 ‰], IAEA-SO-5 [+12.13 ‰] and IAEA-SO-6 [-11.35 ‰]) and for $\delta^{34}S$ (NBS 127 [+21.12 ‰] and IAEA-SO-6 [-34.05 ‰]). Laboratory standards were calibrated to the

international Standard Mean Ocean Water (vSMOW) for $\delta^{18}O$ and Vienna Cañon Diablo Troilite (vCDT) for $\delta^{34}S$. The instrument precision was ± 0.3‰ or better.

To help interpret sulfate-$\delta^{18}O$ data from sulfate in GRSM soil and stream water samples, the $\delta^{18}O$ of water from GRSM streams was analyzed. Stream water was sampled throughout 2016 as part of an ongoing GRSM water quality monitoring program (Schwartz et al. 2014). Filtered stream water samples (N = 100) that had been analyzed by ion chromatography were archived at 4-6 °C for several months prior to $\delta^{18}O$ analysis in December 2016. Samples and laboratory standards were analyzed using a Los Gatos Water Isotope Analyzer located in the Department of Earth and Planetary Sciences at the University of Tennessee, Knoxville, TN, USA. The laboratory standards were calibrated to international standards: Standard Mean Ocean Water (SMOW) and Standard Light Antarctic Precipitation (SLAP). Isotope data from the initial 100 stream water samples were evaluated for evidence of evaporation during storage. It was determined that 80 of the samples showed no evidence of evaporative fractionation during storage.

Chemical and isotope data were analyzed statistically and graphically in JMP® Pro 13 (SAS Corporation 2017).

Results

Surface Water Chemistry

Table 13 shows the results of stream water chemical analyses for each site, arranged left to right by distance from the Anakeesta Ridge (Figure 15). For reference, water chemistry results of the sulfidic bedrock runoff samples are included. Site 4 (overlying the transition zone) had the highest stream water pH and ANC concentrations. Mean values of stream water pH and ANC generally

increased, and mean sulfate concentration decreased, with increasing distance from Anakeesta Ridge. The mean stream water pH at Sites 1 and 2 (pH 4.5; sulfidic bedrock sites) was statistically lower than mean pH at all other Sites (pH 5.8), including Site 3 (pH 5.8; the third sulfidic bedrock site). Sites 1 and 2 (sulfidic) had the largest mean stream water sulfate concentrations (6.9 and 6.5 mg L^{-1}, respectively) and Sites 6 and 7 (sandstone) had the smallest average concentrations (1.1 and 2.3 mg L^{-1}, respectively). Most aluminum, iron and manganese concentrations were near or below analytical quantitation limits (< 0.07 mg L^{-1}) in Sites 6 and 7 (sandstone), Sites 4 and 5 (transition zone), and Site 3 (sulfidic). In stream water from Sites 1 and 2, the aluminum concentrations were < 0.5 mg L^{-1}, and iron and manganese concentrations were < 0.3 and < 0.1 mg L^{-1}, respectively. With respect to stream water chemistry, Site 3 overlying sulfidic bedrock was more similar to sites overlying transition zone and sandstone bedrock than the other two sulfidic bedrock Sites 1 and 2 (Table 13).

Sulfate concentrations relative to the distance from Anakeesta Ridge were fitted to a three-parameter exponential function (Figure 16).

$$SO_4(mg\ L^{-1}) = 2.0\ mg\ L^{-1} + 17.3e^{-1.17(km)}$$

Generally, the sulfate concentrations decreased with increasing distance from the Anakeesta Ridge (high r^2 value of 0.92).

Sulfur Isotope Composition

A summary of the measured $\delta^{34}S$ in main endmembers (bedrock, soil, precipitation) and surface water sulfate are presented in Figure 17, arranged from-top-to-bottom in a similar spatial sequence as found in the sampling locations. Atmospheric sulfate data are presented at the top, data for

various sulfur sources in soil and stream water sulfate below them, and data for bedrock sulfur types are presented at the bottom. All measured $\delta^{34}S$ values were between –10‰ and +10‰. The $\delta^{34}S$ of bedrock sulfur and sulfidic bedrock runoff sulfate usually had lower values (-10 to 0‰) compared to higher $\delta^{34}S$ in stream water sulfate and soil sulfur (0 to 10‰). There was clear distinction in $\delta^{34}S$ of stream water and soil based on sampling location; the $\delta^{34}S$ of soil sulfur and stream water sulfate from Sites 1 and 2 were generally more negative than those from Sites 3 – 7. Variations in the measured $\delta^{34}S$ and corresponding $\delta^{18}O$ are presented in detail in the following sections.

Precipitation and Bedrock Endmembers (Isotope Composition)

The $\delta^{34}S$ and $\delta^{18}O$ of sulfate in GRSM throughfall (ranges: +3.8 to +4.5‰ and +9.4 to +11.1‰, respectively [N = 4]) were both higher than $\delta^{34}S$ and $\delta^{18}O$ of sulfate in GRSM rain (+1.3‰ and +7.3‰, respectively [N = 1]). The $\delta^{18}O$ of surface water collected from GRSM streams in 2016 (not shown on Figure 17) ranged from –8.5‰ to –6.5‰ (N = 80). These GRSM stream $\delta^{18}O_{water}$ results are comparable to the previously reported ranges of $\delta^{18}O$ values of ambient freshwater (e.g., –8.5‰ to –6.1‰ in Canadian rivers near the Canada-US border [Yang et al. 1996]; and –7.6‰ to –1.4‰ in stream water from southwest Western Australia [Turner et al. 1987]).

Table 14 presents the $\delta^{34}S$ of different sulfur types in the GRSM bedrock. Acid-soluble sulfate (ASS) and chromium-reducible sulfur (CRS) were the most common, and acid-volatile sulfide (AVS) was the least common, type of sulfur found in the 12 bedrock samples. Two of the 12 samples (a quartzite sample collected at the top drainage divide of Site 3, and a sandstone sample collected downstream of Site 4) yielded no measurable amounts of any of the four sulfur types. Three shale/slate samples had elemental sulfur with $\delta^{34}S$ of –3.6‰ (Site 1), –3.6‰ and –8.4‰

(downstream of Site 4). Sulfidic carbonaceous slate/shale samples (various sampling locations) had $\delta^{34}S$ of ASS ranging between –9.9 and –2.8‰, and had $\delta^{34}S$ of CRS ranging between –9.2 and +0.3‰. One sample (downstream of Site 4) also yielded measurable amounts of AVS, with $\delta^{34}S$ (–9.2 ‰) that was similar (within margin of error) to $\delta^{34}S$ of CRS (–9.2‰) in the same sample. The $\delta^{18}O$ of ASS extracted from three sulfidic slate/shale samples was +13.8, +17.6 and +20.7‰. The $\delta^{34}S$ of sulfur in the sulfidic bedrock (–9.9 to –2.8‰) was clearly distinguishable from $\delta^{34}S$ of sulfur in the sandstone bedrock (+1.7 to +2.9‰). The $\delta^{34}S$ of sulfidic bedrock samples measured in this study are comparable to the $\delta^{34}S$ value of –6.1‰ (unknown sample size) previously reported for the sulfidic GRSM bedrock by Cook et al. (1987).

The electron-valence state and $\delta^{34}S$ of four types of sulfur measured in the bedrock provide distinctive information about different sources and formation mechanisms of bedrock sulfur. In theory, bedrock ASS (with sulfur in S^{6+} valence state) originating from dissolution of evaporite sulfate minerals should have high $\delta^{34}S$ (e.g., > +12.7, Palmer et al. 2004) associated with sulfur from marine sources (i.e., $\delta^{34}S$ of modern ocean sulfate is +21.0‰ [Rees et al. 1978]). Conversely, the $\delta^{34}S$ of bedrock ASS formed by oxidation of sulfide should be similar to $\delta^{34}S$ of the source sulfide minerals in the same bedrock sample, given that negligible fractionation occurs during sulfide oxidation (Pisapia et al. 2007). Five bedrock samples yielded measurable amounts of ASS and CRS (Table 14). In all cases, the $\delta^{34}S$ of ASS was similar to the $\delta^{34}S$ of CRS, suggesting the ASS in those samples was formed by direct oxidation of sulfides in the bedrock. Elemental sulfur in the bedrock can form from partial oxidation of sulfide minerals (Fuseler and Cypionka 1995) and thus its $\delta^{34}S$ signature can be similar to the source sulfide minerals in the same bedrock sample. Three bedrock samples yielded enough elemental sulfur (S^0) for isotope analysis. The $\delta^{34}S$ of S^0 at Site 1 (–3.6‰) was similar (within margin of error) to $\delta^{34}S$ of CRS in the same sample (–3.6‰);

the $\delta^{34}S$ of S^0 in the two samples collected downstream of Site 4 (–3.6‰ and –8.4‰) were higher than the $\delta^{34}S$ of CRS in their respective samples (–7.3‰ and –9.2‰). Five bedrock samples yielded no measurable amounts of reduced sulfur (CRS or AVS), but did yield measurable amounts of ASS with $\delta^{34}S > +2.0$‰. The source(s) of ASS in those five samples is uncertain, but oxidation of sulfide likely is not the primary source given that no reduced sulfur types were detected. The extracted ASS from three sulfidic slate/shale samples had $\delta^{18}O$ (+13.8, +17.6 and +20.7‰) in the range that could be associated with evaporite sulfate minerals (e.g., $\delta^{18}O > +12.1$‰, Palmer et al. 2004), but their associated $\delta^{34}S$ (–2.8, –2.8 and +1.7‰, respectively) were substantially lower than $\delta^{34}S$ of evaporite sulfate minerals (e.g., $\delta^{34}S > +12.7$‰, Palmer et al. 2004). Instead, the observed low $\delta^{34}S$ and high $\delta^{18}O$ of ASS in these bedrock samples could be an artifact of sample handling/preparation (i.e., sulfide minerals could have oxidized by atmospheric oxygen during storage, grinding, and isotope analysis).

Stream Water Sulfate (Isotope Composition)

Sulfur and oxygen isotope compositions of stream water sulfate is presented at the top of Table 15. The $\delta^{34}S$ of stream water sulfate at Sites 6 and 7 (overlying sandstone bedrock) were statistically higher (range +7.2 to +8.2‰) than those at Sites 1 – 3 overlying sulfidic bedrock (–2.2 to +6.4‰; $p = 0.0012$) and those at Sites 4 and 5 overlying the transition zone (+2.5 to +6.9‰; $p = 0.0429$). The $\delta^{34}S$ of stream water sulfate at Sites 1 – 3 were all statistically different from each other ($p < 0.05$). The lowest $\delta^{34}S$ of stream water sulfate (–2.2 to +1.8‰) were found at Sites 1 and 2 (nearest to Anakeesta Ridge). Notably, the $\delta^{34}S$ of stream water sulfate at Site 3 (+5.7 to +6.4‰) was more similar to those at Sites 6 and 7 (sandstone bedrock) and Site 5 (transition zone) than to those from the sulfidic bedrock of Sites 1 and 2. These same data are presented graphically

as $\delta^{34}S$ of stream water sulfate relative to distance from Anakeesta Ridge (Figure 18). For reference, the $\delta^{34}S$ of sulfate in water directly contacting sulfidic bedrock surfaces (–7.7 ± 0.1‰) was included to represent the sulfur isotope composition controlled primarily by the sulfidic endmember. The $\delta^{34}S$ of stream water sulfate at Sites 5 – 7 were very similar to each other (range +6.9 to +8.2‰), which is notable given that those sites are separated from each other by several kilometers. A similar graphical analysis was done for $\delta^{18}O$ of stream water sulfate relative to the distance from Anakeesta Ridge (Figure 19). The $\delta^{18}O$ of sulfate in water directly contacting sulfidic bedrock surfaces (+0.7 ± 0.5‰) was included to represent the oxygen isotope composition controlled primarily by the sulfidic endmember. The $\delta^{18}O$ of stream water sulfate at Sites 6 and 7 (mean +3.2 ± 0.1‰; N = 9) was the lowest of all study sites, but not as low as the sulfidic endmember (mean +0.7 ± 0.5‰; N = 3). The $\delta^{18}O$ values of stream water sulfate at Sites 1 – 5 clustered together in the wider range of +4.5‰ to +9.0‰.

Distinctive patterns were found between $\delta^{34}S$ of stream water sulfate and acidity metrics (pH and ANC) (Figure 20). The data for the sulfidic bedrock runoff samples are included to represent the pH, ANC and isotope composition controlled primarily by the sulfidic endmember. The data associated with the seven sites appear to cluster into three groups: (1) Sites 1 and 2 (overlying sulfidic bedrock) with lowest pH, ANC and $\delta^{34}S$ of stream water sulfate, (2) Site 4 (overlying the transition zone) with highest pH and ANC, and (3) Sites 3, 5, 6 and 7 (multiple bedrock types) with highest $\delta^{34}S$ of stream water sulfate. Site 1 had significantly lower $\delta^{34}S$ of dissolved sulfate than Site 2 but similar pH and ANC concentrations. The pH, ANC and $\delta^{34}S$ of stream water sulfate from Site 3 (overlying sulfidic bedrock) was more similar to Sites 5, 6 and 7 than in Sites 1 and 2 (overlying sulfidic bedrock). In spite of the measurement variability and the unexplained results for Site 4, the stream pH and $\delta^{34}S$ of stream water sulfate appear to be directly related (dashed

trend line in Figure 20). The stream ANC and $\delta^{34}S$ of dissolved sulfate had a weaker direct relationship (no trend line shown).

Figure 21 shows a graphical analysis of sulfate concentrations (mg L^{-1}) and $\delta^{34}S$ of stream water sulfate, done to complement the previous pH/ANC analysis (Figure 20). For reference, the concentrations and $\delta^{34}S$ of sulfate in water directly contacting sulfidic bedrock surfaces were included to represent the sulfur isotope composition controlled primarily by the sulfidic endmember. Across a wide range of concentrations and $\delta^{34}S$ values of dissolved sulfate, the two parameters appeared to be inversely related (dashed line in Figure 21). One set of data at Site 4 was significantly different from the other set at the same site, and sulfate at Sites 1 and 2 had similar sulfate concentrations (~6 to 7 mg L^{-1}) but significantly different $\delta^{34}S$.

The $\delta^{18}O$ of sulfate in the GRSM stream water ranged between +2.7‰ and +8.9‰ (Table 15). These results are similar to those reported for forest catchment stream water in the northeast U.S. (+1.2 to +10.0‰, Mitchell et al. 2008), for stream water in a Luxembourg watershed (+3.0 to +10.7‰, Rock and Mayer 2002), and for surface water in Poland (+5.4 to +10.0‰, Trembaczowski et al. 2004; and +4.6 to +8.2‰, Szynkiewicz et al. 2008b). Distinctive patterns were found among the $\delta^{18}O$ of stream water sulfate and acidity metrics (pH and ANC) (Figure 22). The data for the sulfidic bedrock runoff samples are included to represent the pH, ANC and isotope composition controlled primarily by the sulfidic endmember. The pH/ANC/$\delta^{18}O$ data from the seven study sites cluster into four groups: (1) Sites 1 and 2 (overlying sulfidic bedrock) with lowest pH and ANC and relatively high $\delta^{18}O$ of stream water sulfate, (2) Site 4 (overlying transition zone) with highest pH and ANC, and relatively high $\delta^{18}O$ of stream water sulfate, (3) Sites 3 and 5, and (4) Sites 6 and 7 (overlying sandstone). Although the stream water pH and ANC at Sites 6 and 7 and Sites 3 and 5 were comparable, the $\delta^{18}O$ of stream water sulfate from Sites 6 and 7 (+2.7 to

+3.6‰) were statistically significantly lower than those from Sites 3 and 5 (+4.9 to +5.6‰) ($p < 0.05$). There appeared to be no clear relationship between pH/ANC and $\delta^{18}O$ of sulfate. Figure 23 shows a comparative analysis of sulfate concentrations (mg L^{-1}) and $\delta^{18}O$ of stream water sulfate (‰), done to complement the previous pH/ANC analysis (Figure 22). For reference, the concentrations and $\delta^{18}O$ of sulfate in water directly contacting sulfidic bedrock surfaces was included to represent the sulfur isotope composition controlled primarily by the sulfidic endmember. Unlike the sulfur isotope analysis, there appeared to be no clear relationship between sulfate concentrations and $\delta^{18}O$ of sulfate. The $\delta^{18}O$ of sulfate in the sulfidic bedrock runoff had significantly lower $\delta^{18}O$ of sulfate with correspondingly high sulfate concentrations.

Soil Sulfur Types (Isotope Composition)

Isotope results for the four types of soil sulfur are summarized in Table 15. The $\delta^{34}S$ of total sulfur (TS) in surface soil were within a relatively narrow range: +3.2 to +5.1‰. Using the non-parametric Wilcoxon Rank Sum pair-wise test ($\alpha = 0.05$), no statistically significant differences ($p > 0.18$) in $\delta^{34}S$ of surface soil TS were found among the sites. In subsurface soil, the $\delta^{34}S$ of TS spanned a wider range: +0.2 and +8.5‰. The $\delta^{34}S$ of TS in subsurface soil from Site 2 (+0.2 to +3.4‰) was significantly lower than $\delta^{34}S$ of TS in subsurface soil from all other Sites (> +3.6‰; $p < 0.03$), including Site 3 (+3.6 to 5.0‰). No statistically significant differences ($p > 0.05$) in $\delta^{34}S$ of subsurface soil TS were found among Sites 3 – 7. With respect to $\delta^{34}S$ of TS, Site 3 (sulfidic bedrock) was more similar to the transition zone and sandstone catchments than to Site 2 (sulfidic bedrock). Attempted extractions of soil organic sulfur from surface soil samples from Sites 2, 3, and 4, and from subsurface soil samples of all studied sites, yielded insufficient $BaSO_4$ mass for isotope analysis. The $\delta^{34}S$ of organic sulfur in surface soil at Sites 5, 6 and 7 was +4.7‰ (N=1),

+3.5‰ (N=1), and +3.8‰ (N=2), respectively. At Sites 5, 6 and 7, the measured $\delta^{34}S$ of organic sulfur and TS were approximately equal.

Sulfur and oxygen isotope compositions of mineral-bound sulfate in subsurface soil are presented in Table 15. Surface soil samples from all sites yielded insufficient $BaSO_4$ mass for isotope analysis. Subsurface soil at Site 2 had the lowest $\delta^{34}S$ values of weakly-bound (+2.6 ± 0.4‰; N=7) and strongly-bound sulfate (+2.3 ± 0.4‰; N=9) among the studied sites. The $\delta^{34}S$ of mineral-bound sulfate in subsurface soil at the other sites were relatively similar to each other (range: +4.4 to +8.1‰). The measured $\delta^{18}O$ of adsorbed sulfate in subsurface soil were consistent across sites (+4.0 to +6.1‰), with the exception of Site 4 which had high $\delta^{18}O$ of +10.5‰ in weakly-bound sulfate (N = 1).

Discussion

Four primary findings were evident in this GRSM study. First, modern atmospheric sulfur input was the primary factor controlling sulfur cycling in high-elevation catchments overlying sandstone bedrock. Second, distinct differences in soil and stream water chemistry were found between catchments overlying sulfidic bedrock and catchments overlying sandstone. Thirdly, Site 3 was distinct from Sites 1 and 2 with respect to soil and stream water chemistry, despite all three sites overlying sulfidic bedrock. These three major findings are discussed below. The fourth (minor) finding was that Site 4 was distinct from all other sites with respect to stream water pH and ANC and isotope composition of sulfate. Although Site 4 was selected to represent a transition zone catchment in the study design, its chemistry was not comparable to Site 5 (the other transition zone catchment). The catchment-specific factors responsible for these unexpected results were not identified, and no further investigation at Site 4 was done.

Modern Atmospheric Sulfur Deposition

Sulfate in the GRSM precipitation showed the highest $\delta^{34}S$ and $\delta^{18}O$ values compared to bedrock endmembers, thus it is a good measure of current contributions from atmospheric deposition (Figure 24). The observed increase in $\delta^{34}S$ and $\delta^{18}O$ of precipitation sulfate (from rain to throughfall; collected near Site 7) could be an interesting aspect of sulfur/sulfate cycling in the high-elevation GRSM catchment; however, little weight can be given to this result given the lack of rain sample replication (N = 1). Previously reported rain-to-throughfall shifts in isotope composition vary widely in the literature. Contrasting examples can be found of increases in $\delta^{34}S$ (e.g., Jedrysek et al. 2002), decreases in $\delta^{34}S$ (e.g., Khenissi 2011), or no apparent effect on $\delta^{34}S$ (e.g., Stam et al. 1992; Mörth et al. 1999). This is expected given that rain-to-throughfall isotope effect is a complex function of atmospheric sulfur isotope composition, deposition rates, canopy characteristics (e.g., tree type, forest density, elevation) and climate factors (e.g., rain composition, temperature, season, etc.).

Despite the measured differences in isotope compositions between rain and throughfall, sulfur and oxygen isotope compositions of sulfate in precipitation helped identify main sulfur sources and transformation mechanism at the seven study sites in the GRSM. As shown in Figure 24, one distinctive mixing line between the throughfall and sulfidic bedrock runoff endmembers is evident for Sites 1 and 2 data. A second mixing line between the throughfall/rain endmember and stream water sulfate from catchments with sandstone (Sites 6 and 7) can be distinguished for Sites 4, 3 and 5 data. The observed relationships between $\delta^{34}S$ and $\delta^{18}O$ show that atmospheric deposition is still an important sulfate source in the GRSM but these contributions appear to change with location and bedrock composition. As has been previously mentioned, the isotope composition of

sulfate in Site 4 has anomalously large variance caused by either analytical error or a substantial within-catchment heterogeneity in the field conditions, bedrock composition, and/or soil properties. Note that this site showed distinctive shifts in $\delta^{34}S$ of stream water sulfate (Figure 24) which might suggest different proportions of sulfate from open rain and throughfall versus bedrock.

Atmospheric deposition appeared to be the dominant source of sulfate at Sites 3 – 7 but there is evidence of microbial cycling of the rain/throughfall sulfate. Cycling of atmospheric sulfur through the GRSM soil at these sites resulted in a small positive sulfur isotope fractionation as indicated by progressively higher $\delta^{34}S$ of stream water sulfate (Figure 24). For example, the $\delta^{34}S$ of stream water sulfate exported from catchments associated with Sites 6 and 7 (+7.2 to +8.2‰; mean = +7.7‰), and the $\delta^{34}S$ of phosphate-extractable mineral-bound soil sulfate at Site 7 (+4.8 and +5.1‰), were higher than $\delta^{34}S$ of throughfall sulfate (+3.8 to +4.5‰; mean = 4.2‰) (Table 15). Conversely, the $\delta^{34}S$ of soil organic sulfur at Sites 6 and 7 (+3.5, +3.8 and +3.8‰) was slightly lower than $\delta^{34}S$ of throughfall sulfate inputs (Table 15). These differences in $\delta^{34}S$ at Sites 6 and 7 (sandstone bedrock catchments) are consistent with isotope fractionations caused by assimilatory sulfate reduction, the microbiological process primarily responsible for sulfate immobilization into organic sulfur (Buchner et al. 2004; Pilsyk and Pazewski 2009). The initial uptake step (sulfate transport across the cell wall into the cell cytoplasm) and the subsequent dissociation of a sulfur-oxygen bond during formation of adenosine-5'-phosphosulfate (APS), favors the ^{32}S-sulfate (Harrison and Thode 1957; Harrison and Thode 1958; Bowen 1960; Kemp and Thode 1968). The sequence of biochemical reactions that initiates the sulfate assimilation/immobilization process (Buchner et al. 2004; Pilsyk and Pazewski 2009) results in the formation of intra-cellular cysteine which contains reduced sulfur (i.e., S^{2-}) with lower $\delta^{34}S$ (Alewell and Gehre 1999; Giesler et al.

2005). Simultaneously, the unassimilated sulfate exported back into stream water would have correspondingly higher $\delta^{34}S$. Similar sulfur isotope fractionations caused by assimilatory sulfate reduction have been reported by others (e.g., +0.5 to –4.4‰ [Kaplan et al. 1963; Mekhtiyeva and Pankina 1968; Mekhtiyeva 1971]; –0.9‰ to –2.8‰ [Kaplan and Rittenberg 1964; Chambers and Trudinger 1979]). The higher $\delta^{34}S$ in Site 5 (transition zone catchment) (Table 15) suggests a similar process may be occurring at that site, although the existence of another source of sulfate with marginally higher $\delta^{34}S$ (e.g., soluble bedrock sulfate minerals) also could have contributed to the observed $\delta^{34}S$ at Site 5.

The $\delta^{18}O$ of stream water sulfate can be used to identify sources of oxygen incorporated into sulfate molecules (e.g., Mayer et al. 1995; Balci et al. 2007; Heidel and Tichomirowa 2010; Müller et al. 2013). Sites 6 and 7 had lower $\delta^{18}O$ values of stream water sulfate (+3.0 to +3.5‰) than stream water from all other catchments (+4.2 to +8.9‰) and throughfall/rain sulfate (+7.3 to +11.0‰). Similar decreases of $\delta^{18}O$ in aqueous sulfate have been linked to microbial mobilization and mineralization of soil organic sulfur back into sulfate that incorporates water-oxygen atoms with negative $\delta^{18}O$ into the sulfate molecules during the re-oxidation reactions (Tichomirowa and Junghans 2009). However, there is some discrepancy between the known microbial processes in soil and the observed low $\delta^{18}O$ and high $\delta^{34}S$ of stream water sulfate. For example, in the studied area the microbial mobilization/mineralization of soil organic sulfur back into sulfate should result in low $\delta^{34}S$, in addition to low $\delta^{18}O$ because the $\delta^{34}S$ of organic sulfur in soil was low (+3.5 to +4.7‰). While assimilatory sulfate reduction (immobilization of sulfate) should increase both $\delta^{34}S$ and $\delta^{18}O$ because of preferential uptake of light ^{32}S and ^{16}O isotopes by microbes (Buchner et al. 2004; Pilsyk and Pazewski 2009), some studies suggest that this process leads to decreases of $\delta^{18}O$ of sulfate (e.g., Mitchell et al. 1998). Unfortunately, there is limited number of studies focused on

oxygen isotope fractionations during assimilatory sulfate reduction, thus we cannot better pinpoint the exact mechanisms of microbial sulfur transformation of sulfate in the studied area.

In addition to microbial processes in soil, there might be also another unidentified local source of sulfate with low $\delta^{18}O$ and high $\delta^{34}S$ values in the sandstone catchments (e.g., evaporitic sulfate minerals) that was not identified using sulfur sequential method. It should be mentioned that adsorption processes on soil particles likely do not result in isotope fractionations sufficiently large (van Stempvoort et al. 1990) to account for the observed shifts in sulfur and oxygen isotope composition at Sites 5, 6 and 7.

It is worth noting that Sites 4 – 7, which are separated from each other by several kilometers and whose sulfur cycle is primarily controlled by atmospheric deposition and soil microbial processes (e.g., higher $\delta^{34}S$ values), show very similar sulfate concentrations. This suggests that the baseline sulfate concentration is consistently low (approximately 2 mg L^{-1} as sulfate) in high-elevation catchments influenced primarily by atmospheric deposition. This low sulfate concentration is consistent with the sulfate concentrations (median 1.1 mg L^{-1} as sulfate; range < 4 mg L^{-1} [N = 7,383]) that have been measured in stream water collected throughout the GRSM for stream water monitoring programs since the early 1990s (STORET 2016).

Conditional Influence of Sulfidic Bedrock

The highest stream water sulfate concentrations and lowest $\delta^{34}S$ and $\delta^{18}O$ values, similar to the sulfidic bedrock, were found at Sites 1 and 2 (nearest to the Anakeesta Ridge) suggesting strong influence of sulfidic bedrock on local stream water chemistry. Additional evidence is found in the high sulfate concentrations and isotope composition in surface water flowing in direct contact with exposed sulfidic bedrock surfaces (> 15 mg L^{-1} as sulfate, $\delta^{34}S$ of –7.5 to –7.9‰).

Steam water chemistry, and $\delta^{34}S$ of stream water sulfate and soil-bound sulfate, was distinctive between Site 3 and Sites 1 and 2 (Table 15), despite all three sites being located within catchments overlying sulfidic bedrock. With respect to low sulfate concentration and higher $\delta^{34}S$ of stream water sulfate and soil sulfate, Site 3 was most comparable to Site 5 (transition zone catchment) and Sites 6 and 7 (sandstone catchments); thus, one or more condition or catchment characteristic is different at Sites 1 and 2 as compared to Site 3. The most viable catchment condition responsible for these differences is the degree to which bedrock surfaces are reactive to weathering conditions versus portions of the bedrock covered by protective barriers (e.g., soil mantel). Sites 1 and 2 are associated with catchments that drain the south-facing slope of Anakeesta Ridge which is characterized by steep slopes and shallow soil mantels. Such conditions are common in the area on and surrounding the Anakeesta Ridge, and are susceptible to landslides that expose underlying bedrock (Ryan 1989). Landslide scars expose fresh sulfidic bedrock surfaces to the atmosphere, and under favorable climate conditions, the previously unweathered, highly reactive sulfide minerals (e.g., pyrite, FeS_2) rapidly oxidize by a sequence of pH- and microbe-dependent reactions (Salmon 2004; Moses and Herman 1991; Lowson 1982). In the GRSM study area, the effect of exposed GRSM sulfidic bedrock on dissolved sulfate was clearly seen in the $\delta^{34}S$ of sulfate in the bedrock runoff (i.e., water flowing in direct contact with exposed sulfidic bedrock surfaces), which ranged between –7.9 and –7.5‰ (Table 15, bottom), and were comparable to those of elemental sulfur, ASS and CRS in the GRSM sulfidic bedrock samples (Table 14). Since there is little sulfur isotope fractionation during oxidation of sulfide (Taylor et al. 1984), the negative $\delta^{34}S$ of sulfate measured in the bedrock runoff indicates that its source was oxidation of sulfide in the Anakeesta Formation bedrock.

The $\delta^{18}O$ of sulfate in the bedrock runoff ranged from 0‰ to +1.6‰ (Table 15, bottom), and were closer to the negative $\delta^{18}O$ of GRSM stream water (–8.5‰ to –6.5‰; N = 80) than to the $\delta^{18}O$ of atmospheric oxygen (+23.5‰; Kroopnick and Craig 1972). This is consistent with other studies of elevated pyrite (FeS_2) mineralization in the bedrock, which reported low $\delta^{18}O$ of sulfate caused by sulfide oxidation reaction(s) involving water-oxygen and Fe^{3+} as the oxidant (e.g., Balci et al. 2007; Müller et al. 2013). Two main sulfide oxidation reaction pathways exist that use 1) molecular oxygen as the oxidant and 2) Fe^{3+} as the oxidant and water-bound oxygen as the source of oxygen for the sulfate ion (Taylor and Wheeler 1994; Balci et al. 2007; Tichomirowa and Junghans 2009). This is significant to sulfate formation because the $\delta^{18}O$ of meteoric water-oxygen (–25‰ to –5‰; Sharp 2007) is significantly lower than the $\delta^{18}O$ of atmospheric oxygen (+23.5‰; Kroopnick and Craig 1972). Sulfate formed from reactions that use water-oxygen will have lower $\delta^{18}O$ than sulfate formed from reactions that use molecular oxygen. Another distinction between these two oxygen sources is fractionation during sulfur-oxygen bond formation. Oxygen isotope enrichment that occurs during sulfur-oxygen bond formation is smaller when water is the source of oxygen (ε = +2.8‰) than when molecular oxygen is the source (ε = –9.8‰) (Balci et al. 2007; Tichomirowa and Junghans 2009). Since each sulfide oxidation mechanism can operate under appropriate environmental conditions, the $\delta^{18}O$ of sulfate in the environment will be comprised of mixtures of sulfate molecules formed by multiple reaction mechanisms and incorporating both sources of oxygen. After formed, sulfate molecules do not exchange sulfur and oxygen isotopes with water under lower temperatures (<25°C) ; therefore, the proportions of different sulfate endmembers in surface water can be quantified using isotope-balance equations (Lloyd 1968; Taylor and Wheeler 1994).

At Sites 1 and 2, the $\delta^{34}S$ values of stream water sulfate fell on the mixing line between atmospheric deposition (throughfall) and sulfidic bedrock endmembers. If one assumes that $\delta^{34}S$ of stream water sulfate at Sites 1 and 2 was comprised of mixtures of bedrock sulfur (–7.45 to –7.90‰) and throughfall (+3.78 to +4.50‰), proportions of each endmember can be calculated from a simple two-component mixing model: $\delta^{34}S_{\text{stream water}} = (X)(\delta^{34}S_{\text{bedrock}}) + (1 - X)(\delta^{34}S_{\text{atmophere}})$, where X represents the fraction of sulfate originating from the bedrock sulfide oxidation. According to this sulfur isotope mass balance constraint, in the investigated seasons approximately 46%-57% of stream water sulfate at Site 1 originated from bedrock and 43%-54% from throughfall. At Site 2, approximately 16%-30% of stream water sulfate originated from bedrock and 70%-84% from throughfall.

A similar two-component mixing model can be applied for oxygen isotope composition of stream water sulfate: $\delta^{18}O_{\text{stream water sulfate}} = (X)(\delta^{18}O_{\text{bedrock runoff}}) + (1 - X)(\delta^{18}O_{\text{atmospheric sulfate}})$, where X represents the fraction of sulfate originating from the bedrock sulfide oxidation. Accordingly, at Site 1, approximately 34%-60% of the stream water sulfate originated from bedrock and 40%-66% from throughfall. At Site 2, with wider variation in measured $\delta^{18}O$ of stream water sulfate, approximately 5%-48% of stream water sulfate originated from bedrock and 52%-95% throughfall. Overall, the results of isotope mass balance imply that contributions of sulfate from bedrock weathering are quite variable in the studied catchments of the GRSM.

The observed influence of weathering of exposed rock on surface water chemistry in the GRSM is directly analogous to acid rock drainage associated with sulfide-rich mine tailings, abandoned coal mines, and hydrothermal deposits (e.g., Evangelou and Zhang 1995; Zhang et al. 1998; Hubbard et al. 2009). Acidity, sulfate, iron and other metals associated with non-ferrous sulfide minerals, etc., are formed initially, followed by secondary reactions among the reaction products

(e.g., precipitation of secondary minerals that exceed saturation indices, oxidation of Fe^{2+} to Fe^{3+}, further oxidation of pyrite by Fe^{3+}, etc.) (Appelo and Postma 2005).

Examples of significant changes in the GRSM stream water pH, ANC, sulfate concentrations and metal concentrations, and their effects on aquatic life, that are directly attributable to the exposed GRSM sulfidic bedrock have been reported previously by Huckabee et al. 1975, Bacon and Maas 1979, and Mathews and Morgan 1982. These studies did not include isotope analysis in their study design, and mainly relied on the stream water chemistry (e.g., pH and dissolved metals) to explain the observed mortality of GRSM fish or amphibians. In those cases, the exposure of sulfidic bedrock was anthropogenic (caused by construction activities). Personal communication with the GRSM biologists provided other, anecdotal examples of aquatic life being extirpated in streams suspected of being affected by natural sulfidic bedrock landslide scars located upgradient of biological monitoring sites. The oxidation rates of sulfidic minerals like pyrite are surface-dependent processes (Singer and Stumm 1970; Hoffmann et al. 1981; Moses et al. 1987; Moses and Herman 1991; Murphy and Strongin 2009), and any process that reduces the "reactive" surface area of the sulfidic minerals also will reduce the production of oxidation byproducts (sulfate, acidity, metals). An effective mechanism by which the surface-reactivity of rock is reduced involves the formation of a protective barrier between the sulfide minerals at the bedrock surface and atmospheric oxygen (which either is the direct oxidizing agent for sulfide oxidation, or oxidizes Fe^{2+} to the other major sulfide oxidizing agent, Fe^{3+}). Two possible barriers are (1) coatings of iron and aluminum oxyhydroxides (formed as byproducts of pyrite oxidation) and (2) protective mantels of soil profiles developed on top of the bedrock. The byproduct ferrous-iron (Fe^{2+}) generated by pyrite oxidation oxidizes to ferric-iron (Fe^{3+}), hydrolyzes into poorly soluble secondary minerals such as ferric-iron oxides, oxyhydroxides, and acid-sulfates. Over time, these

oxidative phases precipitate as minerals buildup and adhere to the surface pores of the bedrock, and partially block the reactive bedrock surface area. The soil mantel functions as a protective barrier between the atmosphere and sulfidic bedrock in the same manner as secondary mineral precipitates. The catchment associated with Site 3 is not known to have exposed outcrops of sulfidic bedrock or natural disturbance scars. Thus, the sulfide weathering rate likely is lower at Site 3 as compared to Sites 1 and 2, thus it was reflected in Site 3 having sulfate with higher $\delta^{34}S$ and lower $\delta^{18}O$, similar to Sites 5-7 overlying sandstone. Consequently, our isotope results indicate that sulfidic bedrock that is covered by an intact soil mantel is not as serious of an environmental threat as exposed sulfidic bedrock.

Conclusions

In this study, the isotope composition of sulfate was used to examine the response of stream water and soil in the GRSM to atmospheric deposition and sulfidic bedrock weathering. The study also focused on small-scale GRSM drainage areas to limit the variability in geochemical results and thus more accurately correlate soil and stream water chemistry to geochemical processes in the catchments. It was hypothesized that $\delta^{34}S$ of stream water sulfate and soil sulfur species would mainly reflect atmospheric sulfate in the absence of significant sulfate inputs from underlying sulfidic bedrock. This was confirmed in our study by high $\delta^{34}S$ and $\delta^{18}O$ of sulfate typical for canopy throughfall and soil recycling in catchments overlying sulfidic-free, sandstone bedrock. While sulfidic bedrock was shown to have significant local impacts on stream water and soil chemistry, its influence was found to be dependent on the exposure of reactive surfaces of sulfidic bedrock to atmospheric oxygen. The studied catchments overlying sulfidic bedrock, but having intact protective soil mantel, showed negligible decreases in stream water pH and ANC, and stream

water sulfate and trace metals concentrations, and they had higher $\delta^{34}S$ of stream water sulfate and soil sulfur species indicative of primary atmospheric inputs and subsequent soil recycling. The results from this study show that sulfidic bedrock significantly decreases the $\delta^{34}S$ of stream water sulfate and soil sulfate, organic sulfur and total sulfur, and increases dissolved sulfate concentrations in stream water, but that the sulfidic bedrock in the catchment must be exposed to the atmosphere for it to manifest those effects. In summary, the characterization of isotope composition of specific sulfur species in soil, sulfur in bedrock, and sulfate in rain and throughfall in the GRSM yielded new details on how sulfur is cycled in the GRSM.

References

Alewell, Christine and Matthias Gehrer (1999). Patterns of stable S isotopes in a forested catchment as indicators for biological S turnover. Biogeochemistry, 47(3):317-331. GRef1058

Appelo, C.A.J., and D. Postma (2005). Geochemistry, Groundwater and Pollution, 2nd Edition. A.A. Balkema Publishers (a member of Taylor & Francis Group plc); Leiden, The Netherlands.

Bacon, J.R. and Richard P. Maas (1979). Contamination of Great Smoky Mountains Trout Streams by Exposed Anakeesta Formations. Journal of Environmental Quality, 8(4):538-543. GRef553

Balci, Nurgul, Wayne C. Shanks III, Bernhard Mayer and Kevin W. Mandernack (2007). Oxygen and sulfur isotope systematics of sulfate produced by bacterial and abiotic oxidation of pyrite. Geochimica et Cosmochimica Acta, 71(15), 3796-3811. GRef234

Balík, J., M Kulhanek, J. Cerny, J. Szakova, D. Pavlikova, and P. Cermak (2009). Differences in soil sulfur fractions due to limitation of atmospheric deposition. Plant, Soil and Environment, 55(8):344-352. GRef990

Bigham, J.M. and Darrell Kirk Nordstrom (2000). Iron and aluminum hydroxysulfates from acid sulfate waters. Reviews in Mineralogy and Geochemistry 40(1), 351-403. GRef582

Bloem, E., S. Haneklaus, and E. Schnug (2002). Optimization of a method for soil sulphur extraction. Communications in Soil Science and Plant Analysis, 33(1-2):41-51. GRef792

Bowen, H.J.M. (1960). Biological fractionation of isotopes. The International Journal of Applied Radiation and Isotopes, 7(4), 261-272. GRef762

Buchner, Peter, Hideki Takahashi and Malcolm J. Hawkesford (2004). Plant sulphate transporters: co-ordination of uptake, intracellular and long-distance transport. Journal of Experimental Botany, 55(404), 1765-1773 GRef1085

Burns, D.A., J.A. Lynch, B.J. Cosby, M.E. Fenn, and J.S. Baron, (2011). US EPA Clean Air Markets Division, National Acid Precipitation Assessment Program Report to Congress 2011: An Integrated Assessment, National Science and Technology Council, Washington, DC, 114 p.

Cai, Meijun, John S. Schwartz, R. Bruce Robinson, Stephen E. Moore, and Matt A. Kulp (2010). Long-Term Effects of Acidic Deposition on Water Quality in a High-Elevation Great Smoky Mountains National Park Watershed: Use of an Ion Input-Output Budget. Water, Air and Soil Pollution, 209(1-4):143-156. GRef591

Cai, Meijun, Amy M. Johnson, John S. Schwartz, Stephen E. Moore, Matt A. Kulp (2011). Response of soil water chemistry to simulated changes in acid deposition in the Great Smoky Mountains. GRef592

Cai, Meijun, Amy M. Johnson, John S. Schwartz, Stephen E. Moore, and Matt A. Kulp (2012). Soil Acid-Base Chemistry of a High-Elevation Forest Watershed in the Great Smoky Mountains National Park: Influence of Acidic Deposition. Water, Air and Soil Pollution, 223(1):289-303. GRef590

Chandra, A.P. and A.R. Gerson (2010). The mechanisms of pyrite oxidation and leaching: A fundamental perspective. Surface Science Reports, 65(9), 293-315. GRef362

Chen, Limin, Charles T. Driscoll, Solomon Gbondo-Tugbawa, Myron J. Mitchell, and Peter S. Murdoch (2004). The application of an integrated biogeochemical model (PnET-BGC) to five

forested watersheds in the Adirondack and Catskill regions of New York. Hydrological Processes, 18(14):2631-2650. GRef726

Cook, Robert B., M.A. Bogle, R.S. Turner, and J.W. Elwood (1987). Biogeochemical controls of sulfate in high-elevation streams: stable sulfur isotope tracers. Abstract in EOS 68(50):1702 (December 15, 1987) GRef559b

David, Mark B. and Myron J. Mitchell (1987). Transformations of Organic and Inorganic Sulfur: Importance to Sulfate Flux in an Adirondack Forest Soil. JAPCA, 37(1), 39-44. GRef125 doi.org/10.1080/08940630.1987.10466198

Dostalova, Z., I. Hunova, V. Novak, J. Ostatnicka, J. Proskova, and J. Sladecek (2004). Air Pollution and Atmospheric Deposition in the Czech Republic in 2003, 132 pp., Czech Hydrometerological Institute, Prague.

Driscoll, Charles T., G.B. Lawrence, A.J. Bulger, T.J. Butler, C.S. Cronan, C. Eagar, K.F. Lambert, Gene E. Likens, J.L. Stoddard, and Kathleen C. Weathers (2001). Acidic deposition in the northeastern United States: Sources and inputs, ecosystem effects, and management strategies. BioScience, 51(3):180-198. GRef1036

Edwards, Pamela J. (1998). Sulfur cycling, retention, and mobility in soils: A review. General technical report NE-250, U.S. Department of Agriculture, Forest Service, Northeastern Research Station. Radnor, PA.

Ensminger, L.E. (1954). Some factors affecting the adsorption of sulfate by Alabama soils. Soil Science Society of America Journal, 18(3), 259-264. GRef844

Espenshade, George H. (1963). Geology of some copper deposits in North Carolina, Virginia, and Alabama: U.S. Geological Survey Bulletin 1142-i, p. i1-i50.

Evangelou, V.P. and Y.L. Zhang (1995). A review: Pyrite oxidation mechanisms and acid mine drainage prevention. Critical Reviews in Environmental Science and Technology, 25(2):141-199. GRef219

Fakhraei, Habibollah, Charles T. Driscoll, James R. Renfro, Matt A. Kulp, Tamara F. Blett, Patricia F. Brewer, and John S. Schwartz (2016). Critical loads and exceedances for nitrogen and sulfur atmospheric deposition in Great Smoky Mountains National Park, United States. Ecosphere, 7(10):e01466. pp. 1-28 GRef1047

Fauville, Andrea, Bernhard Mayer, Rene Frommichen, Kurt Friese and Jan Veizer (2004). Chemical and isotopic evidence for accelerated bacterial sulphate reduction in acid mining lakes after addition of organic carbon: laboratory batch experiments. Chemical Geology, 204, 325-344. GRef285

Fitzgerald, John W., Jaru T. Ash, Timothy C. Strickland, and Wayne T. Swank (1983). Formation of organic sulfur in forest soils: a biologically mediated process. Canadian Journal of Forest Research, 13(6):1077-1082. GRef605

Flohr, Marta J.K., Roberta G. Dillenburg and Geoffrey S. Plumlee (1995). Characterization of secondary mineral formed as the result of weathering of the Anakeesta Formation, Alum Cave, Great Smoky Mountains National Park, Tennessee. U.S. Geological Survey Open-file Report No. 95-477. U.S. Department of the Interior; Reston, Virginia.

Fuller, Robert D., Myron J. Mitchell, R. Krouse, J. Wyskowski, and Charles T. Driscoll (1986). Stable sulfur isotope ratios as a tool for interpreting ecosystem sulfur dynamics. Water, Air and Soil Pollution, 28:163-171. GRef1013

Fuseler, Knut and Heribert Cypionka (1995). Elemental sulfur as an intermediate of sulfide oxidation with oxygen by *Desulfobulbus propionicus*. Archives of Microbiology, 164(2):104-109. GRef1077

Galloway, James N., Stephen A. Norton, and M. Robbins Church (1983). Freshwater acidification from atmospheric deposition of sulfuric acid: A conceptual model. Environmental Science and Technology, 17(11):541A-545A. GRef196

Ghani, A., R.G. Mclaren and R.S. Swift (1993). Mobilization of recently-formed soil organic sulphur. Soil Biology and Biochemistry, 25(12), 1739-1744. GRef668

Giesler, Reiner, Carl Magnus Mörth, Elin Mellqvist, and Peter Torssander (2005). The humus layer determines SO_4^{2-} isotope values in the mineral soil. Biogeochemistry, 74(1):3-20. GRef1055

Gonzalez, Adrian M., Dr. John S. Schwartz, and Matt Kulp (2015). Geochemistry in a high-elevation watershed responds to reductions in acid-pollutant emissions? 2015 World Environmental & Water Resources Congress (EWRI), Austin, Texas, 17-21 May 2015. Platform presentation 19 May 2015.

Grell, Mary Ann Elizabeth (2010). Soil chemistry characterization of acid sensitive watershed in the Great Smoky Mountains National Park. Master of Science Thesis, University of Tennessee, Knoxville; December 2010.

Hadley, Jarvis B. and Richard Goldsmith (1963). Geology of the Eastern Great Smoky Mountains North Carolina and Tennessee. Geological survey professional paper 349-B. U.S. Department of the Interior, U.S. Government Printing Office, Washington, D.C.

Hammarstrom, Jane M., Robert R. Seal, Allen L. Meier, and J.M. Kornfeld (2005). Secondary sulfate minerals associated with acid drainage in the eastern US: recycling of metals and acidity in surficial environments. Chemical Geology, 215(1-4):407-431. GRef486

Harrison A.G. and H. Thode (1957). The kinetic isotope effect in the chemical reduction of sulfate. Transaction of the Faraday Society, 53, 1-4. GRef1087

Harrison A.G. and H. Thode (1958). Mechanism of the bacterial reduction of sulfate from isotope fractionation studies. Transactions of the Faraday Society, 54, 84-92. GRef1088

Heidel, Claudia and Marion Tichomirowa (2010). The role of dissolved molecular oxygen in abiotic pyrite oxidation under acid pH conditions - Experiments with ^{18}O-enriched molecular oxygen. Applied Geochemistry, 25(11):1664-1675. GRef868

Heidel, Claudia, Marion Tichomirowa and Manuela Junghans (2013). Oxygen and sulfur isotope investigations of the oxidation of sulfide mixtures containing pyrite, galena, and sphalerite. Chemical Geology, 342(1), 29-43. GRef321

Herlihy, A.T., P.R. Kaufmann, M.R. Church, P.J. Wigington, J.R. Webb and M.J. Sale (1993). The effects of acidic deposition on streams in the Appalachian Mountain and Piedmont Region of the Mid-Atlantic United States. Water Resources Research, 29(8), 2687-2703. GRef586

Houle, Daniel, Charles Marty, Louis Duchesne and Christian Gagnon (2014). Humus layer in the main locus of secondary SO_4 production in boreal forests. Geochimica et Cosmochimica Acta 126(1), 18-29. GRef287

Hubbard, Christopher G., Stuart Black and Max L. Coleman (2009). Aqueous geochemistry and oxygen isotope compositions of acid mine drainage from the Río Tinto, SW Spain, highlight inconsistencies in current models. Chemical Geology, 265(3-4), 321-334. GRef565

Huckabee, John W., C. Phillip Goodyear and Ronald D. Jones (1975). Acid rock in the Great Smokies: Unanticipated impact on aquatic biota of road construction in regions of sulfide mineralization. Transactions of the American Fisheries Society 104(4):677-684. DOI: 10.1577/1548-8659(1975)104<677:ARITGS>2.0.DO;2

Isil, Selma, Thomas Lavery, Kristi Gebhart, Christopher Rogers, and Carol Armbrust Wanta (2017). Magnitude and Trends of High-elevation Cloud Water Pollutant Concentrations and Modeled Deposition Fluxes. Journal of Environmental Science and Engineering B, 6(2017):127-143. GRefXXX

Jedrysek, Mariusz Orion, Adam Kaluzny, and Jochen Hoefs (2002). Sulphur and oxygen isotope ratios in spruce needles as a tracer of atmospheric pollution. Journal of Geophysical Research: Atmospheres, 107(D18), 4353. GRef855

Johnson, Dale W. and Steven E. Lindberg (ed.) (1992). Atmospheric deposition and forest nutrient cycling: A synthesis of the Integrated Forest Study. Springer-Verlag, New York, NY. GRef1018

Kemp, A.L.W. and H.G. Thode (1968). The mechanism of the bacterial reduction of sulphate and of sulphite from isotope fractionation studies. Geochimica et Cosmochimica Acta, 32(1), 71-91. GRef764

Kendall, C. and E.A. Caldwell (1998). Fundamentals of isotope geochemistry (Chapter 2). In: C. Kendall and J.J. McDonnell (Eds.), Isotope Tracers in Catchment Hydrology, Elsevier Science B.V., Amsterdam. Found online at: http://wwwrcamnl.wr.usgs.gov/isoig/isopubs/itchch2.html

Khenissi, Heyfa (2011). Sulfur isotopic composition and concentration in throughfall and precipitation samples from a suburban forest. Undergraduate research paper submitted to the Department of Geology, University of Maryland. geol.umd.edu/undergraduate/paper/khenissi.pdf (note: report is not dated; therefore, the date/year of publication is uncertain)

King, Philip B. (1964). Geology of the Central Great Smoky Mountains Tennessee. Geological Survey Professional Paper No. 349-C. U.S. Department of the Interior, U.S. Government Printing Office, Washington, D.C.

Kroopnick, P. and H. Craig (1972). Atmospheric oxygen: Isotopic composition and solubility fractionation. Science 175:54-55. GRef525

Likens, Gene E., Charles T. Driscoll, Donald C. Buso, Myron J. Mitchell, Gary M. Lovett, Scott W. Bailey, T.G. Siccama, W.A. Reiners and Christine Alewell (2002). The biogeochemistry of sulfur at Hubbard Brook. Biogeochemistry 60(3), 235-316. GRef632

Likens, Gene E., Thomas J. Butler, and Donald C. Buso (2001). Long- and short-term changes in sulfate deposition: Effects of the 1990 Clean Air Act Amendments. Biogeochemistry, 52(1), 1-11. GRef593

Lloyd, R.M. (1968). Oxygen isotope behavior in the sulfate-water system. Journal of Geophysical Research, 73:6099-6209. Ref. in GRef525

Marnette, Emile C.L. Harm Houweling, Herman van Dam, and Jan Willem Erisman (1993). Effects of decreased atmospheric deposition on the sulfur budgets of two Dutch moorland pools. Biogeochemistry, 23(2):119-144. GRef1039

Marty, Charles, Daniel Houle, Christian Gagnon and Louis Duchesne (2011). Isotopic compositions of S, N and C in soils and vegetation of three forest types in Québec, Canada. Applied Geochemistry 26(12), 2181-2190. GRef290

Mathews, Raymond C. and Eric L. Morgan (1982). Toxicity of Anakeesta Formation Leachates to Shovel-Nosed Salamander, Great Smoky Mountains National Park. Journal of Environmental Quality, 11(1):102-106. GRef1010

Mayer, Bernhard, P. Fritz, Jörg Prietzel, and H. Roy Krouse (1995). The use of stable sulfur and oxygen isotope ratios for interpreting the mobility of sulfate in aerobic forest soils. Applied Geochemistry, 10(2):161-173. GRef158

Mayer, Bernhard, Jörg Prietzel and H. Roy Krouse (2001). The influence of sulfur deposition rates on sulfate retention patterns and mechanisms in aerated forest soils. Applied Geochemistry, 16(9-10):1003-1019. GRef159

Mayer, Bernhard and H. Roy Krouse (2004). Procedures for Sulfur Isotope Abundance Studies (Chapter 26; p.538-596). In: Pier A. Groot, Handbook of Stable Isotope Analytical Techniques. Elsevier, Amsterdam. GRef283

Mayer, Bernhard, James B. Shanley, Scott W. Bailey and Myron J. Mitchell (2010). Identifying sources of stream water sulfate after a summer drought in the Sleepers River watershed (Vermont, USA) using hydrological, chemical, and isotopic techniques. Applied Geochemistry, 25(5), 747-754. GRef289

Maynard, D.G., Y.P. Kalra, and F.G. Radford (1987). Extraction and Determination of Sulfur in Organic Horizons of Forest Soils. Soil Science Society of America Journal, 51(3):801-806. GRef730

Mitchell, M.J., H.R. Krouse, Bernhard Mayer, A.C. Stam, and Y. Zhang (1998). Use of stable isotopes in evaluating sulfur biogeochemistry of forest ecosystems. In: Kendall, C., McDonnell, J.J. (Eds.), Catchment Hydrology. Elsevier, Amsterdam, pp. 489–518. GRef975

Mitchell, Myron J., Scott W. Bailey, James B. Shanley, and Bernhard Mayer (2008). Evaluating sulfur dynamics during storm events for three watersheds in the northeastern USA: a combined hydrological, chemical and isotopic approach. Hydrological Processes, 22(20):4023-4034. GRef515

Mohr, David W. (1973). Stratigraphy and structure of part of the Great Smoky and Murphy Belt Groups, Western North Carolina. American Journal of Science, Cooper 273A:41-71.

Mörth, Carl-Magnus, Peter Torssander, Minoru Kusakabe and Hans Hultberg (1999). Sulfur isotope values in a forested catchment over four years: Evidence for oxidation and reduction processes. Biogeochemistry, 44(1), 51-71. GRef635

Müller, Inigo A., Benjamin Brunner, and Max Coleman (2013). Isotopic evidence of the pivotal role of sulfite oxidation in shaping the oxygen isotope signature of sulfate. Chemical Geology, 354(0):186-202. GRef322

Murphy, Riley and Daniel R. Strongin (2009). Surface reactivity of pyrite and related studies. Surface Science Reports 64(1), 1-45. GRef361

National Parks Service (NPS) (2017). Webpage "World Heritage Sites in the United States: Great Smoky Mountains National Park." U.S. Department of the Interior website URL: https://www.nps.gov/nr/travel/worldheritagesites/Great_Smoky_Mountains_National_Park.htm (accessed August 23, 2017).

National Parks Service (NPS) (2015). Webpage "Program Brief: Inventory and Monitoring." U.S. Department of the Interior website URL: https://science.nature.nps.gov/im/ (accessed July 28, 2017).

Neff, Kiel J., John S. Schwartz, Stephen E. Moore and Matt A. Kulp (2013). Influence of basin characteristics on baseflow and stormflow chemistry in the Great Smoky Mountains National Park, USA. Hydrological Processes 27(14), 2061-2074. GRef484

Neff, Kiel J., John S. Schwartz, Theodore B. Henry, R. Bruce Robinson, Stephen E. Moore, and Matt A. Kulp (2009). Physiological Stress in Native Southern Brook Trout During Episodic Stream Acidification in the Great Smoky Mountains National Park. Archives of Environmental Contamination and Toxicology 57(2):366-376.

Novák, Martin, James W. Kirchner, Daniela Fottova, Eva Prechova, Iva Jacková, Pavel Kram and Jakub Hruska (2005). Isotopic evidence for processes of sulfur retention/release in 13 forested

catchments spanning a strong pollution gradient (Czech Republic, central Europe). Global Biogeochemical Cycles 19(4), GB4012-1 – GB4012-14. GRef183

Novák, Martin, Frantisek Buzek, Anthony F. Harrison, Eva Prechova, Iva Jacková and Daniela Fottova (2003). Similarity between C, N and S stable isotope profiles in European spruce forest soils: Implications for the use of $\delta^{34}S$ as a tracer. Applied Geochemistry 18(5), 765-779. GRef160

Novák, Martin, James W. Kirchner, Hana Groscheová, Miroslav Havel, Jirí Cerny, Rodovan, Krejci, and Frantisek Buzek (2000). Sulfur isotope dynamics in two central European watersheds affected by high atmospheric deposition of SOx. Geochimica et Cosmochimica Acta 64(3):367-383. GRef333

Omernik, James M. and C.F. Powers (1982). Total alkalinity of surface waters: A national map. U.S. Environmental Protection Agency. Corvallis Environmental Research Laboratory, Corvallis, Oregon.

Overton, John H., Jr., Viney P. Aneja and Jack L. Durham (1979). Production of sulfate in rain and raindrops in polluted atmospheres. Atmospheric Environment (1967) 13(3), 355-367.

Palmer, Martin R., Cahit Helvaci, and Anthony E. Fallick (2004). Sulphur, sulphate oxygen and strontium isotope composition of Cenozoic Turkish evaporites. Chemical Geology, 209(3-4):341-356. GRef812

Pilsyk, Sebastian and Andrzej Paszewski (2009). Sulfate permeases – phylogenic diversity of sulfate transport. Acta Biochimica Polonica, 56(3), 375-384. GRef1086

Pisapia, Celine, M. Chaussidon, C. Mustin, and B. Humbert (2007). O and S isotopic composition of dissolved and attached oxidation products of pyrite by Acidithiobacillus ferrooxidans: Comparison with abiotic oxidations. Geochimica et Cosmochimica Acta 71:2474-2490. GRef330

Porter, Ellen, Tamera Blett, Deborah U. Potter, and Cindy Huber (2005). Protecting resources on Federal lands: Implications of critical loads for atmospheric deposition of nitrogen and sulfur. BioScience 55(7):603-612. GRef451

Rees, C.E., W.J. Jenkins, and Jan Monster (1987). The sulfur isotopic composition of ocean water sulfate. Geochimica et Cosmochimica Acta, 42(4):377-381. GRef767

Robison, Andrew L., Todd M. Scanlon, Bernard J. Cosby, James R. Webb, and James N. Galloway (2013). Roles of sulfate adsorption and base cation supply in controlling the chemical response of streams of western Virginia to reduced acid deposition. Biogeochemistry, 116(1-3), 119-130. GRef384

Rock, Luc and Bernhard Mayer (2002). Isotopic assessment of sources and processes affecting sulfate and nitrate in surface water and groundwater of Luxembourg. Isotopes in Environmental and Health Studies, 38(4), 191-206. GRef644

Rock, Luc and Bernhard Mayer (2009). Identifying the influence of geology, land use, and anthropogenic activities on riverine sulfate on a watershed scale by combining hydrometric, chemical and isotopic approaches. Chemical Geology, 262(3-4), 121-130. GRef300

Rossete, Alexssandra Luiza Rodrigues Molina, José Albertino Bendassolli, and Paulo Cesar Ocheuze Trivelin (2008). Organic sulfur oxidation to sulfate in soil samples for total sulfur determination by turbidimetry. Revista Brasileira de Ciência do Solo, 32(6), 2547-2553.GRef662

Ryan, Patrick T. (1989). "Debris Slides and Flows on Anakeesta Ridge within the Great Smoky Mountains National Park, Tennessee, U.S.A. " Master's Thesis, University of Tennessee, 1989. http://trace.tennessee.edu/utk_gradthes/2493 GRef857

Sahrawat, Kanwar L., K.V.S. Murthy, and S.P. Wani (2009). Comparative evaluation of Ca chloride and Ca phosphate for extractable sulfur in soils with a wide range in pH. Journal of Plant Nutrition and Soil Science, 172(3), 404-407. GRef729

Salmon, Sally Ursula (2004). Geochemical processes in mill tailings deposits: modelling of groundwater composition. Applied Geochemistry, 19(1), 1-17. GRef1095

SAS Corporation (2017). JMP® Pro, Version 13.0. SAS Institute Inc., Cary, NC, 1989-2017.

Schwartz, John S., Adrian M. Gonzalez and Matt A. Kulp (2016). Geochemistry in a High-Elevation Watershed Responds to Reductions in Acid-Pollutant Emissions. Abstract No. presented at 2016 Fall Meeting, American Geophysical Union (AGU), San Francisco, Calif., USA; 12-16 Dec.

Schwartz, John S., Meijun Cai, Matt A. Kulp, Stephen E. Moore, Becky Nichols and Charles Parker (2014). Biological effects of stream water quality on aquatic macroinvertebrates and fish communities within the Great Smoky Mountains National Park. U.S. Department of the Interior, National Park Service (NPS) Natural Resources Report (NRR) No. 778; August 2013. GRef584

Sharp, Zachary, 2007. Principles of Stable Isotope Geochemistry. Pearson – Prentice Hall, Upper Saddle River, New Jersey 07458.

Smith S.J., J. van Aardenne, Z. Klimont, R.J. Andres, A. Volke, and Arias S. Delgado (2011). Anthropogenic sulfur dioxide emissions: 1850-2005. Atmospheric Chemistry and Physics 11 (3): 1101-1116. GRef1043

Southworth, Scott, Art Schultz and Danielle Denenny (2005). Geologic map of the Great Smoky Mountains National Park Region, Tennessee and North Carolina. U.S. Geological Survey Open-File Report 2005-1225. URL: http://pubs.usgs.gov/of/2005/1225/OF2005-1225_map.pdf

Southworth, Scott, Art Schultz, and Danielle Denenny (2004). Generalized Geologic map of Bedrock Lithologies and Surficial Deposits in the Great Smoky Mountains National Park region, Tennessee and North Carolina. U.S. Geological Survey Open File Report 2004-1410, scale 1:100,000.

Stam, A.C., Myron J. Mitchell, H. Roy Krouse and Jeffrey S. Kahl (1992). Stable sulfur isotopes of sulfate in precipitation and stream solutions in a northern hardwood watershed. Water Resources Research, 28(1), 231-236. GRef273

STORET (STOrage and RETrieval) Data Warehouse (2016). U.S. Environmental Protection Agency Web site. http://www.epa.gov/storet. Accessed August 8, 2016.

Sullivan, Timothy J., Bernard J. Cosby, James R. Webb, Kai U. Snyder, Alan T. Herlihy, Arthur J. Bulger, Erin H. Gilbert and Deian Moore (2002). Assessment of the effects of acidic deposition on aquatic resources in the Southern Appalachian Mountains. Report prepared for Southern Appalachian Mountains Initiative (SAMI); prepared by E&S Environmental Chemistry, Inc. (Corvallis, Oregon); July 2002. GRef694

Sullivan, Timothy J., Bernard J. Cosby, Kai U. Snyder, Alan T. Herlihy and B. Jackson (2007). Model-based assessment of the effects of acidic deposition on sensitive watershed resources in the National Forests of North Carolina, Tennessee and South Carolina. Final Report prepared for U.S. Department of Agriculture (USDA) Forest Service, Asheville, North Carolina; October 2007.

Sullivan, Timothy J., Bernard J. Cosby and William A. Jackson (2011). Target loads of atmospheric sulfur deposition for the protection and recovery of acid-sensitive streams in the Southern Blue Ridge Province. Journal of Environmental Management, 92(11):2953-2960.

Swank, Wayne T. (1984). Microbial transformation of sulfate in forest soils. Science, 223, 137-145. GRef125

Szynkiewicz, Anna, B. Talon Newton, Stacy S. Timmons and David M. Borrok (2012). The sources and budget for dissolved sulfate in a fractured carbonate aquifer, southern Sacramento Mountains, New Mexico, USA. Applied Geochemistry 27(8), 1451-1462. GRef312

Szynkiewicz, Anna, James C. Witcher, Magdalena Modelska, David M. Borrok and Lisa M. Pratt (2011). Anthropogenic sulfate loads in the Rio Grande, New Mexico (USA). Chemical Geology 283(3-4), 194-209. GRef310

Szynkiewicz, Anna, Miguel Rangel Medina, Magdalena Modelska, Rogelio Monreal and Lisa M. Pratt (2008a). Sulfur isotopic study of sulfate in the aquifer of Costa de Hermosillo (Sonora, Mexico) in relation to upward intrusion of saline groundwater, irrigation pumping and land cultivation. Applied Geochemistry 23(9), 2539-2558. GRef394

Szynkiewicz, Anna, Magdalena Modelska, Mariusz Orion Jedrysek and Maria Mastalerz (2008b). The effect of acid rain and altitude on concentration, $\delta^{34}S$, and $\delta^{18}O$ of sulfate in the water from Sudety Mountains, Poland. Chemical Geology 249(1-2), 36-51. GRef395

Tabatabai, M. Ali, N.T. Basta and H.J. Pirela (1988). Determination of total sulfur in soils and plant materials by ion chromatography. Communications in Soil Science and Plant Analysis, 19(15), 1701-1714. GRef845

Taylor, Bruce E., Mark C. Wheeler and Darrell Kirk Nordstrom (1984). Stable isotope geochemistry of acid mine drainage: Experimental oxidation of pyrite. Geochimica et Cosmochimica Acta, 48(12), 2669-23678. GRef526

Tennessee Valley Authority (TVA) (2017). Environmental stewardship webpage found at: https://www.tva.gov/Environment/Environmental-Stewardship/Air-Quality/Sulfur-Dioxide. Accessed August 10, 2017.

Thornberry-Ehrlich, Trista (2008). Great Smoky Mountains National Park Geologic Resource Evaluation Report. National Resource Report NPS/NRPC/GRD/NRR-2008/048. National Park Service, Denver, Colorado; NPS D-626, September 2008.

Tichomirowa, Marion and Manuela Junghans (2009). Oxygen isotope evidence for sorption of molecular oxygen to pyrite surface sites and incorporation into sulfate in oxidation experiments. Applied Geochemistry, 24(11):2072-2092. GRef329

Trembaczowski, A., J. Szaran and H. Niezgoda (2004). Investigating the Provenance and Seasonal Variations in Sulphate Sulphur and Oxygen Isotopes of Central Roztocze River Water, SE Poland. Water, Air, and Soil Pollution, 157(1-4):65-84. GRef647

Turner, J.V., D.K. MacPherson and R.A. Stokes (1987). The mechanisms of catchment flow processes using natural variations in deuterium and oxygen-18. Journal of Hydrology, 94, 143-162. GRef815

Turner, R.S., P.F. Ryan, D.R. Marmorek, K.W. Thornton, T.J. Sullivan, J.P. Baker, S.W. Christensen, and M.J. Sale (1992). Sensitivity to change for low-ANC eastern US lakes and streams and brook trout populations under alternative sulfate deposition scenarios. Environmental Pollution, 77(2-3):269-277. GRef680

Tuttle, M.L., M.B. Goldhaber, and D.L. Williamson (1986). An analytical scheme for determining forms of sulfur in oil shales and associated rocks. Talanta, 33(12), 953-961. GRef853

USDA-NRCS (2009). Soil survey of Great Smoky Mountains National Park, Tennessee and North Carolina. U.S Department of Agriculture, Natural Resources Conservation Service.

Weathers, Kathleen C., Samuel M. Simkin, Gary M. Lovett and Steven E. Lindberg (2006). Empirical modeling of atmospheric deposition in mountainous landscapes. Ecological Applications 16(4):1590-1607. GRef522

Yang, Chao, Kevin Telmer, and Jan Veizer (1996). Chemical dynamics of the 'St. Lawrence' riverine system: dD_{H2O}, $d^{18}O_{H2O}$, $d^{13}C_{DIC}$, $d^{34}S_{sulfate}$, and dissolved $^{87}Sr/^{86}Sr$. Geochimica et Cosmochimica Acta, 60(5):851-866. GRef649

Zhai, Jing, Charles T. Driscoll, Timothy J. Sullivan, and Bernard J. Cosby (2008). Regional application of the PnET-BGC model to assess historical acidification of Adirondack lakes. Water Resources Research, 44(1), W01421. GRef727

Zhang, Yimin, Myron J. Mitchell, Martin Christ, Gene E. Likens and H. Roy Krouse (1998). Stable sulfur isotope biogeochemistry of the Hubbard Brook Experimental Forest, New Hampshire. Biogeochemistry, 41(3), 259-275. GRef335

Zhou, Qingtao, Charles T. Driscoll, Stephen E. Moore, Matt A. Kulp, James R. Renfro, John S. Schwartz, Meijun Cai, and Jason A. Lynch (2015). Developing Critical Loads of Nitrate and Sulfate Deposition to Watersheds of the Great Smoky Mountains National Park, USA. Water, Air, & Soil Pollution 226(8):1-16. GRef908

Chapter 6 Appendix

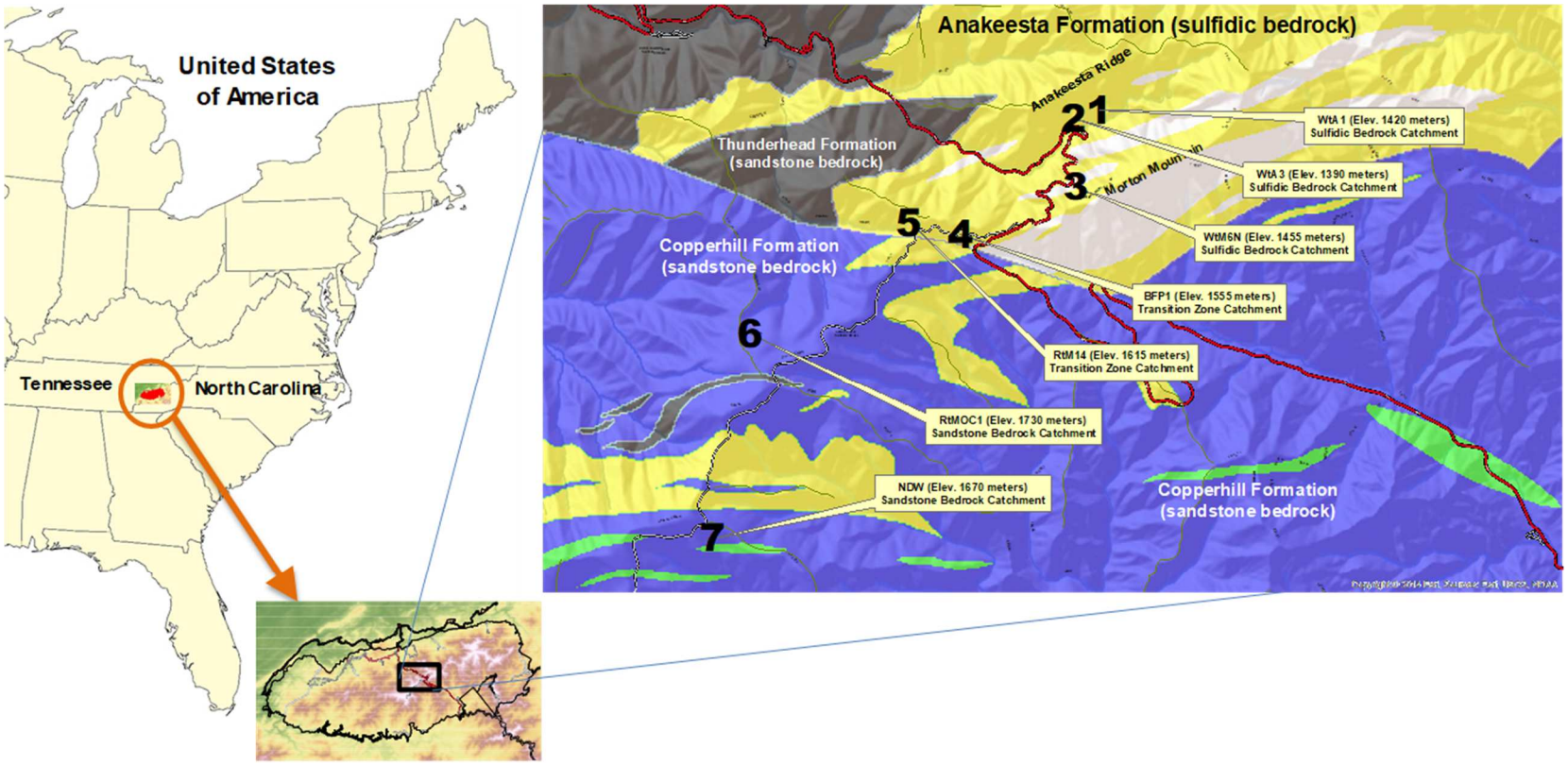

Figure 15. Location of the Great Smoky Mountains National Park (GRSM) and detailed map of sampling locations and major bedrock formations associated with the study areas. Sites 1, 2 and 3 = sulfidic bedrock catchments; Sites 4 and 5 = transition zone bedrock catchments; Sites 6 and 7 = sandstone bedrock catchments (reference sites).

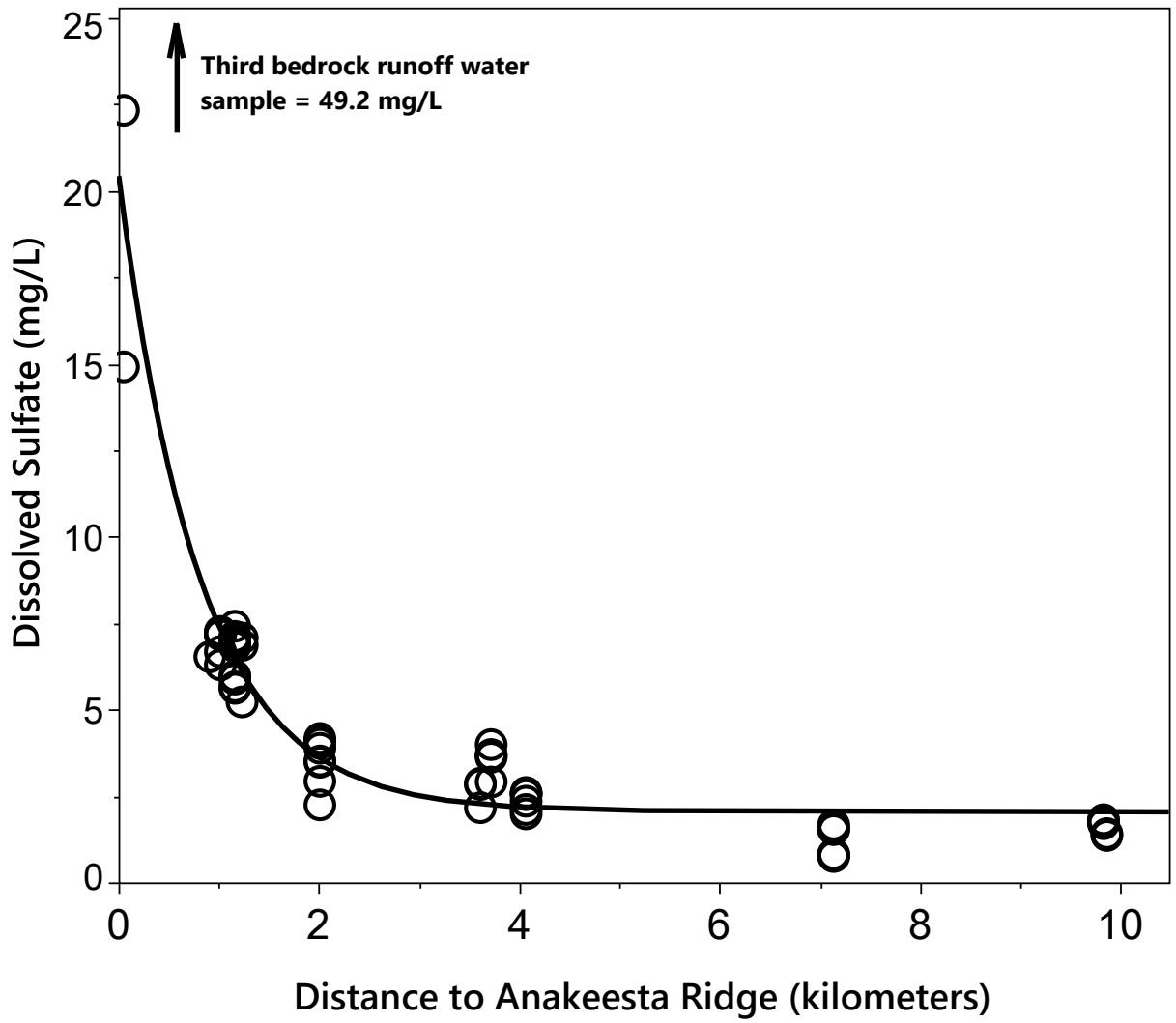

Figure 16. Concentrations of stream water sulfate relative to the approximate distance from Anakeesta Ridge (Fig. 1). Bedrock runoff data were assigned a distance of 0.05 km to reflect direct contact between water and bedrock. Data were fitted to a three-parameter exponential function [$R^2 = 0.92$]: sulfate (mg L^{-1}) = 2.0 + 17.3(exp(–1.17*kilometers))

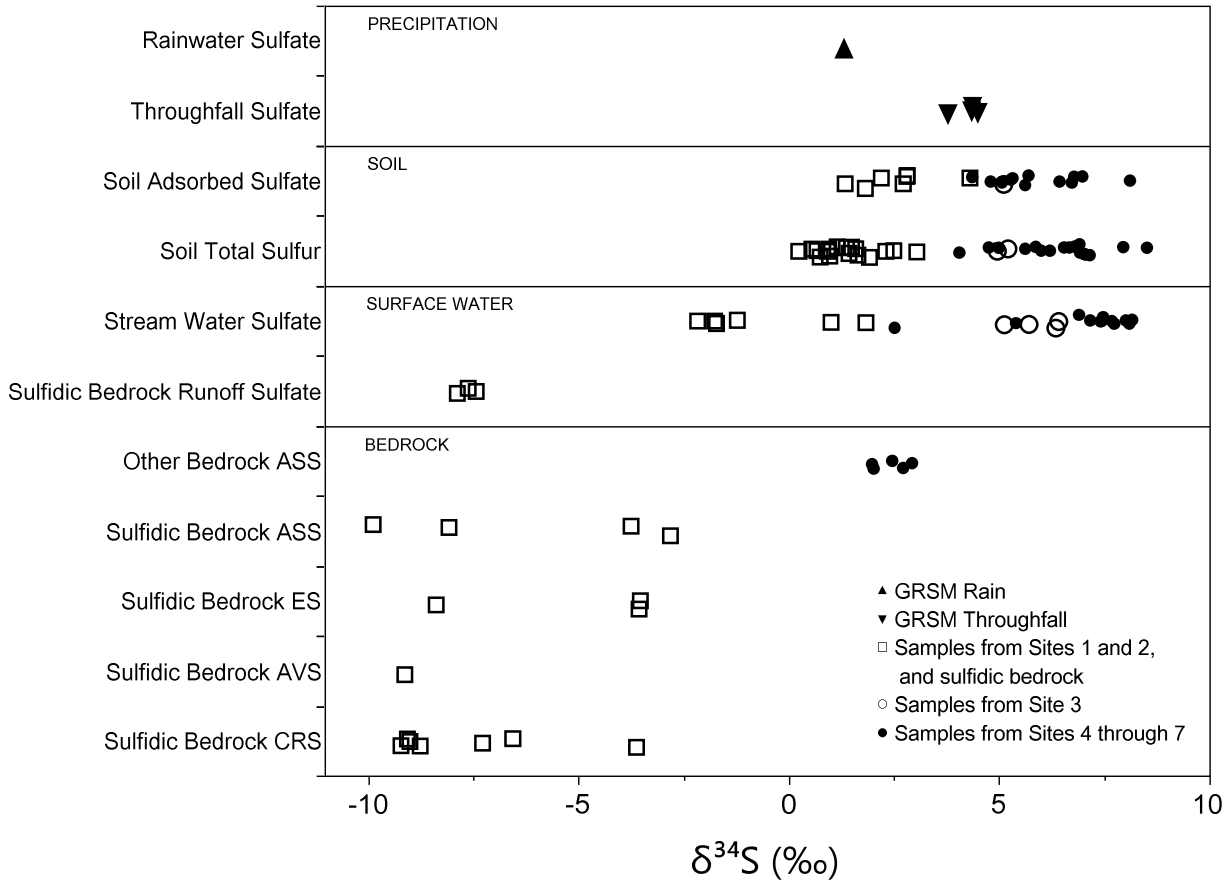

Figure 17. Variations of $\delta^{34}S$ in the samples analyzed for this study. Data are arranged in spatial order: atmospheric samples, surface samples (soil, stream water), bedrock runoff, and bedrock.

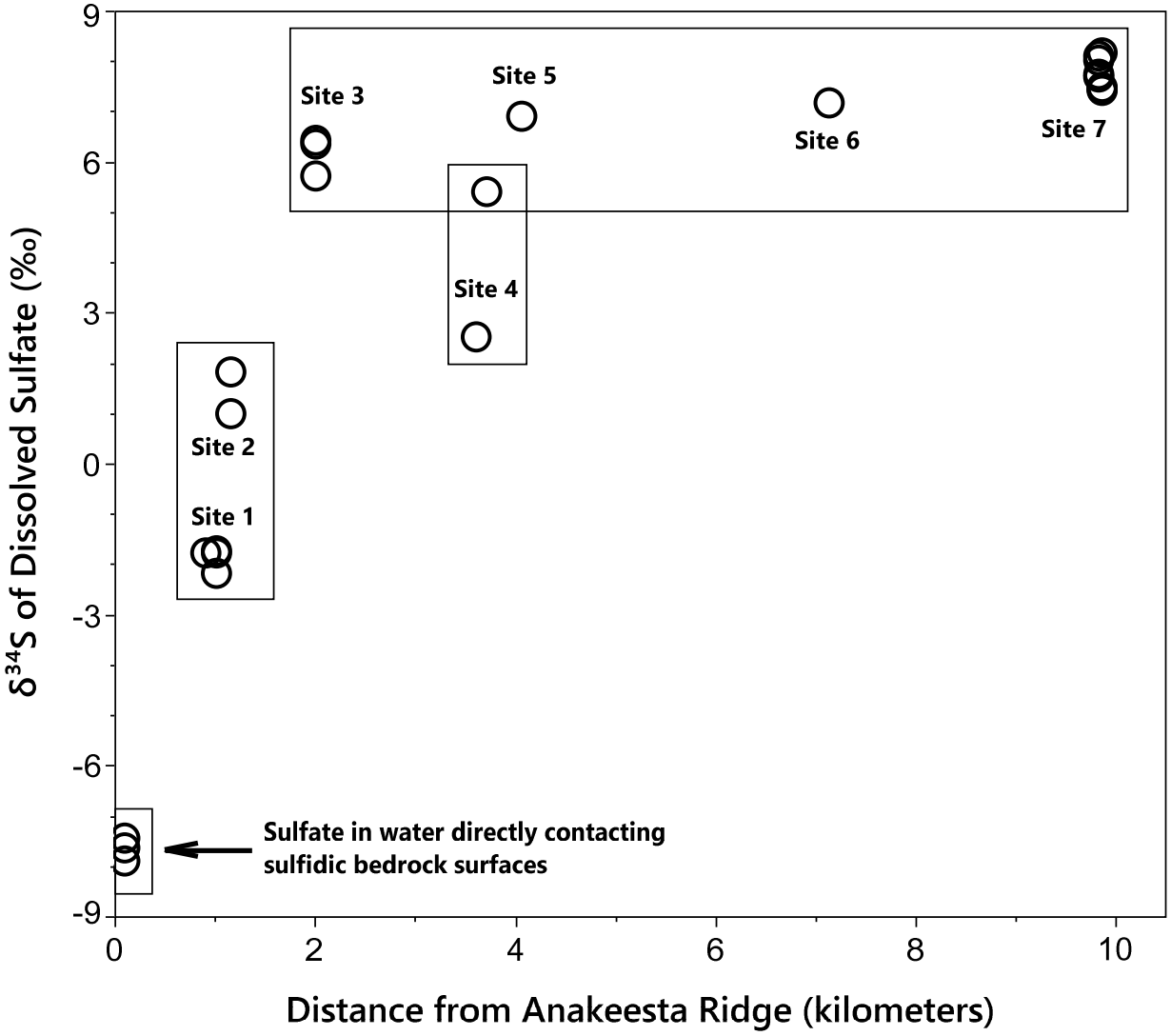

Figure 18. Variation of $\delta^{34}S$ in stream water sulfate relative to the approximate distance from Anakeesta Ridge. Bedrock runoff data were assigned a distance of 0.05 km to reflect direct contact between water and bedrock.

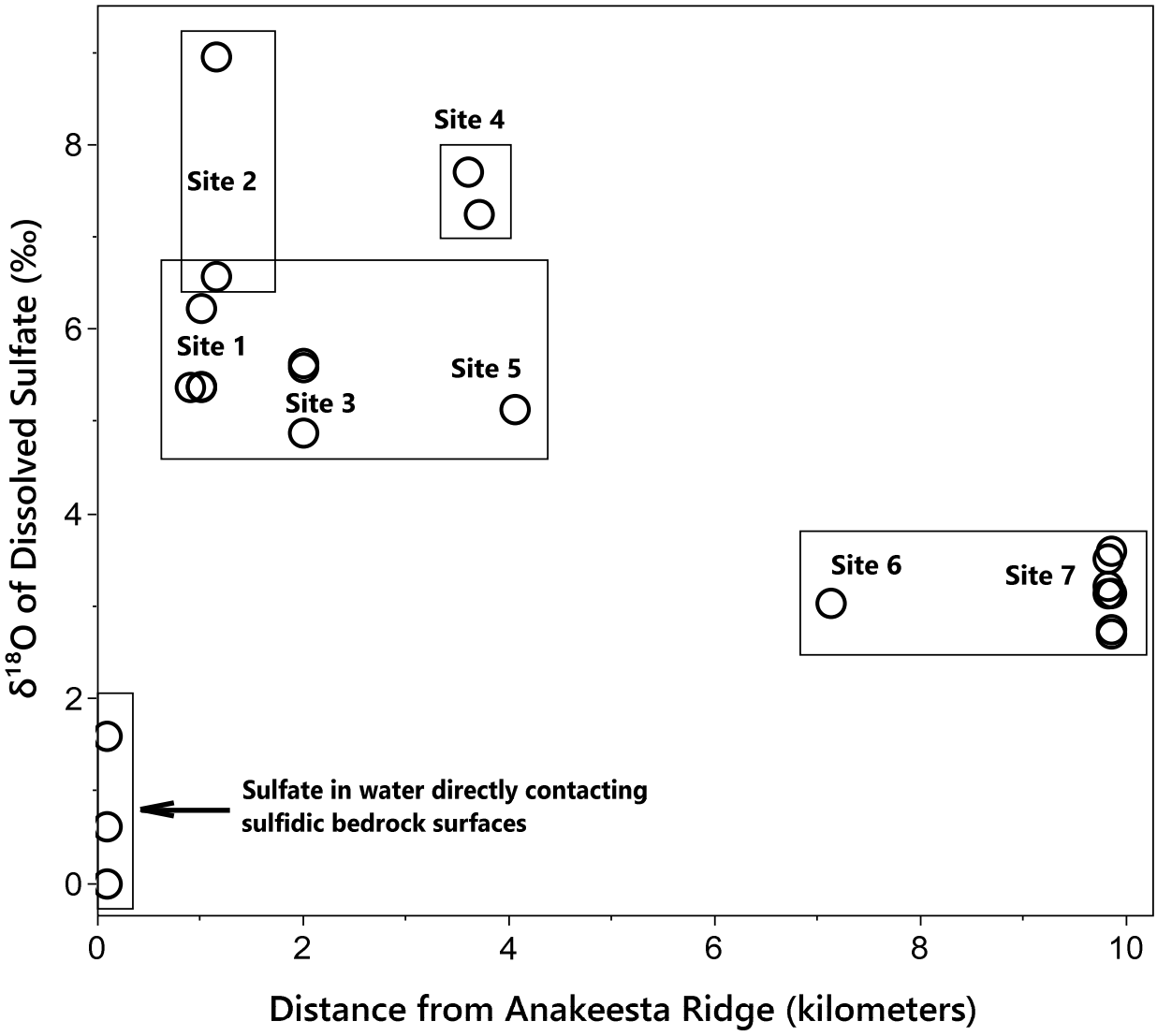

Figure 19. Variation of $\delta^{18}O$ in stream water sulfate relative to the distance from Anakeesta Ridge. Bedrock runoff data were assigned a distance of 0.05 km to reflect direct contact between water and bedrock.

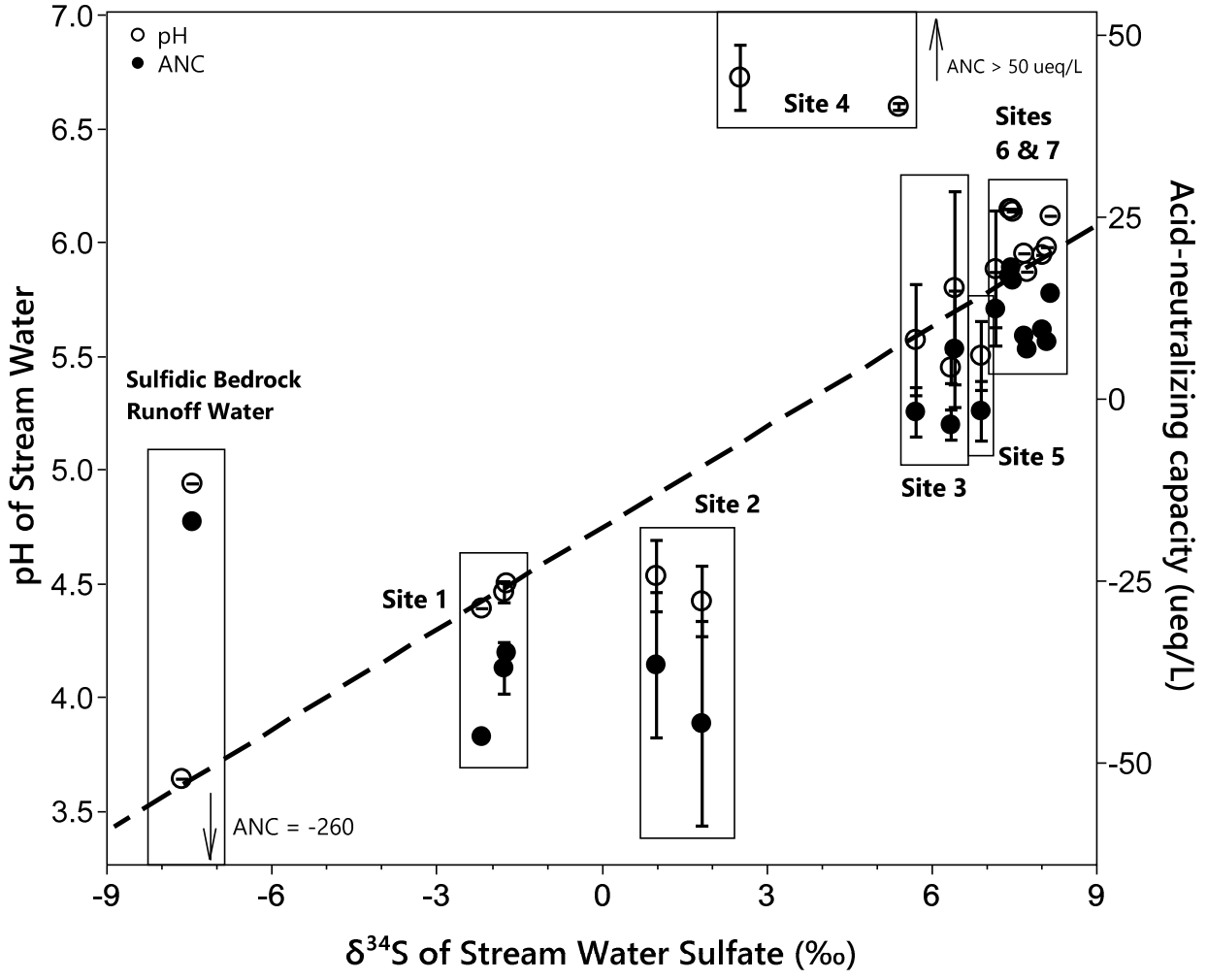

Figure 20. Variations of stream water pH and acid neutralizing capacity (ANC) versus $\delta^{34}S$ of stream water sulfate. For comparison, the data for two sulfidic bedrock runoff samples are included. The error bars represent one standard deviation from the mean value. The dashed trend line was added for visual reference.

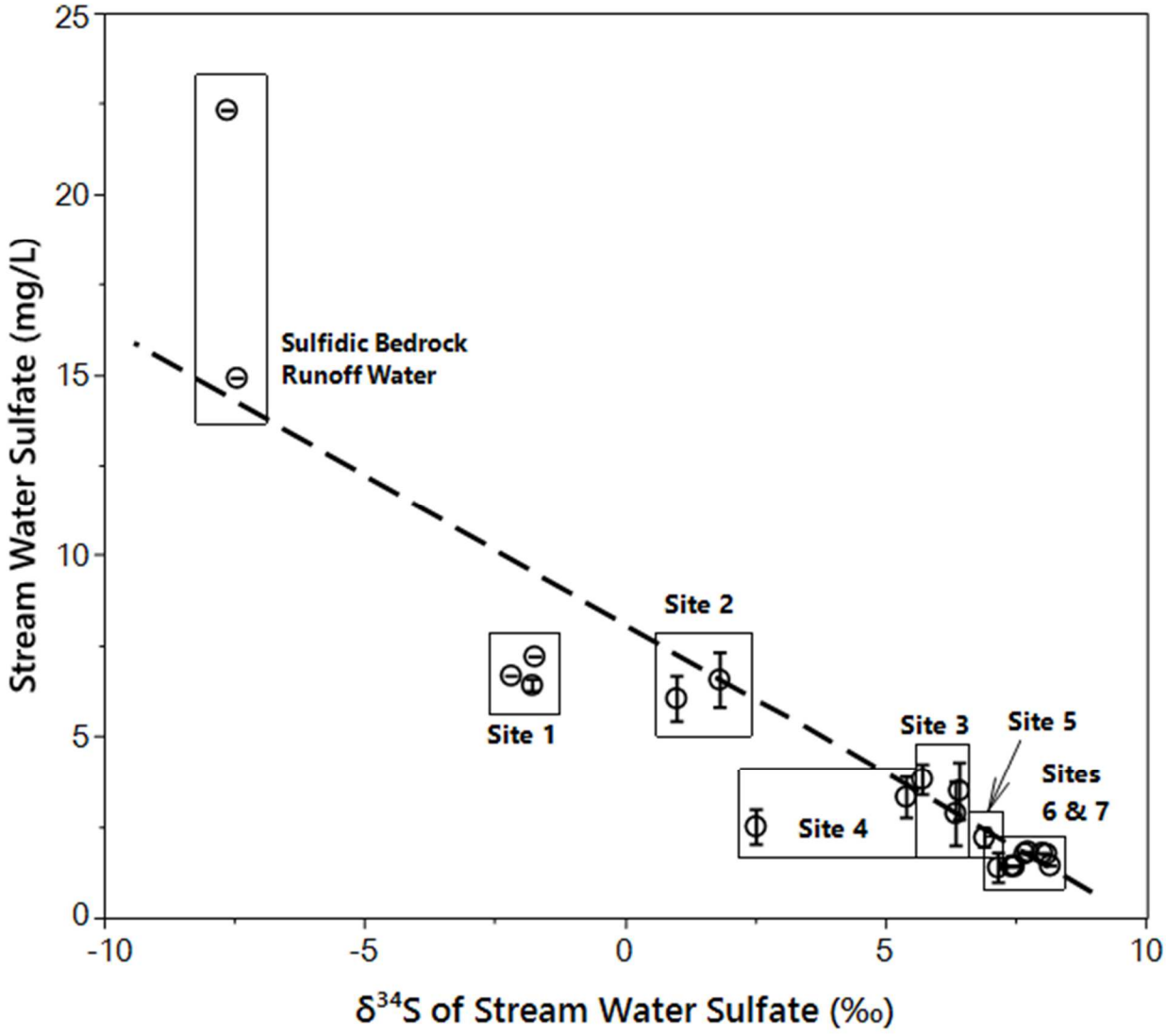

Figure 21. Variations of sulfate concentration versus $\delta^{34}S$ of sulfate in stream water. For comparison, the data for two sulfidic bedrock runoff samples are included. The error bars represent one standard deviation from the mean value. The dashed trend line was added for visual reference.

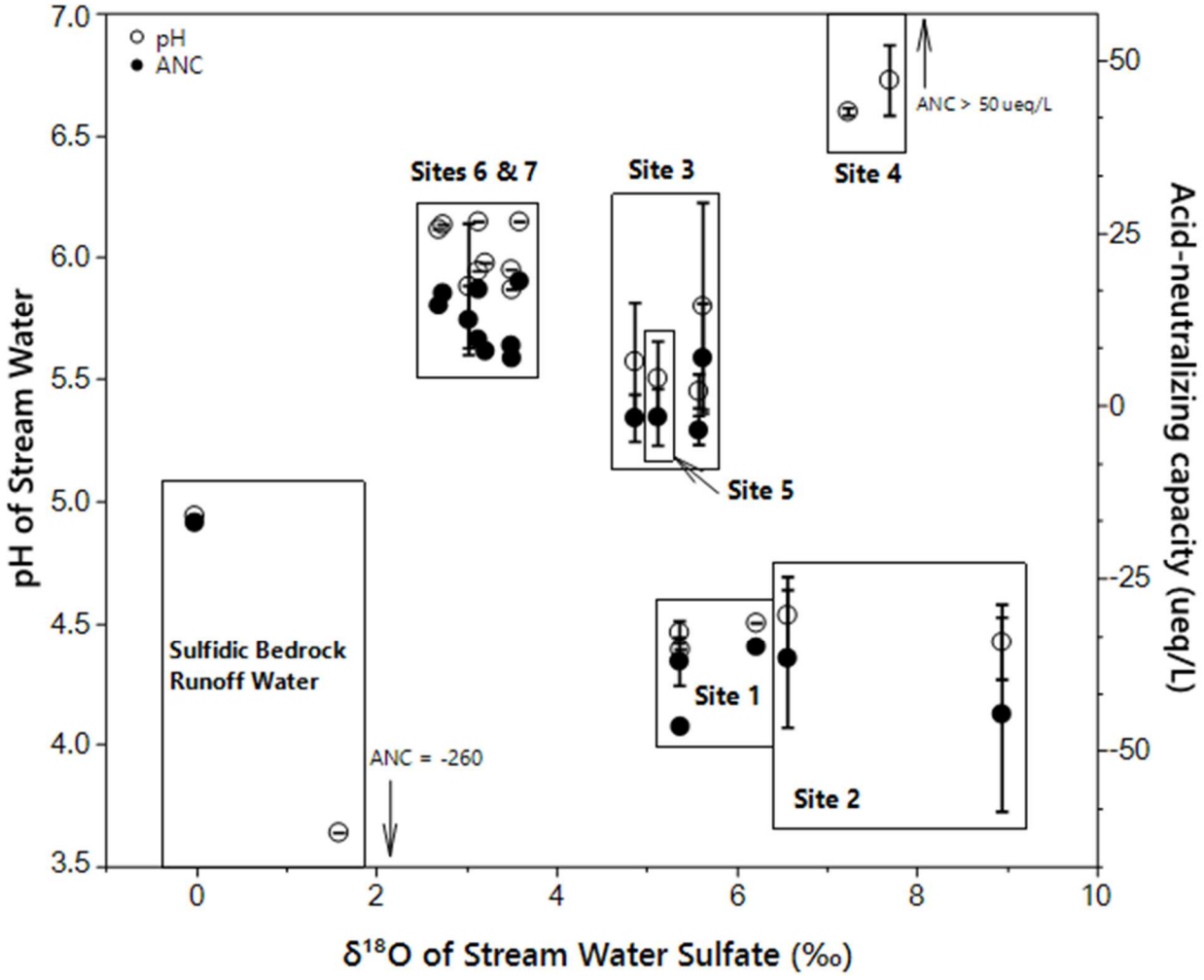

Figure 22. Variations of stream water pH and acid neutralizing capacity (ANC) versus $\delta^{18}O$ of stream water sulfate. For comparison, the data for two sulfidic bedrock runoff samples are included. The error bars represent one standard deviation from the mean value.

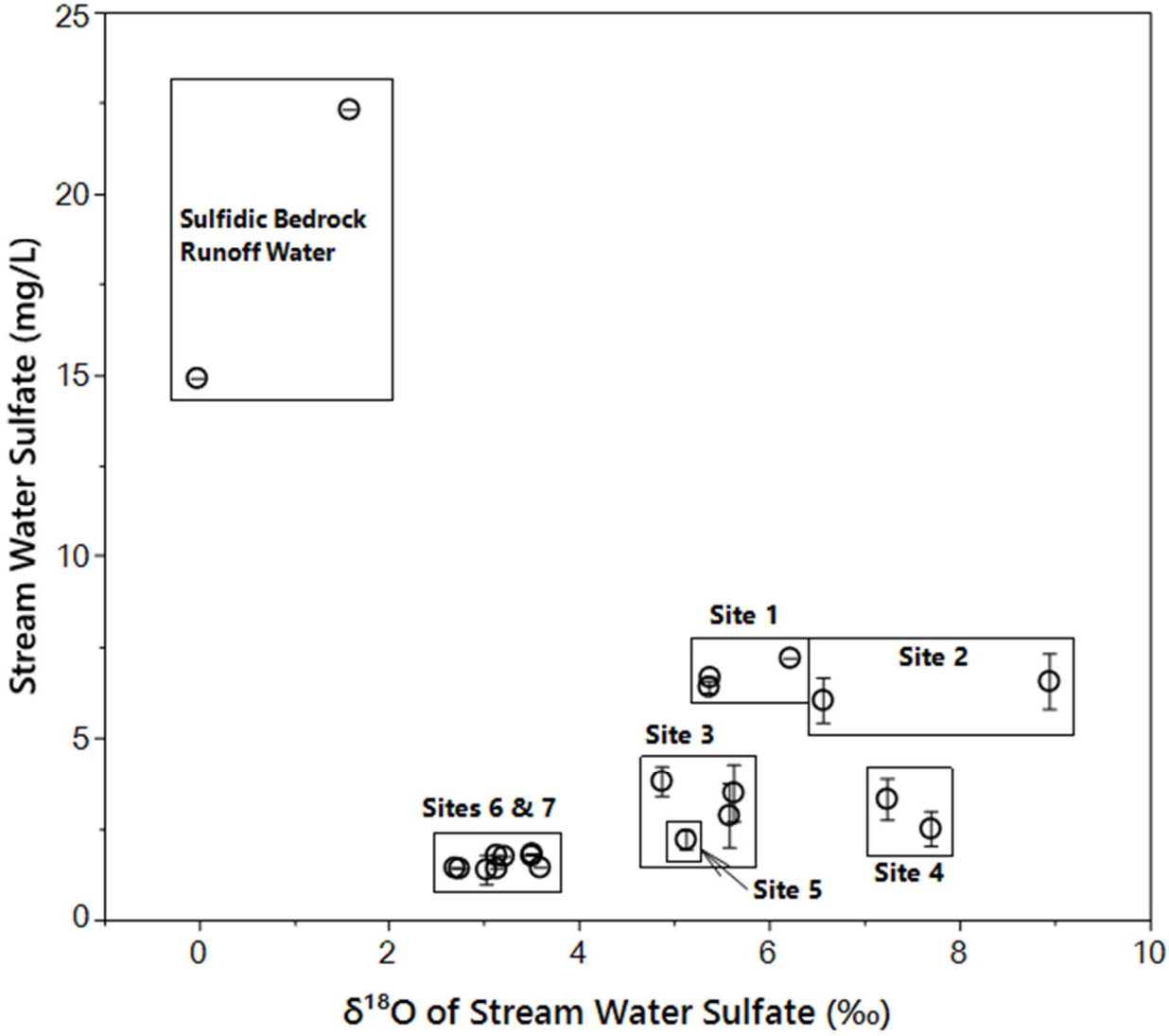

Figure 23. Variations of sulfate concentration versus $\delta^{18}O$ of stream water sulfate. For comparison, the data for two sulfidic bedrock runoff samples are included. The error bars represent one standard deviation from the mean value.

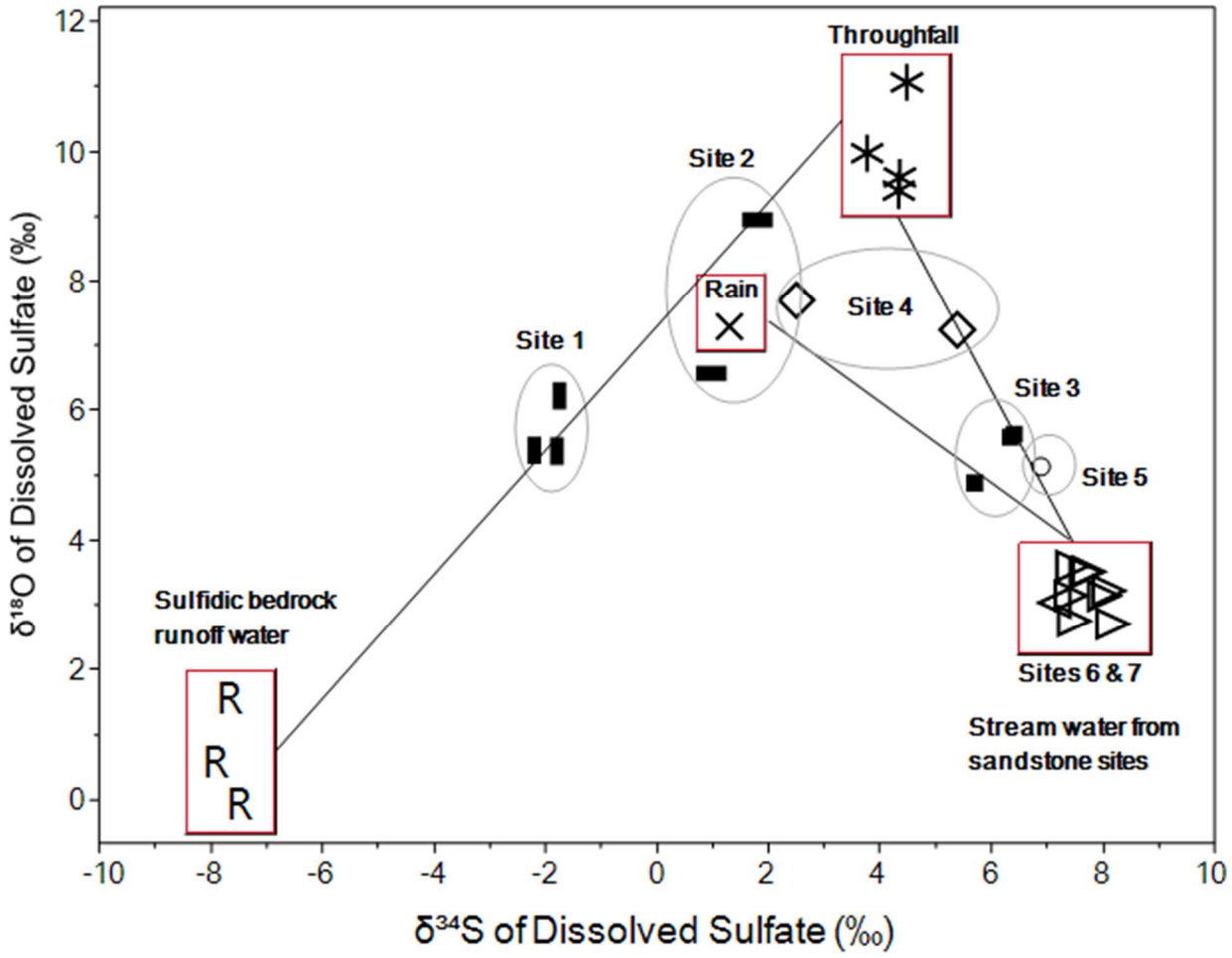

Figure 24. Comparison of $\delta^{34}S$ and $\delta^{18}O$ (‰) of sulfate in precipitation (rain and throughfall) and stream water in the studied sites. Water in direct contact with exposed bedrock (indicated as "R") represents the sulfidic bedrock endmember for stream water.

Table 10. Main characteristics of high-elevation forested catchments used in this study.

Catchment Characteristic	Site Number and Bedrock Type						
	Sulfidic Bedrock			Transition Zone Bedrock		Sandstone Bedrock	
	1	2	3	4	5	6	7
Latitude / Longitude (Decimal Degrees)	35.627 -83.415	35.626 -83.420	35.616 -83.417	35.609 -83.438	35.611 -83.448	35.594 -83.475	35.565 -83.480
Receiving Waterbody at Drainage Outlet	Walker Camp Prong	Walker Camp Prong	Walker Camp Prong	Beach Flats Prong	Road Prong	Moccasin Branch	Noland Creek
Drainage Source	Anakeesta Ridge	Anakeesta Ridge	Morton Mountain	Indian Gap	Mount Mingus	Sugarland Mountain	Mount Love
Drainage Area (hectares)	28.02	14.18	6.96	4.03	2.16	5.02	17.4
Catchment Elevation Span (meters above sea-level)	1410 – 1820	1390 - 1710	1485 - 1670	1545 - 1585	1600 - 1695	1720 -1805	1680 - 1920
Underlying Bedrock Classification* (Southworth et al. 2004; 2005)	(43;Za) with (Qdf) influence	(43;Za) with (Qdf) influence	(43;Za) with minor (45;Zag)	(43;Za) bordering (51;Zch)	(43;Za) bordering (51;Zch)	(51;Zch)	(51;Zch) with minor (52;Zchs)
Soil Classification ** (USDA-NRCS 2009)	HcE and LrF	HcE and LrF	BpF and LrF	LrF	LrF	BpF	SsE and OwF
Soil Taxonomic Class (USDA-NRCS 2009)	Loamy-skeletal, isotic, frigid Humic Dystrudepts	Loamy-skeletal, isotic, frigid Humic Dystrudepts	Fine-loamy, isotic, frigid Humic Dystrudepts	Loamy-skeletal, isotic, frigid Humic Dystrudepts	Loamy-skeletal, isotic, frigid Humic Dystrudepts	Fine-loamy, isotic, frigid Humic Dystrudepts	Fine-loamy, isotic, mesic/frigid Humic Dystrudepts
Soil Thickness (meters) (USDA-NRCS 2009)	0.9 to 1.1	0.9 to 1.1	0.5 to 1.0	0.9 to 1.1	0.9 to 1.1	0.5 to 1.0	> 2.0
Bulk Density (gram cm^{-3}) (USDA-NRCS 2009)	0.29 - 1.68	0.29 - 1.68	0.29 - 1.68	0.37 - 1.68	0.37 - 1.68	0.29 - 1.68	0.54 - 1.55

Table 10 continued

Catchment Characteristic	Site Number and Bedrock Type						
	Sulfidic Bedrock			Transition Zone Bedrock		Sandstone Bedrock	
	1	2	3	4	5	6	7
Surface Soil Organic Carbon (%) (USDA-NRCS 2009)	10 to 15%	10 to 15%	5 to 15%	10 to 15%	10 to 15%	5 to 90%	8 to 31%
Local Slope (degrees from horizonal)	13.5°	18.7°	39.0°	29.6°	25.0°	17.7°	25.5°
Local Aspect (degrees from north)	170°	170°	315°	180°	225°	355°	135°
Dominant Vegetation *** (USDA-NRCS 2009)	Northern hardwood	Northern hardwood	Mixed	Mixed	Mixed	Spruce/fir	Spruce/fir

NOTES:
* Bedrock lithology and deposit map unit codes (text taken from Southworth et al. 2004; 2005):
(1) Code 43 or Za: Anakeesta formation; dark-gray to black slate and phyllite, medium- to coarse-grained feldspathic sandstone, and arkosic conglomerate, thin- to thick-bedded with dolomite beds.
(2) Code Qdf: Debris flows; scars, tracks, and deposits from modern and historic storms with high rainfall (e.g., exposed Anakeesta bedrock "scars").
(3) Code 45 or Zag: Metagraywacke; light-gray, coarse-grained to conglomeratic metagraywacke interbedded with metasiltstone.
(4) Code 51 or Zch: Copperhill formation; Massive to coarse-grained metagraywacke and metaconglomerate interbedded with locally sulfidic quartz-garnet-muscovite phyllite and schist.
(5) Code 52 or Zchs: Quartz-muscovite schist; quartz-muscovite and phyllite interbedded with metagraywacke. Phyllite locally graphitic and sulfidic. Schist contains porphyroblasts of garnet, kyanite, or staurolite, corresponding to metamorphic grade.

** Soil classification codes (descriptions taken from USDA-NRCS 2009):
(1) Code HcE: Heintooga-Chiltoskie complex, 30 to 50 percent slopes, stony
(2) Code LrF: Luftee-Anakeesta complex, 30 to 95% slopes, very rocky (50% Luftee soil; 30% Anakeesta soil; 20% other)
(3) Code BpF: Breakneck-Pullback complex, 30 to 94 percent slopes, very rocky
(4) Code SsE: Spivey-Santeetlah complex, 30 to 50 percent slopes, very stony
(5) Code OwS: Oconoluftee-Guyot-Cataloochie complex, 50 to 95 percent slopes, stony, windswept

*** Vegetation Type: Spruce/fir refers to red spruce and Fraser fir. Northern hardwoods refer to such trees as northern red oak, black cherry, yellow birch, sugar maple, beech, and serviceberry. Mixed refers to both spruce/fir and Northern hardwoods.

Table 11. Bedrock samples collected throughout the study areas.

Sample ID (Date)	Description	Notes	Latitude	Longitude	Elevation (m)
RK-WC4(237) (150912)	Shale/Slate	Loose rock near bedrock	35.62953	-83.40920	1455
RK-WtM6N.3-1 (151023)	Sandstone (brown)	Loose rock near bedrock	35.61501	-83.41575	1645
RK-WtM6N.3-2 (151023)	Shale	Loose rock near bedrock	35.61501	-83.41575	1645
RK-ACtP1-1s (160407)	Shale (dark grey "coal")	Half of unattached specimen	35.63157	-83.44673	1206
RK-ACtP1-1q (160407)	Quartzite (opaque white)	Half of unattached specimen	35.63157	-83.44673	1206
RK-WtA1.2-1 (160414)	Slate (glisten/reflective)	From bedrock outcrop	35.62688	-83.41469	1423
RK-WtA3.2-1 (160604)	Shale	Loose rock near bedrock	35.62002	-83.47074	1247
RK-RtS7.1-1 (160425)	Sandstone (brown-grey)	Loose rock near bedrock	35.62197	-83.47031	1220
RK-RtS6.1-1 (160425)	Shale (granular/platy)	Loose rock near bedrock	35.62583	-83.41968	1390
RK-BFP3-1 (150208)	Shale	Loose rock; base of roadbed	35.60700	-83.43469	1441
RK-BFP3-2 (150208)	Sandstone	Loose rock; base of roadbed	35.60700	-83.43469	1441
RK-BFP3-3 (150208)	Black carbonaceous slate	Loose rock; base of roadbed	35.60700	-83.43469	1441

Table 12. Soil samples collected from the studied catchment sites. Geographic coordinates for each site are the median latitude and longitude of all collected soil cores (World Geodetic System 1984).

Site Number	Sub-Watershed	Bedrock Formation [1]	Soil [2] Class	Sampling Month/Year	No. of Cores	No. of O + A	No. of B soil	No. of C soil	Latitude Longitude	Elevation (meters)	Distance (km) [3]
1	Walker Camp Prong	Anakeesta	L	n/a	n/a	n/a	n/a	n/a	35.62688 -83.41469	1427	1.02
2	Walker Camp Prong	Anakeesta	L	May & Aug 2016 [4]	6	4	6	3	35.62591 -83.41999	1397	1.16
3	Walker Camp Prong	Anakeesta	F	August 2016	3	0	3	3	35.61668 -83.41774	1486	2.07
4	Oconoluftee	Anakeesta	L	August 2016	4	3	5	3	35.60941 -83.43854	1560	3.63
5	Road Prong	Anakeesta	L	August 2016	3	3	1	2	35.61110 -83.44766	1625	4.06
6	Road Prong	Copperhill / Thunderhead	F	August 2016	3	3	3	0	35.59446 -83.47501	1740	7.15
7	Noland Divide	Copperhill / Thunderhead	Fm	July 2016	4	4	4	0	35.56517 -83.48053	1722	9.84

(1) Based on National Park Service bedrock geology GIS layer.

(2) SOURCE: United States Department of Agriculture, Natural Resources Conservation Service (2009). Soil survey of Great Smoky Mountains National Park, TN and NC.
Fm - Fine-loamy, isotic, mesic/frigid Humic Dystrudepts; F - Fine-loamy, isotic, frigid Humic Dystrudepts;
L - Loamy-skeletal, isotic, frigid Humic Dystrudepts

(3) Distance = distance (in kilometers) between catchment soil cores and Anakeesta Ridge at the Boulevard Trail crossing (coordinates: 35.63506°N, -83.41373°E)

(4) Cores 1 - 4 were collected in May; Cores 5 and 6 were collected in August

Table 13. Stream water and bedrock runoff chemistry.

Chemical Parameter	Site Number and Bedrock Type							Sulfidic Bedrock Runoff **
	Sulfidic Bedrock			Transition Zone Bedrock		Sandstone Bedrock		
	1	2	3	4 *	5	6	7	
pH	4.5 ± 0.02	4.5 ± 0.04	5.8 ± 0.10	6.7 ± 0.04	5.6 ± 0.05	6.0 ± 0.07	6.0 ± 0.03	3.6 ± 0.02
Acid-neutralizing capacity (µeq L^{-1})	-36.9 ± 1.8	-36.1 ± 3.5	5.3 ± 2.5	118.1 ± 8.1	1.5 ± 1.7	15.6 ± 1.7	12.5 ± 1.4	-265 ± 7.1
Sulfate (mg L^{-1})	6.94 ± 0.13	6.53 ± 0.19	3.65 ± 0.20	3.15 ± 0.16	2.37 ± 0.09	1.08 ± 0.15	2.30 ± 0.70	35.8 ± 19
Total Aluminum (mg L^{-1})	0.38 ± 0.08	0.40 ± 0.02	0.04 ± 0.01	< 0.02	0.06 ± 0.02	< 0.02	< 0.02	> 0.73
Total Iron (mg L^{-1})	0.05 ± 0.02	0.10 ± 0.02	< 0.02	< 0.02	< 0.02	< 0.02	< 0.02	> 0.72
Total Manganese (mg L^{-1})	0.09 ± 0.02	0.07 ± 0.01	< 0.02	< 0.02	< 0.02	< 0.02	< 0.02	> 0.90

* Site 4 stream water pH and ANC results were distinct from other sites.

** Results from water in direct contact with sulfidic bedrock at Site 2 (N = 2)

µeq L^{-1} = micro-equivalents per liter; mg L^{-1} = milligrams per liter

Table 14. Sulfur and oxygen isotope composition of bedrock samples.

Sample ID	Description	SSE Fraction Isotope Composition (‰ vCDT)				
		Elem. S Step 1	AVS Step 2a	ASS_d^{34}S Step 2b	ASS_d^{18}O Step 2b	CRS Step 3
RK-WC4(237) (150912)	Shale/Slate	n.s.	n.s.	1.69	20.70	0.28
RK-WtM6N.3-1 (151023)	Sandstone (brown)	n.s.	n.s.	2.72	n.s.	n.s.
RK-WtM6N.3-2 (151023)	Shale	n.s.	n.s.	2.02	n.s.	n.s.
RK-ACtP1-1s (160407)	Shale (dark grey "coal")	n.s.	n.s.	1.98	n.s.	n.s.
RK-ACtP1-1q (160407)	Quartzite (opaque white)	n.s.	n.s.	n.s.	n.s.	n.s.
RK-WtA1.2-1 (160414)	Slate (glisten/reflective)	-3.55	n.s.	-2.83	13.80	-3.64
RK-WtA3.2-1 (160604)	Shale	n.s.	n.s.	-3.77	17.60	-6.58
RK-RtS7.1-1 (160425)	Sandstone (brown-grey)	n.s.	n.s.	2.46	n.s.	n.s.
RK-RtS6.1-1 (160425)	Shale (granular/platy)	n.s.	n.s.	2.93	n.s.	n.s.
RK-BFP3-1 (150208)	Shale	-3.58	n.s.	-8.10	n.s.	-7.30
RK-BFP3-2 (150208)	Sandstone	n.s.	n.s.	n.s.	n.s.	n.s.
RK-BFP3-3a (150208)	Black carbonaceous slate	-8.40	-9.15	-9.90	n.s.	-9.24
RK-BFP3-3b (150208)	Black carbonaceous slate	n.m.	n.m.	n.m.	n.m.	-9.09
RK-BFP3-3c (150208)	Black carbonaceous slate	n.m.	n.m.	n.m.	n.m.	-8.78
RK-BFP3-3d (150208)	Black carbonaceous slate	n.m.	n.m.	n.m.	n.m.	-9.03

SSE - Sequential Sulfur Extraction (method); ‰ vCDT - per mil relative to Vienna Cañon Diablo Troilite reference
Elem. S = elemental sulfur; AVS = acid-volatile sulfides; ASS = acid-soluble sulfates; CRS = chromium-reducible disulfides
Steps 1, 2a, 2b and 3 refer to methodological stages in the SSE procedure. Sulfur fraction extracted from each step is indicated.
n.s. = no detectable amount extracted from rock sample; n.m. = SSE step not performed on rock sample

Table 15. Sulfur and oxygen isotope composition of stream water sulfate, soil, rain, throughfall and bedrock runoff.

Sample	Site Number and Bedrock Type						
	Sulfidic Bedrock			Transition Zone Bedrock		Sandstone Bedrock	
	1	2	3	4	5	6	7
Stream Water							
Sulfate $\delta^{34}S$ *	-1.9 ± 0.1 (3)	1.0, 1.8	6.2 ± 0.2 (3)	2.5, 5.4	6.9	7.2	7.8 ± 0.1 (8)
Sulfate $\delta^{18}O$ **	5.6 ± 0.3 (3)	6.6, 8.9	5.4 ± 0.2 (3)	7.2, 7.7	5.1	3.0	3.2 ± 0.1 (8)
Surface Soil							
Total Sulfur $\delta^{34}S$	no data	3.2, 3.4	3.6, 4.0	3.8 ± 0.2 (5)	4.5 ± 0.4 (3)	3.5 ± 0.1 (4)	4.1 ± 0.2 (5)
Organic Sulfur $\delta^{34}S$	no data	no data	no data	no data	4.7	3.5	3.8, 3.8
Subsurface Soil							
Total Sulfur $\delta^{34}S$	no data	1.4 ± 0.2 (17)	5.0, 5.2	6.5 ± 0.2 (7)	6.2	6.1 ± 0.5 (4)	7.9 ± 0.4 (3)
Extractable Sulfate							
Weakly-bound $\delta^{34}S$	no data	2.6 ± 0.4 (7)	5.1	6.3 ± 0.5 (7)	5.3	4.4	5.9 ± 0.3 (3)
Strongly-bound $\delta^{34}S$	no data	2.3 ± 0.4 (9)	4.4, 4.5	5.0 ± 0.5 (3)	4.5 ± 0.1 (3)	no data	4.8, 5.1
Weakly-bound $\delta^{18}O$	no data	5.6	no data	10.5	no data	no data	no data
Strongly-bound $\delta^{18}O$	no data	4.9 ± 0.2 (9)	5.3	4.4 ± 0.2 (3)	5.1 ± 0.6 (3)	no data	4.9

Rain (N=1), Throughfall (N=4), and Bedrock Runoff (N=3): Data are: ($\delta^{34}S$ values) // ($\delta^{18}O$ values)

Rain: (+1.3‰) // (+7.3‰) Throughfall: (4.3 ± 0.2‰) // (10.0 ± 0.4‰) Bedrock Runoff: (–7.7 ± 0.1‰) // (+0.7 ± 0.5‰)

* Sulfur isotope composition (‰) relative to Vienna Cañon Diablo Troilite (vCDT) reference.
** Oxygen isotope composition (‰) relative to Vienna Standard Mean Ocean Water (vSMOW) reference.
Values presented as mean ± standard error of the mean (replicates). Singlet and duplicate data shown where appropriate.

CHAPTER 7: SUMMARY AND CONCLUSIONS

Based on the results of this study, and reviews of other published studies of forested ecosystems, the original conceptual model of sulfur cycling in small-area catchments of the GRSM (see Conceptual Model chapter) was revised to reflect improved understanding of sulfur cycling and biogeochemistry of stream water and soil in high-elevation headwater catchments.

Revised Conceptual Model

Atmospheric sulfur inputs as wet or dry deposition are intercepted by canopy foliage. Chemical transformations and sulfate mass consolidation (combining of wet + dry deposition) generates canopy throughfall sulfate enriched in $\delta^{34}S$ and $\delta^{18}O$, which is one of the major sources of sulfur to forest soil. In catchments with soil profiles comprised of thick O- and A-horizons and high organic matter content, a portion of throughfall sulfate is absorbed by microbial biomass consisting of numerous species of sulfate-transforming micro-organisms. Some microbial species catalyze simple condensation reactions that convert free sulfate (6+ valence state) into sulfate-ester and sulfonate (6+) functional groups attached to soil organic matter. Others reduce sulfate (6+) into stable organo-sulfur compounds (4+ and 2-) such as amino acids (methionine, cysteine, homocysteine and taurine). Simple organo-sulfur compounds may be further transformed chemically into recalcitrant forms of organo-sulfur which stable C-S bonds such as found in humic substances. These immobilization reactions reducing sulfate 6+ to organo-sulfur compounds in lower valence states create an isotope effect by preferential (energetically less costly) absorption of the lighter ^{32}S atom over the heavier ^{34}S atom. This results in organo-sulfur species having smaller $\delta^{34}S$ relative to that of the sulfate source. The balance of throughfall sulfate not absorbed and immobilized has relatively higher proportion of ^{34}S atoms, resulting in sulfate dissolved in the

soil solution phase (and ultimately in the discharged stream water) having larger $\delta^{34}S$ relative to the original throughfall sulfate.

As enriched dissolved sulfate migrates down into the subsurface soil, it is acted upon by additional abiotic mineral adsorption reactions and secondary mineral crystallization. Organic sulfur immobilization is less of a factor in the subsurface given the lower organic matter concentrations and lower microbial activity in the lower soil profile. Abiotic processes involving sulfur in the subsurface are not energetically costly and thus negligible isotope fractionation occurs in the subsurface. Retention/export of sulfur in the subsurface is primarily from dissolution/precipitation of sulfate-containing secondary minerals and surface sorption reactions.

Future Studies

The conclusions supported by these geochemical studies have spawned more research questions regarding various aspects of the GRSM ecosystems.

With respect to the observation that mere presence of underlying sulfidic bedrock is insufficient to induce acidification effects in soil and stream water:

- What is threshold soil profile composition and thickness between no effects and measurable acidification effects from sulfidic bedrock?

With respect to the sensitivity of acidification effects on local bedrock composition:

- How variable is GRSM bedrock mineralogy within a given catchment with respect to total sulfur content, composition (elemental sulfur, acid-volatile sulfides, acid-soluble sulfates, polysulfides, kerogen/organic sulfur), and isotopic composition?

With respect to the unknown variability in isotope composition of precipitation over the GRSM:

- How spatially variable are the sulfur and oxygen isotope compositions of throughfall and rain in the GRSM?
- How temporally variable are the sulfur and oxygen isotope compositions of throughfall and rain in the GRSM?

With respect to details of the biogeochemistry of GRSM soils:

- What is the nature of soil organic sulfur in GRSM catchments with respect to forms of organic sulfur (sulfonate, sulfate-ester, amino acids, carbon-bound sulfur, humic-bound)?
- How easily/quickly is organic sulfur mineralized back to sulfate in GRSM soil?
- How does microbial sulfate transformation vary within GRSM catchments? Across GRSM catchments? With catchment-specific factors such as soil organic matter content?

With respect to details of the export of sulfur from GRSM catchments:

- How does hydrological factors influence the nature of stream water sulfate exported from GRSM catchments? Is through-flow predominantly through subsurface soil? Surface soil? How does this change with moisture profile?
- Are there seasonal/temporal patterns to the sulfur and oxygen isotope composition of surface water draining high-elevation forested catchments in GRSM?

With respect to details of the retention of sulfur in GRSM catchments:

- How variable is the geochemical sulfur composition of soil within a catchment (inorganic/sulfate vs. organic; non-specific adsorbed vs. chemically bound)?

- Is there a systematic spatial pattern to the geochemical sulfur composition of soil within a catchment (e.g., relative to proximity to the drainage channel)?

- How spatially variable is the sulfur isotope composition of soil within a catchment?

- Is there a systematic spatial pattern to the sulfur and oxygen isotope composition of soil within a catchment (e.g., relative to proximity to the drainage channel)?

- How does catchment biomass (vegetation amount, vegetation type, microbial communities) influence the composition of soil sulfur in GRSM catchments?

- What proportion of retained sulfur is tied up in catchment biomass?

- What is the sulfur and oxygen isotope composition of vegetation species in the GRSM (e.g., moss, lichen, shrub, tree)?

- What are the total mass budgets of sulfur in GRSM catchments?

APPENDICES

APPENDIX A

DETAILED PROTOCOLS AND ANALYTICAL METHODS

Field Work Preparations

Permits to sample environmental media in the GRSM were obtained from Paul Super, Science Coordinator at the Appalachian Highlands Science Learning Center. Sampling was done with appropriate weather/safety gear and sampling equipment. Field conditions and GPS coordinates were documented on prepared log sheets; digital photographs were taken, as appropriate.

Sampling Procedures

The following sections detail field documentation and measurements, sample collection, and sample handling and preservation. At each site, ambient water temperature was measured using a digital thermometer with stainless-steel thermistor probe (to ± 0.1 °C). Geographic coordinates of sample locations (waypoints) were recorded using a handheld geographic positioning system (GPS) receiver (based on the World Geodetic System (WGS) 1984 coordinate system). Digital photographs of the sampling sites may be taken.

Soil Samples

Soil sample collection was done with minimal alteration to the natural environment by coring with stainless steel augers and soil scoops (versus pit excavation). Soil was cored at locations well-distant from trails and foot-traffic, and unsampled soil was replaced into the core. Soil from each location was sampled only once during the study. Samples from soil horizons O/A and B/C were collected (in duplicate). Each soil sample (> 1000 grams each) were placed into individual 1-gallon plastic Ziploc baggies (labeled with site ID, soil horizon, replicate A or B, date, time and collector's initials). Bagged soil samples were placed in a cooler, transported back to the laboratory and stored at ~4 to 6 °C until processed.

Soil analysis were done on the size fraction of particles less than 2 millimeters (mm); soil samples were press-sieved (at field moisture) through a 2-mm screen to remove gravel and large organic debris. Portions of each sieved soil sample were taken immediately for soil pH and soil moisture (solids) analysis; the remaining portion of each soil sample were allowed to air-dry for several days in clean plastic bins or trays (protected from cross-contamination). Air-dry soil samples were stored in 1-gallon plastic Ziploc baggies at ~6 °C until analyzed.

Bedrock Samples

Representative, pristine bedrock samples were mechanically removed from accessible outcrops near each soil sampling location. Samples were placed into individual 1-gallon plastic Ziploc baggies (labeled with site ID, geographic coordinates, brief identifying description, date, time and collector's initials). Bagged samples were transported back to the laboratory and stored at ~6 °C until analyzed. Bedrock sulfur composition were determined on internal material from each rock sample, ground to powder by mechanical grinding (manual or electrical). Rock samples were analyzed immediately after grinding to minimize alteration of composition.

Water Samples

Collecting meteoric and surface water samples is not expected to permanently alter the natural environment at the sampling locations; therefore, no special precautions are necessary for water sampling activities. Stream water samples were collected coincident with the soil samples at the headwaters and the outlet of each study catchment.

Stream samples were collected by two methods. Water samples collected in duplicate were collected in pairs of 50-ml conical bottom High-Density Polyethylene (HDPE) tubes (vials) with

threaded screw caps. Water samples collected in singlet were collected in clean, 175-ml HDPE bottles with threaded screw caps. In both cases, they were filled and capped under water surface to prevent trapping air. Stream water samples were transported back to the laboratory in a cooler containing several frozen chill-packs, and stored at ~6 °C until analyzed. Larger volumes (> 10 liters) of stream water were collected using a clean, 0.5-liter stainless-steel scoop and transferred into a distilled water-rinsed, 10- or 20-liter, Low-Density Polyethylene (LDPE) Cubitainer® (Fisher Scientific; Pittsburgh, PA; item no.: 05-721-122) through a clean, plastic funnel fitted with clean 250-micron mesh to strain out larger entrained debris. Filled Cubitainers® were transported back to the laboratory and stored at ~6 °C until analyzed.

Rain water samples were captured during storm events with a distilled water-rinsed, 5-ft by 5-ft (~ 7.25 m2) clear plastic sheet (~ 2 mil thickness) supported by a 1/2-inch PVC-pipe frame. The intercepted rain was diverted into a 20-liter LDPE Cubitainer® through a clean, plastic funnel fitted with clean 250-micron mesh to strain out larger debris. Snow samples were collected using a clean, 0.5-liter stainless-steel scoop and >5-gallon plastic bucket lined with a clean plastic bag. Snow-filled bags were sealed, transported back to the laboratory and stored at ~6 °C until analyzed.

Laboratory Activities

Samples were analyzed and characterized using standard laboratory practices and established methods published in peer-reviewed scientific articles or in government agency standard operating procedure documents. Details of sample analysis and characterization for each category of samples are given in the following sections.

Soil Samples – Analysis and Characterization

Physical and chemical analytical procedures (or calculated parameters) for characterizing soil samples are summarized and referenced in Tables 16 and 17, and are listed below:

- pH (potentiometric) and moisture content
- grain size composition (GSC) and total soil organic matter (TSOM)
- Total and amorphous metal oxides (iron, aluminum, and manganese)
- exchangeable acidity (EA)
- exchangeable base cations (EBC), aluminum, and iron
- cation exchange capacity (CEC) and effective CEC (ECEC; calculated)
- base saturation (BS; calculated) and anion exchange capacity (AEC)
- total-S, inorganic-S, and organic-S content; with extracted sulfur-fractions
- Sulfur isotope composition ($\delta^{34}S$)

A subset of soil samples was analyzed in triplicate to assess variability in soil data.

SOIL SAMPLE ANALYSIS – PHYSICAL AND CHEMICAL PROPERTIES

Soil pH were determined potentiometrically by two methods (Thomas 1996): a 1:2 (weight/volume) mixture of field-moist soil and deionized water (DIWtr), and a 1:2 (wt./vol.) mixture of field-moist soil and a 10 milli-molar (mM) calcium chloride ($CaCl_2$) solution. Soil moisture content were determined gravimetrically by drying 5-gram portions of soil at 105ºC to constant weight (Or and Wraith 2000). Grain size composition (GSC; fractions of sand [2000 µm – 63 µm], silt [63 µm – 2.0 µm] and clay [< 2.0 µm]) were determined gravimetrically (Kettler et al. 2001) by shaking overnight 100-gram portions of air-dried soil with 3% (w/v) sodium hexametaphosphate solution (dispersing agent), pouring the soil slurry (in series) through a 2-mm

sieve to remove gravel and large debris, then through a 63-µm sieve (demarcation of sand/silt). The material on the 2-mm sieve was dried and weighed. This mass was subtracted from the original sample weight to correct for gravel content. The silt/clay slurry was collected into a separate bottle and homogenized. The contents were allowed to settle for six hours at which time the clay suspension was removed. The silt residue remaining on the bottom of the bottle was rinsed and settled repeatedly to remove residual dispersing agent solution, and finally dried at 105 ^{o}C to constant weight.

SOIL SAMPLE ANALYSIS – SOIL BULK COMPOSITION

Total soil volatile matter (surrogate of total soil organic matter; TSOM) were determined gravimetrically by burning 5-gram portions of soil at 430 oC to constant weight (Davies 1974).

Total ferric oxy-hydroxide (TFO) content were determined by treating soil with sodium citrate and sodium dithionite (Holmgren 1967; Claff et al. 2010), followed by iCAP-OES analysis. Amorphous aluminum and ferric oxides (AAFO) content were determined by treating soil with acidic (pH 3) ammonium oxalate (Loeppert and Inskeep 1996), followed by iCAP-OES analysis.

SOIL SAMPLE ANALYSIS – SURFACE EXCHANGE CHEMISTRY

Exchangeable base cations (EBC; sodium (Na), potassium (K), magnesium (Mg), calcium (Ca)) were determined by overnight washing 5-gram portions of air-dry soil with 50 ml of 1 M ammonium chloride (NH_4Cl) (Sumner and Miller 1996), filtering through 0.45 µm membrane filters, and analyzing the filtered leachate for Na, K, Mg and Ca by iCAP-OES. Exchangeable aluminum (Al), manganese (Mn) and iron (Fe) were determined simultaneously on the filtered EBC leachate samples by iCAP-OES analysis (Sims 1996).

Cation exchange capacity (CEC) at field conditions were determined by saturating exchange complex sites with unbuffered 1 M NH_4Cl, rinsing to remove excess indicator ion, then removal of the adsorbed indicator cation by treatment with 1 M KCl. The extract solution is analyzed for NH_4^+ by IC (Sumner and Miller 1996). Base saturation (BS) is calculated parameter: the ratio of EBC to ECEC, respectively (Coleman et al. 1959). Soil anion exchange capacity (AEC) were determined by overnight washing 5-gram portions of air-dry soil with 50 ml of 1 M KCl, rinsing to remove excess indicator ion solution, and overnight washing the same soil sample with 1 M sodium nitrate ($NaNO_3$) (Zelanzny et al. 1996). The leachate from the second overnight washing were analyzed for potassium and chloride by IC. Exchangeable acidity (EA) is defined as sum of exchangeable proton concentration and any other acid-reacting species with a pKa less than the titration endpoint (Essington 2015). EA was computed by difference: CEC – EBC.

SOIL SAMPLE ANALYSIS – SOIL SULFUR FRACTIONS

Total soil sulfur (TS) was determined by dry thermal oxidation of soil samples (< 1 gram dry) with a 25:1 sodium bicarbonate and silver oxide (Ag_2O) mixture at 550 °C (Tabatabai et al. 1988; Rossete et al. 2008). Cooled residues were transferred with minimum deionized water into a flask, followed by neutralization of the carbonate content with minimum volume of ultrapure HCl. A stream of pure nitrogen gas was passed through the resulting extract solution (pH < 3) to remove all traces of carbon dioxide. Dissolved sulfate in the leachate was analyzed by IC, and the remaining sulfate content was transformed to $BaSO_4$ for sulfur isotope composition analysis.

The identity and distribution of inorganic sulfur (primarily sulfate) species were determined by a three-step sequential extraction procedure. Unbound (soil solution) and weakly associated (electrostatically adsorbed) soil sulfate was extracted by three consecutive washings of 5-gram portions of air-dry soil with 1M NH_4Cl solution (Bloem et al. 2002; Maynard et al. 1987).

Specifically-adsorbed (inner-sphere) sulfate (ISI) were extracted by overnight washing with 500 mg L^{-1} (as P) KH_2PO_4 solution (Ensminger 1954; Sahrawat et al. 2009). Leachate samples from all extraction steps were filtered through 0.45 µm membrane filters, and analyzed for sulfate by IC and total extractable sulfur by ICP-OES. Total inorganic sulfur (TIS) was calculated as the sum of the inorganic-S fractions (Tabatabai 1996).

Characterizing soil organic-S is much more difficult than characterizing soil inorganic-S, in part because of the plethora of possible organic compounds and isomers that can contain at least one sulfur atom (Tabatabai 1996). Methods currently do not exist for chemically extracting or directly analyzing soil organic-S. For this study, soil organic-S content was estimated in two ways. One estimate was calculated as difference between total sulfur (TS) and total inorganic sulfur (TIS). The major source of error in calculating soil organic S this way is the possible presence of mineral sulfur forms in the soil matrix (e.g., pyrite, pyrrhotite, gypsum, secondary aluminum-sulfate or iron-sulfate minerals, etc.).

SOIL SAMPLE ANALYSIS – SULFUR ISOTOPE COMPOSITION

Soil inorganic-S fractions (weakly associated and strongly bound sulfate) were treated to recover extracted sulfate for sulfur and oxygen isotope composition. Extract liquids with dissolved sulfate were acidified to pH < 3 with ultrapure hydrochloric acid (HCl) followed by addition of 10% (w/v) aqueous barium chloride solution (1 mL $BaCl_2$ per 100 mL sample) to precipitate the sulfate as $BaSO_4$ (Mayer and Krouse 2004; Kendall and Caldwell 1998). The $BaSO_4$ solids were rinsed and dried for isotopic composition analysis.

It was observed that recovery of sulfate as $BaSO_4$ was affected by dissolved organic sulfur (DOS) in stream water samples or soil-sulfate extractions (Alewell 1993), by dissolved phosphate

introduced during extraction of strongly bound soil sulfate with hydrogen phosphate, and by suppression of sulfate ion activity by high ionic strength generated by the cumulative additions of hydrogen phosphate (for sulfate anion-exchange), potassium hydroxide (for increasing pH > 12), magnesium and ammonium chlorides (for struvite precipitation), and hydrochloric acid (for decreasing pH < 3). In the first two cases, barium forms insoluble compounds which interfere with IRMS analysis. Concentrations of DOS typically were low in surface water samples and moderate in soil extracts; interference was compensated with additional $BaCl_2$. Phosphate concentrations in soil extracts were too large to be compensated; interference was eliminated by precipitating the phosphate as insoluble struvite (magnesium ammonium phosphate) at pH > 11 and filtration (Bouropoulos and Koutsoukos 2000; Stratful et al. 2001; Foletto et al. 2013). Filtrate pH was reduced to below 3 with ultrapure HCl before proceeding with $BaCl_2$ addition. Interference due to high ionic strength was unable to be counteracted successfully.

Bedrock Samples – Analysis and Characterization

Bedrock samples collected from the field were fractured to expose the core. Any weathered "outer rind" were removed, and unweathered portions were ground to fine powder in a ceramic ball-mill. Portions of the prepared rock-core subsamples were processed through a series of treatments designed to sequentially extract specific chemical fractions of sulfur based on oxidation-reduction state (Tuttle et al. 2003; Fauville et al. 2004) (Table 18). Reduced sulfur fractions in bedrock (elemental sulfur, acid-volatile monosulfides [S(-II)], acid-soluble sulfates [S(6+)], and polysulfides [S(-I)]) were reduced to hydrogen sulfide (H_2S) and captured as silver sulfide (Ag_2S) precipitate. The precipitates were rinsed and dried for isotopic composition analysis.

Water Samples – Analysis and Characterization

Physical and chemical analytical procedures for characterizing water samples are summarized and referenced in Table 19, and are listed below:

- pH and specific conductance (unfiltered)
- ANC (unfiltered; acid neutralizing capacity)
- Dissolved anions (filtered; chloride [Cl^-], nitrate [NO_3^-], sulfate [SO_4^{2-}], nitrite [NO_2^-], and phosphate [$H_2PO_4^-$])
- Dissolved cations (filtered; ammonium [NH_4^+], sodium [Na^+], potassium [K^+], magnesium [Mg^{2+}] and calcium [Ca^{2+}])
- Dissolved trace metals (filtered; aluminum [Al_{total}], copper [Cu_{total}], iron [Fe_{total}], manganese [Mn_{total}], silica [SiO_2] and zinc [Zn_{total}])
- Sulfate-sulfur isotope composition ($\delta^{34}S_{SO4}$)
- Sulfate-oxygen isotope composition ($\delta^{18}O_{SO4}$)

These procedures will apply to stream water, meteoric water and soil/interflow water samples. Portions of unfiltered water samples were analyzed for general water quality parameters (pH, specific conductance and ANC) using an automated titration system (Mantech PC-Titrate® system). Sample portions were filtered through 0.45 micrometer (µm) membrane filters and analyzed for dissolved anions and cations by ion chromatography (IC) using a Dionex 2100/1100 dual column system with background suppression. Sample portions were filtered through 0.45 µm membrane filters and preserved with ultra-pure (trace metals grade) nitric acid to a final concentration of 1% by volume (pH < 2) and analyzed for dissolved trace metals by inductively

coupled argon plasma (iCAP) optical emission spectrometry (OES) using a Thermo-Elemental iCAP DUO 7400.

Large volumes of water samples were filtered through 0.45 µm membrane filters, acidified to pH < 3 with concentrated hydrochloric acid (HCl), and treated with 10% (w/v) barium chloride to extract the sulfate content as $BaSO_4$ (Mayer and Krouse 2004; Kendall and Caldwell 1998). The $BaSO_4$ solids were rinsed and dried for isotopic composition analysis.

Stable Isotope Composition Analysis

Samples of stream water, rain/ice/snow, bedrock, soil horizons and representative vegetation were characterized for sulfur and oxygen isotopic composition. The sulfur content was extracted and converted into a form amenable to analysis by isotope ratio mass spectrometry (IRMS). The extraction procedures have been described previously, in respective sections. The BaSO4 and Ag2S samples generated by these extraction procedures were prepared for IRMS analysis by combining < 1 mg of sample with co-reagent in corresponding crucible cups. Table 20 shows masses, co-reagent, type of crucible and corresponding laboratory standards used to determine sulfur and oxygen isotopic composition.

Oxygen in the BaSO4 samples for oxygen isotope composition analysis were converted to carbon monoxide in a Thermo Scientific TC/EA High Temperature Conversion Elemental Analyzer. The CO were analyzed in a Delta Plus XL mass spectrometer. Sulfur in the $BaSO_4$ and Ag_2S samples for sulfur isotope composition analysis were converted into sulfur dioxide (SO_2) by combustion with vanadium pentoxide (V_2O_5) at 1150°C in a Costech Elemental Analyzer. The sulfur dioxide was analyzed in a Delta Plus XL mass spectrometer. The same analysis was done on laboratory standards for $\delta^{18}O$ (UTK-Gyp1 [+16.83 ‰], SC-1std [-2.52 ‰], IAEA-SO-5 [+12.13 ‰] and

IAEA-SO-6 [-11.35 ‰]) or $\delta^{34}S$ (NBS 127 [+21.12 ‰] and IAEA-SO-6 [-34.05 ‰]). These laboratory standards were calibrated to international standards SMOW (for $\delta^{18}O$) and CDT (for $\delta^{34}S$). Raw $\delta^{18}O$ and $\delta^{34}S$ data measured in samples were recalibrated to international standards through the laboratory standards calibration.

References

Alewell, Christine (1993). Effects of organic sulfur compounds on extraction and determination of inorganic sulfate. Plant and Soil, 149(1):141-144. GRef951

Autry, Andrew R., John W. Fitzgerald, and Penny R. Caldwell (1990). Sulfur fractions and retention mechanisms in forest soils. Canadian Journal of Forest Research, 20(3), 337-342. GRef120

Autry, Andrew R. and John W. Fitzgerald (1990). Sulfonate S: A major form of forest soil organic sulfur. Biology and Fertility of Soils, 10(1), 50-56. GRef657

Canfield, Donald E., Robert Raiswell, Joseph T. Westrich, Christopher M. Reaves and Robert A. Berner (1986). The use of chromium reduction in the analysis of reduced inorganic sulfur in sediments and shales. Chemical Geology, 54(1-2), 149-155. GRef795

Claff, S.R., L.A. Sullivan, E.D. Burton, and R.T. Bush (2010). A sequential extraction procedure for acid sulfate soils: Partitioning of iron. Geoderma, 155, 224-230. GRef838

Coleman, N.T., S.B. Weed and R.J. McCracken (1959). Cation-exchange capacity and exchangeable cations in Piedmont soils in North Carolina. Soil Science Society of America Journal, 23(2), 146-149. GRef841

Davies, Brian E. (1974). Loss-on-ignition as an estimate of soil organic matter. Soil Science Society of America Journal, 38(1), 150-151. GRef840.

Ensminger, L.E. (1954). Some factors affecting the adsorption of sulfate by Alabama soils. Soil Science Society of America Journal, 18(3), 259-264. GRef844

Essington, Michael E. (2015). Soil and Water Chemistry: An Integrative Approach (2nd Edition). CRC Press, Boca Raton, Florida.

Fauville, Andrea, Bernhard Mayer, Rene Frommichen, Kurt Friese and Jan Veizer (2004). Chemical and isotopic evidence for accelerated bacterial sulphate reduction in acid mining lakes after addition of organic carbon: laboratory batch experiments. Chemical Geology, 204, 325-344. GRef285

Freney, J.R. (1958). Determination of water-soluble sulfate in soils. Soil Science, 86(5):241-244. GRef1081

Ghabbour, Elham A. and Geoffrey Davies (2009). Spectrophotometric Analysis of Fulvic Acid Solutions – A Second Look. Annals of Environmental Science, 3(1), 131-138. GRef837

Hayes, T.M., Michael H.B. Hayes, Jan O. Skjemstad, R.S. Swift, and Ronald L. Malcolm (1996). Isolation of humic substances from soil using aqueous extractants of different pH and XAD resins, and their characterization by 13C-NMR. Chapter 2, 13-24. In: Clapp, C. Edward, Michael H.B. Hayes, Nicola Senesi and S.M. Griffith (editors). 1996. Humic Substances and Organic Matter in Soil and Water Environments: Characterization, Transformations, and Interactions. International Humic Substances Society; St. Paul, Minnesota.

Hillman, D.C., J.F. Potter, and S.J. Simon (1986). National Surface Water Survey, Eastern Lake Survey (Phase I: Synoptic Chemistry). Analytical Methods Manuel. EPA-600/4-86/009. U.S. Environmental Protection Agency; Las Veges, Nevada.

Holmgren, George G.S. (1967). A rapid citrate-dithionite extractable iron procedure. Soil Science Society of America Proceedings, 31(2), 210-211. GRef839

Holmgren, George G.S. and J.M. Kimble (1984). Field estimation of amorphous aluminum with 4M potassium hydroxide. Soil Science Society of America Journal, 48(6), 1378-1382. GRef831

Johnson, C.M. and Hideo Nishita (1952). Microestimation of Sulfur in Plant Materials, Soils, and Irrigation Waters. Analytical Chemistry, 24(4):736-742. GRef799

Kang, Phil-Goo, Bernhard Mayer and Myron J. Mitchell (2012). Comparison of sample preparation methods for stable isotope analysis of dissolved sulphate in forested watersheds. Isotopes in Environmental and Health Studies, iFirst, 1-11. GRef187

Kendall, C. and E.A. Caldwell (1998). Fundamentals of isotope geochemistry (Chapter 2). In: C. Kendall and J.J. McDonnell (Eds.), Isotope Tracers in Catchment Hydrology, Elsevier Science B.V., Amsterdam. Found online at: http://wwwrcamnl.wr.usgs.gov/isoig/isopubs/itchch2.html

Ketterings Q, Miyamoto C, Mathur RR, Dietzel K, and Gami S. (2011). A Comparison of Soil Sulfur Extraction Methods. Soil Science Society of America Journal, 75(4), 1578-1583.GRef731

Kettler, T.A., J.W. Doran and T.L. Gilbert (2001). Simplified Method for Soil Particle-Size Determination to Accompany Soil-Quality Analyses. Soil Science Society of America Journal, 65(3), 849-852. GRef836

Loeppert, Richard H. and William P. Inskeep (1996). Iron. Chapter 23, 639-664. In: D.L. Sparks (ed.), Methods of Soil Analysis, Part 3, Chemical Methods. Soil Science Society of America. Book Series 5. ASA and SSSA, Madison, WI.

Mayer, Bernhard and H. Roy Krouse (2004). Procedures for Sulfur Isotope Abundance Studies (Chapter 26; p.538-596). In: Pier A. Groot, Handbook of Stable Isotope Analytical Techniques. Elsevier, Amsterdam.

Maynard D.G., Y.P. Kalra and F.G. Radford (1987). Extraction and Determination of Sulfur in Organic Horizons of Forest Soils. Soil Science Society of America Journal, 51(3), 801-806. GRef730

Metson, A.J. (1979). Sulfur in New Zealand soils: I. A review of Sulphur in soils with particular reference to adsorbed sulphate-sulphur. New Zealand Journal of Agricultural Research, 22, 95-114. GRef846

Mizutani, Y. and T.A. Rafter (1969). Isotopic composition of sulphate in rainwater, Gracefield, New Zealand. New Zealand Journal of Science, 12, 69-80. GRef1098

Or, Dani and Jon M. Wraith (2000). Soil Water Content and Water Potential Relationships. Chapter 3, pp. A53-A63. In: Handbook of Soil Science. Malcolm E. Sumner (Editor-in-Chief), CRC Press, New York, N.Y.

Rossete, Alexssandra Luiza Rodrigues Molina, José Albertino Bendassolli, and Paulo Cesar Ocheuze Trivelin 2008. Organic sulfur oxidation to sulfate in soil samples for total sulfur determination by turbidimetry. Revista Brasileira de Ciência do Solo, 32(6), 2547-2553.GRef662

Sahrawat, Kanwar L., K.V.S. Murthy, and S.P. Wani. 2009. Comparative evaluation of Ca chloride and Ca phosphate for extractable sulfur in soils with a wide range in pH. Journal of Plant Nutrition and Soil Science, 172(3), 404-407. GRef729

Sims, J. Thomas. 1996. Lime Requirement. Chapter 17, p.491-515. In: D.L. Sparks (ed.), Methods of Soil Analysis, Part 3, Chemical Methods. Soil Science Society of America. Book Series 5. ASA and SSSA, Madison, WI.

Sumner, M.E. and W.P. Miller. 1996. Cation Exchange Capacity and Exchange Coefficients. Chapter 40, p.1201-1229. In: In: D.L. Sparks (ed.), Methods of Soil Analysis, Part 3, Chemical Methods. Soil Science Society of America. Book Series 5. ASA and SSSA, Madison, WI.

Swift, Roger S. 1985. Fractionation of soil humic substances. P. 387-408. In: G.R. Aiken et al. (editors). Humic Substances in Soils, Sediment, and Water. Wiley-Interscience, New York, N.Y.

Tabatabai, M. Ali and J.M. Bremner (1972). Forms of sulfur, and carbon, nitrogen and sulfur relationships in Iowa soils. Soil Science, 114(5), 39-44. GRef660

Tabatabai, M. Ali, N.T. Basta and H.J. Pirela (1988). Determination of total sulfur in soils and plant materials by ion chromatography. Communications in Soil Science and Plant Analysis, 19(15), 1701-1714. GRef845

Tabatabai, M. Ali (1996). Sulfur. Chapter 33, p.921-960. In: In: D.L. Sparks (ed.), Methods of Soil Analysis, Part 3, Chemical Methods. Soil Science Society of America. Book Series 5. ASA and SSSA, Madison, WI.

Tanikawa, Toko, Masamichi Takahashi, Akihiro Imaya, and Kazuhiro Ishizuka (2009). Highly accumulated sulfur constituents and their mineralogical relationships in Andisols from central Japan. Geoderma, 151(1-2), 42-49. GRef722

Thomas, G.W. 1996. Soil pH and soil acidity. Chapter 16, p.475-490. In: In: D.L. Sparks (ed.), Methods of Soil Analysis, Part 3, Chemical Methods. Soil Science Society of America. Book Series 5. ASA and SSSA, Madison, WI.

Tuttle, M.L., M.B. Goldhaber, and D.L. Williamson (1986). An analytical scheme for determining forms of sulfur in oil shales and associated rocks. Talanta, 33(12), 953-961. GRef853

Zelazny, Lucian W., Liming He, and An Vanwormhoudt. 1996. Charge Analysis of Soils and Anion Exchange. Chapter 41, p.1231-1253. In: D.L. Sparks (ed.), Methods of Soil Analysis, Part 3, Chemical Methods. Soil Science Society of America. Book Series 5. ASA and SSSA, Madison, WI.

Table 16. Procedures for soil analysis

Analytical Parameter	Symbol	Summary of Method or Calculation	Reference
pH (potentiometric)	pH_{H2O} pH_{CaCl2}	Slurry: 5g soil + 10 ml of Milli-Q Type-1 deionized water Slurry: 5g soil + 10 ml of 10 mM $CaCl_2$	Thomas 1996 in MofSA [1]
Moisture content	%water	Dry at 105°C to constant mass	Or and Wraith 2000
Particle size analysis	PSA	Bulk fractions: sand/silt/clay; report as % of total mass	Kettler et al. 2001
Total soil organic matter	TSOM	Loss-on-ignition (LOI) at 550° C to constant mass	Davies 1974
Total ferric oxides	TFOs	Treat[2] with citrate-dithionate reagent; analyze for Fe, Al, Mn by iCAP-OES[3]	Holmgren 1967; Claff et al. 2010
Amorphous aluminum and ferric oxides	AAFOs	Treat[2] with ammonium oxalate acidified to pH 3.0; analyze for Fe, Al, Mn by iCAP-OES[3]	Loeppert and Inskeep 1996 in MofSA [1]
Exchangeable acidity	EA	Calculated: EA = CEC – EBC	Sims 1996 in MofSA [1]
Exchangeable base cations, aluminum, iron	EBC, Al/Fe	Treat[2] with 1 M NH_4Cl; adjust filtered extract to 1% HNO_3; analyze for Na, K, Mg, Ca, Al, Fe, Mn by iCAP-OES[3]	Sumner and Miller 1996 in MofSA [1]
Cation exchange capacity (field value)	CEC	Treat[2] with unbuffered 1 M $NH_4CH3COOH$, followed by 1 M KCl; analyze for NH_4^+ by IC	Sumner and Miller 1996 in MofSA [1]
Base saturation	BS	Calculated: BS = EBC/CEC (%)	Coleman et al. 1959
Anion exchange capacity	AEC	Treat[2] with 1 M NH_4Cl; rinse soil sample of excess and treat[2] with 1 M $NaNO_3$; analyze for chloride by IC	Zelanzny et al. 1996 in MofSA [1]
Total Sulfur and Total Organic Sulfur	TS TOS	Oxidize with sodium bicarbonate ($NaHCO_3$) and silver oxide (Ag_2O) at 550 °C; extract sulfate from ash with hot water and analyze by IC	Tabatabai et al. 1988; Rossete et al. 2008
Sulfate (weakly associated)	SO_4-out	Treat[2] with 1 M NH_4Cl; analyze leachate by IC (SO_4^{2-})	Bloem et al. 2002; Maynard et al. 1987
Sulfate (strongly bound)	SO_4-inn	Treat[2] with 500 mg-P L^{-1} KH_2PO_4; analyze leachate by IC (SO_4^{2-})	Ensminger 1954; Sahrawat et al. 2009
Total Inorganic Sulfur	TIS	Calculated: Sum {UIS + OSIS + ISIS}	Tabatabai 1996 in MofSA [1]

NOTES:

[1] MofSA - D.L. Sparks (ed.), Methods of Soil Analysis, Part 3, Chemical Methods. Book Series 5. ASA and SSSA, Madison, WI; 1996.

[2] Generic soil leaching procedure: 5.0 grams air-dry soil + 50 ml of extractant; shake overnight; decant leachate and filter through 0.4 µm membrane filter; store in clean plastic (preferably low-density polyethylene [LDPE]) bottle until processed.

[3] iCAP-OES – inductively-coupled argon plasma optical emission spectrometry

Table 17. Procedures for characterizing the sulfur composition (total, inorganic, and organic) in soil samples

Analytical Parameter	Symbol	Summary of Method or Calculation	Reference
Total Sulfur	TS	Oxidize with sodium bicarbonate ($NaHCO_3$) and silver oxide (Ag_2O) at 550 °C; dissolve sulfate in ash with water and analyze by IC	Tabatabai et al. 1988; Rossete et al. 2008
Total Inorganic Sulfur	TIS	Calculated: Sum {UIS + OSIS + ISIS}	Tabatabai 1996 in MofSA [1]
Total Organic Sulfur (can miss some *soluble polar org-S species*)	TOS	Calculated: {TS} - {TIS}	Tabatabai 1996 in MofSA [1]
Unbound Inorganic Sulfur (can include some *soluble polar org-S species*)	U-IS	Treat[2] with water; analyze same leachate by IC (SO_4^{2-}) and iCAP-OES [3] (total soluble-S)	Freney 1958
Outer-Sphere Inorganic Sulfur; exchangeable, electrostatic (correct for FIS and *soluble org-S*)	OS-IS	Treat[2] with 0.025 M KCl (or 0.01 M NH_4Cl); analyze leachate by IC (SO_4^{2-})	Bloem et al. 2002; Maynard et al. 1987
Inner-Sphere Inorganic Sulfur; specific adsorbed (correct for U-IS, OS-IS, and *soluble org-S*)	IS-IS	Treat[2] with 500 mg-P L^{-1} KH_2PO_4; analyze leachate by IC (SO_4^{2-})	Ensminger 1954; Sahrawat et al. 2009
Labile Sulfonate Sulfur (-C-O-SO_3 sulfate ester; -C-N-SO_3 sulfate amine) (correct for TIS)	LSS	Hydro-iodic acid (HI) reduction with capture of H_2S for analysis	Johnson and Nashita 1952; Tabatabai and Bremner 1972
Labile Carbon-Bound Sulfur; amino acids (-C-SH or –C-S-CH3)	LCS	Raney Nickel catalyst reduction with capture of H_2S for analysis	Lowe and DeLong 1963
Recalcitrant Carbon-Bound Sulfur Non-Amino Acid type (-C-S-C-)	RCS	Calculated: {TOS} – Sum {LSS + LCS}	Tabatabai 1996 in MofSA [1]

NOTES:

[1] MofSA - D.L. Sparks (ed.), Methods of Soil Analysis, Part 3, Chemical Methods. Book Series 5. ASA and SSSA, Madison, WI; 1996.

[2] Generic soil leaching procedure: 5.0 grams air-dry soil + 50 ml of extractant; shake overnight; decant leachate and filter through 0.4 µm membrane filter; store in clean plastic (preferably low-density polyethylene [LDPE]) bottle until processed.

[3] iCAP-OES – inductively-coupled argon plasma optical emission spectrometry

Table 18. Procedures for sequential extraction of sulfur-fractions from soil and bedrock samples, and for preparing samples for stable isotope analysis

Analytical Parameter	Symbol	Summary of Method or Calculation	Reference
Elemental sulfur	ES°	Add 125 ml acetone to 15 grams of sample (in an HDPE bottle); 24 hrs.; filter (0.45 µm polycarbonate); Reduce by "Canfield chromium reduction" method; trap in $AgNO_3$ solution; collect Ag_2S	Tuttle et al. 1986; Tuttle et al. 2003; Fauville et al. 2004; Canfield et al. 1986
Water-extractable sulfate	WXS	Add 100 ml of DI water to solid residue from "S°" step; 30 minutes; filter; add 10% $BaCl_2$; collect $BaSO_4$	Tuttle et al. 2003; Fauville et al. 2004
Acid-volatile monosulfides (S(-II) sulfur)	MS	Add hot 6M HCl to solid residue from "WXS" step under N_2 atmosphere; trap in $AgNO_3$ solution; collect Ag_2S	Tuttle et al. 2003; Fauville et al. 2004
Polysulfides (S(-I) sulfur)	PS	Treat residue from "MS" step by "Canfield chromium reduction" method; trap in $AgNO_3$ solution; collect Ag_2S	Tuttle et al. 2003; Fauville et al. 2004; Canfield et al. 1986
Residual sulfur	RS	Oxidize residue from "PS" step with sodium bicarbonate ($NaHCO_3$) and silver oxide (Ag_2O) at 550 °C; extract sulfate from ash with hot water; filter; add 10% $BaCl_2$; collect $BaSO_4$	Tabatabai et al. 1988; Rossete et al. 2008
Total sulfur	TS	Oxidize portion of original sample with sodium bicarbonate ($NaHCO_3$) and silver oxide (Ag_2O) at 550 °C; extract sulfate from ash with hot water; filter; add 10% $BaCl_2$; collect $BaSO_4$	Tabatabai et al. 1988; Rossete et al. 2008
Sulfur isotope composition (as barium sulfate or silver sulfide)	$\delta^{34}S_{(BaSO4)}$ $\delta^{34}S_{(Ag2S)}$	In a tin cup, combine $BaSO_4$ (0.4-0.6 mg) or Ag_2S (0.3-0.4 mg) with vanadium pentoxide (1.5-5.0 mg); analyze by isotope ratio mass spectrometry (IRMS)	Mayer and Krouse 2004 Kendall and Caldwell 1998

Table 19. Procedures for characterizing the chemical and isotopic composition of water samples

Analytical Parameter	Symbol	Summary of Method or Calculation	Reference
pH (temperature-compensated)	pH	Electrometric	EPA Method 150.1
Specific Conductance (25°C)	SPC	Electrometric	EPA Method 120.1
Acid neutralizing capacity	ANC	Automated Titration	Automated Gran Titration (low ionic strength waters; e.g., Hillman et al. 1986)
Anions (Cl^-, NO_3^-, SO_4^{2-}, NO_3^-, $H_2PO_4^-$)	IC_{AN}	Ion Chromatography (IC)	Standard Methods 4110
Ammonium (NH_4^+) and Base cations[1] (Na^+, K^+, Mg^{2+}, Ca^{2+})	IC_{CAT}	Ion Chromatography (IC)	Standard Methods 4110
Total base cations[1] (Na, K, Mg, Ca), trace metals (Al, Cu, Fe, Mn, Si & Zn), and total dissolved sulfur (S)	BC TM TDS	Inductively Coupled Argon Plasma Optical Emission Spectrometry (iCAP-OES)	Standard Methods 3120B EPA Method 6010B EPA Method 3005A
Sulfate extraction for stable isotope analysis – Direct precipitation		Filter and acidify (pH < 3) water sample; add 10% barium chloride ($BaCl_2$); collect/dry barium sulfate ($BaSO_4$)	Kendall and Caldwell 1998
Sulfate extraction for stable isotope analysis – Anionic resin[2]		Pass large volume (> 20 liters) of water sample over 1 to 3 grams of anionic exchange resin for > 3 days; treat SO_4-saturated resin with 3 x 5 ml of 3 M HCl; add 10% barium chloride ($BaCl_2$); collect/dry barium sulfate ($BaSO_4$)	Kang et al. 2012; Mizutani and Rafter 1969
Sulfate-oxygen isotope composition[3]	$\delta^{18}O_{(SO4)}$	In a silver cup, combine $BaSO_4$ (0.2-0.4 mg) and graphite (0.2-0.3 mg); analyze by isotope ratio mass spectrometry (IRMS)	Mayer and Krouse 2004 Kendall and Caldwell 1998
Sulfate-sulfur isotope composition[3]	$\delta^{34}S_{(SO4)}$	In a tin cup, combine $BaSO_4$ (0.4-0.6 mg) and vanadium pentoxide (1.5-5.0 mg); analyze by isotope ratio mass spectrometry (IRMS)	Mayer and Krouse 2004 Kendall and Caldwell 1998

NOTES:
1 Non-hydrolysable cations that do not influence water pH; thus, historically they have been called “base cations.”
2 Amberlite® IRA-400, chloride form (Alfa Aesar®, lot number N20A050), conditioned with 1 M KCl (24 hrs.) and water rinsed
3 These procedures also are applicable to sulfate in aqueous leachate samples extracted from soil, rock or vegetation samples.

Table 20. Sample preparation details for sulfur and sulfate-oxygen isotope composition analysis

Isotope	Mass (mg)	Co-reagent, mass	Crucible	Lab Standard
$\delta^{18}O_BaSO_4$	0.2 – 0.4 mg	NaF*, 0.2 – 0.3 mg	silver	UTK-Gyp1; SC-1std; IAEA-SO-5
$\delta^{34}S_BaSO_4$	0.4 – 0.6 mg	V_2O_5*, 1.5 – 5.0 mg	tin	NBS 127; IAEA-SO-6
$\delta^{34}S_Ag_2S$	0.3 – 0.4 mg	V_2O_5*, 1.5 – 5.0 mg	tin	NBS 127; IAEA-SO-6

* NaF = sodium fluoride; V_2O_5 = vanadium pentoxide

APPENDIX B

RAW DATA – CHAPTER 4

SampleID	Site Code	Catchment	Date	Year	Month	cond. uS/cm	pH	ANC ueq/L	Cl umol/L	NO3 umol/L	SO4 umol/L	Na umol/L	K umol/L	Mg umol/L	Ca umol/L	Al umol/L	Fe umol/L	Mn umol/L	Si umol/L	Elevation meters	Stream Order
ACtP1-1/A 150710 82	ACtP1-1	ACC	150710	2015	7	20.46	4.81	-20.26	3.89	9.53	12.98	9.74	2.89	10.12	7.09	4.703	0.052	0.464	28.48	1189.5	1
ACtP1-1/B 150710 85	ACtP1-1	ACC	150710	2015	7	20.81	4.77	-21.07	4.12	5.34	12.81	13.14	6.24	12.63	10.16	22.653	21.510	1.919	40.13	1189.5	1
ACtP1-1/x 160407 5914	ACtP1-1	ACC	160407	2016	4	24.53	4.45	-43.18	18.33	6.03	27.60	16.57	5.40	13.12	7.44	10.303	2.174	0.783	28.84	1189.5	1
ACtP2-1/x 150710 48	ACtP2-1	ACC	150710	2015	7	19.65	4.80	-17.22	5.22	19.13	10.07	12.05	3.53	21.35	11.58	4.714	0.090	0.535	44.33	1197.6	1
ACtP1-3/x 160428 2977	ACtP1-3	ACC	160428	2016	4	22.02	4.38	-51.65	8.83	5.14	28.98	11.96	2.43	12.51	7.19	8.780	1.669	0.526	28.13	1207.4	1
ACtP1-3/x 160506 5965	ACtP1-3	ACC	160506	2016	5	23.13	4.42	-46.68	9.00	4.69	25.16	11.53	2.12	12.75	8.08	13.520	3.954	0.621	33.65	1207.4	1
ACtP3-1/x 150710 84	ACtP3-1	ACC	150710	2015	7	30.16	4.62	-33.38	4.74	13.31	28.55	12.83	4.12	28.35	18.09	13.109	0.073	1.212	45.72	1208.3	1
ACtP1-2/A 160428 2981	ACtP1-2	ACC	160428	2016	4	19.16	4.73	-21.89	18.02	47.88	23.55	19.10	6.09	22.46	11.85	4.803	0.158	0.670	47.39	1210.7	1
ACtP1-2/B 160428 3165	ACtP1-2	ACC	160428	2016	4	18.86	4.75	-19.86	17.97	49.29	23.50	16.01	5.35	22.42	12.15	4.321	0.066	0.672	47.71	1210.7	1
ACtP1-2/x 160506 6092	ACtP1-2	ACC	160506	2016	5	19.49	4.79	-16.14	12.64	48.67	23.69	13.31	4.91	20.90	13.90	4.562	0.002	0.746	47.07	1210.7	1
StyxBr-1/A 150710 80	ACtSTYX1	ACC	150710	2015	7	15.91	5.68	3.78	4.77	10.35	13.16	14.92	3.71	21.48	22.66	1.027	0.118	0.033	41.41	1273.2	2
StyxBr-1/B 150710 81	ACtSTYX1	ACC	150710	2015	7	16.11	5.75	4.89	4.34	10.35	13.09	14.48	3.32	21.72	24.70	1.805	0.288	0.371	40.98	1273.2	2
StyxBr-2/A 150710 03	ACtSTYX2	ACC	150710	2015	7	16.64	5.89	7.51	4.23	10.56	12.30	13.92	3.09	22.18	23.18	1.230	0.419	0.035	40.02	1355.6	2
StyxBr-2/B 150710 61	ACtSTYX2	ACC	150710	2015	7	15.70	5.93	8.21	4.20	10.18	12.30	12.83	3.35	22.22	23.55	0.189	0.063	0.009	40.52	1355.6	2
BFP2/x 150304 V500	BFP2	BFP	150304	2015	3	22.62	6.38	56.99	13.12	53.69	25.50	32.75	9.64	22.26	46.88	0.697	0.047	0.033	73.60	1491.9	1
BFP2/x 150407a V250	BFP2	BFP	150407	2015	4	24.03	6.37	94.73	5.92	23.27	11.29	49.98	11.10	24.27	58.59	0.219	0.070	0.009	111.80	1491.9	1
BFP2/A 151023 1916	BFP2	BFP	151023	2015	10	39.11	6.55	111.05				119.84	31.41	28.31	62.45	0.200	0.036	0.002	121.41	1491.9	1
BFP2/B 151023 1877	BFP2	BFP	151023	2015	10	29.76	6.68	89.36				57.81	11.71	27.81	60.61	0.100	0.056	0.000	121.09	1491.9	1
BFP2/x 161007 V175	BFP2	BFP	161007	2016	10	27.10	6.61	87.29	17.69	52.64	30.28	64.64	10.03	29.58	63.08	0.282	0.021	0.011	129.68	1491.9	1
BFP2/A 161123	BFP2	BFP	161123	2016	11	29.18	6.53	95.76	19.63	51.69	41.48	68.90	12.38	36.12	70.61	0.078	0.140	0.102	121.24	1491.9	1
BFP2/B 161123	BFP2	BFP	161123	2016	11	29.59	6.60	87.85	16.84	52.93	38.55	63.94	11.41	35.22	68.34	0.193	0.002	0.011	120.56	1491.9	1
BFP2/C 161123	BFP2	BFP	161123	2016	11	30.10	6.57	92.82	22.85	51.92	38.06	71.77	13.12	35.18	67.77	0.004	0.002	0.007	121.13	1491.9	1
BFP2/D 161123	BFP2	BFP	161123	2016	11	30.00	6.60	103.98	18.31	51.40	37.69	67.51	11.05	35.55	69.76	0.096	0.002	0.011	121.02	1491.9	1
BFP2/E 161123	BFP2	BFP	161123	2016	11	29.49	6.63	91.64	16.11	51.69	37.48	63.33	9.87	35.26	66.97	0.119	0.002	0.009	120.10	1491.9	1
BFP1b/x 160801 V175	BFP1b	BFP	160801	2016	8	24.67	6.59	96.39	17.18	55.11	28.22	63.25	11.66	29.75	66.20	0.237	0.213	0.004	140.50	1510.9	1
BFP1/x 150407a V500	BFP1	BFP	150407	2015	4	21.92	5.95	80.59	5.13	27.93	4.24	55.46	10.61	20.78	47.21	0.675	0.115	0.060	126.44	1555.7	1
BFP1/x 161007 V175	BFP1	BFP	161007	2016	10	28.25	6.63	117.23	12.52	53.32	22.51	63.72	9.87	32.26	72.21	0.096	0.014	0.013	146.16	1555.7	1
BFP1/A 161115	BFP1	BFP	161115	2016	11	26.75	6.78	145.35	14.53	52.00	29.86	76.73	11.28	39.87	84.76	0.004	0.002	0.027	149.08	1555.7	1
BFP1/B 161115	BFP1	BFP	161115	2016	11	27.09	6.83	157.98	15.40	50.71	29.48	76.03	11.77	38.80	85.83	0.004	0.002	0.002	149.51	1555.7	1
BFP1/C 161115	BFP1	BFP	161115	2016	11	27.68	6.85	154.31	14.92	50.90	29.43	76.77	11.36	40.03	86.86	0.004	0.002	0.002	150.83	1555.7	1
BFP1/D 161115	BFP1	BFP	161115	2016	11	27.86	6.84	140.06	14.98	51.69	29.49	74.90	12.76	39.42	86.76	0.004	0.002	0.000	151.00	1555.7	1
BFP1/E 161115	BFP1	BFP	161115	2016	11	27.34	6.84	142.66	13.68	51.33	29.28	72.60	10.87	39.29	86.66	0.004	0.002	0.002	150.47	1555.7	1
WLPt14/A 150630 71	WLPt14	LWPLPR	150630	2015	6	23.53	6.87	178.37	4.91	1.19	3.13	77.90	22.53	19.46	37.90	0.308	0.152	0.004	200.71	466.9	1
BullheadBr-1/A 150630 75	WLPtBULL1	LWPLPR	150630	2015	6	26.44	6.94	203.55	5.22	1.18	4.17	87.91	19.46	22.71	45.41	0.767	0.374	0.004	186.82	473.6	2
BullheadBr-1/B 150630 27	WLPtBULL1	LWPLPR	150630	2015	6	26.34	6.94	201.27	4.88	1.24	4.10	86.39	18.42	22.88	45.34	0.649	0.360	0.004	185.61	473.6	2
WLPt15/A 150630 63	WLPt15	LWPLPR	150630	2015	6	24.73	6.78	190.49	4.60	1.18	4.37	87.34	27.67	19.91	35.56	0.419	0.131	0.004	218.83	475.2	1
WLPt15/B 150630 34	WLPt15	LWPLPR	150630	2015	6	24.83	6.79	190.28	4.60	1.10	4.32	88.47	28.29	20.04	36.08	0.385	0.183	0.004	220.86	475.2	1
SugarlandBr-1/A 150630 66	WLPtSugar1	LWPLPR	150630	2015	6	25.14	6.96	190.70	5.61	3.27	3.54	72.64	16.88	21.07	50.00	0.782	0.779	0.004	159.90	475.6	2
SugarlandBr-1/B 150630 68	WLPtSugar1	LWPLPR	150630	2015	6	24.73	6.96	191.03	4.29	3.24	3.41	70.64	16.14	20.70	48.95	0.463	0.211	0.002	157.84	475.6	2
HuskeyGapCr1/A 150630 78	WLPtHusk1	LWPLPR	150630	2015	6	50.17	7.20	443.79	6.88	2.61	3.22	110.22	24.17	51.18	127.70	0.237	0.059	0.000	222.75	492.2	2
HuskeyGapCr1/B 150630 12	WLPtHusk1	LWPLPR	150630	2015	6	51.48	7.17	431.06	5.75	2.58	2.99	105.96	22.61	51.02	127.13	0.878	1.311	0.004	224.53	492.2	2
WLPt13/A 150630 60	WLPt13	LWPLPR	150630	2015	6	75.21	7.32	527.41	15.29	7.26	17.24	110.05	25.83	69.49	211.14	1.527	0.802	0.002	183.62	547.1	1
WLPt13/B 150630 77	WLPt13	LWPLPR	150630	2015	6	75.51	7.33	516.11	15.80	7.50	17.36	110.61	26.98	69.62	212.64	0.256	0.156	0.004	181.77	547.1	1
HuskeyGapCr-Tr01/A 150716 141	HuskeyGAP1	LWPLPR	150716	2015	7	27.85	6.90	193.93	5.84	0.02	5.49	113.62	12.94	29.75	61.33	0.923	0.141	0.000	247.89	588.4	1
HuskeyGapCr-Tr01/B 150716 151	HuskeyGAP1	LWPLPR	150716	2015	7	29.06	7.01	208.41	6.37	0.00	5.47	106.92	12.07	27.03	51.45	0.645	0.136	0.142	244.82	588.4	1
CritterBr1/A 150716 40	WLPtCRITT1	LWPLPR	150716	2015	7	24.53	6.53	54.28	5.53	24.93	9.50	46.19	20.08	15.43	51.00	0.111	0.030	-0.002	104.18	608.7	1
CritterBr1/B 150716 59	WLPtCRITT1	LWPLPR	150716	2015	7	24.94	6.62	59.28	5.47	22.66	9.48	48.24	20.13	15.96	53.62	0.163	0.048	0.004	107.17	608.7	1
HickoryKingBr1/A 150716 131	WLPtHick1	LWPLPR	150716	2015	7	18.93	6.25	35.47	6.29	9.45	10.46	41.98	18.44	12.10	46.18	0.767	0.045	0.011	89.33	613.2	2
HickoryKingBr1/B 150716 154	WLPtHick1	LWPLPR	150716	2015	7	22.92	6.37	32.76	16.98	9.53	10.45	59.20	28.62	11.93	37.43	0.738	0.082	0.000	87.45	613.2	2
HuskeyGapCr2/A 150716 142	WLPtHusk2	LWPLPR	150716	2015	7	30.57	7.00	210.37	7.76	1.69	3.73	104.39	14.91	28.97	56.32	0.356	0.050	0.009	226.42	629	1
HuskeyGapCr2/B 150716 150	WLPtHusk2	LWPLPR	150716	2015	7	29.66	6.96	220.90	6.66	0.00	3.74	106.74	14.53	28.27	54.59	1.030	0.111	-0.002	227.31	629	1
SteepBr-1/A 150630 42	WLPtSteep1	LWPLPR	150630	2015	6	23.13	6.40	57.93	9.53	12.68	10.09	41.89	26.42	23.25	39.80	0.096	0.014	0.005	89.87	759.7	2
SteepBr-1/B 150630 58	WLPtSteep1	LWPLPR	150630	2015	6	21.72	6.45	0.00	6.23	12.48	10.01	39.23	19.75	22.26	37.93	0.152	0.030	0.011	89.80	759.7	2
FlintRockBr1/A 150716 155	FlintRockBr1	LWPLPR	150716	2015	7	13.39	6.35	30.00	3.41	5.18	6.09	35.84	12.38	7.61	20.29	0.841	0.100	0.000	102.54	785.1	1
FlintRockBr1/B 150716 157	FlintRockBr1	LWPLPR	150716	2015	7	13.82	6.39	31.46	4.03	5.08	6.12	37.67	12.89	7.32	20.61	0.830	0.048	0.013	103.40	785.1	1
WtCHT1-1/x 150407a V500	WLPtCT1-1	LWPLPR	150407	2015	4	21.92	6.03	26.58	4.54	14.71	23.66	22.05	9.90	26.21	46.31	0.141	0.030	0.009	50.81	866	2
ColeCr1/A 150630 22	WtCOLE1	MtLC	150630	2015	6	17.91	6.20	27.76	4.80	14.66	9.86	27.45	8.24	20.82	29.54	1.746	0.095	0.013	69.29	1105.2	2
ColeCr1/B 150630 31	WtCOLE1	MtLC	150630	2015	6	17.65	6.23	23.87	4.51	14.66	9.71	24.79	7.95	20.61	29.07	2.094	0.127	0.015	68.93	1105.2	2
BearpenBr-1/A 150630 43	WtBEAR1	MtLC	150630	2015	6	18.92	5.29	-3.41	5.58	19.35	12.71	21.66	4.32	20.90	24.35	1.282	0.039	0.198	65.30	1119.4	1
BearpenBr-1/B 150630 18	WtBEAR1	MtLC	150630	2015	6	19.82	5.35	7.91	6.01	19.21	12.74	23.10	5.29	20.98	24.43	1.264	0.029	0.187	65.76	1119.4	1
TroutBr-1/A 150630 32	WtTROUT1	MtLC	150630	2015	6	19.76	5.10	13.17	4.32	11.66	16.73	15.31	4.60	20.61	22.18	3.121	0.088	0.624	44.47	1125	2
TroutBr-1/B 150630 39	WtTROUT1	MtLC	150630	2015	6	19.48	5.02	10.96	3.78	11.68	16.65	14.18	3.68	20.24	21.18	3.165	0.079	0.635	43.44	1125	2

SampleID	Site Code	Latitude	Longitude	UTM	Easting meters	Northing meters	Dist2Knob meters	Dist2Blvd meters	SubWtrShed	Distrubance	Bedrock Code	Bedrock GROUP
ACtP1-1/A 150710 82	ACtP1-1	35.6306	-83.4471	17	278405	3945740	1834.09	3060.41	ACC	0	43	sulfidic
ACtP1-1/B 150710 85	ACtP1-1	35.6306	-83.4471	17	278405	3945740	1834.09	3060.41	ACC	0	43	sulfidic
ACtP1-1/x 160407 5914	ACtP1-1	35.6306	-83.4471	17	278405	3945740	1834.09	3060.41	ACC	0	43	sulfidic
ACtP2-1/x 150710 48	ACtP2-1	35.6312	-83.4462	17	278489	3945797	1764.07	2969.78	ACC	0	43	sulfidic
ACtP1-3/x 160428 2977	ACtP1-3	35.6316	-83.4467	17	278443	3945841	1819.30	3010.53	ACC	0	43	sulfidic
ACtP1-3/x 160506 5965	ACtP1-3	35.6316	-83.4467	17	278443	3945841	1819.30	3010.53	ACC	0	43	sulfidic
ACtP3-1/x 150710 84	ACtP3-1	35.6323	-83.4448	17	278615	3945920	1676.64	2831.85	ACC	0	43	sulfidic
ACtP1-2/A 160428 2981	ACtP1-2	35.6317	-83.4467	17	278441	3945861	1826.31	3010.49	ACC	0	43	sulfidic
ACtP1-2/B 160428 3165	ACtP1-2	35.6317	-83.4467	17	278441	3945861	1826.31	3010.49	ACC	0	43	sulfidic
ACtP1-2/x 160506 6092	ACtP1-2	35.6317	-83.4467	17	278441	3945861	1826.31	3010.49	ACC	0	43	sulfidic
StyxBr-1/A 150710 80	ACtSTYX1	35.6350	-83.4379	17	279253	3946199	1250.61	2184.42	ACC	0	43	sulfidic
StyxBr-1/B 150710 81	ACtSTYX1	35.6350	-83.4379	17	279253	3946199	1250.61	2184.42	ACC	0	43	sulfidic
StyxBr-2/A 150710 03	ACtSTYX2	35.6397	-83.4377	17	279278	3946726	1627.75	2232.98	ACC	yes	43	sulfidic
StyxBr-2/B 150710 61	ACtSTYX2	35.6397	-83.4377	17	279278	3946726	1627.75	2232.98	ACC	yes	43	sulfidic
BFP2/x 150304 V500	BFP2	35.6077	-83.4375	17	279206	3943174	2428.95	3724.20	BFP	0	43	sulfidic
BFP2/x 150407a V250	BFP2	35.6077	-83.4375	17	279206	3943174	2428.95	3724.20	BFP	0	43	sulfidic
BFP2/A 151023 1916	BFP2	35.6077	-83.4375	17	279206	3943174	2428.95	3724.20	BFP	0	43	sulfidic
BFP2/B 151023 1877	BFP2	35.6077	-83.4375	17	279206	3943174	2428.95	3724.20	BFP	0	43	sulfidic
BFP2/x 161007 V175	BFP2	35.6077	-83.4375	17	279206	3943174	2428.95	3724.20	BFP	0	43	sulfidic
BFP2/A 161123	BFP2	35.6077	-83.4375	17	279206	3943174	2428.95	3724.20	BFP	0	43	sulfidic
BFP2/B 161123	BFP2	35.6077	-83.4375	17	279206	3943174	2428.95	3724.20	BFP	0	43	sulfidic
BFP2/C 161123	BFP2	35.6077	-83.4375	17	279206	3943174	2428.95	3724.20	BFP	0	43	sulfidic
BFP2/D 161123	BFP2	35.6077	-83.4375	17	279206	3943174	2428.95	3724.20	BFP	0	43	sulfidic
BFP2/E 161123	BFP2	35.6077	-83.4375	17	279206	3943174	2428.95	3724.20	BFP	0	43	sulfidic
BFP1b/x 160801 V175	BFP1b	35.6082	-83.4384	17	279128	3943230	2411.82	3727.33	BFP	0	43	sulfidic
BFP1/x 150407a V500	BFP1	35.6095	-83.4386	17	279117	3943379	2284.69	3618.58	BFP	0	43	sulfidic
BFP1/x 161007 V175	BFP1	35.6095	-83.4386	17	279117	3943379	2284.69	3618.58	BFP	0	43	sulfidic
BFP1/A 161115	BFP1	35.6095	-83.4386	17	279117	3943379	2284.69	3618.58	BFP	0	43	sulfidic
BFP1/B 161115	BFP1	35.6095	-83.4386	17	279117	3943379	2284.69	3618.58	BFP	0	43	sulfidic
BFP1/C 161115	BFP1	35.6095	-83.4386	17	279117	3943379	2284.69	3618.58	BFP	0	43	sulfidic
BFP1/D 161115	BFP1	35.6095	-83.4386	17	279117	3943379	2284.69	3618.58	BFP	0	43	sulfidic
BFP1/E 161115	BFP1	35.6095	-83.4386	17	279117	3943379	2284.69	3618.58	BFP	0	43	sulfidic
WLPt14/A 150630 71	WLPt14	35.6796	-83.5316	17	270886	3951367	11072.14	11767.67	LWPLPR	0	67	sandstone
BullheadBr-1/A 150630 75	WLPtBULL1	35.6773	-83.5272	17	271279	3951098	10596.11	11296.39	LWPLPR	0	67	sandstone
BullheadBr-1/B 150630 27	WLPtBULL1	35.6773	-83.5272	17	271279	3951098	10596.11	11296.39	LWPLPR	0	67	sandstone
WLPt15/A 150630 63	WLPt15	35.6802	-83.5290	17	271129	3951428	10902.08	11577.95	LWPLPR	0	67	sandstone
WLPt15/B 150630 34	WLPt15	35.6802	-83.5290	17	271129	3951428	10902.08	11577.95	LWPLPR	0	67	sandstone
SugarlandBr-1/A 150630 66	WLPtSugar1	35.6768	-83.5286	17	271157	3951051	10674.07	11385.93	LWPLPR	0	67	sandstone
SugarlandBr-1/B 150630 68	WLPtSugar1	35.6768	-83.5286	17	271157	3951051	10674.07	11385.93	LWPLPR	0	67	sandstone
HuskeyGapCr1/A 150630 78	WLPtHusk1	35.6731	-83.5264	17	271342	3950628	10296.13	11041.19	LWPLPR	0	67	sandstone
HuskeyGapCr1/B 150630 12	WLPtHusk1	35.6731	-83.5264	17	271342	3950628	10296.13	11041.19	LWPLPR	0	67	sandstone
WLPt13/A 150630 60	WLPt13	35.6627	-83.5226	17	271658	3949472	9472.61	10325.92	LWPLPR	0	67	sandstone
WLPt13/B 150630 77	WLPt13	35.6627	-83.5226	17	271658	3949472	9472.61	10325.92	LWPLPR	0	67	sandstone
HuskeyGapCr-Tr01/A 150716 141	HuskeyGAP1	35.6630	-83.5278	17	271185	3949518	9920.55	10789.19	LWPLPR	0	67	sandstone
HuskeyGapCr-Tr01/B 150716 151	HuskeyGAP1	35.6630	-83.5278	17	271185	3949518	9920.55	10789.19	LWPLPR	0	67	sandstone
CritterBr1/A 150716 40	WLPtCRITT1	35.6580	-83.5197	17	271906	3948945	9029.16	9930.68	LWPLPR	0	56	sandstone
CritterBr1/B 150716 59	WLPtCRITT1	35.6580	-83.5197	17	271906	3948945	9029.16	9930.68	LWPLPR	0	56	sandstone
HickoryKingBr1/A 150716 131	WLPtHick1	35.6565	-83.5164	17	272201	3948771	8689.57	9599.06	LWPLPR	0	56	sandstone
HickoryKingBr1/B 150716 154	WLPtHick1	35.6565	-83.5164	17	272201	3948771	8689.57	9599.06	LWPLPR	0	56	sandstone
HuskeyGapCr2/A 150716 142	WLPtHusk2	35.6617	-83.5307	17	270918	3949377	10107.45	11001.10	LWPLPR	0	67	sandstone
HuskeyGapCr2/B 150716 150	WLPtHusk2	35.6617	-83.5307	17	270918	3949377	10107.45	11001.10	LWPLPR	0	67	sandstone
SteepBr-1/A 150630 42	WLPtSteep1	35.6428	-83.5062	17	273083	3947227	7355.60	8422.37	LWPLPR	0	76	sandstone
SteepBr-1/B 150630 58	WLPtSteep1	35.6428	-83.5062	17	273083	3947227	7355.60	8422.37	LWPLPR	0	76	sandstone
FlintRockBr1/A 150716 155	FlintRockBr1	35.6567	-83.5386	17	270189	3948838	10593.52	11563.33	LWPLPR	0	56	sandstone
FlintRockBr1/B 150716 157	FlintRockBr1	35.6567	-83.5386	17	270189	3948838	10593.52	11563.33	LWPLPR	0	56	sandstone
WtCHT1-1/x 150407a V500	WLPtCT1-1	35.6368	-83.4871	17	274801	3946481	5513.43	6643.95	LWPLPR	0	76	sandstone
ColeCr1/A 150630 22	WtCOLE1	35.6376	-83.4650	17	276798	3946554	3601.00	4656.04	MtLC	0	76	sandstone
ColeCr1/B 150630 31	WtCOLE1	35.6376	-83.4650	17	276798	3946554	3601.00	4656.04	MtLC	0	76	sandstone
BearpenBr-1/A 150630 43	WtBEAR1	35.6366	-83.4624	17	277035	3946440	3340.00	4411.15	MtLC	0	76	sandstone
BearpenBr-1/B 150630 18	WtBEAR1	35.6366	-83.4624	17	277035	3946440	3340.00	4411.15	MtLC	0	76	sandstone
TroutBr-1/A 150630 32	WtTROUT1	35.6344	-83.4615	17	277106	3946189	3200.84	4331.13	MtLC	yes	76	sandstone
TroutBr-1/B 150630 39	WtTROUT1	35.6344	-83.4615	17	277106	3946189	3200.84	4331.13	MtLC	yes	76	sandstone

SampleID	Site Code	Catchment	Date	Year	Month	cond. uS/cm	pH	ANC ueq/L	Cl umol/L	NO3 umol/L	SO4 umol/L	Na umol/L	K umol/L	Mg umol/L	Ca umol/L	Al umol/L	Fe umol/L	Mn umol/L	Si umol/L	Elevation meters	Stream Order
NDNE/A 161116	NDNE	NDW	161116	2016	11	11.48	5.87	6.83	10.41	18.51	18.90	28.97	6.65	8.68	18.69	0.612	0.124	0.020	72.21	1670.3	1
NDNE/B 161116	NDNE	NDW	161116	2016	11	11.26	5.98	7.86	10.61	19.16	18.17	29.10	6.68	8.64	18.76	0.408	0.002	0.005	71.96	1670.3	1
NDNE/C 161116	NDNE	NDW	161116	2016	11	11.16	5.95	9.53	9.99	18.55	18.48	28.71	6.75	9.01	20.76	0.530	0.072	0.016	71.60	1670.3	1
NDNE/D 161116	NDNE	NDW	161116	2016	11	11.27	5.98	9.65	9.87	19.58	18.43	28.97	6.65	8.80	18.99	0.326	0.002	0.007	71.50	1670.3	1
NDNE/E 161116	NDNE	NDW	161116	2016	11	11.08	5.99	9.44	10.04	19.08	17.70	29.10	6.42	8.68	19.39	0.463	0.002	0.009	71.32	1670.3	1
NDSW/A 161116	NDSW	NDW	161116	2016	11	11.02	6.15	16.89	9.51	19.53	14.68	32.45	6.62	8.52	19.34	0.519	0.106	0.016	75.41	1670.3	1
NDSW/B 161116	NDSW	NDW	161116	2016	11	10.71	6.12	14.04	8.97	23.53	89.00	30.88	6.16	10.12	79.40	1.356	1.271	0.076	76.34	1670.3	1
NDSW/C 161116	NDSW	NDW	161116	2016	11	10.61	6.15	18.08	8.72	19.95	14.93	29.49	6.06	8.68	18.56	0.245	0.032	0.004	76.30	1670.3	1
NDSW/D 161116	NDSW	NDW	161116	2016	11	10.95	6.12	14.50	9.28	20.24	14.89	29.45	6.14	8.60	18.41	0.523	0.002	0.013	76.55	1670.3	1
NDSW/E 161116	NDSW	NDW	161116	2016	11	10.50	6.15	18.17	8.66	19.61	14.18	29.80	6.01	8.52	18.51	0.248	0.002	0.004	76.12	1670.3	1
RtM12-1/x 160220 v14a	RtM12-1	RP	160220	2016	2	14.21	6.31	31.04	8.83	26.06	34.39	19.66	2.07	21.19	39.25	0.152	0.011	0.004	54.69	1094.2	1
RtM11-1/x 150714 104	RtM11-1	RP	150714	2015	7	18.74	6.64	52.34	5.11	12.66	7.94	38.15	9.87	31.35	63.33	0.615	0.098	0.000	91.79	1120.6	1
RtM11-1/x 160220 v13a	RtM11-1	RP	160220	2016	2	12.45	6.10	15.28	9.14	40.88	21.78	33.84	6.75	16.46	24.50	0.385	0.041	0.005	89.62	1120.6	1
RtM10-1/x 150714 113	RtM10-1	RP	150714	2015	7	17.82	6.23	34.97	3.86	11.21	7.95	36.02	11.61	16.99	37.28	1.167	0.287	-0.002	86.66	1138.6	1
RtM10-1/x 160220 v12a	RtM10-1	RP	160220	2016	2	12.87	6.25	22.68	9.20	35.37	22.35	30.67	9.72	13.62	29.79	0.460	0.064	0.002	84.95	1138.6	1
RtM9-1/x 150714 103	RtM9-1	RP	150714	2015	7	15.29	5.91	8.35	3.07	8.24	10.05	26.71	13.48	11.23	26.22	2.439	0.145	0.005	71.57	1150.8	1
RtM9-1/x 160220 v11a	RtM9-1	RP	160220	2016	2	12.59	6.05	12.43	11.14	29.29	24.46	27.19	11.15	11.85	29.09	2.179	0.183	0.016	69.57	1150.8	1
RtM11-2/x 160407 5660	RtM11-2	RP	160407	2016	4	16.53	6.19	20.01	9.42	39.51	20.37	34.49	8.39	18.14	26.45	0.719	0.333	0.016	90.40	1152.8	1
RtS8-1/x 150714 115	RtS8-1	RP	150714	2015	7	17.03	6.41	40.98	4.17	10.61	7.62	34.75	10.13	13.70	31.69	0.882	0.163	-0.002	86.24	1177.9	1
RtS8-1/x 160220 v10a	RtS8-1	RP	160220	2016	2	12.78	6.24	24.81	10.32	34.48	20.66	32.49	9.41	13.82	31.26	0.949	0.125	0.002	82.21	1177.9	1
RtS6-1/x 150714 110	RtS6-1	RP	150714	2015	7	18.23	6.36	41.37	4.03	11.71	11.04	26.19	10.18	15.92	44.96	1.301	0.124	0.005	62.49	1215.3	1
RtS6-1/x 160220 v9a	RtS6-1	RP	160220	2016	2	14.77	6.30	40.23	8.94	26.47	28.55	23.01	12.61	15.51	42.94	2.012	0.199	0.016	63.91	1215.3	1
RtS6-2/x 160407 5810	RtS6-2	RP	160407	2016	4	18.91	6.53	46.30	9.03	26.90	27.78	22.84	12.94	16.33	43.39	0.489	0.175	0.002	61.28	1221.4	1
RtS6-2/x 160425 5753	RtS6-2	RP	160425	2016	4	17.88	6.25	55.97	12.16	25.59	30.91	26.79	13.15	17.57	47.53	0.793	0.124	0.009	63.84	1221.4	1
CHt1A/x 160303 5751	ChTt1-1	RP	160303	2016	3	14.25	5.80	13.65	11.48	30.34	20.18	28.23	10.56	11.27	23.30	0.085	0.002	0.002	71.46	1230.7	1
CHt1B/x 160303 6163	ChTt1-1	RP	160303	2016	3	14.55	5.90	12.95	10.69	34.05	21.02	26.75	10.21	11.89	23.85	0.004	0.002	0.004	72.56	1230.7	1
RtS10-1/x 160220 v8a	RtS10-1	RP	160220	2016	2	19.12	4.53	-35.45	9.25	33.85	20.66	17.05	17.62	8.93	19.59	16.615	1.787	0.286	73.45	1234.6	1
RtS7-1/x 150714 101	RtS7-1	RP	150714	2015	7	25.14	4.57	-39.86	6.21	6.64	8.66	25.62	13.04	8.52	21.48	18.553	1.481	0.218	66.40	1241.4	1
RtS7-1/x 160220 v7a	RtS7-1	RP	160220	2016	2	17.20	4.66	-25.66	10.24	30.74	25.16	15.05	15.53	9.63	20.66	8.217	0.897	0.335	56.47	1241.4	1
CHt2A/x 160303 5762	ChTt2-1	RP	160303	2016	3	15.62	5.90	19.19	18.22	9.27	22.59	19.97	10.82	11.27	33.91	0.630	0.002	0.002	61.99	1244	1
CHt2C/x 160303 5928	ChTt2-1	RP	160303	2016	3	15.76	5.95	15.98	9.62	22.30	26.71	22.27	10.92	10.99	33.66	0.741	0.004	0.002	61.28	1244	1
CHt2B/x 160303 6132	ChTt2-1	RP	160303	2016	3	15.50	6.02	16.56	9.05	24.19	26.92	19.57	10.69	11.07	32.96	0.612	0.002	0.004	61.99	1244	1
RtS7-2/x 160425 5776	RtS7-2	RP	160425	2016	4	19.34	4.72	-19.76	10.30	26.98	24.96	18.40	13.94	9.42	20.88	8.139	0.550	0.319	72.42	1250.3	1
RtM13-1/x 160220 v6a	RtM13-1	RP	160220	2016	2	11.60	5.74	5.22	10.49	32.79	25.58	19.92	9.97	9.46	30.19	3.484	0.098	0.084	58.57	1271.1	1
RtChT1/A 160303 5927	RtChT1-1	RP	160303	2016	3	16.69	6.09	27.90	9.14	25.21	27.13	25.49	9.26	13.95	36.75	0.534	0.018	0.002	70.78	1286.4	2
RtChT1/B 160303 6121	RtChT1-1	RP	160303	2016	3	16.89	6.13	26.39	9.34	27.00	27.87	25.88	9.23	14.03	36.18	0.482	0.007	0.002	71.00	1286.4	2
RtM1-1/A 150716 133	RtM1-1	RP	150716	2015	7	19.94	4.87	-16.67	4.77	9.58	13.68	29.36	8.41	6.42	23.35	5.889	0.197	0.422	54.01	1321.9	1
RtM1-1/B 150716 147	RtM1-1	RP	150716	2015	7	18.31	4.90	-13.97	3.75	9.43	12.46	19.92	7.67	6.17	24.03	5.960	0.082	0.410	53.98	1321.9	1
RtM1-1/x 160220 v3a	RtM1-1	RP	160220	2016	2	14.34	4.93	-13.45	11.42	25.45	27.59	17.40	11.20	6.91	25.33	4.844	0.113	0.353	48.25	1321.9	1
RtM2-1/A 150716 118	RtM2-1	RP	150716	2015	7	14.89	4.99	-12.15	3.33	5.84	8.02	23.97	10.05	4.73	12.00	4.247	0.288	0.222	75.98	1326.8	1
RtM2-1/B 150716 123	RtM2-1	RP	150716	2015	7	16.13	5.02	-11.65	6.46	6.24	8.35	35.15	12.61	5.14	13.85	4.277	0.276	0.249	75.02	1326.8	1
RtM1-2/x 160412 5919	RtM1-2	RP	160412	2016	4	17.74	5.42	-2.92	53.45	28.95	37.16	24.58	11.82	6.95	24.00	5.730	0.766	0.302	88.91	1329.5	1
RtM7-1/A 150716 129	RtM7-1	RP	150716	2015	7	13.39	5.87	7.56	3.70	7.95	8.36	25.49	7.93	9.18	22.91	2.220	0.079	0.005	68.86	1334.8	1
RtM7-1/B 150716 140	RtM7-1	RP	150716	2015	7	13.39	5.95	7.46	3.95	7.92	8.36	25.05	8.01	9.22	22.96	2.183	0.199	0.004	69.32	1334.8	1
RtM3-1/A 150716 143	RtM3-1	RP	150716	2015	7	18.01	6.39	27.86	4.91	11.43	11.72	25.40	13.02	9.22	45.66	0.526	0.018	0.000	72.78	1366.6	1
RtM3-1/B 150716 145	RtM3-1	RP	150716	2015	7	18.41	6.36	25.38	4.65	11.71	11.73	26.27	11.33	9.22	40.92	1.149	0.090	0.004	73.17	1366.6	1
RtTOM2/x 150804 H5012	RtTOM2	RP	150804	2015	8	12.37	6.10	14.70	9.65	15.84	18.31	27.84	6.09	8.85	21.88	3.439	0.299	0.009	80.90	1383.4	2
RtM4-1/A 150716 119	RtM4-1	RP	150716	2015	7	28.05	4.45	-46.36	4.94	12.82	8.91	21.31	13.73	6.25	22.51	19.928	1.864	0.426	82.93	1412.2	1
RtM4-1/B 150716 127	RtM4-1	RP	150716	2015	7	27.75	4.47	-44.10	4.99	13.26	9.03	21.97	13.50	6.34	22.31	18.672	1.576	0.471	84.17	1412.2	1
RtM4-1/x 160412 2308	RtM4-1	RP	160412	2016	4	21.62	4.73	-19.51	80.61	36.14	21.65	14.44	4.60	18.84	17.19	16.897	1.189	1.092	34.29	1412.2	1
RtM5-1/A 150716 138	RtM5-1	RP	150716	2015	7	16.69	5.21	-9.11	5.16	10.16	10.65	25.19	7.65	10.74	26.87	5.708	0.654	0.186	70.82	1417.8	1
RtM5-1/B 150716 139	RtM5-1	RP	150716	2015	7	16.51	5.22	-6.92	5.05	9.82	10.64	26.19	7.75	10.70	25.95	5.507	0.476	0.131	70.53	1417.8	1
RtM4-2/x 160412 6152	RtM4-2	RP	160412	2016	4	21.02	4.77	-17.82	30.77	36.80	23.84	12.05	2.76	19.75	17.52	18.346	1.051	1.101	34.79	1419.6	1
RtS9-1/A 150716 121	RtS1-1	RP	150716	2015	7	13.24	6.06	12.16	2.79	9.64	8.53	23.01	8.06	10.62	26.70	0.423	0.039	0.004	65.62	1436.2	1
RtS9-1/B 150716 134	RtS1-1	RP	150716	2015	7	13.38	6.02	9.63	2.71	9.84	8.54	22.88	7.72	9.55	23.80	0.434	0.034	0.002	66.08	1436.2	1
RtM6-1/A 150716 152	RtM6-1	RP	150716	2015	7	16.25	6.27	17.31	9.34	15.74	6.78	38.28	6.14	15.35	54.17	0.600	0.181	0.016	79.72	1518.4	1
RtM6-1/B 150716 156	RtM6-1	RP	150716	2015	7	14.83	6.22	13.63	5.84	15.60	6.77	35.10	4.19	14.77	26.52	0.448	0.091	0.002	84.74	1518.4	1
RtM14-2/x 160412 5835	RtM14-2	RP	160412	2016	4	13.32	5.30	-4.33	33.03	26.92	20.65	24.88	12.89	6.05	22.58	8.176	1.112	0.379	88.55	1616.7	1
RtM14-2/x 160523 V175	RtM14-2	RP	160523	2016	5	11.92	5.44	-4.13	12.92	20.05	20.52	34.71	3.17	7.12	12.43	1.256	0.084	0.064	88.41	1616.7	1
RtM14-2/x 160701 V250	RtM14-2	RP	160701	2016	7	11.23	5.67	1.95												1616.7	1
RtM14-2/x 160816 V175	RtM14-2	RP	160816	2016	8	12.37	5.48	-3.76	20.17	24.08	21.94	43.76	4.81	9.18	14.22	2.435	0.272	0.126	97.24	1616.7	1
RtM14-2/x 161007 v175	RtM14-2	RP	161007	2016	10	13.08	5.61	-1.52	21.63	9.89	24.47	46.72	7.49	8.85	15.52	4.014	0.654	0.180	99.66	1616.7	1

SampleID	Site Code	Latitude	Longitude	UTM	Easting meters	Northing meters	Dist2Knob meters	Dist2Blvd meters	SubWtrShed	Distrubance	Bedrock Code	Bedrock GROUP
NDNE/A 161116	NDNE	35.5646	-83.4797	17	275270	3938492	8479.92	9837.11	NDW	0	51	sandstone
NDNE/B 161116	NDNE	35.5646	-83.4797	17	275270	3938492	8479.92	9837.11	NDW	0	51	sandstone
NDNE/C 161116	NDNE	35.5646	-83.4797	17	275270	3938492	8479.92	9837.11	NDW	0	51	sandstone
NDNE/D 161116	NDNE	35.5646	-83.4797	17	275270	3938492	8479.92	9837.11	NDW	0	51	sandstone
NDNE/E 161116	NDNE	35.5646	-83.4797	17	275270	3938492	8479.92	9837.11	NDW	0	51	sandstone
NDSW/A 161116	NDSW	35.5645	-83.4797	17	275241	3938472	8513.07	9870.88	NDW	0	51	sandstone
NDSW/B 161116	NDSW	35.5645	-83.4797	17	275241	3938472	8513.07	9870.88	NDW	0	51	sandstone
NDSW/C 161116	NDSW	35.5645	-83.4797	17	275241	3938472	8513.07	9870.88	NDW	0	51	sandstone
NDSW/D 161116	NDSW	35.5645	-83.4797	17	275241	3938472	8513.07	9870.88	NDW	0	51	sandstone
NDSW/E 161116	NDSW	35.5645	-83.4797	17	275241	3938472	8513.07	9870.88	NDW	0	51	sandstone
RtM12-1/x 160220 v14a	RtM12-1	35.6309	-83.4686	17	276457	3945815	3772.25	4991.66	RP	0	76	sandstone
RtM11-1/x 150714 104	RtM11-1	35.6288	-83.4696	17	276359	3945590	3851.30	5109.45	RP	0	43	sulfidic
RtM11-1/x 160220 v13a	RtM11-1	35.6288	-83.4696	17	276359	3945590	3851.30	5109.45	RP	0	43	sulfidic
RtM10-1/x 150714 113	RtM10-1	35.6278	-83.4695	17	276366	3945470	3839.88	5117.19	RP	0	43	sulfidic
RtM10-1/x 160220 v12a	RtM10-1	35.6278	-83.4695	17	276366	3945470	3839.88	5117.19	RP	0	43	sulfidic
RtM9-1/x 150714 103	RtM9-1	35.6266	-83.4698	17	276337	3945367	3868.06	5160.67	RP	0	43	sulfidic
RtM9-1/x 160220 v11a	RtM9-1	35.6266	-83.4698	17	276337	3945367	3868.06	5160.67	RP	0	43	sulfidic
RtM11-2/x 160407 5660	RtM11-2	35.6284	-83.4682	17	276485	3945543	3723.23	4989.80	RP	0	43	sulfidic
RtS8-1/x 150714 115	RtS8-1	35.6246	-83.4702	17	276295	3945127	3918.70	5243.95	RP	0	43	sulfidic
RtS8-1/x 160220 v10a	RtS8-1	35.6246	-83.4702	17	276295	3945127	3918.70	5243.95	RP	0	43	sulfidic
RtS6-1/x 150714 110	RtS6-1	35.6222	-83.4701	17	276300	3944854	3941.34	5299.43	RP	0	76	sandstone
RtS6-1/x 160220 v9a	RtS6-1	35.6222	-83.4701	17	276300	3944854	3941.34	5299.43	RP	0	76	sandstone
RtS6-2/x 160407 5810	RtS6-2	35.6220	-83.4703	17	276274	3944837	3969.43	5328.82	RP	0	76	sandstone
RtS6-2/x 160425 5753	RtS6-2	35.6220	-83.4703	17	276274	3944837	3969.43	5328.82	RP	0	76	sandstone
CHt1A/x 160303 5751	ChTt1-1	35.6253	-83.4745	17	275906	3945212	4302.60	5610.98	RP	0	43	sulfidic
CHt1B/x 160303 6163	ChTt1-1	35.6253	-83.4745	17	275906	3945212	4302.60	5610.98	RP	0	43	sulfidic
RtS10-1/x 160220 v8a	RtS10-1	35.6207	-83.4704	17	276264	3944692	4001.99	5376.17	RP	0	76	sandstone
RtS7-1/x 150714 101	RtS7-1	35.6199	-83.4706	17	276246	3944601	4036.47	5418.90	RP	0	76	sandstone
RtS7-1/x 160220 v7a	RtS7-1	35.6199	-83.4706	17	276246	3944601	4036.47	5418.90	RP	0	76	sandstone
CHt2A/x 160303 5762	ChTt2-1	35.6252	-83.4754	17	275828	3945205	4380.82	5689.05	RP	0	43	sulfidic
CHt2C/x 160303 5928	ChTt2-1	35.6252	-83.4754	17	275828	3945205	4380.82	5689.05	RP	0	43	sulfidic
CHt2B/x 160303 6132	ChTt2-1	35.6252	-83.4754	17	275828	3945205	4380.82	5689.05	RP	0	43	sulfidic
RtS7-2/x 160425 5776	RtS7-2	35.6200	-83.4709	17	276222	3944612	4057.89	5438.76	RP	0	76	sandstone
RtM13-1/x 160220 v6a	RtM13-1	35.6187	-83.4705	17	276248	3944471	4061.86	5455.73	RP	0	76	sandstone
RtChT1/A 160303 5927	RtChT1-1	35.6250	-83.4766	17	275720	3945181	4489.77	5799.54	RP	0	43	sulfidic
RtChT1/B 160303 6121	RtChT1-1	35.6250	-83.4766	17	275720	3945181	4489.77	5799.54	RP	0	43	sulfidic
RtM1-1/A 150716 133	RtM1-1	35.6152	-83.4702	17	276270	3944078	4147.33	5569.20	RP	yes	76	sandstone
RtM1-1/B 150716 147	RtM1-1	35.6152	-83.4702	17	276270	3944078	4147.33	5569.20	RP	yes	76	sandstone
RtM1-1/x 160220 v3a	RtM1-1	35.6152	-83.4702	17	276270	3944078	4147.33	5569.20	RP	yes	76	sandstone
RtM2-1/A 150716 118	RtM2-1	35.6145	-83.4704	17	276251	3943999	4190.88	5616.69	RP	0	76	sandstone
RtM2-1/B 150716 123	RtM2-1	35.6145	-83.4704	17	276251	3943999	4190.88	5616.69	RP	0	76	sandstone
RtM1-2/x 160412 5919	RtM1-2	35.6153	-83.4700	17	276286	3944085	4129.94	5551.74	RP	yes	76	sandstone
RtM7-1/A 150716 129	RtM7-1	35.6146	-83.4702	17	276270	3944016	4167.33	5592.63	RP	0	76	sandstone
RtM7-1/B 150716 140	RtM7-1	35.6146	-83.4702	17	276270	3944016	4167.33	5592.63	RP	0	76	sandstone
RtM3-1/A 150716 143	RtM3-1	35.6123	-83.4674	17	276511	3943746	4042.50	5483.94	RP	0	76	sandstone
RtM3-1/B 150716 145	RtM3-1	35.6123	-83.4674	17	276511	3943746	4042.50	5483.94	RP	0	76	sandstone
RtTOM2/x 150804 H5012	RtTOM2	35.6083	-83.4667	17	276566	3943306	4192.50	5643.50	RP	0	51	sandstone
RtM4-1/A 150716 119	RtM4-1	35.6114	-83.4644	17	276783	3943642	3841.69	5289.60	RP	0	76	sandstone
RtM4-1/B 150716 127	RtM4-1	35.6114	-83.4644	17	276783	3943642	3841.69	5289.60	RP	0	76	sandstone
RtM4-1/x 160412 2308	RtM4-1	35.6114	-83.4644	17	276783	3943642	3841.69	5289.60	RP	0	76	sandstone
RtM5-1/A 150716 138	RtM5-1	35.6110	-83.4607	17	277119	3943592	3570.58	5021.87	RP	yes	76	sandstone
RtM5-1/B 150716 139	RtM5-1	35.6110	-83.4607	17	277119	3943592	3570.58	5021.87	RP	yes	76	sandstone
RtM4-2/x 160412 6152	RtM4-2	35.6116	-83.4645	17	276778	3943668	3834.41	5281.71	RP	0	76	sandstone
RtS9-1/A 150716 121	RtS1-1	35.6101	-83.4588	17	277290	3943489	3479.00	4930.57	RP	0	43	sulfidic
RtS9-1/B 150716 134	RtS1-1	35.6101	-83.4588	17	277290	3943489	3479.00	4930.57	RP	0	43	sulfidic
RtM6-1/A 150716 152	RtM6-1	35.6104	-83.4531	17	277807	3943510	3045.86	4492.02	RP	0	43	sulfidic
RtM6-1/B 150716 156	RtM6-1	35.6104	-83.4531	17	277807	3943510	3045.86	4492.02	RP	0	43	sulfidic
RtM14-2/x 160412 5835	RtM14-2	35.6110	-83.4477	17	278292	3943565	2642.52	4074.84	RP	0	43	sulfidic
RtM14-2/x 160523 V175	RtM14-2	35.6110	-83.4477	17	278292	3943565	2642.52	4074.84	RP	0	43	sulfidic
RtM14-2/x 160701 V250	RtM14-2	35.6110	-83.4477	17	278292	3943565	2642.52	4074.84	RP	0	43	sulfidic
RtM14-2/x 160816 V175	RtM14-2	35.6110	-83.4477	17	278292	3943565	2642.52	4074.84	RP	0	43	sulfidic
RtM14-2/x 161007 v175	RtM14-2	35.6110	-83.4477	17	278292	3943565	2642.52	4074.84	RP	0	43	sulfidic

SampleID	Site Code	Catchment	Date	Year	Month	cond. uS/cm	pH	ANC ueq/L	Cl umol/L	NO3 umol/L	SO4 umol/L	Na umol/L	K umol/L	Mg umol/L	Ca umol/L	Al umol/L	Fe umol/L	Mn umol/L	Si umol/L	Elevation meters	Stream Order
RtM14-2/A 161115	RtM14-2	RP	161115	2016	11	15.18	5.68	6.01	36.30	19.60	26.68	68.38	24.22	12.59	19.16	0.819	0.134	0.215	98.88	1616.7	1
RtM14-2/B 161115	RtM14-2	RP	161115	2016	11	14.63	5.67	6.31	34.75	20.00	26.92	63.64	23.76	11.97	16.82	0.997	0.075	0.242	98.56	1616.7	1
RtM14-2/C 161115	RtM14-2	RP	161115	2016	11	14.78	5.63	4.69	36.50	20.47	27.06	66.64	24.94	11.40	16.17	1.301	0.267	0.249	99.52	1616.7	1
RtM14-2/D 161115	RtM14-2	RP	161115	2016	11	14.67	5.79	8.34	34.24	20.10	26.92	63.20	24.17	11.85	16.52	1.245	0.109	0.208	99.27	1616.7	1
RtM14-2/E 161115	RtM14-2	RP	161115	2016	11	15.51	5.68	1.58	40.98	20.42	26.43	68.16	28.11	11.97	16.92	1.097	0.122	0.204	99.45	1616.7	1
RtTOM1/A 150527 04	RtTOM1	RP	150527	2015	5	20.20	5.35	50.98	6.49	10.39	10.47	32.10	13.12	13.25	28.20	0.259	0.029	0.211	75.20	1710.4	1
RtTOM1/B 150527 16	RtTOM1	RP	150527	2015	5	20.03	5.42	45.44	6.88	10.52	10.70	33.10	13.45	13.41	28.54	1.390	0.195	0.220	78.23	1710.4	1
RtMOC2/x 160816 V175	RtMOC2	RP	160816	2016	8	11.90	5.50	6.64	10.77	21.00	17.29	27.62	5.29	13.74	20.34	2.090	0.002	0.204	71.32	1727.9	1
RtMOC2/A 161007 V175	RtMOC2	RP	161007	2016	10	12.76	5.96	11.04	17.91	20.14	16.11	36.19	12.81	8.85	19.64	0.663	0.023	0.133	78.90	1727.9	1
RtMOC2/B 161007 V175	RtMOC2	RP	161007	2016	10	11.37	6.05	12.94	11.28	20.40	15.89	28.49	9.72	9.67	20.11	0.560	0.045	0.127	78.76	1727.9	1
RtMOC2/A 161115	RtMOC2	RP	161115	2016	11	8.96	5.97	16.87	14.19	18.95	8.50	36.15	9.54	9.09	15.35	0.541	0.002	0.084	81.68	1727.9	1
RtMOC2/B 161115	RtMOC2	RP	161115	2016	11	9.22	6.02	19.21	16.59	19.21	8.15	38.45	10.82	8.80	16.89	0.248	0.002	0.102	81.71	1727.9	1
RtMOC2/C 161115	RtMOC2	RP	161115	2016	11	9.01	6.02	19.23	14.86	19.82	7.92	40.19	9.62	8.97	15.67	0.637	0.016	0.098	81.86	1727.9	1
RtMOC2/D 161115	RtMOC2	RP	161115	2016	11	9.40	6.03	19.48	17.54	19.13	7.97	40.58	10.64	9.22	15.84	0.441	0.034	0.086	82.04	1727.9	1
RtMOC2/E 161115	RtMOC2	RP	161115	2016	11	9.65	6.08	19.43	17.71	19.24	7.85	41.45	11.59	8.72	14.65	0.352	0.025	0.087	81.89	1727.9	1
RtMOC1/ 160801 V175	RtMOC1	RP	160801	2016	8	9.34	5.23	-6.85	7.36	8.37	23.00	26.58	5.45	6.75	9.88	3.202	0.473	0.333	75.16	1751.9	1
WtGRASS1/A 150527 14	WtGRASS1	WCP	150527	2015	5	15.53	5.03	-8.22	3.44	3.95	11.44	16.18	5.42	6.75	21.31	3.076	0.312	0.703	52.16	1209.8	1
WtGRASS1/B 150527 23	WtGRASS1	WCP	150527	2015	5	15.84	5.03	-7.95	3.78	4.35	11.23	17.23	5.73	6.42	21.11	3.221	0.090	0.666	51.95	1209.8	1
WtM11-1/A 150527 37	WtM11-1	WCP	150527	2015	5	20.81	6.39	129.04	5.75	2.95	2.96	25.75	5.65	16.17	54.89	1.649	0.308	0.005	58.82	1233.9	1
WtM11-1/B 150527 38	WtM11-1	WCP	150527	2015	5	19.44	6.52	126.60	7.64	5.77	2.93	29.19	7.98	15.06	48.13	1.805	0.202	0.013	59.64	1233.9	1
WtM10-1/A 150527 07	WtM10-1	WCP	150527	2015	5	15.24	5.98	29.86	5.05	14.87	5.61	27.49	4.50	15.18	25.13	1.067	0.385	0.013	69.54	1268.5	1
WtM10-1/B 150527 29	WtM10-1	WCP	150527	2015	5	15.39	6.05	30.38	5.11	16.00	5.28	28.75	4.63	15.22	25.05	0.641	0.163	0.015	70.11	1268.5	1
WtM8-1/A 150527 08	WtM8-1	WCP	150527	2015	5	34.99	6.50	93.23	13.09	12.06	30.92	48.20	7.98	30.90	82.21	0.734	0.111	-0.002	68.72	1282.9	1
WtM8-1/B 150527 52	WtM8-1	WCP	150527	2015	5	35.49	6.67	111.96	13.17	11.81	31.15	47.24	7.93	30.41	80.79	0.215	0.023	0.002	68.47	1282.9	1
WtM8-1/A 151023 3056	WtM8-1	WCP	151023	2015	10	37.00	6.64	83.39				53.33	8.47	32.09	83.04	0.285	0.034	0.004	70.68	1282.9	1
WtM8-1/B 151023 3165	WtM8-1	WCP	151023	2015	10	36.90	6.62	74.16				52.68	8.52	32.30	83.71	1.019	0.057	0.011	70.29	1282.9	1
WtM7-1/A 150527 10	WtM7-1	WCP	150527	2015	5	10.28	5.79	12.40	4.23	5.26	3.34	20.88	3.50	9.34	13.07	2.984	0.398	0.113	67.54	1285.4	1
WtM7-1/B 150527 26	WtM7-1	WCP	150527	2015	5	11.35	5.99	20.91	4.71	7.53	3.49	23.40	4.48	10.66	21.11	2.439	0.557	0.098	68.68	1285.4	1
WtA6-1/A 150527 06	WtA6-1	WCP	150527	2015	5	21.20	6.27	49.68	7.14	11.64	12.50	49.02	6.19	21.72	30.27	0.975	0.072	0.016	98.77	1312	1
WtA6-1/B 150527 33	WtA6-1	WCP	150527	2015	5	20.14	6.45	44.40	5.27	11.56	12.22	47.02	4.65	22.34	30.81	2.227	0.697	0.016	104.43	1312	1
WtA6-1/x 160414 6136	WtA6-1	WCP	160414	2016	4	18.68	6.22	27.62	47.84	28.35	30.84	36.93	4.83	7.24	13.02	0.997	0.009	0.104	86.34	1312	1
WtA5-1/A 150527 11	WtA5-1	WCP	150527	2015	5	18.93	5.04	0.42	6.04	9.64	13.65	39.71	2.43	16.13	16.57	3.984	0.432	0.291	81.00	1354.1	1
WtA5-1/B 150527 55	WtA5-1	WCP	150527	2015	5	18.88	5.03	-2.98	6.21	10.22	13.83	39.41	2.66	17.65	22.01	3.135	0.335	0.271	79.58	1354.1	1
WtA5-1/B 160506 6149	WtA5-1	WCP	160506	2016	5	24.13	4.49	-39.40	7.02	14.87	33.46	14.66	1.97	13.04	15.94	14.043	4.645	0.411	36.71	1354.1	1
WtA5-1/A 160506 5900	WtA5-1	WCP	160506	2016	5	23.93	4.49	-39.47	7.25	14.84	33.11	14.79	1.92	12.92	15.64	14.202	4.683	0.410	36.71	1354.1	1
WtA5-1/x 160521 3496	WtA5-1	WCP	160521	2016	5	23.63	4.50	-35.31	6.60	14.74	37.43	14.40	1.99	13.91	16.74	14.273	4.720	0.440	37.49	1354.1	1
WtA5-1/x 160604 V175	WtA5-1	WCP	160604	2016	6	21.52	4.62	-26.63	7.28	15.40	36.77	16.27	1.76	14.28	17.37	11.300	4.106	0.451	45.47	1354.1	1
WtA5-1/A 160816 V175	WtA5-1	WCP	160816	2016	8	15.78	4.97	-11.26	13.71	15.48	32.42	35.67	8.93	1.52	15.35	5.018	2.383	0.324	80.65	1354.1	1
WtA5-1/B 160816 V175	WtA5-1	WCP	160816	2016	8	15.78	4.97	-11.26	13.71	19.42	31.26	35.84	8.95	1.52	15.25	4.963	2.382	0.324	81.93	1354.1	1
WtA5-1/A 161117	WtA5-1	WCP	161117	2016	11	19.12	6.11	19.99	18.39	36.90	39.34	61.85	4.14	29.09	34.36	1.949	2.253	0.195	105.11	1354.1	1
WtA5-1/B 161117	WtA5-1	WCP	161117	2016	11	18.88	6.16	23.52	17.35	37.16	32.47	60.24	2.89	28.51	29.12	2.094	1.257	0.169	104.57	1354.1	1
WtA4-1/A 150527 05	WtA4-1	WCP	150527	2015	5	17.76	5.15	5.37	6.97	3.16	16.85	33.62	2.71	11.97	19.31	4.051	0.183	0.390	63.20	1357.5	1
WtA4-1/B 150527 49	WtA4-1	WCP	150527	2015	5	17.60	5.04	0.19	5.92	3.03	16.51	32.45	1.97	11.85	18.79	4.644	0.143	0.391	62.81	1357.5	1
WtA4-1/A 160506 5916	WtA4-1	WCP	160506	2016	5	16.62	4.92	-11.80	10.55	17.16	31.21	20.14	2.15	12.43	20.96	6.575	0.260	0.282	48.78	1357.5	1
WtA4-1/B 160506 1877	WtA4-1	WCP	160506	2016	5	17.29	4.89	-13.11	10.46	17.10	31.23	20.27	2.28	12.38	20.88	6.553	0.279	0.278	48.32	1357.5	1
WtA4-1/x 160521 3386	WtA4-1	WCP	160521	2016	5	16.01	4.93	-11.53	10.13	11.64	31.45	22.75	2.10	11.15	18.11	7.227	0.331	0.253	48.21	1357.5	1
WtA4-1/x 160604 V175	WtA4-1	WCP	160604	2016	6	16.55	4.91	-13.81	10.92	12.82	34.25	23.62	1.89	11.36	18.69	6.771	0.278	0.302	53.19	1357.5	1
WtA4-1/x 160816 V175	WtA4-1	WCP	160816	2016	8	15.14	4.92	-14.11	13.14	3.79	36.53	25.97	6.68	1.40	17.07	6.430	0.389	0.552	64.66	1357.5	1
WtA4-1/A 161117	WtA4-1	WCP	161117	2016	11	16.97	5.16	-7.94	15.57	16.63	37.77	40.06	2.66	16.09	18.21	5.808	0.245	0.706	67.19	1357.5	1
WtA4-1/B 161117	WtA4-1	WCP	161117	2016	11	18.02	5.03	-9.48	18.70	16.24	37.98	42.67	5.37	16.38	18.76	5.367	0.167	0.775	67.08	1357.5	1
WtA3-1/A 150527 41	WtA3-1	WCP	150527	2015	5	42.53	4.31	-62.37	3.38	3.08	42.10	13.22	2.69	24.27	29.14	13.076	1.296	1.316	40.59	1368.8	2
WtA3-1/B 150527 47	WtA3-1	WCP	150527	2015	5	43.64	4.29	-70.71	3.70	3.60	42.57	13.92	3.45	23.82	19.46	15.711	0.845	1.010	38.74	1368.8	2
WtA3-1/x 150829 146	WtA3-1	WCP	150829	2015	8	45.25	4.41	-53.61	24.65	22.71	97.99	15.27	4.04	28.02	31.01	14.873	1.545	0.954	45.47	1368.8	2
WtA3-1/A 151023 3323	WtA3-1	WCP	151023	2015	10	47.86	4.32	-57.93				18.88	4.65	29.62	23.63	16.645	1.132	1.292	47.89	1368.8	2
WtA3-1/B 151023 3496	WtA3-1	WCP	151023	2015	10	47.96	4.33	-60.74				22.97	6.09	29.05	22.86	18.401	0.779	1.292	47.82	1368.8	2
WtA3-1/x 151229	WtA3-1	WCP	151229	2015	12	32.17	4.40	-59.63	10.30	11.93	54.33	10.40	2.92	15.59	16.39	11.500	2.057	0.795	29.05	1368.8	2
WtA3-1/x 160220 JUG	WtA3-1	WCP	160220	2016	2	28.10	4.35	-50.56	8.07	8.42	71.38	10.83	1.76	23.95	20.88	16.200	1.467	1.076	32.05	1368.8	2
WtA3-1/x 160604 V175	WtA3-1	WCP	160604	2016	6	34.99	4.32	-55.66	5.95	13.02	73.56	9.92	2.05	21.19	19.91	13.910	2.867	0.990	34.86	1368.8	2
WtM1-1/B 150311 3282	WtM1-1	WCP	150311	2015	3	15.89	5.12	-7.01	9.34	27.79	27.50									1386.3	1
WtM1-1/A 150311 3056	WtM1-1	WCP	150311	2015	3	15.79	5.13	-7.76	8.49	28.32	27.29	53.33	8.47	32.09	83.04	0.285	0.034	0.004	70.68	1386.3	1
WtM1-1/A 150527 01	WtM1-1	WCP	150527	2015	5	18.08	5.62	6.96	5.05	5.19	18.57	24.36	4.78	17.40	26.05	1.082	0.134	0.040	54.23	1386.3	1
WtM1-1/B 150527 02	WtM1-1	WCP	150527	2015	5	18.58	5.56	19.70	7.31	5.24	18.61	29.75	7.14	17.98	26.87	0.960	0.047	0.049	55.44	1386.3	1

SampleID	Site Code	Latitude	Longitude	UTM	Easting meters	Northing meters	Dist2Knob meters	Dist2Blvd meters	SubWtrShed	Distrubance	Bedrock Code	Bedrock GROUP
RtM14-2/A 161115	RtM14-2	35.6110	-83.4477	17	278292	3943565	2642.52	4074.84	RP	0	43	sulfidic
RtM14-2/B 161115	RtM14-2	35.6110	-83.4477	17	278292	3943565	2642.52	4074.84	RP	0	43	sulfidic
RtM14-2/C 161115	RtM14-2	35.6110	-83.4477	17	278292	3943565	2642.52	4074.84	RP	0	43	sulfidic
RtM14-2/D 161115	RtM14-2	35.6110	-83.4477	17	278292	3943565	2642.52	4074.84	RP	0	43	sulfidic
RtM14-2/E 161115	RtM14-2	35.6110	-83.4477	17	278292	3943565	2642.52	4074.84	RP	0	43	sulfidic
RtTOM1/A 150527 04	RtTOM1	35.5963	-83.4613	17	277026	3941960	4675.17	6087.97	RP	0	51	sandstone
RtTOM1/B 150527 16	RtTOM1	35.5963	-83.4613	17	277026	3941960	4675.17	6087.97	RP	0	51	sandstone
RtMOC2/x 160816 V175	RtMOC2	35.5945	-83.4750	17	275775	3941797	5702.65	7145.57	RP	0	51	sandstone
RtMOC2/A 161007 V175	RtMOC2	35.5945	-83.4750	17	275775	3941797	5702.65	7145.57	RP	0	51	sandstone
RtMOC2/B 161007 V175	RtMOC2	35.5945	-83.4750	17	275775	3941797	5702.65	7145.57	RP	0	51	sandstone
RtMOC2/A 161115	RtMOC2	35.5945	-83.4750	17	275775	3941797	5702.65	7145.57	RP	0	51	sandstone
RtMOC2/B 161115	RtMOC2	35.5945	-83.4750	17	275775	3941797	5702.65	7145.57	RP	0	51	sandstone
RtMOC2/C 161115	RtMOC2	35.5945	-83.4750	17	275775	3941797	5702.65	7145.57	RP	0	51	sandstone
RtMOC2/D 161115	RtMOC2	35.5945	-83.4750	17	275775	3941797	5702.65	7145.57	RP	0	51	sandstone
RtMOC2/E 161115	RtMOC2	35.5945	-83.4750	17	275775	3941797	5702.65	7145.57	RP	0	51	sandstone
RtMOC1/ 160801 V175	RtMOC1	35.5944	-83.4733	17	275929	3941782	5593.52	7033.49	RP	0	51	sandstone
WtGRASS1/A 150527 14	WtGRASS1	35.6247	-83.4472	17	278378	3945080	1852.78	3242.72	WCP	yes	76	sandstone
WtGRASS1/B 150527 23	WtGRASS1	35.6247	-83.4472	17	278378	3945080	1852.78	3242.72	WCP	yes	76	sandstone
WtM11-1/A 150527 37	WtM11-1	35.6224	-83.4419	17	278852	3944817	1468.55	2911.21	WCP	0	76	sandstone
WtM11-1/B 150527 38	WtM11-1	35.6224	-83.4419	17	278852	3944817	1468.55	2911.21	WCP	0	76	sandstone
WtM10-1/A 150527 07	WtM10-1	35.6197	-83.4347	17	279494	3944501	1136.79	2552.31	WCP	0	43	sulfidic
WtM10-1/B 150527 29	WtM10-1	35.6197	-83.4347	17	279494	3944501	1136.79	2552.31	WCP	0	43	sulfidic
WtM8-1/A 150527 08	WtM8-1	35.6185	-83.4312	17	279811	3944354	1106.52	2427.15	WCP	0	43	sulfidic
WtM8-1/B 150527 52	WtM8-1	35.6185	-83.4312	17	279811	3944354	1106.52	2427.15	WCP	0	43	sulfidic
WtM8-1/A 151023 3056	WtM8-1	35.6185	-83.4312	17	279811	3944354	1106.52	2427.15	WCP	0	43	sulfidic
WtM8-1/B 151023 3165	WtM8-1	35.6185	-83.4312	17	279811	3944354	1106.52	2427.15	WCP	0	43	sulfidic
WtM7-1/A 150527 10	WtM7-1	35.6184	-83.4305	17	279870	3944349	1091.67	2391.81	WCP	0	43	sulfidic
WtM7-1/B 150527 26	WtM7-1	35.6184	-83.4305	17	279870	3944349	1091.67	2391.81	WCP	0	43	sulfidic
WtA6-1/A 150527 06	WtA6-1	35.6196	-83.4260	17	280281	3944469	922.14	2045.07	WCP	0	43	sulfidic
WtA6-1/B 150527 33	WtA6-1	35.6196	-83.4260	17	280281	3944469	922.14	2045.07	WCP	0	43	sulfidic
WtA6-1/x 160414 6136	WtA6-1	35.6196	-83.4260	17	280281	3944469	922.14	2045.07	WCP	0	43	sulfidic
WtA5-1/A 150527 11	WtA5-1	35.6240	-83.4213	17	280721	3944946	679.43	1405.97	WCP	yes	43	sulfidic
WtA5-1/B 150527 55	WtA5-1	35.6240	-83.4213	17	280721	3944946	679.43	1405.97	WCP	yes	43	sulfidic
WtA5-1/B 160506 6149	WtA5-1	35.6240	-83.4213	17	280721	3944946	679.43	1405.97	WCP	yes	43	sulfidic
WtA5-1/A 160506 5900	WtA5-1	35.6240	-83.4213	17	280721	3944946	679.43	1405.97	WCP	yes	43	sulfidic
WtA5-1/x 160521 3496	WtA5-1	35.6240	-83.4213	17	280721	3944946	679.43	1405.97	WCP	yes	43	sulfidic
WtA5-1/x 160604 V175	WtA5-1	35.6240	-83.4213	17	280721	3944946	679.43	1405.97	WCP	yes	43	sulfidic
WtA5-1/A 160816 V175	WtA5-1	35.6240	-83.4213	17	280721	3944946	679.43	1405.97	WCP	yes	43	sulfidic
WtA5-1/B 160816 V175	WtA5-1	35.6240	-83.4213	17	280721	3944946	679.43	1405.97	WCP	yes	43	sulfidic
WtA5-1/A 161117	WtA5-1	35.6240	-83.4213	17	280721	3944946	679.43	1405.97	WCP	yes	43	sulfidic
WtA5-1/B 161117	WtA5-1	35.6240	-83.4213	17	280721	3944946	679.43	1405.97	WCP	yes	43	sulfidic
WtA4-1/A 150527 05	WtA4-1	35.6244	-83.4206	17	280790	3944993	705.87	1330.86	WCP	0	43	sulfidic
WtA4-1/B 150527 49	WtA4-1	35.6244	-83.4206	17	280790	3944993	705.87	1330.86	WCP	0	43	sulfidic
WtA4-1/A 160506 5916	WtA4-1	35.6244	-83.4206	17	280790	3944993	705.87	1330.86	WCP	0	43	sulfidic
WtA4-1/B 160506 1877	WtA4-1	35.6244	-83.4206	17	280790	3944993	705.87	1330.86	WCP	0	43	sulfidic
WtA4-1/x 160521 3386	WtA4-1	35.6244	-83.4206	17	280790	3944993	705.87	1330.86	WCP	0	43	sulfidic
WtA4-1/x 160604 V175	WtA4-1	35.6244	-83.4206	17	280790	3944993	705.87	1330.86	WCP	0	43	sulfidic
WtA4-1/x 160816 V175	WtA4-1	35.6244	-83.4206	17	280790	3944993	705.87	1330.86	WCP	0	43	sulfidic
WtA4-1/A 161117	WtA4-1	35.6244	-83.4206	17	280790	3944993	705.87	1330.86	WCP	0	43	sulfidic
WtA4-1/B 161117	WtA4-1	35.6244	-83.4206	17	280790	3944993	705.87	1330.86	WCP	0	43	sulfidic
WtA3-1/A 150527 41	WtA3-1	35.6251	-83.4199	17	280854	3945064	725.38	1237.88	WCP	yes	43	sulfidic
WtA3-1/B 150527 47	WtA3-1	35.6251	-83.4199	17	280854	3945064	725.38	1237.88	WCP	yes	43	sulfidic
WtA3-1/x 150829 146	WtA3-1	35.6251	-83.4199	17	280854	3945064	725.38	1237.88	WCP	yes	43	sulfidic
WtA3-1/A 151023 3323	WtA3-1	35.6251	-83.4199	17	280854	3945064	725.38	1237.88	WCP	yes	43	sulfidic
WtA3-1/B 151023 3496	WtA3-1	35.6251	-83.4199	17	280854	3945064	725.38	1237.88	WCP	yes	43	sulfidic
WtA3-1/x 151229	WtA3-1	35.6251	-83.4199	17	280854	3945064	725.38	1237.88	WCP	yes	43	sulfidic
WtA3-1/x 160220 JUG	WtA3-1	35.6251	-83.4199	17	280854	3945064	725.38	1237.88	WCP	yes	43	sulfidic
WtA3-1/x 160604 V175	WtA3-1	35.6251	-83.4199	17	280854	3945064	725.38	1237.88	WCP	yes	43	sulfidic
WtM1-1/B 150311 3282	WtM1-1	35.6237	-83.4165	17	281156	3944904	1067.08	1283.15	WCP	0	43	sulfidic
WtM1-1/A 150311 3056	WtM1-1	35.6237	-83.4165	17	281156	3944904	1067.08	1283.15	WCP	0	43	sulfidic
WtM1-1/A 150527 01	WtM1-1	35.6237	-83.4165	17	281156	3944904	1067.08	1283.15	WCP	0	43	sulfidic
WtM1-1/B 150527 02	WtM1-1	35.6237	-83.4165	17	281156	3944904	1067.08	1283.15	WCP	0	43	sulfidic

SampleID	Site Code	Catchment	Date	Year	Month	cond. uS/cm	pH	ANC ueq/L	Cl umol/L	NO3 umol/L	SO4 umol/L	Na umol/L	K umol/L	Mg umol/L	Ca umol/L	Al umol/L	Fe umol/L	Mn umol/L	Si umol/L	Elevation meters	Stream Order
WtM1-1/A 150829 B05	WtM1-1	WCP	150829	2015	8	16.35	5.69	4.09	10.18	13.29	39.33	22.31	3.12	16.83	23.73	0.838	0.025	0.031	58.07	1386.3	1
WtM1-1/B 150829 B06	WtM1-1	WCP	150829	2015	8	15.74	5.67	4.25	7.25	13.11	39.23	20.88	2.25	16.58	23.85	0.993	0.133	0.031	58.18	1386.3	1
WtM1-1/A 150925 B11	WtM1-1	WCP	150925	2015	9	19.95	5.50	1.94	13.65	33.71	41.67	23.49	8.95	23.25	30.42	2.976	0.238	0.220	53.05	1386.3	1
WtM1-1/B 150925 B20	WtM1-1	WCP	150925	2015	9	19.81	5.56	2.11	13.65	34.09	41.55	23.66	9.05	23.66	31.04	3.047	0.210	0.106	53.80	1386.3	1
WtM1-1/A 151023 3168	WtM1-1	WCP	151023	2015	10	17.76	5.65	2.63				32.45	6.34	18.84	27.42	0.597	0.070	0.022	58.50	1386.3	1
WtM1-1/B 151023 3174	WtM1-1	WCP	151023	2015	10	17.16	5.70	2.11				25.53	4.17	18.31	26.45	0.586	0.038	0.033	56.90	1386.3	1
WtM1-1/x 151229	WtM1-1	WCP	151229	2015	12	17.81	5.19	-7.52	9.90	31.42	37.98	20.53	4.60	16.83	27.32	4.032	0.233	0.319	56.04	1386.3	1
WtM1-1/x 160604 V175	WtM1-1	WCP	160604	2016	6	14.68	5.51	-2.98	8.55	17.43	37.02	19.53	3.40	14.77	23.98	1.531	0.079	0.042	53.52	1386.3	1
WtM1-1/x 160816 V175	WtM1-1	WCP	160816	2016	8	14.57	5.68	1.14	13.43	15.03	38.54	27.19	10.21	4.81	25.97	1.338	0.027	0.051	60.96	1386.3	1
WtM1-1/x 161007 v175	WtM1-1	WCP	161007	2016	10	17.56	6.06	12.03	13.76	20.06	42.00	28.45	5.50	24.52	38.62	1.605	0.140	0.162	64.20	1386.3	1
WtA3-2/x 160407 6123	WtA3-2	WCP	160407	2016	4	31.77	4.40	-44.65	9.56	11.40	61.19	11.79	1.87	20.70	21.18	10.915	2.888	0.950	29.20	1392.5	1
WtA3-2b/A 160506 6125	WtA3-2	WCP	160506	2016	5	30.36	4.47	-42.29	6.94	24.58	58.90	10.61	2.48	20.20	24.13	16.808	1.280	1.101	33.75	1392.5	1
WtA3-2/x 160506 1916	WtA3-2	WCP	160506	2016	5	31.57	4.39	-45.39	5.64	7.69	62.12	11.27	1.28	20.61	21.38	11.986	4.944	0.868	28.27	1392.5	1
WtA3-2b/B 160506 5860	WtA3-2	WCP	160506	2016	5	30.47	4.47	-37.04	7.56	24.29	58.48	10.83	2.71	20.12	23.20	17.034	1.257	1.101	33.68	1392.5	1
WtA3-2/x 160521 3168	WtA3-2	WCP	160521	2016	5	37.30	4.26	-61.55	6.01	8.68	77.14	10.13	2.51	22.34	24.23	14.832	3.716	0.956	30.05	1392.5	1
WtA3-2/x 160604 V175	WtA3-2	WCP	160604	2016	6	29.06	4.43	-44.68	5.78	5.53	61.97	12.53	1.84	19.05	20.34	8.795	1.415	0.874	33.22	1392.5	1
WtA3-2/x 160816 V175	WtA3-2	WCP	160816	2016	8	30.11	4.41	-47.15	10.21	10.02	60.89	13.35	12.12	3.62	21.03	10.318	2.398	0.963	45.90	1392.5	1
WtA3-2/x 161007 v175	WtA3-2	WCP	161007	2016	10	29.71	4.77	-22.39	17.66	8.05	72.35	21.40	4.96	29.29	31.31	14.525	1.293	1.338	59.32	1392.5	1
WtA3-2/A 161117	WtA3-2	WCP	161117	2016	11	30.58	4.76	-19.38	18.00	11.03	73.60	19.97	3.58	32.38	28.02	16.789	0.673	1.460	58.57	1392.5	1
WtA3-2/B 161117	WtA3-2	WCP	161117	2016	11	31.09	4.61	-28.06	17.38	10.71	74.02	20.14	3.35	32.50	27.75	16.474	0.417	1.456	57.89	1392.5	1
WtA3-2/C 161117	WtA3-2	WCP	161117	2016	11	30.89	4.58	-32.96	18.95	10.76	72.23	21.84	3.91	31.80	30.42	16.111	1.422	1.471	58.61	1392.5	1
WtA3-2/D 161117	WtA3-2	WCP	161117	2016	11	30.27	4.62	-26.87	18.64	10.52	72.91	25.45	4.25	32.75	28.29	16.926	0.702	1.471	58.25	1392.5	1
WtA3-2/E 161117	WtA3-2	WCP	161117	2016	11	30.78	4.61	-28.23	20.03	11.64	70.97	26.66	4.40	32.01	31.21	15.414	0.535	1.423	59.43	1392.5	1
WtM1-2/x 160521 3393	WtM1-2	WCP	160521	2016	5	14.50	5.59	2.57	7.47	15.95	36.41	20.23	3.58	15.02	23.75	1.531	0.073	0.046	50.35	1402.5	1
WtM1-2/A 161117	WtM1-2	WCP	161117	2016	11	17.76	5.53	-0.38	11.54	33.77	41.90	30.06	3.40	26.33	30.17	0.371	0.002	0.046	57.00	1402.5	1
WtM1-2/B 161117	WtM1-2	WCP	161117	2016	11	17.64	5.61	1.26	10.24	33.56	40.73	29.53	3.17	26.46	29.79	0.363	0.002	0.036	57.04	1402.5	1
WtM1-2/C 161117	WtM1-2	WCP	161117	2016	11	17.82	5.65	3.83	10.35	34.24	41.30	30.01	3.50	26.37	30.02	0.267	0.002	0.036	57.11	1402.5	1
WtM1-2/D 161117	WtM1-2	WCP	161117	2016	11	17.71	5.69	1.01	11.96	33.90	40.75	31.01	4.35	26.33	30.14	0.163	0.002	0.038	56.97	1402.5	1
WtM1-2/E 161117	WtM1-2	WCP	161117	2016	11	17.76	5.65	0.30	10.63	33.34	40.98	29.62	3.43	26.50	30.02	0.241	0.047	0.042	57.47	1402.5	1
WtA1-1/A 150912 B15	WtA1-1	WCP	150912	2015	9	33.38	4.45	-42.94	14.39	3.03	76.31	10.96	4.17	20.98	19.31	13.398	1.062	1.443	41.52	1403.9	1
WtA1-1/B 150912 B14	WtA1-1	WCP	150912	2015	9	34.59	4.44	-44.38	10.61	9.34	76.28	11.92	3.94	21.07	19.16	13.531	1.019	1.478	41.77	1403.9	1
WtA1-1/A 150918 B18	WtA1-1	WCP	150918	2015	9	35.69	4.51	-40.24	16.36	11.71	73.87	19.62	5.09	21.68	21.18	14.495	0.636	1.567	43.76	1403.9	1
WtA1-1/B 150918 B24	WtA1-1	WCP	150918	2015	9	35.59	4.50	-48.01	9.79	11.48	75.24	13.05	3.96	21.89	19.49	14.228	0.861	1.469	42.48	1403.9	1
WtA1-1/x 160414 6155	WtA1-1	WCP	160414	2016	4	31.87	4.43	-39.55	13.88	17.31	65.54	18.18	11.94	8.06	34.56	1.208	0.036	0.080	53.55	1403.9	1
WtA1-1/x 160831 JUG	WtA1-1	WCP	160831	2016	8	31.57	4.39	-46.48	7.47	17.93	69.47	9.87	2.10	22.42	19.96	17.508	3.393	1.516	45.43	1403.9	1
WtA1-1/A 161115	WtA1-1	WCP	161115	2016	11	25.81	4.61	-29.56	11.90	12.13	75.16	17.05	3.17	30.57	24.83	17.293	0.793	2.131	48.35	1403.9	1
WtA1-1/B 161115	WtA1-1	WCP	161115	2016	11	26.49	4.48	-33.89	12.61	11.93	74.86	16.18	3.32	29.05	23.10	19.002	1.098	2.164	48.42	1403.9	1
WtA1-1/C 161115	WtA1-1	WCP	161115	2016	11	26.32	4.48	-34.63	11.90	12.35	74.56	15.35	3.17	29.50	23.80	19.069	0.833	2.192	48.14	1403.9	1
WtA1-1/D 161115	WtA1-1	WCP	161115	2016	11	26.57	4.47	-39.90	11.40	11.98	74.68	14.27	2.94	28.88	22.86	19.784	0.917	2.175	48.28	1403.9	1
WtA1-1/E 161115	WtA1-1	WCP	161115	2016	11	26.83	4.47	-36.64	13.09	12.08	75.51	15.70	3.27	28.84	22.81	18.946	0.023	2.175	48.64	1403.9	1
WtA1-1/B 161115	WtA1-1	WCP	161115	2016	11	26.49	4.48	-33.89	12.61	11.93	74.86	16.18	3.32	29.05	23.10	19.002	1.098	2.164	48.42	1403.9	1
WtA1-1/C 161115	WtA1-1	WCP	161115	2016	11	26.32	4.48	-34.63	11.90	12.35	74.56	15.35	3.17	29.50	23.80	19.069	0.833	2.192	48.14	1403.9	1
WtA1-1/D 161115	WtA1-1	WCP	161115	2016	11	26.57	4.47	-39.90	11.40	11.98	74.68	14.27	2.94	28.88	22.86	19.784	0.917	2.175	48.28	1403.9	1
WtA1-1/E 161115	WtA1-1	WCP	161115	2016	11	26.83	4.47	-36.64	13.09	12.08	75.51	15.70	3.27	28.84	22.81	18.946	0.023	2.175	48.64	1403.9	1
WtX1-1/x 160831 V175	WtX1-1	WCP	160831	2016	8	11.13	5.55	1.45	8.94	21.89	22.99	22.44	2.07	13.21	19.99	0.619	0.125	0.102	63.06	1404.3	1
WtX1-1/A 161115	WtX1-1	WCP	161115	2016	11	11.23	5.53	0.18	11.28	22.26	26.17	32.58	4.99	15.84	19.94	0.400	0.029	0.100	69.64	1404.3	1
WtM2-2/x 150208 3386	WtM2-2	WCP	150208	2015	2	18.21	5.79	9.24	8.49	25.47	32.78	49.46	12.05	90.97	27.99	0.897	0.064	0.007	56.19	1426	1
WtM2-2/x 150304 2977	WtM2-2	WCP	150304	2015	3	17.14	5.34	-2.61	8.35	32.35	28.42	51.20	12.61	91.83	27.86	0.808	0.034	0.000	55.47	1426	1
WtM2-2/A 150716 122	WtM2-2	WCP	150716	2015	7	16.07	5.76	5.04	4.12	8.29	14.51	25.45	4.60	13.00	29.32	1.182	0.054	0.049	61.10	1426	1
WtM2-2/B 150716 144	WtM2-2	WCP	150716	2015	7	16.54	5.95	7.08	4.85	8.40	14.54	26.97	4.81	13.04	30.24	1.538	0.133	0.015	62.02	1426	1
WtM2-2/A 150829 B03	WtM2-2	WCP	150829	2015	8	18.08	6.00	11.49	11.73	20.50	39.17	26.58	3.89	18.27	31.84	0.675	0.043	0.002	62.74	1426	1
WtM2-2/B 150829 B04	WtM2-2	WCP	150829	2015	8	18.01	6.00	17.86	11.14	20.30	39.15	26.23	4.09	18.35	31.71	0.697	0.020	0.004	63.34	1426	1
WtM2-2/x 150925 136	WtM2-2	WCP	150925	2015	9	18.72	5.93	14.11	13.23	36.17	35.11	26.66	9.28	20.98	34.63	1.972	0.066	0.013	53.55	1426	1
WtM2-2/A 151023 B30	WtM2-2	WCP	151023	2015	10	22.02	5.92	7.35				29.58	5.47	19.54	34.31	1.175	0.068	0.046	63.73	1426	1
WtM2-2/B 151023 137	WtM2-2	WCP	151023	2015	10	19.42	6.14	15.29				29.06	5.37	19.75	33.66	1.075	0.070	0.020	63.81	1426	1
WtM2-2/x 151229	WtM2-2	WCP	151229	2015	12	14.75	5.20	-7.31	10.35	23.22	32.44	17.83	4.78	10.62	24.48	3.473	0.179	0.209	55.12	1426	1
WtM2-2b/x 151229	WtM2-2	WCP	151229	2015	12	11.99	5.14	-8.55	10.97	10.32	23.29	13.44	2.20	7.74	13.90	5.782	0.090	0.289	46.61	1426	1
WtM2-2/x 160521 3380	WtM2-2	WCP	160521	2016	5	14.48	5.68	5.25	6.97	20.87	33.02	20.36	3.71	13.82	26.57	2.038	0.052	0.027	51.84	1426	1
WtM2-2/x 160701 V250	WtM2-2	WCP	160701	2016	7	16.60	6.08	16.27												1426	1
WtM2-2/x 160816 V175	WtM2-2	WCP	160816	2016	8	17.15	6.33	29.07	10.97	20.80	39.58	27.23	10.84	4.98	43.76	1.271	0.061	0.025	66.76	1426	1
WtA1-2/x 160414 5824	WtA1-2	WCP	160414	2016	4	31.37	4.50	-34.54	23.92	17.43	67.93	47.20	7.65	20.61	30.12	0.274	0.020	0.016	93.75	1426.6	1
WtK1b/A 150912 B12	WtK1b	WCP	150912	2015	9	16.72	5.79	11.70	9.82	16.97	37.73	22.31	4.73	18.02	27.37	1.205	0.267	0.046	51.66	1431	1

SampleID	Site Code	Latitude	Longitude	UTM	Easting meters	Northing meters	Dist2Knob meters	Dist2Blvd meters	SubWtrShed	Distrubance	Bedrock Code	Bedrock GROUP
WtM1-1/A 150829 B05	WtM1-1	35.6237	-83.4165	17	281156	3944904	1067.08	1283.15	WCP	0	43	sulfidic
WtM1-1/B 150829 B06	WtM1-1	35.6237	-83.4165	17	281156	3944904	1067.08	1283.15	WCP	0	43	sulfidic
WtM1-1/A 150925 B11	WtM1-1	35.6237	-83.4165	17	281156	3944904	1067.08	1283.15	WCP	0	43	sulfidic
WtM1-1/B 150925 B20	WtM1-1	35.6237	-83.4165	17	281156	3944904	1067.08	1283.15	WCP	0	43	sulfidic
WtM1-1/A 151023 3168	WtM1-1	35.6237	-83.4165	17	281156	3944904	1067.08	1283.15	WCP	0	43	sulfidic
WtM1-1/B 151023 3174	WtM1-1	35.6237	-83.4165	17	281156	3944904	1067.08	1283.15	WCP	0	43	sulfidic
WtM1-1/x 151229	WtM1-1	35.6237	-83.4165	17	281156	3944904	1067.08	1283.15	WCP	0	43	sulfidic
WtM1-1/x 160604 V175	WtM1-1	35.6237	-83.4165	17	281156	3944904	1067.08	1283.15	WCP	0	43	sulfidic
WtM1-1/x 160816 V175	WtM1-1	35.6237	-83.4165	17	281156	3944904	1067.08	1283.15	WCP	0	43	sulfidic
WtM1-1/x 161007 v175	WtM1-1	35.6237	-83.4165	17	281156	3944904	1067.08	1283.15	WCP	0	43	sulfidic
WtA3-2/x 160407 6123	WtA3-2	35.6258	-83.4200	17	280846	3945150	683.76	1166.75	WCP	yes	43	sulfidic
WtA3-2b/A 160506 6125	WtA3-2	35.6258	-83.4200	17	280846	3945150	683.76	1166.75	WCP	yes	43	sulfidic
WtA3-2/x 160506 1916	WtA3-2	35.6258	-83.4200	17	280846	3945150	683.76	1166.75	WCP	yes	43	sulfidic
WtA3-2b/B 160506 5860	WtA3-2	35.6258	-83.4200	17	280846	3945150	683.76	1166.75	WCP	yes	43	sulfidic
WtA3-2/x 160521 3168	WtA3-2	35.6258	-83.4200	17	280846	3945150	683.76	1166.75	WCP	yes	43	sulfidic
WtA3-2/x 160604 V175	WtA3-2	35.6258	-83.4200	17	280846	3945150	683.76	1166.75	WCP	yes	43	sulfidic
WtA3-2/x 160816 V175	WtA3-2	35.6258	-83.4200	17	280846	3945150	683.76	1166.75	WCP	yes	43	sulfidic
WtA3-2/x 161007 v175	WtA3-2	35.6258	-83.4200	17	280846	3945150	683.76	1166.75	WCP	yes	43	sulfidic
WtA3-2/A 161117	WtA3-2	35.6258	-83.4200	17	280846	3945150	683.76	1166.75	WCP	yes	43	sulfidic
WtA3-2/B 161117	WtA3-2	35.6258	-83.4200	17	280846	3945150	683.76	1166.75	WCP	yes	43	sulfidic
WtA3-2/C 161117	WtA3-2	35.6258	-83.4200	17	280846	3945150	683.76	1166.75	WCP	yes	43	sulfidic
WtA3-2/D 161117	WtA3-2	35.6258	-83.4200	17	280846	3945150	683.76	1166.75	WCP	yes	43	sulfidic
WtA3-2/E 161117	WtA3-2	35.6258	-83.4200	17	280846	3945150	683.76	1166.75	WCP	yes	43	sulfidic
WtM1-2/x 160521 3393	WtM1-2	35.6221	-83.4157	17	281222.8	3944722.3	1216.17	1449.61	WCP	0	43	sulfidic
WtM1-2/A 161117	WtM1-2	35.6221	-83.4157	17	281222.8	3944722.3	1216.17	1449.61	WCP	0	43	sulfidic
WtM1-2/B 161117	WtM1-2	35.6221	-83.4157	17	281222.8	3944722.3	1216.17	1449.61	WCP	0	43	sulfidic
WtM1-2/C 161117	WtM1-2	35.6221	-83.4157	17	281222.8	3944722.3	1216.17	1449.61	WCP	0	43	sulfidic
WtM1-2/D 161117	WtM1-2	35.6221	-83.4157	17	281222.8	3944722.3	1216.17	1449.61	WCP	0	43	sulfidic
WtM1-2/E 161117	WtM1-2	35.6221	-83.4157	17	281222.8	3944722.3	1216.17	1449.61	WCP	0	43	sulfidic
WtA1-1/A 150912 B15	WtA1-1	35.6259	-83.4144	17	281350	3945142	1171.13	1017.73	WCP	yes	43	sulfidic
WtA1-1/B 150912 B14	WtA1-1	35.6259	-83.4144	17	281350	3945142	1171.13	1017.73	WCP	yes	43	sulfidic
WtA1-1/A 150918 B18	WtA1-1	35.6259	-83.4144	17	281350	3945142	1171.13	1017.73	WCP	yes	43	sulfidic
WtA1-1/B 150918 B24	WtA1-1	35.6259	-83.4144	17	281350	3945142	1171.13	1017.73	WCP	yes	43	sulfidic
WtA1-1/x 160414 6155	WtA1-1	35.6259	-83.4144	17	281350	3945142	1171.13	1017.73	WCP	yes	43	sulfidic
WtA1-1/x 160831 JUG	WtA1-1	35.6259	-83.4144	17	281350	3945142	1171.13	1017.73	WCP	yes	43	sulfidic
WtA1-1/A 161115	WtA1-1	35.6259	-83.4144	17	281350	3945142	1171.13	1017.73	WCP	yes	43	sulfidic
WtA1-1/B 161115	WtA1-1	35.6259	-83.4144	17	281350	3945142	1171.13	1017.73	WCP	yes	43	sulfidic
WtA1-1/C 161115	WtA1-1	35.6259	-83.4144	17	281350	3945142	1171.13	1017.73	WCP	yes	43	sulfidic
WtA1-1/D 161115	WtA1-1	35.6259	-83.4144	17	281350	3945142	1171.13	1017.73	WCP	yes	43	sulfidic
WtA1-1/E 161115	WtA1-1	35.6259	-83.4144	17	281350	3945142	1171.13	1017.73	WCP	yes	43	sulfidic
WtA1-1/B 161115	WtA1-1	35.6259	-83.4144	17	281350	3945142	1171.13	1017.73	WCP	yes	43	sulfidic
WtA1-1/C 161115	WtA1-1	35.6259	-83.4144	17	281350	3945142	1171.13	1017.73	WCP	yes	43	sulfidic
WtA1-1/D 161115	WtA1-1	35.6259	-83.4144	17	281350	3945142	1171.13	1017.73	WCP	yes	43	sulfidic
WtA1-1/E 161115	WtA1-1	35.6259	-83.4144	17	281350	3945142	1171.13	1017.73	WCP	yes	43	sulfidic
WtX1-1/x 160831 V175	WtX1-1	35.6255	-83.4146	17	281332.7	3945101.5	1163.52	1059.65	WCP	0	43	sulfidic
WtX1-1/A 161115	WtX1-1	35.6255	-83.4146	17	281332.7	3945101.5	1163.52	1059.65	WCP	0	43	sulfidic
WtM2-2/x 150208 3386	WtM2-2	35.6200	-83.4178	17	281028	3944498	1212.20	1707.70	WCP	0	43	sulfidic
WtM2-2/x 150304 2977	WtM2-2	35.6200	-83.4178	17	281028	3944498	1212.20	1707.70	WCP	0	43	sulfidic
WtM2-2/A 150716 122	WtM2-2	35.6200	-83.4178	17	281028	3944498	1212.20	1707.70	WCP	0	43	sulfidic
WtM2-2/B 150716 144	WtM2-2	35.6200	-83.4178	17	281028	3944498	1212.20	1707.70	WCP	0	43	sulfidic
WtM2-2/A 150829 B03	WtM2-2	35.6200	-83.4178	17	281028	3944498	1212.20	1707.70	WCP	0	43	sulfidic
WtM2-2/B 150829 B04	WtM2-2	35.6200	-83.4178	17	281028	3944498	1212.20	1707.70	WCP	0	43	sulfidic
WtM2-2/x 150925 136	WtM2-2	35.6200	-83.4178	17	281028	3944498	1212.20	1707.70	WCP	0	43	sulfidic
WtM2-2/A 151023 B30	WtM2-2	35.6200	-83.4178	17	281028	3944498	1212.20	1707.70	WCP	0	43	sulfidic
WtM2-2/B 151023 137	WtM2-2	35.6200	-83.4178	17	281028	3944498	1212.20	1707.70	WCP	0	43	sulfidic
WtM2-2/x 151229	WtM2-2	35.6200	-83.4178	17	281028	3944498	1212.20	1707.70	WCP	0	43	sulfidic
WtM2-2b/x 151229	WtM2-2	35.6200	-83.4178	17	281028	3944498	1212.20	1707.70	WCP	0	43	sulfidic
WtM2-2/x 160521 3380	WtM2-2	35.6200	-83.4178	17	281028	3944498	1212.20	1707.70	WCP	0	43	sulfidic
WtM2-2/x 160701 V250	WtM2-2	35.6200	-83.4178	17	281028	3944498	1212.20	1707.70	WCP	0	43	sulfidic
WtM2-2/x 160816 V175	WtM2-2	35.6200	-83.4178	17	281028	3944498	1212.20	1707.70	WCP	0	43	sulfidic
WtA1-2/x 160414 5824	WtA1-2	35.6269	-83.4147	17	281328	3945251	1131.33	911.54	WCP	yes	43	sulfidic
WtK1b/A 150912 B12	WtK1b	35.6280	-83.4098	17	281778	3945366	1573.15	860.45	WCP	0	43	sulfidic

SampleID	Site Code	Catchment	Date	Year	Month	cond. uS/cm	pH	ANC ueq/L	Cl umol/L	NO3 umol/L	SO4 umol/L	Na umol/L	K umol/L	Mg umol/L	Ca umol/L	Al umol/L	Fe umol/L	Mn umol/L	Si umol/L	Elevation meters	Stream Order
WtK1b/B 150912 B28	WtK1b	WCP	150912	2015	9	16.80	5.83	8.77	9.53	21.95	37.25	22.05	3.91	18.14	27.67	0.775	0.082	0.022	52.16	1431	1
WtK1/x 150422 NPS	WtK1	WCP	150422	2015	4	13.42	5.52	3.23	2.62	8.43	11.60	17.66	3.81	13.25	20.58	2.431	0.127	0.042	47.46	1438.1	1
WtM6N-2/x 150829 B02	WtM6N-2	WCP	150829	2015	8	19.04	5.68	4.19	16.95	25.29	37.88	31.67	7.34	16.33	28.49	1.130	0.088	0.038	61.70	1455.6	1
WtM6N-2/A 151023 3128	WtM6N-2	WCP	151023	2015	10	17.57	5.71	3.09				28.32	5.88	16.25	29.17	1.138	0.048	0.024	64.70	1455.6	1
WtM6N-2/B 151023 3500	WtM6N-2	WCP	151023	2015	10	22.92	5.34	-7.92				26.32	5.65	16.75	30.09	2.020	0.398	0.035	64.37	1455.6	1
WtM6N-2/x 151229	WtM6N-2	WCP	151229	2015	12	14.81	5.40	-5.05	18.08	29.43	23.34	17.40	5.75	9.26	20.24	4.510	0.054	0.269	55.01	1455.6	1
WtM6N-2/x 160220a v16	WtM6N-2	WCP	160220	2016	2	12.34	5.40	-4.20	8.26	30.64	36.53	18.49	4.58	14.07	27.35	1.668	0.023	0.075	46.32	1455.6	1
WtM6-2N/x 160521 3500	WtM6N-2	WCP	160521	2016	5	14.34	5.50	1.21	6.94	26.90	30.46	17.40	5.14	12.71	24.90	1.634	0.036	0.040	49.35	1455.6	1
WtM6N-2/x 160816 V175	WtM6N-2	WCP	160816	2016	8	14.18	5.50	-2.09	7.93	22.71	36.25	21.23	8.88	2.55	27.10	1.883	0.030	0.078	63.02	1455.6	1
WtM6N-2/x 161007 v175	WtM6N-2	WCP	161007	2016	10	18.50	5.75	0.59	13.91	43.16	42.70	34.71	3.22	22.09	33.68	1.672	0.100	0.066	74.13	1455.6	1
WtM6N-2/A 161117	WtM6N-2	WCP	161117	2016	11	20.51	6.07	10.84	10.58	43.06	42.30	34.89	6.09	25.63	40.17	0.752	0.500	0.015	69.47	1455.6	1
WtM6N-2/B 161117	WtM6N-2	WCP	161117	2016	11	20.72	6.08	12.47	11.03	45.11	43.35	36.67	15.09	25.84	40.77	0.871	0.138	0.016	69.22	1455.6	1
WtM6N-2/C 161117	WtM6N-2	WCP	161117	2016	11	20.72	6.09	11.62	10.58	43.69	42.45	34.15	5.88	25.92	40.80	0.838	0.090	0.018	68.54	1455.6	1
WtM6N-2/D 161117	WtM6N-2	WCP	161117	2016	11	20.41	6.09	12.03	10.63	42.77	41.91	33.80	5.63	25.22	40.25	0.467	0.147	0.016	68.61	1455.6	1
WtM6N-2/E 161117	WtM6N-2	WCP	161117	2016	11	20.92	6.19	15.63	9.65	42.40	40.42	32.80	5.60	25.67	40.60	0.823	0.292	0.024	67.61	1455.6	1
WtM6S-2/A 150716 132	WtM6S-2	WCP	150716	2015	7	14.83	5.50	-2.80	4.43	12.98	9.85	26.58	9.72	9.50	21.38	1.390	0.038	0.115	65.30	1463.5	1
WtM6S-2/B 150716 136	WtM6S-2	WCP	150716	2015	7	14.20	5.39	-3.41	3.33	12.98	9.79	25.14	5.58	9.59	22.26	1.475	0.134	0.113	65.91	1463.5	1
WtM6S-2/x 150829 B01	WtM6S-2	WCP	150829	2015	8	14.52	5.39	-4.13	8.01	26.80	24.09	23.49	2.97	10.53	19.19	0.871	0.034	0.067	67.37	1463.5	1
WtM6S-2/A 151023 2991	WtM6S-2	WCP	151023	2015	10	14.78	5.59	0.86				27.10	5.50	10.99	21.91	0.856	0.030	0.033	71.28	1463.5	1
WtM6S-2/B 151023 3380	WtM6S-2	WCP	151023	2015	10	14.90	5.51	-2.64				26.93	5.45	11.60	22.21	0.908	0.029	0.073	70.96	1463.5	1
WtM6S-2/x 151229	WtM6S-2	WCP	151229	2015	12	14.37	5.14	-9.77	8.41	20.45	28.69	28.45	9.57	8.60	18.16	3.106	0.097	0.200	61.13	1463.5	1
WtM6S-2/x 160220a v15	WtM6S-2	WCP	160220	2016	2	11.44	5.54	0.20	10.97	34.14	24.32	25.88	6.57	11.15	23.18	1.056	0.029	0.044	64.91	1463.5	1
WtM6-2S/x 160521 3128	WtM6S-2	WCP	160521	2016	5	12.70	5.46	-1.80	7.16	27.56	23.65	21.84	5.58	10.08	20.11	1.227	0.030	0.024	62.77	1463.5	1
WtM6S-2/x 160816 V175	WtM6S-2	WCP	160816	2016	8	13.10	5.50	-3.93	14.86	29.22	25.25	29.97	6.37	7.49	21.01	1.405	0.020	0.047	69.47	1463.5	1
WtM6-2Sb/x 151229	WtM6S-2b	WCP	151229	2015	12	12.97	5.05	-11.42	9.84	12.92	26.44	17.88	5.14	5.88	13.85	6.338	0.063	0.229	57.68	1463.5	1
WtM6-2Sb/x 160521 3056	WtM6S-2b	WCP	160521	2016	5	12.35	5.21	-5.79	6.91	18.39	24.69	17.57	4.42	8.27	16.24	2.576	0.047	0.124	57.40	1463.5	1
WtA2-1/A 150912 B21	WtA2-1	WCP	150912	2015	9	19.23	4.90	-16.06	12.04	23.77	43.01	15.62	2.35	14.89	21.51	3.962	0.161	0.626	38.45	1465.1	1
WtA2-1/B 150912 B23	WtA2-1	WCP	150912	2015	9	19.19	4.92	-13.20	11.09	23.74	37.52	15.05	2.15	14.65	21.28	4.132	0.251	0.593	38.63	1465.1	1
WtM2-4/A 161117	WtM2-4	WCP	161117	2016	11	19.72	6.04	10.48	12.16	45.85	39.39	33.19	4.83	24.89	37.20	0.597	0.002	0.018	66.65	1466.8	1
WtM2-4/B 161117	WtM2-4	WCP	161117	2016	11	19.63	5.98	10.43	11.62	48.00	39.32	34.71	5.42	25.14	37.40	0.586	0.133	0.024	67.01	1466.8	1
WtM2-4/C 161117	WtM2-4	WCP	161117	2016	11	20.21	6.05	11.22	13.29	46.32	39.46	34.97	5.55	25.02	37.53	0.497	0.002	0.022	66.94	1466.8	1
WtM2-4/D 161117	WtM2-4	WCP	161117	2016	11	20.51	6.03	10.83	13.91	46.92	40.42	35.23	5.55	25.10	37.53	0.597	0.002	0.020	67.22	1466.8	1
WtM2-4/E 161117	WtM2-4	WCP	161117	2016	11	20.31	5.99	9.01	12.35	47.00	40.48	34.49	5.42	25.06	37.68	0.504	0.002	0.024	67.29	1466.8	1
WtK2/x 150803 H5010	WtK2	WCP	150803	2015	8	14.13	6.08	11.19	6.91	19.21	29.38	20.97	3.22	14.32	26.27	0.604	0.029	0.016	55.08	1556.2	1

SampleID	Site Code	Latitude	Longitude	UTM	Easting meters	Northing meters	Dist2Knob meters	Dist2Blvd meters	SubWtrShed	Distrubance	Bedrock Code	Bedrock GROUP
WtK1b/B 150912 B28	WtK1b	35.6280	-83.4098	17	281778	3945366	1573.15	860.45	WCP	0	43	sulfidic
WtK1/x 150422 NPS	WtK1	35.6279	-83.4095	17	281806	3945349	1601.47	887.36	WCP	0	43	sulfidic
WtM6N-2/x 150829 B02	WtM6N-2	35.6174	-83.4188	17	280932	3944208	1385.98	2012.39	WCP	0	43	sulfidic
WtM6N-2/A 151023 3128	WtM6N-2	35.6174	-83.4188	17	280932	3944208	1385.98	2012.39	WCP	0	43	sulfidic
WtM6N-2/B 151023 3500	WtM6N-2	35.6174	-83.4188	17	280932	3944208	1385.98	2012.39	WCP	0	43	sulfidic
WtM6N-2/x 151229	WtM6N-2	35.6174	-83.4188	17	280932	3944208	1385.98	2012.39	WCP	0	43	sulfidic
WtM6N-2/x 160220a v16	WtM6N-2	35.6174	-83.4188	17	280932	3944208	1385.98	2012.39	WCP	0	43	sulfidic
WtM6-2N/x 160521 3500	WtM6N-2	35.6174	-83.4188	17	280932	3944208	1385.98	2012.39	WCP	0	43	sulfidic
WtM6N-2/x 160816 V175	WtM6N-2	35.6174	-83.4188	17	280932	3944208	1385.98	2012.39	WCP	0	43	sulfidic
WtM6N-2/x 161007 v175	WtM6N-2	35.6174	-83.4188	17	280932	3944208	1385.98	2012.39	WCP	0	43	sulfidic
WtM6N-2/A 161117	WtM6N-2	35.6174	-83.4188	17	280932	3944208	1385.98	2012.39	WCP	0	43	sulfidic
WtM6N-2/B 161117	WtM6N-2	35.6174	-83.4188	17	280932	3944208	1385.98	2012.39	WCP	0	43	sulfidic
WtM6N-2/C 161117	WtM6N-2	35.6174	-83.4188	17	280932	3944208	1385.98	2012.39	WCP	0	43	sulfidic
WtM6N-2/D 161117	WtM6N-2	35.6174	-83.4188	17	280932	3944208	1385.98	2012.39	WCP	0	43	sulfidic
WtM6N-2/E 161117	WtM6N-2	35.6174	-83.4188	17	280932	3944208	1385.98	2012.39	WCP	0	43	sulfidic
WtM6S-2/A 150716 132	WtM6S-2	35.6166	-83.4201	17	280815	3944124	1403.49	2125.07	WCP	0	43	sulfidic
WtM6S-2/B 150716 136	WtM6S-2	35.6166	-83.4201	17	280815	3944124	1403.49	2125.07	WCP	0	43	sulfidic
WtM6S-2/x 150829 B01	WtM6S-2	35.6166	-83.4201	17	280815	3944124	1403.49	2125.07	WCP	0	43	sulfidic
WtM6S-2/A 151023 2991	WtM6S-2	35.6166	-83.4201	17	280815	3944124	1403.49	2125.07	WCP	0	43	sulfidic
WtM6S-2/B 151023 3380	WtM6S-2	35.6166	-83.4201	17	280815	3944124	1403.49	2125.07	WCP	0	43	sulfidic
WtM6S-2/x 151229	WtM6S-2	35.6166	-83.4201	17	280815	3944124	1403.49	2125.07	WCP	0	43	sulfidic
WtM6S-2/x 160220a v15	WtM6S-2	35.6166	-83.4201	17	280815	3944124	1403.49	2125.07	WCP	0	43	sulfidic
WtM6-2S/x 160521 3128	WtM6S-2	35.6166	-83.4201	17	280815	3944124	1403.49	2125.07	WCP	0	43	sulfidic
WtM6S-2/x 160816 V175	WtM6S-2	35.6166	-83.4201	17	280815	3944124	1403.49	2125.07	WCP	0	43	sulfidic
WtM6-2Sb/x 151229	WtM6S-2b	35.6166	-83.4201	17	280815	3944124	1403.49	2125.07	WCP	0	43	sulfidic
WtM6-2Sb/x 160521 3056	WtM6S-2b	35.6166	-83.4201	17	280815	3944124	1403.49	2125.07	WCP	0	43	sulfidic
WtA2-1/A 150912 B21	WtA2-1	35.6298	-83.4076	17	281976	3945559	1779.24	804.32	WCP	0	43	sulfidic
WtA2-1/B 150912 B23	WtA2-1	35.6298	-83.4076	17	281976	3945559	1779.24	804.32	WCP	0	43	sulfidic
WtM2-4/A 161117	WtM2-4	35.6189	-83.4167	17	281122	3944372	1368.63	1811.60	WCP	0	43	sulfidic
WtM2-4/B 161117	WtM2-4	35.6189	-83.4167	17	281122	3944372	1368.63	1811.60	WCP	0	43	sulfidic
WtM2-4/C 161117	WtM2-4	35.6189	-83.4167	17	281122	3944372	1368.63	1811.60	WCP	0	43	sulfidic
WtM2-4/D 161117	WtM2-4	35.6189	-83.4167	17	281122	3944372	1368.63	1811.60	WCP	0	43	sulfidic
WtM2-4/E 161117	WtM2-4	35.6189	-83.4167	17	281122	3944372	1368.63	1811.60	WCP	0	43	sulfidic
WtK2/x 150803 H5010	WtK2	35.6269	-83.4004	17	282622	3945222	2422.69	1508.83	WCP	0	43	sulfidic

APPENDIX C
RAW DATA – CHAPTER 5

SampleID	Site Code	Catchment	Date	Year	Month	Cond.	pH	ANC	Cl	NO3	SO4	SO4 uEqL	Na	K	Mg	Mg uEqL	Ca	Ca uEqL	Al	Fe	Mn	Si	Elevation
						uS/cm		ueq/L	umol/L	umol/L	umol/L		umol/L	umol/L	umol/L		umol/L		umol/L	umol/L	umol/L	umol/L	meters
BFP1b/x 160801 V175	BFP1b	BFP	160801	2016	8	24.67	6.59	96.39	17.18	55.11	56.44	28.22	63.25	11.66	59.49	29.75	132.39	66.20	0.237		0.007	140.50	1510.9
BFP1/x 161007 V175	BFP1	BFP	161007	2016	10	28.25	6.63	117.23	12.52	53.32	45.01	22.51	63.72	9.87	64.51	32.26	144.42	72.21	0.096	0.029	0.025	146.16	1555.7
BFP2/x 161007 V175	BFP2	BFP	161007	2016	10	27.10	6.61	87.29	17.69	52.64	60.56	30.28	64.64	10.03	59.16	29.58	126.15	63.08	0.282	0.043	0.022	129.68	1491.9
BFP1/M 161115	BFP1	BFP	161115	2016	11	27.34	6.83	148.07	14.70	51.32	59.02	29.51	75.41	11.61	78.96	39.48	172.34	86.17	0.004	0.004	0.003	150.18	1555.7
BFP2/M 161123	BFP2	BFP	161123	2016	11	29.67	6.59	94.41	18.75	51.92	77.30	38.65	67.09	11.57	70.93	35.47	137.38	68.69	0.098	0.004	0.019	120.81	1491.9
NDNE/M 161116	NDNE	NDW	161116	2016	11	11.25	5.95	8.66	10.18	18.98	36.67	18.33	28.97	6.63	17.53	8.76	38.63	19.32	0.468	0.080	0.023	71.72	1670.3
NDNE 2016 Mean	NDNE	NDW	161231	2016	12	11.75	5.82	5.89	12.08	18.56	41.62	20.81	25.18	8.69	16.82	8.41	42.33	21.17	1.121	0.095	0.044	62.78	1670.3
NDNE 2016 Median	NDNE	NDW	161231	2016	12	11.92	5.83	5.72	11.17	19.08	41.77	20.89	23.04	8.39	16.61	8.31	41.53	20.77	0.981	0.086	0.036	60.64	1670.3
NDNE 2016 Min	NDNE	NDW	161231	2016	12	10.00	5.68	0.91	9.48	12.29	34.06	17.03	19.07	6.75	14.25	7.13	38.75	19.38	0.610	0.001	0.008	55.54	1670.3
NDNE 2016 Max	NDNE	NDW	161231	2016	12	12.96	6.02	10.94	19.24	22.01	49.84	24.92	38.10	19.00	19.93	9.97	49.28	24.64	3.409	0.392	0.127	75.61	1670.3
NDSW/M 161116	NDSW	NDW	161116	2016	11	10.76	6.14	16.34	9.03	20.57	29.34	14.67	30.41	6.20	17.77	8.89	37.41	18.71	0.384	0.071	0.018	76.15	1670.3
NDSW 2016 Mean	NDSW	NDW	161231	2016	12	10.71	6.03	12.46	11.64	18.24	32.72	16.36	24.26	5.96	15.79	7.90	38.62	19.31	0.922	0.124	0.015	68.11	1670.3
NDSW 2016 Median	NDSW	NDW	161231	2016	12	10.71	6.01	11.72	8.61	17.30	32.75	16.38	23.13	6.10	15.62	7.81	38.70	19.35	0.758	0.116	0.009	66.84	1670.3
NDSW 2016 Min	NDSW	NDW	161231	2016	12	9.11	5.91	8.43	7.17	13.41	25.50	12.75	20.84	4.87	14.39	7.20	35.08	17.54	0.410	0.004	0.001	61.19	1670.3
NDSW 2016 Max	NDSW	NDW	161231	2016	12	15.23	6.18	19.27	33.11	38.57	44.24	22.12	31.27	6.81	17.47	8.74	42.77	21.39	2.899	0.364	0.093	78.60	1670.3
RtM14-2/x 160412 5835	RtM14-2	RtM14	160412	2016	4	13.32	5.30	-4.33	33.03	26.92	41.31	20.65	24.88	12.89	12.10	6.05	45.16	22.58	8.176	2.224	0.757	88.55	1616.7
RtM14-2/x 160523 V175	RtM14-2	RtM14	160523	2016	5	11.92	5.44	-4.13	12.92	20.05	41.04	20.52	34.71	3.17	14.24	7.12	24.85	12.43	1.256	0.168	0.127	88.41	1616.7
RtM14-2/x 160816 V175	RtM14-2	RtM14	160816	2016	8	12.37	5.48	-3.76	20.17	24.08	43.89	21.94	43.76	4.81	18.35	9.18	28.44	14.22	2.435	0.544	0.251	97.24	1616.7
RtM14-2/x 161007 v175	RtM14-2	RtM14	161007	2016	10	13.08	5.61	-1.52	21.63	9.89	48.95	24.47	46.72	7.49	17.69	8.85	31.04	15.52	4.014	1.307	0.360	99.66	1616.7
RtM14-2/M 161115	RtM14-2	RtM14	161115	2016	11	14.95	5.69	5.38	36.56	20.11	53.60	26.80	66.00	25.04	23.91	11.96	34.23	17.12	1.092	0.283	0.447	99.13	1616.7
RtMOC2/x 160816 V175	RtMOC2	RtMOC	160816	2016	8	11.90	5.50	6.64	10.77	21.00	34.58	17.29	27.62	5.29	27.48	13.74	40.67	20.34	2.090	0.004	0.408	71.32	1727.9
RtMOC2/A 161007 V175	RtMOC2	RtMOC	161007	2016	10	12.76	5.96	11.04	17.91	20.14	32.23	16.11	36.19	12.81	17.69	8.85	39.27	19.64	0.663	0.047	0.266	78.90	1727.9
RtMOC2/B 161007 V175	RtMOC2	RtMOC	161007	2016	10	11.37	6.05	12.94	11.28	20.40	31.77	15.89	28.49	9.72	19.34	9.67	40.22	20.11	0.560	0.090	0.255	78.76	1727.9
RtMOC2/M 161115	RtMOC2	RtMOC	161115	2016	11	9.25	6.03	18.84	16.18	19.27	16.16	8.08	39.37	10.44	17.92	8.96	31.36	15.68	0.444	0.032	0.183	81.84	1727.9
WtA1-1/x 160414 6155	WtA1-1	WtA1	160414	2016	4	31.87	4.43	-39.55	13.88	17.31	131.08	65.54	18.18	11.94	16.13	8.06	69.12	34.56	1.208	0.072	0.160	53.55	1403.9
WtA1-2/x 160414 5824	WtA1-2	WtA1	160414	2016	4	31.37	4.50	-34.54	23.92	17.43	135.87	67.93	47.20	7.65	41.23	20.61	60.23	30.12	0.274	0.039	0.033	93.75	1426.6
WtA1-1/x 160831 JUG	WtA1-1	WtA1	160831	2016	8	31.57	4.39	-46.48	7.47	17.93	138.93	69.47	9.87	2.10	44.85	22.42	39.92	19.96	17.508	6.787	3.033	45.43	1403.9
WtA1-1/M 161115	WtA1-1	WtA1	161115	2016	11	26.40	4.50	-34.92	12.18	12.10	149.91	74.95	15.71	3.18	58.74	29.37	46.96	23.48	18.819	1.820	4.335	48.37	1403.9
WtA3-1/x 151229	WtA3-1	WtA3	151229	2015	12	32.17	4.40	-59.63	10.30	11.93	108.66	54.33	10.40	2.92	31.19	15.59	32.79	16.39	11.500	4.115	1.591	29.05	1368.8
WtA3-1/x 160220 JUG	WtA3-1	WtA3	160220	2016	2	28.10	4.35	-50.56	8.07	8.42	142.76	71.38	10.83	1.76	47.89	23.95	41.77	20.88	16.200	2.933	2.152	32.05	1368.8
WtA3-2/x 160407 6123	WtA3-2	WtA3	160407	2016	4	31.77	4.40	-44.65	9.56	11.40	122.38	61.19	11.79	1.87	41.39	20.70	42.37	21.18	10.915	5.777	1.900	29.20	1392.5
WtA3-2b/A 160506 6125	WtA3-2	WtA3	160506	2016	5	30.36	4.47	-42.29	6.94	24.58	117.80	58.90	10.61	2.48	40.40	20.20	48.26	24.13	16.808	2.561	2.202	33.75	1392.5
WtA3-2/x 160506 1916	WtA3-2	WtA3	160506	2016	5	31.57	4.39	-45.39	5.64	7.69	124.23	62.12	11.27	1.28	41.23	20.61	42.77	21.38	11.986	9.888	1.737	28.27	1392.5
WtA3-2b/B 160506 5860	WtA3-2	WtA3	160506	2016	5	30.47	4.47	-37.04	7.56	24.29	116.97	58.48	10.83	2.71	40.24	20.12	46.41	23.20	17.034	2.514	2.202	33.68	1392.5
WtA3-2/x 160521 3168	WtA3-2	WtA3	160521	2016	5	37.30	4.26	-61.55	6.01	8.68	154.27	77.14	10.13	2.51	44.68	22.34	48.46	24.23	14.832	7.431	1.911	30.05	1392.5
WtA3-2/x 160604 V175	WtA3-2	WtA3	160604	2016	6	29.06	4.43	-44.68	5.78	5.53	123.94	61.97	12.53	1.84	38.10	19.05	40.67	20.34	8.795	2.829	1.747	33.22	1392.5
WtA3-1/x 160604 V175	WtA3-1	WtA3	160604	2016	6	34.99	4.32	-55.66	5.95	13.02	147.11	73.56	9.92	2.05	42.38	21.19	39.82	19.91	13.910	5.734	1.980	34.86	1368.8
WtA3-2/x 160816 V175	WtA3-2	WtA3	160816	2016	8	30.11	4.41	-47.15	10.21	10.02	121.77	60.89	13.35				42.07	21.03	10.318	4.795	1.926	45.90	1392.5
WtA3-2/x 161007 v175	WtA3-2	WtA3	161007	2016	10	29.71	4.77	-22.39	17.66	8.05	144.70	72.35	21.40	4.96	58.59	29.29	62.63	31.31	14.525	2.586	2.676	59.32	1392.5
WtA3-2/M 161117	WtA3-2	WtA3	161117	2016	11	30.72	4.64	-27.10	18.60	10.93	145.50	72.75	22.81	3.90	64.58	32.29	58.28	29.14	16.343	1.500	2.912	58.55	1392.5
WtM6N-2/x 151229	WtM6N-2	WtM6N	151229	2015	12	14.81	5.40	-5.05	18.08	29.43	46.68	23.34	17.40	5.75	18.51	9.26	40.47	20.24	4.510	0.107	0.539	55.01	1455.6
WtM6N-2/x 160220a v16	WtM6N-2	WtM6N	160220	2016	2	12.34	5.40	-4.20	8.26	30.64	73.06	36.53	18.49	4.58	28.14	14.07	54.69	27.35	1.668	0.047	0.149	46.32	1455.6
WtM6-2N/x 160521 3500	WtM6N-2	WtM6N	160521	2016	5	14.34	5.50	1.21	6.94	26.90	60.92	30.46	17.40	5.14	25.43	12.71	49.80	24.90	1.634	0.072	0.080	49.35	1455.6
WtM6N-2/x 160816 V175	WtM6N-2	WtM6N	160816	2016	8	14.18	5.50	-2.09	7.93	22.71	72.49	36.25	21.23	8.88	5.10	2.55	54.19	27.10	1.883	0.061	0.157	63.02	1455.6
WtM6N-2/x 161007 v175	WtM6N-2	WtM6N	161007	2016	10	18.50	5.75	0.59	13.91	43.16	85.40	42.70	34.71	3.22	44.19	22.09	67.37	33.68	1.672	0.201	0.131	74.13	1455.6
WtM6N-2/M 161117	WtM6N-2	WtM6N	161117	2016	11	20.66	6.10	12.52	10.49	43.41	84.17	42.09	34.46	5.80	51.31	25.66	81.03	40.52	0.821	0.466	0.036	68.69	1455.6

SampleID	Site Code	Steam Order	Latitude	Longitude	UTM	Easting meters	Northing meters	Dist2Knob meters	SumAnions	SumCats	%Diff	CO3	HCO3	Al + H3O	S+N/BC	SubWtrShed	SumBC-uEqL
BFP1b/x 160801 V175	BFP1b	1	35.60819	-83.43841	17	279128	3943230	2411.82	225.09	267.47	0.09	0.01	96.36	0.49	0.42	BFP	170.85
BFP1/x 161007 V175	BFP1	1	35.60953	-83.43858	17	279117	3943379	2284.69	228.05	282.68	0.11	0.02	117.20	0.33	0.35	BFP	178.06
BFP2/x 161007 V175	BFP2	1	35.60770	-83.43754	17	279206	3943174	2428.95	218.16	260.33	0.09	0.01	87.27	0.53	0.44	BFP	167.32
BFP1/M 161115	BFP1	1	35.60953	-83.43858	17	279117	3943379	2284.69	273.05	338.34	0.11	0.03	148.01	0.15	0.33	BFP	212.67
BFP2/M 161123	BFP2	1	35.60770	-83.43754	17	279206	3943174	2428.95	242.36	287.18	0.08	0.01	94.39	0.36	0.45	BFP	182.81
NDNE/M 161116	NDNE	1	35.56464	-83.47965	17	275270	3938492	8479.92	74.49	92.33	0.11	0.00	8.66	1.59	0.61	NDW	63.68
NDNE 2016 Mean	NDNE	1	35.56464	-83.47965	17	275270	3938492	8479.92	74.49							NDW	63.45
NDNE 2016 Median	NDNE	1	35.56464	-83.47965	17	275270	3938492	8479.92	74.49							NDW	60.50
NDNE 2016 Min	NDNE	1	35.56464	-83.47965	17	275270	3938492	8479.92	74.49							NDW	52.32
NDNE 2016 Max	NDNE	1	35.56464	-83.47965	17	275270	3938492	8479.92	74.49							NDW	91.71
NDSW/M 161116	NDSW	1	35.56445	-83.47972	17	275241	3938472	8513.07	105.00	117.27	0.08	0.00	16.34	1.31	0.62	NDW	64.21
NDSW 2016 Mean	NDSW	1	35.56445	-83.47972	17	275241	3938472	8513.07								NDW	57.43
NDSW 2016 Median	NDSW	1	35.56445	-83.47972	17	275241	3938472	8513.07								NDW	56.39
NDSW 2016 Min	NDSW	1	35.56445	-83.47972	17	275241	3938472	8513.07								NDW	50.45
NDSW 2016 Max	NDSW	1	35.56445	-83.47972	17	275241	3938472	8513.07								NDW	68.20
RtM14-2/x 160412 5835	RtM14-2	1	35.61102	-83.44772	17	278292	3943565	2642.52	101.25	106.19	0.02	0.00	0.00	13.22	0.72	RP	66.40
RtM14-2/x 160523 V175	RtM14-2	1	35.61102	-83.44772	17	278292	3943565	2642.52	74.00	78.52	0.03	0.00	0.00	4.90	0.79	RP	57.43
RtM14-2/x 160816 V175	RtM14-2	1	35.61102	-83.44772	17	278292	3943565	2642.52	88.13	98.59	0.06	0.00	0.00	5.72	0.71	RP	71.96
RtM14-2/x 161007 v175	RtM14-2	1	35.61102	-83.44772	17	278292	3943565	2642.52	80.47	108.62	0.15	0.00	0.00	6.47	0.57	RP	78.58
RtM14-2/M 161115	RtM14-2	1	35.61102	-83.44772	17	278292	3943565	2642.52	115.66	151.01	0.13	0.00	5.38	3.16	0.49	RP	120.12
RtMOC2/x 160816 V175	RtMOC2	1	35.59452	-83.47500	17	275775	3941797	5702.65	72.99	103.57	0.17	0.00	6.63	5.24	0.55	RP	66.99
RtMOC2/A 161007 V175	RtMOC2	1	35.59452	-83.47500	17	275775	3941797	5702.65	81.32	106.95	0.14	0.00	11.04	1.76	0.49	RP	77.49
RtMOC2/B 161007 V175	RtMOC2	1	35.59452	-83.47500	17	275775	3941797	5702.65	76.40	98.67	0.13	0.00	12.94	1.46	0.53	RP	67.99
RtMOC2/M 161115	RtMOC2	1	35.59452	-83.47500	17	275775	3941797	5702.65	70.45	99.75	0.17	0.00	18.84	1.39	0.36	RP	74.45
WtA1-1/x 160414 6155	WtA1-1	1	35.62591	-83.41442	17	281350	3945142	1171.13	162.26	116.81	-0.16	0.00	0.00	38.36	1.29	WCP	72.75
WtA1-2/x 160414 5824	WtA1-2	1	35.62688	-83.41469	17	281328	3945251	1131.33	177.22	156.65	-0.06	0.00	0.00	32.19	0.98	WCP	105.57
WtA1-1/x 160831 JUG	WtA1-1	1	35.62591	-83.41442	17	281350	3945142	1171.13	164.34	124.07	-0.14	0.00	0.00	58.25	1.62	WCP	54.36
WtA1-1/M 161115	WtA1-1	1	35.62591	-83.41442	17	281350	3945142	1171.13	174.18	149.20	-0.08	0.00	0.00	50.55	1.30	WCP	71.74
WtA3-1/x 151229	WtA3-1	2	35.62510	-83.41987	17	280854	3945064	725.38	130.89	94.49	-0.16	0.00	0.00	51.68	1.56	WCP	45.30
WtA3-1/x 160220 JUG	WtA3-1	2	35.62510	-83.41987	17	280854	3945064	725.38	159.25	123.54	-0.13	0.00	0.00	61.07	1.48	WCP	57.43
WtA3-2/x 160407 6123	WtA3-2	1	35.62578	-83.41998	17	280846	3945150	683.76	143.34	116.00	-0.11	0.00	0.00	50.91	1.37	WCP	55.53
WtA3-2b/A 160506 6125	WtA3-2	1	35.62578	-83.41998	17	280846	3945150	683.76	149.32	123.32	-0.10	0.00	0.00	50.85	1.40	WCP	57.42
WtA3-2/x 160506 1916	WtA3-2	1	35.62578	-83.41998	17	280846	3945150	683.76	137.57	120.15	-0.07	0.00	0.00	52.54	1.37	WCP	54.54
WtA3-2b/B 160506 5860	WtA3-2	1	35.62578	-83.41998	17	280846	3945150	683.76	148.81	121.94	-0.10	0.00	0.00	51.00	1.41	WCP	56.87
WtA3-2/x 160521 3168	WtA3-2	1	35.62578	-83.41998	17	280846	3945150	683.76	168.96	129.95	-0.13	0.00	0.00	69.41	1.54	WCP	59.21
WtA3-2/x 160604 V175	WtA3-2	1	35.62578	-83.41998	17	280846	3945150	683.76	135.25	106.51	-0.12	0.00	0.00	46.03	1.39	WCP	53.75
WtA3-1/x 160604 V175	WtA3-1	2	35.62510	-83.41987	17	280854	3945064	725.38	166.08	115.79	-0.18	0.00	0.00	61.44	1.70	WCP	53.06
WtA3-2/x 160816 V175	WtA3-2	1	35.62578	-83.41998	17	280846	3945150	683.76	142.00	91.83	-0.21	0.00	0.00	48.87	1.76	WCP	
WtA3-2/x 161007 v175	WtA3-2	1	35.62578	-83.41998	17	280846	3945150	683.76	170.40	167.37	-0.01	0.00	0.00	31.59	1.04	WCP	86.97
WtA3-2/M 161117	WtA3-2	1	35.62578	-83.41998	17	280846	3945150	683.76	175.03	170.32	-0.01	0.00	0.00	39.73	1.05	WCP	88.14
WtM6N-2/x 151229	WtM6N-2	1	35.61740	-83.41878	17	280932	3944208	1385.98	94.19	87.30	-0.04	0.00	0.00	8.48	0.93	WCP	52.65
WtM6N-2/x 160220a v16	WtM6N-2	1	35.61740	-83.41878	17	280932	3944208	1385.98	111.96	107.76	-0.02	0.00	0.00	5.66	0.98	WCP	64.48
WtM6-2N/x 160521 3500	WtM6N-2	1	35.61740	-83.41878	17	280932	3944208	1385.98	95.97	99.56	0.02	0.00	1.21	4.80	0.90	WCP	60.15
WtM6N-2/x 160816 V175	WtM6N-2	1	35.61740	-83.41878	17	280932	3944208	1385.98	103.13	91.50	-0.06	0.00	0.00	5.05	1.06	WCP	59.75
WtM6N-2/x 161007 v175	WtM6N-2	1	35.61740	-83.41878	17	280932	3944208	1385.98	143.06	151.49	0.03	0.00	0.59	3.47	0.86	WCP	93.71
WtM6N-2/M 161117	WtM6N-2	1	35.61740	-83.41878	17	280932	3944208	1385.98	150.58	175.72	0.08	0.00	12.51	1.55	0.73	WCP	106.43

			Grain Size Analysis (4-phase; dry)					Particle Size Analysis (3-phase; wet)					Lab pH			ExAcidity	EBC	Exch-Al	Exch-Fe	CEC	%BSat	AEC	Soluble-SO4 (0.025M KCl)	PO4 Extractable SO4 (Ca(H2PO4)2)	
51		4																						
Site Code		**Sample ID**	**% Water**	**%Crs**	**%Fine**	**%Silt+Clay**	**% <250 um**	**Sand%**	**Silt%**	**Clay**	**% Water**	**% Water**	**(1:2 water)**	**(1:2 $CaCl_2$)**	**Duplicate**	**$cmol_c$/kg**	**$cmol_c$/kg**	**cmol/kg**	**cmol/kg**	**$cmol_c$/kg**	**EBC/(CEC)**	**$cmol_c$/kg**	**ug[SO4]/g dry**	**ug-S/g dry**	**IS ug[SO4]/g**	**IS ug-S/g dry**
SiteCode	**A**	**SampleID**	**B**					**%Sand**	**%Silt**	**%Clay**	**%Water1**	**%Water2**	**pHwtr**	**pHCaCl2**	**pHDup**	**ExAc**	**EBC**	**ExAl**	**ExFe**	**CEC**	**%BSat**	**AEC**	**SO4-Out**	**S-Out**	**SO4-Inn**	**S-Inn**
WtA3	A	SL-WtA3-1T						0.615	0.121	0.263	0.472		4.38	3.76		6.68	1.16	2.170	0.040	7.84	0.148	0.08	18.47	6.17	184.60	61.62
WtA3	A	SL-WtA3-1B	57.5%	86.3%	12.2%	1.5%	13.65%	0.596	0.024	0.380	0.624		4.06	3.84		5.28	1.18	1.576	0.010	6.46	0.183	0.04	17.39	5.81	252.43	84.26
WtA3	A	SL-WtA3-2T						0.523	0.095	0.382	0.541		4.01	3.73		9.89	2.18	3.224	0.103	12.07	0.181	0.08	7.57	2.53	107.81	35.98
WtA3	A	SL-WtA3-2B	59.8%	83.8%	13.4%	2.7%	16.19%	0.522	0.113	0.365	0.658		4.12	3.91		9.64	0.62	2.458	0.012	10.27	0.061	0.05	6.72	2.24	100.37	33.50
WtA3		SL-WtA3-2Bb	B 60.1%	88.6%	10.7%	0.7%	11.40%	0.505	0.188	0.308	0.669		4.11	3.98		7.89	0.61	2.294	0.010	8.51	0.072	0.09	7.22	2.41	106.26	35.47
WtA3	A	SL-WtA3-3T									0.814		4.06	3.77		12.37	3.28	3.309	0.718	15.65	0.210	0.20	14.44	4.82	81.08	27.06
WtA3		SL-WtA3-3Tb	B								0.862		4.31	4.05		12.92	2.23	2.373	0.281	15.15	0.147	0.13	14.50	4.84	58.49	19.52
WtA3	A	SL-WtA3-3B	37.5%	72.8%	19.2%	8.0%	27.19%	0.535	0.124	0.341	0.424		4.08	3.83		4.40	0.63	1.084	0.060	5.02	0.125	0.03	12.15	4.05	66.60	22.23
WtA3	A	SL-WtA3-4T						0.529	0.071	0.400	0.558		3.97	3.60		8.30	2.02	1.856	0.390	10.32	0.196	0.03	9.69	3.23	104.38	34.84
WtA3		SL-WtA3-4Tb	B					0.530	0.058	0.412	0.605		3.93	3.34		8.81	1.93	1.762	0.117	10.74	0.180	0.09			85.77	28.63
WtA3	A	SL-WtA3-4B	47.7%	78.6%	16.8%	4.5%	21.39%	0.525	0.190	0.285	0.540		4.11	3.63		7.94	2.57	2.072	0.092	10.51	0.245	0.15	27.12	9.05	171.16	57.13
WtA3	A	SL-WtA3-5T	29.9%	78.1%	16.4%	5.5%	21.92%	0.725	0.116	0.159	0.385	0.375	4.25	3.59		6.25	1.17	2.079	0.090	7.42	0.157	0.15	28.86	9.63	93.76	31.30
WtA3	A	SL-WtA3-5B	25.5%	68.9%	15.7%	15.4%	31.13%	0.511	0.154	0.335	0.394	0.237	4.59	3.88		3.72	0.70	1.762	0.019	4.42	0.157	0.09	18.81	6.28	114.46	38.20
WtA3	A	SL-WtA3-6T						0.820	0.074	0.106	0.511	0.373	4.03	3.01		7.59	6.35	3.271	0.354	13.94	0.455	0.74	11.05	3.69	62.94	21.01
WtA3	A	SL-WtA3-6B	17.2%	60.2%	14.3%	25.5%	39.81%	0.531	0.128	0.340	0.267	0.152	4.36	3.32		4.82	0.53	1.260	0.041	5.35	0.099	0.13	9.53	3.18	69.87	23.32
WtA3	A	SL-WtA3-6C	24.0%	79.5%	14.1%	6.4%	20.49%				0.297	0.220	4.24	3.49		7.69	0.56	3.101	0.035	8.25	0.068	0.18	15.97	5.33	177.21	59.15
NDW.NE1	A	SL-NDNE-1T						0.344	0.059	0.597	0.830	0.825	3.69	3.32	3.31	21.03	1.24	3.870	0.020	22.27	0.056	0.89	16.33	5.45	13.19	4.40
NDW.NE1	A	SL-NDNE-1B	51.8%	61.3%	25.0%	13.7%	38.68%	0.576	0.158	0.267	0.585	0.587	4.53	4.24	4.30	8.27	0.62	1.791	0.004	8.89	0.069	0.03	11.04	3.69	96.70	32.28
NDW.NE2	A	SL-NDNE-2T						0.394	0.069	0.537	0.800	0.747	3.52	3.13	3.10	17.12	1.33	5.110	0.053	18.46	0.072	0.80	26.67	8.90	10.55	3.52
NDW.NE2	A	SL-NDNE-2B	45.6%	63.0%	24.1%	12.9%	37.01%	0.423	0.269	0.308	0.506	0.503	3.99	3.81	3.69	12.06	0.36	2.638	0.008	12.42	0.029	0.03	8.37	2.80	21.81	7.28
NDW.SW1	A	SL-NDSW-1T						0.392	0.123	0.485	0.749	0.730	4.02	3.32	3.34	22.41	1.29	3.310	0.042	23.70	0.054	1.27	25.05	8.36	29.83	9.96
NDW.SW1	A	SL-NDSW-1B	45.7%	55.8%	34.6%	9.7%	44.24%	0.626	0.133	0.241	0.465	0.513	4.35	3.89	3.92	7.02	0.50	1.548	0.005	7.52	0.067	0.03	10.34	3.45	26.63	8.89
NDW.SW2	A	SL-NDSW-2T						0.357	0.028	0.615	0.822	0.792	3.69	2.78	2.80	13.01	1.86	2.960	0.073	14.87	0.125	1.00	17.13	5.72	17.64	5.89
NDW.SW2	A	SL-NDSW-2B	51.7%	34.1%	38.1%	27.8%	65.87%	0.443	0.109	0.447	0.588	0.674	4.26	3.90	3.91	12.87	0.46	2.707	0.011	13.33	0.034	0.04	13.36	4.46	46.34	15.47
RtM14	A	SL-RtM14-1T						0.543	0.316	0.141	0.522		3.91	3.05	3.24	12.98	1.62	2.817	0.250	14.60	0.111	0.01	4.29	1.43	24.60	8.21
RtM14	A	SL-RtM14-1B	27.6%	78.2%	14.0%	7.8%	21.84%	0.518	0.317	0.165	0.305		4.67	4.09	4.06	4.26	0.35	1.099	0.008	4.61	0.076	0.01	8.02	2.68	335.63	112.03
RtM14	A	SL-RtM14-2T						0.531	0.082	0.387	0.578		4.08	3.25	3.36	14.50	1.78	3.048	0.153	16.28	0.109	0.02	2.54	0.85	40.14	13.40
RtM14	A	SL-RtM14-2B	35.0%	58.4%	26.8%	14.8%	41.59%	0.566	0.266	0.168	0.333		4.61	4.23	4.15	5.30	0.48	1.245	0.008	5.78	0.084	0.00	7.28	2.43	164.53	54.92
RtM14	A	SL-RtM14-3T						0.560	0.201	0.239	0.755		4.11	3.53	3.53	22.21	1.56	5.508	0.095	23.77	0.066	0.11	2.68	0.90	23.65	7.90
RtM14	A	SL-RtM14-3B	42.9%	59.4%	28.9%	11.7%	40.59%	0.514	0.324	0.162	0.461		4.39	3.83	3.75	9.01	0.65	2.049	0.011	9.66	0.067	0.01	6.34	2.12	127.04	42.41
BFP1	A	SL-BFP1-1T						0.794	0.134	0.073	0.552		4.58	3.56		2.52	15.48	0.983	0.021	18.00	0.860	0.84	11.42	3.81	16.78	5.60
BFP1	A	SL-BFP1-1B	29.3%	77.2%	12.4%	10.4%	22.85%	0.471	0.386	0.143	0.301		5.18	4.15		2.05	1.88	0.798	0.007	3.93	0.477	0.10	8.70	2.90	243.19	81.18
BFP1	A	SL-BFP1-1C	27.6%	62.0%	23.0%	15.0%	37.97%	0.491	0.430	0.079	0.292		5.26	4.27		1.64	1.49	0.856	0.007	3.13	0.475	0.12	14.67	4.90	377.89	126.14
BFP1	A	SL-BFP1-2T	38.5%	59.6%	29.8%	10.6%	40.35%	0.642	0.257	0.102	0.391		4.88	3.95		3.10	11.75	0.784	0.008	14.85	0.791	0.40	12.98	4.33	43.02	14.36
BFP1	A	SL-BFP1-2B	36.9%	68.9%	20.1%	11.0%	31.09%	0.555	0.349	0.095	0.378		4.29	3.70		6.00	1.62	1.792	0.008	7.62	0.213	0.16	7.20	2.40	43.78	14.61
BFP1	A	SL-BFP1-2C	28.6%	72.4%	16.7%	10.8%	27.56%	0.425	0.419	0.156	0.294		4.56	4.01		3.78	0.57	1.329	0.005	4.34	0.130	0.07	14.72	4.91	355.06	118.52
BFP1		SL-BFP1-2Cb	B 29.7%	76.7%	15.0%	8.3%	23.32%				0.300		4.54	4.06		3.96	0.53	1.282	0.006	4.49	0.117	0.07				
BFP1	A	SL-BFP1-3T						0.630	0.080	0.289	0.650		6.02	5.15		32.10	8.41	0.023	0.002	40.51	0.208	0.42	17.50	5.84	10.99	3.67
BFP1	A	SL-BFP1-3B	30.3%	67.8%	18.4%	13.9%	32.23%	0.660	0.270	0.070	0.372		5.79	4.73		2.31	4.61	0.177	0.002	6.92	0.666	0.02	10.78	3.60	23.54	7.86
BFP1	A	SL-BFP1-4T						0.807	0.088	0.105	0.716		3.66	2.73		18.25	7.06	2.596	0.173	25.31	0.279	2.21	7.83	2.61	8.33	2.78
BFP1	A	SL-BFP1-4B	41.9%	82.0%	15.3%	2.8%	18.05%	0.689	0.234	0.077	0.427		4.05	3.48		11.42	0.98	3.056	0.040	12.40	0.079	0.07	12.37	4.13	50.41	16.83
BFP1	A	SL-BFP1-4C	38.7%	78.0%	17.0%	5.1%	22.04%	0.717	0.263	0.021	0.397		4.17	3.75		10.04	0.55	2.446	0.013	10.59	0.052	0.07	12.88	4.30	57.50	19.19
RtMOC	A	SL-RtMOC-1T						0.773	0.052	0.175	0.748		3.57	2.69	2.92	21.35	3.25	3.871	0.269	24.60	0.132	0.34	8.68	2.90	11.13	3.71
RtMOC	A	SL-RtMOC-1B	42.9%	35.1%	37.4%	27.5%	64.93%	0.610	0.277	0.114	0.454		4.08	3.61	3.61	8.82	0.88	2.102	0.036	9.71	0.091	0.01	2.60	0.87	20.47	6.83
RtMOC	A	SL-RtMOC-2T						0.782	0.113	0.104	0.514		3.46	2.81	3.07	15.09	2.27	3.050	0.300	17.36	0.131	0.02	4.82	1.61	16.21	5.41
RtMOC	A	SL-RtMOC-2B	30.7%	57.5%	27.5%	15.0%	42.50%	0.581	0.270	0.149	0.319		4.51	4.01	4.05	5.82	0.89	1.293	0.010	6.71	0.133	0.00	11.45	3.82	18.05	6.03
RtMOC	A	SL-RtMOC-3T						0.777	0.028	0.194	0.697		4.02	3.21	3.39	19.81	2.20	4.792	0.273	22.00	0.100	0.18	4.86	1.62	17.40	5.81
RtMOC	A	SL-RtMOC-3B	69.0%	59.6%	27.6%	12.8%	40.39%	0.616	0.279	0.105	0.333	0.317	4.33	3.67	3.69	14.23	1.36	3.622	0.075	15.60	0.087	0.01	2.47	0.82	20.40	6.81
RtMOC	A	SL-RtMOC-3B(dupl)	68.0%	42.0%	35.0%	23.0%	58.01%									14.49	1.45	3.566	0.074	15.94	0.091	0.01	2.46	0.82		
WtM6N	A	SL-WtM6N-1T						0.608	0.266	0.126	0.529		4.47	4.00	4.06	7.83	1.16	1.604	0.004	9.00	0.129	0.03	4.06	1.35	78.73	26.28
WtM6N	A	SL-WtM6N-1B	42.7%	58.4%	25.3%	16.3%	41.65%	0.608	0.286	0.106	0.436		4.80	4.51	4.48	2.50	0.56	0.622	0.003	3.07	0.183	0.00	8.19	2.73	332.10	110.85
WtM6N	A	SL-WtM6N-2T						0.789	0.162	0.049	0.612		4.55	3.85	4.10	8.26	2.22	1.971	0.003	10.48	0.212	0.03	5.78	1.93	48.03	16.03
WtM6N	A	SL-WtM6N-2B	34.0%	78.6%	17.1%	4.3%	21.45%	0.788	0.123	0.089	0.347		4.61	3.98	4.03	5.25	1.22	0.939	0.003	6.47	0.189	0.01	5.92	1.98	84.53	28.22
WtM6N	A	SL-WtM6N-3T						0.735	0.126	0.138	0.699		4.01	3.29	3.59	8.09	4.90	2.298	0.083	12.99	0.377	0.03	6.48	2.16	25.25	8.43
WtM6N	A	SL-WtM6N-3B						0.596	0.247	0.156	0.451		4.17	3.70	3.74	9.10	1.23	0.933	0.003	10.33	0.119	0.01	3.76	1.26		

51		4	Bound-S	Bound-Extrctbl-OS	TIS (SO4-S)	TS (< 250 um)		OrgS by diffnc	OrgS meas'd (< 250 um)		%OrgS by diffnc	%OrgS meas'd	TOC (< 250 um)			TC (< 250 um)			C/S ratio
Site Code		Sample ID	ug/g dry	ug/g dry	ug-S/g dry	ug-S/g	StdDev	ug-S/g dry	ug-S/g	StdDev	% OrgS	% OrgS	% TOC	StdDev	ug-C/g	% TC	StdDev	ug-C/g	
SiteCode	A	SampleID	B	TotSO4	Sol-OrgS	TIS-S	TS	sd	OrgsDiff	OrgsMeas	sd	%OrgSDiff	%OrgSMeas	%TOC	sd	TOC	%TC	sd	TC	C/S
WtA3	A	SL-WtA3-1T		82.24	20.62	67.78	779	27	711	544	nm	0.913	0.699	8.2	0.36	81989	2.3	0.07	22778	41.8
WtA3	A	SL-WtA3-1B		125.88	41.62	90.06	783	109	693	755	nm	0.885	0.964	4.7	0.4	47081	5.9	0.8	59170	78.3
WtA3	A	SL-WtA3-2T		61.68	25.70	38.51	937	5	898	717	nm	0.959	0.766	14.6	0.56	145506	5.6	0.5	55529	77.4
WtA3	A	SL-WtA3-2B		54.07	20.57	35.75	922	59	886	888	nm	0.961	0.964	16.2	0.77	162015	11.3	0.1	113066	127.3
WtA3		SL-WtA3-2Bb	B	55.07	19.60	37.88	866	64	828	888	nm	0.956	1.026	13.1	0.54	130730	15.7	0.0	156893	176.6
WtA3	A	SL-WtA3-3T		63.64	36.58	31.88	1666	41	1634	1197	nm	0.981	0.719	25.5	0.90	254844	27.6	1.3	276201	230.7
WtA3		SL-WtA3-3Tb	B	47.36	27.84	24.36	1602	97	1577	1197	nm	0.985	0.748	21.7	0.05	216565	27.6	1.3	276201	230.7
WtA3	A	SL-WtA3-3B		32.50	10.27	26.29	605	3	579	416	nm	0.957	0.688	5.3	0.13	52686	8.0	0.1	79682	191.4
WtA3	A	SL-WtA3-4T		60.12	25.28	38.07	881	15	843	615	nm	0.957	0.697	12.0	0.08	120050	10.2	1.1	101845	165.7
WtA3		SL-WtA3-4Tb	B	48.57	19.94	28.63	890	12	862	615	nm	0.968	0.690	14.4	0.34	143936	14.3	1.9	143368	233.2
WtA3	A	SL-WtA3-4B		82.70	25.57	66.19	705	3	639	465	nm	0.906	0.660	3.4	0.8	34301	10.3	0.7	103458	222.5
WtA3	A	SL-WtA3-5T		47.89	16.60	40.93	541	2	500	382	nm	0.924	0.706	6.1	0.44	61015	8.8	0.001	87765	229.7
WtA3	A	SL-WtA3-5B		46.56	8.35	44.48	293	4	248	186	nm	0.848	0.637	2.7	0.2	26695	3.3	0.02	32880	176.5
WtA3	A	SL-WtA3-6T		27.14	6.14	24.70	959	20	934	594	nm	0.974	0.620	14.9	1.3	149256	18.7	1.0	187105	314.9
WtA3	A	SL-WtA3-6B		24.25	0.93	26.51	254	7	227	125	nm	0.896	0.492	3.5	0.2	35486	4.0	0.02	40312	322.6
WtA3	A	SL-WtA3-6C		68.88	9.73	64.48	353	1	289	262	nm	0.817	0.742	2.3	0.1	23207	2.3	0.04	22870	87.3
NDW.NE1	A	SL-NDNE-1T		8.71	4.31	9.85	1988	61	1978	1623	nm	0.995	0.817	25.1	1.3	250707	37.3	2.1	373198	229.9
NDW.NE1	A	SL-NDNE-1B		51.86	19.58	35.96	517	11	481	204	nm	0.930	0.394	6.0	0.8	60120	2.9	0.1	29056	142.7
NDW.NE2	A	SL-NDNE-2T		6.04	2.52	12.42	2153	40	2140	1872	nm	0.994	0.870	22.5	2.8	225025	35.6	1.8	356347	190.4
NDW.NE2	A	SL-NDNE-2B		10.59	3.31	10.07	131	17	121	49	nm	0.923	0.373	5.1	0.9	51021	1.3	0.1	13474	275.9
NDW.SW1	A	SL-NDSW-1T		18.01	8.05	18.32	1082	93	1063	1069	nm	0.983	0.988	23.0	1.3	229697	19.9	1.1	198600	185.8
NDW.SW1	A	SL-NDSW-1B		17.14	8.25	12.34	407	17	395	201	nm	0.970	0.494	5.0	0.3	49901	2.2	0.2	21789	108.2
NDW.SW2	A	SL-NDSW-2T		8.82	2.94	11.60	1918	79	1906	1517	nm	0.994	0.791	15.7	1.0	157162	35.5	0.8	354857	233.9
NDW.SW2	A	SL-NDSW-2B		24.84	9.37	19.92	470	13	450	472	nm	0.958	1.005	5.5	1.4	55170	2.8	0.4	27521	58.3
RtM14	A	SL-RtM14-1T		13.29	5.08	9.64	899	14	889	788	nm	0.989	0.876	11.8	1.0	117581	15.4	1.0	154449	196.1
RtM14	A	SL-RtM14-1B		145.26	33.23	114.71	300	6	186	50	nm	0.618	0.166	1.5	0.1	14953	1.8	0.0	18480	370.9
RtM14	A	SL-RtM14-2T		27.00	13.60	14.24	899	26	884	797	nm	0.984	0.887	12.0	1.4	120108	13.2	0.2	131664	165.1
RtM14	A	SL-RtM14-2B		76.29	21.37	57.35	294	10	236	115	nm	0.805	0.390	2.9	0.3	29219	3.4	0.4	34460	300.5
RtM14	A	SL-RtM14-3T		26.22	18.32	8.79	1480	10	1472	1475	nm	0.994	0.996	22.5	0.6	225013	29.3	0.4	292579	198.4
RtM14	A	SL-RtM14-3B		64.12	21.72	44.52	397	10	352	235	nm	0.888	0.592	4.6	0.7	45513	5.7	0.4	56554	240.7
BFP1	A	SL-BFP1-1T		10.48	4.88	9.41	1121	24	1111	884	nm	0.992	0.789	18.9	2.0	189321	21.6	0.6	216097	244.4
BFP1	A	SL-BFP1-1B		103.44	22.27	84.08	285	5	201	106	nm	0.705	0.372	1.5	0.1	14830	1.6	0.1	16358	154.1
BFP1	A	SL-BFP1-1C		166.80	40.66	131.03	264	15	133	71	nm	0.504	0.267	1.2	0.4	11505	1.1	0.0	10901	154.4
BFP1	A	SL-BFP1-2T		24.29	9.93	18.69	690	39	671	617	nm	0.973	0.895	9.6	0.2	96054	10.6	0.6	106142	172.0
BFP1	A	SL-BFP1-2B		29.81	15.19	17.02	496	9	479	289	nm	0.966	0.582	4.3	0.2	42610	4.5	0.2	45210	156.6
BFP1	A	SL-BFP1-2C		163.07	44.55	123.43	337	7	214	150	nm	0.634	0.445	1.8	0.4	18237	1.7	0.1	17336	115.5
BFP1		SL-BFP1-2Cb	B				336	1						2.0	0.1	20472	1.8	0.1	18020	
BFP1	A	SL-BFP1-3T		6.18	2.52	9.51	830	16	821	590	nm	0.989	0.710	18.2	1.1	182231	17.8	1.1	177964	301.8
BFP1	A	SL-BFP1-3B		10.09	2.23	11.46	235	5	223	142	nm	0.951	0.605	1.6	0.5	16127	2.5	0.1	25310	178.2
BFP1	A	SL-BFP1-4T		4.78	2.00	5.39	2010	5	2005	2099	nm	0.997	1.044	29.4	1.0	294350	42.9	0.1	429382	204.6
BFP1	A	SL-BFP1-4B		23.23	6.41	20.96	506	18	485	316	nm	0.959	0.623	6.8	0.03	68286	8.7	0.3	87341	276.8
BFP1	A	SL-BFP1-4C		26.00	6.81	23.49	315	2	291	204	nm	0.925	0.649	4.8	0.1	48414	6.2	0.7	62184	304.5
RtMOC	A	SL-RtMOC-1T		6.63	2.92	6.61	1672	8	1666	1573	nm	0.996	0.941	25.4	1.16	254243	43.6	1.1	435524	276.9
RtMOC	A	SL-RtMOC-1B		16.31	9.48	7.70	379	38	371	313	nm	0.980	0.828	3.9	0.06	39013	4.5	0.5	44562	142.1
RtMOC	A	SL-RtMOC-2T		12.87	7.46	7.02	1130	97	1123	838	nm	0.994	0.742	12.2	1.41	121590	17.3	1.2	172850	206.4
RtMOC	A	SL-RtMOC-2B		77.41	71.38	9.85	206	0	196	47	nm	0.952	0.228	1.4	0.15	14485	1.7	0.0	17014	362.4
RtMOC	A	SL-RtMOC-3T		10.09	4.28	7.43	1293	125	1286	1144	nm	0.994	0.885	16.3	0.44	163076	27.3	2.2	273457	238.9
RtMOC	A	SL-RtMOC-3B		21.39	14.59	7.63	736	25	728	605	41	0.990	0.822	9.9	0.47	99094	11.0	1.0	109877	181.6
RtMOC	A	SL-RtMOC-3B(dupl)					736	nm	n/a	605	nm		0.822	9.0	0.07	89678	11	nm	109877	181.6
WtM6N	A	SL-WtM6N-1T		63.58	37.30	27.63	772	36	745				0.000	8.1	0.4	81150	8.3	0.1	83156	
WtM6N	A	SL-WtM6N-1B		161.13	50.28	113.59	504	11	391				0.000	4.1	0.5	41079	4.6	0.3	45774	
WtM6N	A	SL-WtM6N-2T		39.16	23.13	17.96	1123	42	1105				0.000	9.9	0.3	98652	14.5	1.3	145288	
WtM6N	A	SL-WtM6N-2B		44.29	16.07	30.19	681	7	651				0.000	3.7	0.1	36844	7.0	0.6	69677	
WtM6N	A	SL-WtM6N-3T		14.32	5.89	10.59	1110	27	1099				0.000	17.1	0.03	170586	20.0	2.8	200442	
WtM6N	A	SL-WtM6N-3B					557	24	n/a				0.000	5.7	0.46	56657	6.9	0.1	69082	

APPENDIX D

RAW DATA – CHAPTER 6

Site Code	Sample Type	Sample Name	d34Svcdt ‰ (± SD)	d18Ovsmow ‰ (± 0.4)
BFP1	INN SL	INN SL-BFP1-2B	5.964	4.047
BFP1	INN SL	INN SL-BFP1-2C	4.539	4.723
BFP1	INN SL	INN SL-BFP1-2Cb	4.518	4.494
NDNE	INN SL	INN SL-NDNE-1B	4.833	4.923
RtM14	INN SL	INN SL-RtM14-1B	4.502	6.120
RtM14	INN SL	INN SL-RtM14-2B	4.726	5.011
RtM14	INN SL	INN SL-RtM14-3B	4.367	4.061
WtA3	INN SL	INN SL-WtA3-1B	1.526	5.635
WtA3	INN SL	INN SL-WtA3-2B	2.286	**4.784**
WtA3	INN SL	INN SL-WtA3-2Bb	2.633	4.766
WtA3	INN SL	INN SL-WtA3-3B	0.808	5.708
WtA3	INN SL	INN SL-WtA3-4B	0.816	4.679
WtA3	INN SL	INN SL-WtA3-5B	1.982	4.580
WtA3	INN SL	INN SL-WtA3-5T	3.319	4.408
WtA3	INN SL	INN SL-WtA3-6B	3.644	4.661
WtA3	INN SL	INN SL-WtA3-6C	3.804	5.077
WtM6.2N	INN SL	INN SL-WtM6.2N-1B	4.479	5.257
BFP1	OU SL	OU SL-BFP1-2C	5.069	10.537
WtA3	OU SL	OU SL-WtA3-4B	1.324	5.626

Site ID	Sample ID	Sample Type	Sample Name	$\delta^{34}S$ ‰	$\delta^{18}O$ ‰
ACC	ACC1	WQ	WQ-ACC01(150304)	2.080	4.670
BFP1	BFP1	WQ	WQ-BFP1 (160825)	2.515	7.692
BFP1	BFP2	WQ	WQ-BFP2 (161123)	5.401	7.233
BFP1	BFP3	LEACH	WQ-BFP3(150208)	-7.900	0.600
BFP1	BFP3	LEACH	WQ-BFP3(150304)	-7.450	-0.020
WtA3	WtA3.3	LEACH	WQ-WtA3.3 (160604)	-7.640	1.580
NDW	NDNE	WQ	WQ-NDNE (160701)	7.682	3.494
NDW	NDNE	WQ	WQ-NDNE-170224	7.737	3.500
NDW	NDSW	WQ	WQ-NDSW (160701)	8.097	3.206
NDW	NDSW	WQ	WQ-NDSW-170224	8.012	3.125
RAIN	RAIN	RN	KnoxRain-2015Summer	-0.610	9.080
RAIN	RAIN	RN	Noland Divide Open Site July 2016	1.314	7.284
RAIN	RAIN	TF	RN TF-NDW 170310	6.622	8.000
RtM14	RtM14.2	WQ	WQ-RtM14-2(160523)	6.900	5.120
RtMOC	RtMOC	WQ	WQ-RtMOC1 (160815)	7.165	3.020
WtA1	WtA1.1	WQ	WQ-WtA1.1 (160831)	-2.184	5.370
WtA1	WtA1.1	WQ	WQ-WtA1.1 (161115)	-1.734	6.214
WtA1	WtA1.1	WQ	WQ-WtA1-1(150918)	-1.780	5.360
WtA3	WtA3.1	WQ	WQ-WtA3.1 (160220)	-1.240	4.170
WtA3	WtA3.2	WQ	WQ-WtA3.2 (160604)	0.990	6.560
WtA3	WtA3.2	WQ	WQ-WtA3.2 (161117)	1.818	8.939
WtM1	WtM1.1	WQ	WQ-WtM1.1 (150311)	5.124	4.742
WtM2	WtM2.1	WQ	WQ-WtM2.1 (150927)	4.230	4.540
WtM2	WtM2.1	WQ	WQ-WtM2.1 (150927)	4.170	4.730
WtM2	WtM2.1	WQ	WQ-WtM2.1 (161117)	3.964	5.063
WtM2	WtM2.2	WQ	WQ-WtM2.2 (150208)	6.351	5.574
WtM2	WtM2.2	WQ	WQ-WtM2.2 (150304)	5.711	4.865
WtM2	WtM2.2	WQ	WQ-WtM2.2 (150925)	6.420	5.620
WtM6	WtM6.1	WQ	WQ-WtM6.1 (160825)	3.019	2.621
WtM6	WtM6.1	WQ	WQ-WtM6.1 (161116)	2.939	2.923

Sample ID	Site Code	Collection Date	Elevation		dDvsmow	d18Ovsmow
RtM4-1 (160324)	RtM4-1	3/24/2016	1412.2	m	-44.70	-7.45
B15	WtA1-1	9/12/2015	1403.9	m	-31.09	-5.03
B16	WtA1-1	9/12/2015	1403.9	m	-31.40	-5.25
B21	WtA2-1	9/12/2015	1465.1	m	-36.53	-6.02
B23	WtA2-1	9/12/2015	1465.1	m	-35.28	-5.52
B27	WC4b	9/12/2015	1456.5	m	-34.96	-5.16
B12	WtK1b	9/12/2015	1431	m	-37.85	-5.95
B28	WtK1b	9/12/2015	1431	m	-38.15	-6.01
B13	WC4Fe	9/12/2015	1445.8	m	-36.08	-5.91
B26	WC4Fe	9/12/2015	1445.8	m	-35.24	-5.51
WC1	WC1	12/29/2015	1381.7	m	-42.69	-6.69
WtM1-1	WtM1-1	12/29/2015	1386.3	m		
WtA3-1	WtA3-1	12/29/2015	1368.8	m	-39.19	-6.25
WtM2-2	WtM2-2	12/29/2015	1426	m	-44.31	-6.83
WtM2-2b (new)	WtM2-2	12/29/2015	1426	m	-43.50	-6.77
WtM6N-2	WtM6N-2	12/29/2015	1455.6	m	-46.54	-7.37
WtM6S-2	WtM6S-2	12/29/2015	1463.5	m	-44.97	-6.78
WtM6S-2b (new)	WtM6S-2	12/29/2015	1463.5	m	-44.47	-6.91
RPv2	RtM1-1	2/20/2016	1321.9	m	-51.17	-8.18
RPv6	RtM13-1	2/20/2016	1271.1	m	-52.20	-8.17
RPv7	RtS7-1	2/20/2016	1241.4	m	-51.01	-8.05
RPv8	RtS10-1	2/20/2016	1234.6	m	-47.13	-7.76
RPv9	RtS6-1	2/20/2016	1215.3	m	-46.97	-7.64
RPv10	RtS8-1	2/20/2016	1177.9	m	-44.84	-7.34
RPv11	RtM9-1	2/20/2016	1150.8	m	-48.44	-7.81
RPv12	RtM10-1	2/20/2016	1138.6	m	-45.51	-7.29
RPv13	RtM11-1	2/20/2016	1120.6	m	-45.48	-7.32
RPv14	RtM12-1	2/20/2016	1094.2	m	-46.33	-7.40
RPv15	WtM6S-2	2/20/2016	1463.5	m	-48.56	-7.94
RPv16	WtM6N-2	2/20/2016	1455.6	m	-50.81	-7.81
WtA3-1	WtA3-1	2/20/2016	1368.8	m	-53.21	-8.51
6163	ChTt1-1	3/3/2016	1230.7	m	-43.42	-7.48
5762	ChTt2-1	3/3/2016	1244	m	-48.22	-7.70
5927	RtChT1-1	3/3/2016	1286.4	m	-46.93	-7.78
5751	ChTt1-1	3/3/2016	1230.7	m	-46.60	-7.49
6163	ChTt1-1	3/3/2016	1230.7	m	-46.37	-7.53
6132	ChTt2-1	3/3/2016	1244	m	-47.54	-7.48
6121	RtChT1-1	3/3/2016	1286.4	m	-47.65	-7.71
5660	RtM11-2	4/7/2016	1152.8	m		
5810	RtS6-2	4/7/2016	1221.4	m	-46.57	-7.81
5914	ACtP1-2	4/7/2016	1210.7	m	-39.58	-7.04
6123	WtA3-2	4/7/2016	1392.5	m	-38.22	-6.86
5835	RtM14-2	4/12/2016	1616.7	m	-43.20	-7.42
6152	RtM4-2	4/12/2016	1419.6	m	-43.41	-7.37
5919	RtM1-2	4/12/2016	1329.5	m	-48.06	-7.90
2308	RtM4-1	4/12/2016	1412.2	m		
6167	WtM2-1	4/14/2016	1329.8	m	-45.15	-7.63
6139	WtM2-1	4/14/2016	1329.8	m	-46.02	-7.73

Sample ID	Site Code	Collection Date	Elevation		dDvsmow	d18Ovsmow
5824	WtA1-2	4/14/2016	1426.6	m	-42.52	-7.21
6155	WtA1-1	4/14/2016	1403.9	m	-43.15	-7.48
6059	WtM2-1	4/14/2016	1329.8	m	-45.58	-7.81
5776	RtS7-2	4/25/2016	1250.3	m	-43.25	-7.33
5753	RtS6-2	4/25/2016	1221.4	m	-46.22	-7.47
2981	ACtP1-2	4/28/2016	1210.7	m	-46.37	-7.66
3165	ACtP1-2	4/28/2016	1210.7	m	-46.20	-7.69
5916	WtA4-1	5/6/2016	1357.5	m	-41.87	-7.42
5965	ACtP1-3	5/6/2016	1207.4	m	-37.51	-6.75
6125	WtA3-3	5/6/2016	1390.4	m	-33.82	-6.11
6092	ACtP1-2	5/6/2016	1210.7	m	-44.59	-6.80
1916	WtA3-2	5/6/2016	1392.5	m	-34.77	-5.16
6149	WtA5-1	5/6/2016	1354.1	m	-37.25	-6.71
1877	WtA4-1	5/6/2016	1357.5	m	-33.76	-4.01
5860	WtA3-3	5/6/2016	1390.4	m	-32.60	-6.17
5900	WtA5-1	5/6/2016	1354.1	m	-36.92	-6.76
3128	WtM6S-2	5/21/2016	1463.5	m	-47.25	-7.88
3056	WtM6S-2b	5/21/2016	1463.5	m	-45.46	-7.74
3500	WtM6N-2	5/21/2016	1455.6	m	-42.11	-7.38
3380	WtM2-2	5/21/2016	1426	m	-41.46	-7.47
3393	WtM1-2	5/21/2016	1402.5	m	-41.58	-7.23
3174	WC1	5/21/2016	1381.7	m	-36.92	-6.70
3168	WtA3-2	5/21/2016	1392.5	m	-33.78	-6.23
3496	WtA5-1	5/21/2016	1354.1	m	-36.12	-6.70
3386	WtA4-1	5/21/2016	1357.5	m	-39.23	-6.89
RtM14-2	RtM14-2	5/23/2016	1616.7	m	-42.74	-7.39
WtA5-1a	WtA5-1	8/16/2016	1354.1	m	-38.98	-7.10
WtA5-1b	WtA5-1	8/16/2016	1354.1	m	-40.67	-7.29
RtM14-2	RtM14-2	8/16/2016	1616.7	m	-39.93	-6.60
WtM6N-2	WtM6N-2	8/16/2016	1455.6	m	-38.32	-7.07
WtM6S-2	WtM6S-2	8/16/2016	1463.5	m	-44.73	-7.82
WtM1-1	WtM1-1	8/16/2016	1386.3	m	-37.04	-6.83
WtM2-2	WtM2-2	8/16/2016	1426	m	-38.00	-7.01
WC2 (237)	WC2	8/16/2016	1389.2	m	-37.23	-6.61
WtA3-2	WtA3-2	8/16/2016	1392.5	m	-22.85	-5.25
WtA4-1	WtA4-1	8/16/2016	1357.5	m	-36.65	-7.00
RtMOC1-2	RtMOC2	8/16/2016	1727.9	m	-47.47	-8.08
WtA3-2	WtA3-2	10/7/2016	1392.5	m	-24.93	-4.96
RtMOC1	RtMOC1a	10/7/2016	1751.9	m	-47.11	-7.82
RtMOC2	RtMOC1b	10/7/2016	1751.9	m	-49.04	-8.03
BFP1	BFP1	10/7/2016	1555.7	m	-41.28	-7.05
BFP2 (253)	BFP2	10/7/2016	1491.9	m	-42.32	-7.65
RtM14-2	RtM14-2	10/7/2016	1616.7	m	-41.51	-7.14
WtM6N-2	WtM6N-2	10/7/2016	1455.6	m	-39.99	-6.78
WtM6-1	WtM6-1	10/7/2016	1325.1	m	-40.67	-6.87
WtM1-1	WtM1-1	10/7/2016	1386.3	m	-37.79	-6.73
WtM2-1	WtM2-1	10/7/2016	1329.8	m	-35.81	-6.54

Site ID	Core ID	Core Section	Soil Horizon	Replicate	Soil Sample	Soluble SO4 d34S‰	Sorbed SO4 d34S‰	Organic S d34S‰	Total S d34S‰
BFP1	1	Surface	A		BFP1-1T				3.5
BFP1	1	Subsurface	B		BFP1-1B	7.0			7.0
BFP1	1	Subsurface	B/C		BFP1-1C	6.8			7.0
BFP1	2	Surface	A		BFP1-2T				4.4
BFP1	2	Subsurface	B		BFP1-2B	6.7	6.0		6.0
BFP1	2	Subsurface	C	prime	BFP1-2C	5.1	4.5		6.7
BFP1	2	Subsurface	C	duplicate	BFP1-2C	4.8	4.5		6.5
BFP1	3	Subsurface	A		BFP1-3T				4.1
BFP1	3	Subsurface	B		BFP1-3B	5.3			5.6
BFP1	4	Surface	A		BFP1-4T				3.2
BFP1	4	Subsurface	B		BFP1-4B				6.9
BFP1	4	Subsurface	C		BFP1-4C	8.1			
BFP1	9	Surface	O/A		BFP1-T combo				3.8
NDW	1	Surface	O/A	prime	NDNE-1T				3.7
NDW	1	Surface	O/A	duplicate	NDNE-1T				3.8
NDW	1	Subsurface	B		NDNE-1B	6.4	4.8		8.0
NDW	2	Surface	O/A		NDNE-2T				4.6
NDW	2	Subsurface	B		NDNE-2B	5.6			8.5
NDW	9	Surface	O/A		NDNE-T(combo)			3.8	
NDW	1	Surface	O/A		NDSW-1T				4.3
NDW	1	Subsurface	B		NDSW-1B		5.1		7.2
NDW	2	Surface	O/A		NDSW-2T				4.0
NDW	2	Subsurface	B		NDSW-2B				5.0
NDW	9	Surface	O/A		NDSW-T(combo)			3.8	
NDW	9	Subsurface	B		NDSW-1B & 2B (combo)	5.7			
RtM14	1	Surface	O/A		RtM14-1T				4.9
RtM14	1	Subsurface	B		RtM14-1B	5.3	4.5		
RtM14	2	Surface	O/A		RtM14-2T				4.8
RtM14	2	Subsurface	C		RtM14-2B		4.7		
RtM14	3	Surface	O/A		RtM14-3T				3.7
RtM14	3	Subsurface	C		RtM14-3B		4.4		6.2
RtM14	9	Surface	O/A		RtM14-T(combo)			4.7	
RtMOC	1	Surface	A	prime	RtMOC-1T				3.4
RtMOC	1	Surface	A	duplicate	RtMOC-1T				3.4
RtMOC	1	Subsurface	B		RtMOC-1B				5.9
RtMOC	2	Surface	A		RtMOC-2T				3.7
RtMOC	2	Subsurface	B	prime	RtMOC-2B	4.4			6.8
RtMOC	2	Subsurface	B	duplicate	RtMOC-2B				6.9
RtMOC	3	Surface	A		RtMOC-3T				3.4
RtMOC	3	Subsurface	B		RtMOC-3B				4.8
RtMOC	9	Surface	A		RtMOC-T(combo)			3.5	
WtA3	1	Subsurface	B		WtA3-1T				0.9
WtA3	1	Subsurface	B		WtA3-1B	2.2	1.5		1.1
WtA3	2	Subsurface	B		WtA3-2T				1.4
WtA3	2	Subsurface	B	prime	WtA3-2B	2.8	2.3		0.2
WtA3	2	Subsurface	B	duplicate	WtA3-2B	2.8	2.6		0.7
WtA3	3	Subsurface	B	prime	WtA3-3T				0.7
WtA3	3	Subsurface	B	duplicate	WtA3-3T				0.5
WtA3	3	Subsurface	B	prime	WtA3-3B	1.8	0.8		1.0
WtA3	3	Subsurface	B	duplicate	WtA3-3B				0.9
WtA3	4	Subsurface	B	prime	WtA3-4T				1.5
WtA3	4	Subsurface	B	duplicate	WtA3-4T				1.6
WtA3	4	Subsurface	B	prime	WtA3-4B	1.3	0.8		2.3
WtA3	4	Subsurface	B	duplicate	WtA3-4B				1.4
WtA3	5	Subsurface	B		WtA3-5T	4.3	3.3		1.9
WtA3	5	Subsurface	C		WtA3-5B	2.7	2.0		1.6
WtA3	6	Surface	A	prime	WtA3-6T				3.4
WtA3	6	Surface	A	duplicate	WtA3-6T				3.2
WtA3	6	Subsurface	C		WtA3-6B		3.6		2.5
WtA3	6	Subsurface	C		WtA3-6C		3.8		3.0
WtM6.2N	1	Subsurface	B		WtM6.2N-1T				5.212
WtM6.2N	1	Subsurface	C	prime	WtM6.2N-1B	5.112	4.479		
WtM6.2N	1	Subsurface	C	duplicate	WtM6.2N-1B		4.381		
WtM6.2N	2	Surface	A		WtM6.2N-2T				3.964
WtM6.2N	2	Subsurface	B		WtM6.2N-2B				4.959
WtM6.2N	3	Surface	A		WtM6.2N-3T				3.607

VITA

Adrian Gonzalez was born at Bergstrom Air Force Base, Austin, Texas, to Mike and Iris Gonzalez in 1966. His family settled in Southern California, and he remained a resident of California through his high school (Chaffee H.S.) and undergraduate (Pomona College) years. After graduating with a B.A. in Chemistry, he moved to the U.S. East Coast to begin his career as a bench chemist for a major chemical company in Stamford, Connecticut. After taking an evening college course in environmental science, he applied to a full-time Master's program at Manhattan College, Riverdale, NY. He worked with Drs. John Mahony and Dominic Di Toro on EPA-funded research in acid-volatile sulfides and sediment organic carbon mitigating metals toxicity in aquatic sediment. He earned a M.S. in Environmental Science and Engineering in 1992 and was hired as a research associate at the College. In that time period, he married Catherine Savarese, and accepted an environmental scientist position at the Oak Ridge National Laboratory (ORNL) in Oak Ridge, TN. In 1993 and 1996, he and his wife welcomed Elizabeth and Nicole into their family, respectively. Over the next 20 years, he worked for engineering consulting firms as an environmental scientist focused on ecological risk assessments for Superfund project remedial investigations. In 2012, he accepted a 12-month science fellowship at the U.S. Food and Drug Administration, College Park, Maryland. He accepted a graduate research assistantship in the Civil and Environmental Engineering department at the University of Tennessee, Knoxville, in 2013. For the next five years, he collaborated with National Park Service professionals and university principle investigators as the water quality laboratory manager, providing experiment support and monitoring analysis expertise, while working on his dissertation. He earned his Ph.D. in Civil Engineering in May 2018.